TAMOXIFEN IN RESIDUAL NON-FUNCTIONING PITUITARY NEUROENDOCRINE TUMOURS: AN INTEGRATED CLINICAL, MOLECULAR AND COMPUTATIONAL STUDY

DR. AMALINA BINTI HAYDAR ALI TAJUDDIN

UNIVERSITI KEBANGSAAN MALAYSIA

UNIVERSITI KEBANGSAAN MALAYSIA The National University of Malaysia	UKM-SPKPPP-PT(PdP)-05-AK04-BO07	No. Semakan: 02	Tarikh Kuat Kuasa: 27/01/2026
	BORANG DAN SENARAI SEMAK PENYERAHAN TESIS/DISERTASI SELEPAS PEMBETULAN ***FORM AND CHECKLIST OF AMENDED THESIS/DISSERTATION SUBMISSION***		

F. KELULUSAN DEKAN/PENGARAH / *APPROVAL FROM DEAN/DIRECTOR*

Tandatangan: *Signature*

Tarikh: *Date* 14/8/26

Nama dan Cap Rasmi: *Name and Official Stamp*

PROFESOR DATO' DR MARINA MAT BAKI
MD (UKM), MS ORL-HNS (UKM), PhD (UCL)
Dekan Fakulti Perubatan
Pakar Perunding Kanan ORL-HNS
Universiti Kebangsaan Malaysia

G. PERAKUAN TESIS/ DISERTASI SARJANA / DOKTOR FALSAFAH (*CERTIFICATION OF MASTER'S / DOCTORAL THESIS / DISSERTATION*)

Nama penuh pengarang (*Author's Full Name*)	DR AMALINA BINTI HAYDAR ALI TAJUDDIN		
No. Pendaftaran Pelajar (Student's Registration No.)	P100288	Sesi Akademik (*Academic Session*)	SEM 2 2025/2026
Tajuk Tesis / Disertasi (*Thesis / Dissertation Title*)	TAMOXIFEN IN RESIDUAL NON-FUNCTIONING PITUITARY NEUROENDOCRINE TUMOURS: AN INTEGRATED CLINICAL, MOLECULAR AND COMPUTATIONAL STUDY		

Semua tesis/disertasi dan penerbitan berkaitan hasil penyelidikan pelajar adalah tertakluk kepada Dasar Harta Intelek Universiti Kebangsaan Malaysia.
All theses/ dissertations and publications relating to the research work of a student are subject to the Intellectual Property Policy of Universiti Kebangsaan Malaysia.

Saya mengaku bahawa tahap akses tesis/disertasi ini sebagai (*Tandakan ✓ dalam kotak bagi maklumat yang berkaitan; tandakan satu (1) kotak di bawah sahaja):
I hereby declare the level of access for this thesis/dissertation as follows (tick ✓ the relevant box below; tick only one option).

Pilihan Tahap Akses *Access Level Selection*		Tafsiran Tahap Akses Tesis/Disertasi *Definition of Thesis/Dissertation Access Level*
☐	**RAHSIA** ***(CONFIDENTIAL)***	Mengandungi maklumat rahsia sepertimana yang diperuntukan bawah Akta Rahsia Rasmi 1972. *Contains classified information as stipulated under the Official Secrets Act 1972.*
☐	**TERHAD** ***(RESTRICTED)***	Mengandungi maklumat yang hanya boleh diakses oleh pihak yang mempunyai kebenaran atau keperluan tertentu untuk mengetahuinya yang ditentukan oleh organisasi/ badan di mana penyelidikan dijalankan. *Contains information that may only be accessed by parties with specific authorization*

Universiti Kebangsaan Malaysia The National University of Malaysia	UKM-SPKPPP-PT(PdP)-05-AK04-BO07	No. Semakan: 02	Tarikh Kuat Kuasa: 27/01/2026
	BORANG DAN SENARAI SEMAK PENYERAHAN TESIS/DISERTASI SELEPAS PEMBETULAN ***FORM AND CHECKLIST OF AMENDED THESIS/DISSERTATION SUBMISSION***		

		or a defined need to know, as determined by the organization or body where the research is conducted.
☑	**AKSES TERBUKA** ***(OPEN ACCESS)***	Tesis/disertasi versi akhir dalam format PDF yang boleh diakses secara percuma secara dalam talian dan bebas dari isu hak cipta dan pelesenan *The final version of the thesis/dissertation in PDF format that is freely accessible online and free from copyright and licensing issues.* Kementerian Pendidikan Tinggi melalui surat bertarikh 27 Mac 2025 memutuskan bahawa kebenaran akses tesis / disertasi dalam borang serahan akses terbuka ditentukan oleh penyelia (bukan pelajar). *The Ministry of Higher Education, through a letter dated 27 March 2025, has decided that permission for thesis / dissertation access in the open access submission form shall be determined by the supervisor (not the student).*
☐	**EMBARGO**	Tempoh masa di mana akses kepada tesis/disertasi disekat (ditutup) selama dua (2) tahun atas sebab-sebab tertentu sebagai contoh kerahsiaan atau hak cipta. Tesis/disertasi akan berstatus akses terbuka selepas tamat tempoh *embargo.* *The period during which access to the thesis/dissertation is restricted for two (2) years due to specific reasons, such as confidentiality or copyright. The thesis/dissertation will be granted open-access status upon the expiry of the embargo period.*

PENGESAHAN PELAJAR *(STUDENT VERIFICATION)*	**PENGESAHAN PENYELIA *(SUPERVISOR VERIFICATION)***
TANDATANGAN PELAJAR ***(STUDENT'S SIGNATURE)***	PROFESSOR DR. NORLELA SUKOR Full Registration Number : 31347 MD (USM), MMed (UKM), PhD (QLD), FACE (US) Consultant Endocrinologist National University of Malaysia **TANDATANGAN PENYELIA / PENGERUSI JK SISWAZAH** ***(SUPERVISOR'S / CHAIRPERSON SUPERVISION COMMITTEE SIGNATURE)***
Nama Pelajar *(Student name)*: DR AMALINA BINTI HAYDAR ALI TAJUDDIN No. Pendaftaran Pelajar *(Student's Registration No.)* P100288 Tarikh: 11/8/2026 *(Date)*	Nama Penyelia / Pengerusi JK Siswazah : PROF DR NORLELA SUKOR *(Supervisor's / Chairperson Supervision Committee Name)* Tarikh: 11.8.2026 *(Date)*

TAMOXIFEN IN RESIDUAL NON-FUNCTIONING PITUITARY NEUROENDOCRINE TUMOURS: AN INTEGRATED CLINICAL, MOLECULAR AND COMPUTATIONAL STUDY

DR. AMALINA BINTI HAYDAR ALI TAJUDDIN

THESIS SUBMITTED IN FULFILMENT FOR THE DEGREE OF DOCTOR OF PHILOSOPHY (MEDICINE)

FACULTY OF MEDICINE
UNIVERSITI KEBANGSAAN MALAYSIA
KUALA LUMPUR

2026

TAMOKSIFEN DALAM SISA TUMOR PITUITARI JENIS NEUROENDOKRIN TANPA FUNGSI: SATU KAJIAN BERSEPADU KLINIKAL, MOLEKULAR DAN KOMPUTASIONAL

DR. AMALINA BINTI HAYDAR ALI TAJUDDIN

TESIS YANG DIKEMUKAKAN UNTUK MEMPEROLEH
IJAZAH DOKTOR FALSAFAH (PERUBATAN)

FAKULTI PERUBATAN
UNIVERSITI KEBANGSAAN MALAYSIA
KUALA LUMPUR

2026

DECLARATION

I hereby declare that the work in this thesis is my own except for quotations and summaries which have been duly acknowledged.

11 August 2026

AMALINA BINTI
HAYDAR ALI TAJUDDIN
P100288

ACKNOWLEDGEMENT

First and foremost, all praise and thanks are due to Almighty Allah for His countless blessings, mercy, and guidance, and for granting me patience, strength, and good health throughout my PhD research journey. Without His will and sustenance, this work would not have been possible.

I consider myself truly fortunate and deeply honoured to have Professor Dr Norlela Sukor as my main supervisor. I wish to express my sincere gratitude for her invaluable guidance, continuous support, insightful advice, and unwavering encouragement throughout the planning, execution, and completion of this research. Her dedication, critical thinking, and mentorship have profoundly shaped my academic development and greatly enhanced the quality of this work.

I would also like to convey my highest appreciation to my co-supervisor, Associate Professor Dr Elena Aisha Azizan, for her constructive comments, thoughtful suggestions, and constant encouragement. Her expertise, patience, and willingness to share her knowledge have been instrumental in refining both the scientific direction and the presentation of this thesis.

Moreover, I am deeply grateful to the Endocrine Unit, Hospital Canselor Tuanku Muhriz (HCTM), and the Department of Neurosurgery, Hospital Kuala Lumpur (HKL), for their support, collaboration, and assistance throughout this study. I extend my sincere thanks to all the supporting staff at HCTM and HKL for their invaluable help, friendship, and for creating a pleasant and supportive working environment during my doctoral years. Their professionalism and kindness made the demanding journey of this research both manageable and meaningful.

To my beloved family, my heartfelt gratitude goes to my dearest husband, Mohd Hazman Hashim, for his endless patience, sacrifices, understanding, and unwavering [illegible] support, and steadfast belief in me throughout this journey. Their support was especially invaluable during one of the most challenging periods of my life, when I was diagnosed with Guillain–Barré syndrome following a COVID-19 vaccine booster. The illness significantly affected my physical strength and emotional resilience, and it profoundly disrupted my motivation and ability to continue patient recruitment at that time. The long recovery process, which took nearly a year, tested both my body and spirit. It was through their constant care, encouragement, and prayers that I was able to regain my strength, rebuild my motivation, and continue this PhD journey. My greatest inspiration is my beloved son, Mirza Hakim, whose presence, love, and smiles gave me renewed strength and determination to persevere, even during the most difficult moments.

Last but not least, I gratefully acknowledge the financial support provided by the Ministry of Higher Education under the Fundamental Research Grant Scheme (FRGS) 2018, as well as the research matching grant (RMGS) from the International Islamic University Malaysia (IIUM). This support was crucial in enabling the successful completion of this research.

ABSTRAK

Sisa tumor pituitari jenis neuroendokrin tanpa fungsi (NF-PitNET) selepas pembedahan mempunyai pilihan rawatan yang terhad untuk mencegah pertumbuhan semula. Kajian translasi bukti-konsep ini menilai potensi tamoksifen pada sisa NF-PitNET menggunakan rangka kerja klinikal, molekul dan komputasional bersepadu. Analisis [illegible] β) [illegible] ajian rintis rawak selama 12 bulan merekrut orang dewasa dengan penyakit sisa yang disahkan melalui pengimejan resonans magnetik (MRI) dan diagihkan secara 1:1 kepada tamoksifen 20–40 mg sehari atau pemantauan aktif. Isipadu tumor dinilai pada garis dasar, enam bulan dan dua belas bulan menggunakan segmentasi MRI tiga dimensi kuantitatif. Sepuluh serum penandabio yang merangkumi laluan pertumbuhan, angiogenik, keradangan dan pemodulasi *Wingless-Integrated* diukur secara longitudinal. Manakala aliran rangkaian farmakologi, analisis pengayaan laluan, pemetaan interaksi protin dan pemeringkatan gen hab digunakan untuk mencirikan sasaran dan laluan molekul berkaitan tamoksifen. Sembilan puluh enam pesakit disaring, dengan dua puluh melengkapkan susulan; setiap kumpulan mempunyai profil klinikal, radiologi, histologi dan penandabio asas [illegible] % [illegible] β [illegible] % [illegible] menunjukkan kesan signifikan, analisis berpasangan dalam kumpulan tamoksifen menunjukkan pengurangan isipadu tumor yang signifikan daripada garis dasar hingga dua belas bulan ($p = 0.045$). Pengecutan tumor berlaku dalam 40% pesakit yang dirawat dengan tamoksifen tanpa kes pertumbuhan semula, manakala 20% pesakit di bawah pemantauan aktif menunjukkan perkembangan tumor ($p = 0.014$). Dalam analisis regresi linear berganda, protin berkaitan *Dickkopf 1* selepas rawatan secara bebas dan [illegible] $p = 0.010$). [illegible] ≈ [illegible] Pemodelan multivariat mengenalpasti paksi pertumbuhan dan angiogenik yang menjadi penyumbang terbesar dalam varians respons volumetrik. Analisis rangkaian komputasional menunjukkan penglibatan rangkaian isyarat utama, khususnya laluan fosfatidilinositol 3-kinase/*protein kinase B* dan *mitogen-activated protein kinase*, yang menyokong modulasi peringkat sistem berkaitan tamoksifen. Kesimpulannya, tamoksifen menunjukkan kesan volumetrik yang menggalakkan, disokong oleh bukti radiologi, biokimia dan komputasional. Walaupun bersifat penerokaan, dapatan ini menghasilkan bukti yang koheren secara biologi dan menjana hipotesis bahawa tamoksifen mungkin memberikan kesan pengubahsuaian penyakit untuk sisa NF-PitNET, justeru menyokong keperluan kajian terkawal berskala lebih besar.

ABSTRACT

Post-operative residual non-functioning pituitary neuroendocrine tumours (NF-PitNETs) have limited medical treatment options to prevent tumour regrowth. This translational proof-of-concept study evaluated the therapeutic potential of tamoxifen in patients with residual NF-PitNETs using an integrated clinical, molecular, and computational framework. Immunohistochemical analysis quantified oestrogen [illegible] α) [illegible] archival tumour tissues. A 12-month randomised pilot trial enrolled adults with magnetic resonance imaging (MRI)-confirmed residual disease and allocated them in a 1:1 ratio to tamoxifen at 20–40 mg daily or active surveillance. Tumour volumes were assessed at baseline, six months, and twelve months using quantitative three-dimensional MRI segmentation. A panel of ten serum biomarkers spanning growth, angiogenic, inflammatory, and Wingless and Integrated-modulating pathways was measured longitudinally. In parallel, a network pharmacology workflow, pathway enrichment analysis, protein–protein interaction mapping, and hub gene ranking was applied to characterise tamoxifen-associated molecular targets and pathways. Ninety-six patients were screened, with twenty completing follow up; each group had [illegible] % [illegible] analyses did not show significant overall time or time-by-treatment effects, paired analysis within the tamoxifen group demonstrated a significant reduction in tumour volume from baseline to twelve months (p = 0.045). Tumour shrinkage occurred in 40% of tamoxifen-treated patients, with no cases of regrowth observed, whereas 20% of patients under active surveillance demonstrated tumour progression (p = 0.014). In multiple linear regression analysis, post-treatment Dickkopf-related protein 1 [illegible] − [illegible] 5 [illegible] p = 0.010). Multivariate modelling identified a dominant growth and angiogenic axis explaining the largest proportion of variance in volumetric response. Computational network analyses implicated key signalling networks, particularly the phosphatidylinositol 3-kinase/protein kinase B and mitogen-activated protein kinase pathways, supporting tamoxifen-associated systems-level modulation. In conclusion, tamoxifen was associated with favourable volumetric trends supported by radiological, biochemical, and computational evidence. While exploratory, these findings provide biologically coherent, hypothesis-generating evidence that tamoxifen may exert disease-modifying effects in selected patients with residual NF-PitNETs and justify larger controlled trials.

TABLE OF CONTENTS

LIST OF TABLES

LIST OF ILLUSTRATIONS

LIST OF ABBREVIATIONS

ACTH	Adrenocorticotropin hormone
AKT	Protein Kinase B
ANCOVA	Analysis of covariance
ANOVA	Analysis of variance
ARG2	Arginase-2
BCL2	B-Cell Lymphoma 2
B-raf	proto-oncogene serine/threonine-protein kinase
BRD4	Bromodomain-Containing Protein 4
CBG	Cabergoline
CD206	Mannose Receptor, C-Type 1 (M2 Macrophage Marker)
CD56	Neural Cell Adhesion Molecule (NK-Cell Marker)
CD8	Cluster of Differentiation 8 (Cytotoxic T Cell Marker)
CDKN2A	Cyclin-Dependent Kinase Inhibitor 2A
circRNA	Circular RNA
circVPS13C	Circular RNA Derived from VPS13C Gene
c-MYC	MYC Proto-Oncogene
CRH	Corticotrophin-releasing hormone
CS	□ □ □ □ □ □ □ ’ □□ □□ □ □ □ □ □ □ □
CTNNB1	Catenin Beta-1(β-Catenin)
CV	Coefficient of Variability
Cyclin D1	G1/S-Specific Cyclin-D1
DA	Dopamine agonist
DAVID	Database for Annotation, Visualization and Integrated Discovery

DDAVP	1-deamino-8-D-arginine vasopressin or desmopressin
DEX	Dexamethasone
DKK1	Dickkopf-related protein 1
DKK1post	Dickkopf-related protein 1 post tamoxifen
DKK1pre	Dickkopf-related protein 1 at baseline
DLK1	Delta-Like Non-Canonical Notch Ligand 1
DR	Dopamine receptor
E2F1	E2F Transcription Factor 1
ECM	Extracellular Matrix
EGFR	Epidermal Growth Factor Receptor
ELISA	Enzyme-linked immunosorbent Assay
EMT	Epithelial–Mesenchymal Transition
EphB6	Ephrin Type-B Receptor 6
ER	Oestrogen receptor
ERK	Extracellular signal-regulated kinase
ERK5	Extracellular signal regulated kinase 5
□ □ α	Oestrogen receptor alpha
ERβ	Oestrogen receptor beta
ESR1	Oestrogen receptor 1 gene
ESR2	Oestrogen receptor 2 gene
EZRIN	Cytoskeletal Linker Protein
FGF	Fibroblast Growth Factor
FGFpost	Fibroblast Growth Factor post tamoxifen
FGFpre	Fibroblast Growth Factor at baseline
FGFR4	Fibroblast Growth Factor Receptor 4
FIPA	Familial isolated pituitary adenoma

FOXP3	Forkhead Box P3 (Regulatory T Cell Marker)
FSH	Follicular stimulating hormone
□ □ □ □ □ 5 γ	Growth Arrest and DNA Damage-Inducible Gamma
GATA3	GATA-binding protein 3
GH	Growth hormone
GH3	Growth hormone-3
GnRH	Gonadotropin-releasing hormone
GO	Gene Ontology
GPCR	G-Protein–Coupled Receptor
□ α □	G-Protein Alpha-q Subunit
HCTM	Hospital Canselor Tuanku Muhriz
HGF	Hepatocyte Growth Factor
HGFpost	Hepatocyte Growth Factor post tamoxifen
HGFpre	Hepatocyte Growth Factor at baseline
Hippo Pathway	Developmental Pathway Regulating Proliferation and Organ Size
HKL	Hospital Kuala Lumpur
HLA-B	Human Leukocyte Antigen-B
HMG	High mobility group proteins
HMGA1	High Mobility Group AT-Hook 1
hpNF-PitNETs	High-proliferative nonfunctioning pituitary neuroedocrine tumors
HRP	Horseradish peroxidase
HTR2B	5-Hydroxytryptamine (Serotonin) Receptor 2B
IF	Immunofluorescence
IL-10	Interleukin-10

IL-6	Interleukin-6
IL-6R	Interleukin-6 Receptor
IRS	Immunoreactivity score
Jak	Janus kinase
JAK2	Janus Kinase 2
KEGG	Kyoto Encyclopaedia of Genes and Genomes
LAR	Long acting release
LH	Luteinizing hormone
lpNF-PitNETs	Low-proliferative non-functioning pituitary neuroedocrine tumors
MAPK	Mitogen-Activated Protein Kinase
MDM2	Murine Double Minute 2 Oncogene
MEG3	Maternally Expressed Gene 3
MEN1	Multiple endocrine neoplasia type 1
MEN4	Multiple endocrine neoplasia type 4
MET	Mesenchymal-epithelial transition factor
miRNA	Micro ribonucleic acid
MMP1	Matrix Metalloproteinase-1
MMP2	Matrix Metalloproteinase-2
MMP9	Matrix Metalloproteinase-9
MRI	Magnetic resonance imaging
mRNA	Messenger ribonucleic acid
mTOR	Mammalian target of rapamycin
NFPA	Non-functioning pituitary adenoma
NF-PitNET	Non-functioning pituitary neuroendocrine tumors
NF-κ □	Nuclear Factor Kappa-B

NOTCH3	Neurogenic Locus Notch Homolog 3
Nrf2	Nuclear factor erythroid 2-related factor 2
OCT	Optical coherence tomography
OD	Optical density
p16	Cyclin-Dependent Kinase Inhibitor 2A (INK4A)
$p18^{INK4C}$	Cyclin-Dependent Kinase Inhibitor 2C
P38-MAPK	p38-Mitogen activated protein kinases
PA	Pituitary adenoma
p-Akt	Phosphorylated protein kinase B
PAR-1	Protease-Activated Receptor 1
PCNA	Proliferating Cell Nuclear Antigen
PD-1	Programmed Cell Death Protein-1
PD-L1	Programmed Death-Ligand 1
PI3K	Phosphoinositide 3-Kinase
PI3K-PKB/Akt	Phosphoinositide-3-kinase-protein kinase B
PIK3CA	Phosphatidylinositol-4,5-Bisphosphate 3-Kinase Catalytic Subunit Alpha
PIT1	Pituitary-specific transcription factor 1
PitNET	Pituitary neuroendocrine tumor
PITX2	Paired-Like Homeodomain Transcription Factor 2
PKC-α	Protein kinase C alpha
□ □ □ γ	Protein Kinase C-Gamma
PLC	Phospholipase C
p-MEK	phosphorylated-mitogen-activated protein kinase kinase
POMC	Proopiomelanocortin
PPI	Protein-protein Interaction

PR	Progesterone receptor
PRL	Prolactin
PRRT	Peptide receptor radionuclide therapy
PT	Pituitary tumour
PTTG	Pituitary Tumour-transforming Gene
PVN	Paraventricular nucleus
Raf	proto-oncogene serine/threonine-protein kinase
RAPTOR	Regulatory-associated protein of mammalian target of rapamycin
Ras	Rat sarcoma genes
Rb	Retinoblastoma Protein
RICTOR	Rapamycin-insensitive companion of mammalian target of rapamycin
RM-GLM	Generalised Linear Model of Repeated Measures
ROS/RNS	Reactive oxygen/ nitrogen species
RT-dPCR	Reverse transcription digital polymerase chain reaction
RT-qPCR	Reverse transcription quantitative polymerase chain reaction
SCA	Stem Cell Antigen
SCF	Stem cell factor-c-kit
SDF-□ α	Stromal-Derived Factor 1 Alpha
SEMA3A	Semaphorin 3A
SF-1	Steroidogenic factor-1
sFRP1	Secreted Frizzled-Related Protein-1
sFRP1post	Secreted Frizzled-Related Protein-1 post tamoxifen
sFRP1pre	Secreted Frizzled-Related Protein-1 at baseline
sFRP2	Secreted Frizzled-Related Protein-2
sFRP4	Secreted Frizzled-Related Protein-4

SGA	Silent Gonadotroph Adenoma
SLA	Silent Lactotroph Adenoma
Smad	Mothers Against Decapentaplegic Homolog
Smad3	Mothers Against Decapentaplegic Homolog 3
SMILES	Simplified Molecular Input Line Entry System
SON	Supraoptic nucleus
SRL	Somatostatin receptor ligand
SSA	Silent Somatotroph Adenoma
SSA	Somatostatin analogue
SSTR	Somatostatin receptor
SSTR2	Somatostatin receptor type 2
STA	Silent Thyrotroph Adenoma
STAT	Signal Transducer and Activator of Transcription
STAT3	Signal Transducer and Activator of Transcription 3
T_0	Time-point at baseline
$T0VOL_2$	Tumour volume at baseline
T_1	Time-point at 6 months
$T1VOL_2$	Tumour volume at 6 months / interim
T_2	Time-point at 12 months
$T2VOL_2$	Tumour volume at 12 months / final
T3	Triiodothyronine
T4	Tetraiodothyronine or thyroxine
TAM	Tamoxifen
TGFSR	Tumor growth-free survival rate
TGF-α	Transforming Growth Factor-Alpha
TGF-α □ □ □ □	Transforming Growth Factor-Alpha post tamoxifen
TGF-α □ □ □	Transforming Growth Factor-Alpha at baseline

TGF-β	Transforming Growth Factor-Beta
TGF-β □ □ □	Transforming Growth Factor-Beta Receptor II
TLE2	Transducin-Like Enhancer of Split 2
TMZ	Temozolamide
TNBC	Triple-negative breast cancer
TNF-α	Tumour Necrosis Factor-Alpha
TPIT	T-box transcription factor
TSH	Thyroid-stimulating hormone
TVDT	Tumor volume doubling time
TX	Triphenylethylene tamoxifen
UKM	Universiti Kebangsaan Malaysia
VEGF	Vascular Endothelial Growth Factor
VEGFR	Vascular Endothelial Growth Factor Receptor
VEGFA	Vascular Endothelial Growth Factor A
VEGFpost	Vascular Endothelial Growth Factor post tamoxifen
VEGFpre	Vascular Endothelial Growth Factor at baseline
WB	Western blot
WHO	World Health Organization
WIF1	Wnt Inhibitory Factor 1
Wnt	Wingless-related integration site

CHAPTER I

INTRODUCTION

1.1 INTRODUCTION

In the rapidly advancing field of neuroendocrinology, pituitary neuroendocrine tumours (PitNETs) present a distinct clinical challenge owing to their heterogeneous biological behaviour, variable hormonal activity, and inconsistent treatment outcomes. Among these, non-functioning pituitary neuroendocrine tumours (NF-PitNETs) are particularly challenging. These tumours lack overt hormone hypersecretion and are often clinically silent until they cause compressive symptoms such as headaches, hypopituitarism, or visual disturbances. Their silent progression, frequent invasiveness, and the absence of validated medical therapies highlight the urgent need for novel diagnostic and therapeutic approaches.

This study addresses two interrelated aspects of NF-PitNET biology: (i) the expression patterns □ □ □□ □ □ □ □ □ □ □ □ □□ □ □ □ □ □ □ □ □□ □ □ □ □ □ □ □ □ □□ □ identification of putative protein profiles associated with tamoxifen therapy in residual tumours. By integrating clinical, molecular, and proteomic approaches, the research aims to advance current understanding of NF-PitNET pathophysiology and to elucidate the potential role of anti-oestrogen strategies in the management of these tumours.

1.2 BACKGROUND OF THE STUDY

Pituitary adenomas, now classified as PitNETs under the 2022 World Health Organization (WHO) framework (Asa et al., 2017), are among the most common intracranial neoplasms, accounting for approximately 15% of primary central nervous system tumours (Ostrom et al., 2022). Within this group, non-functioning PitNETs (NF-

PitNETs) constitute a substantial and clinically important subset, representing approximately 14–54% of pituitary adenomas across surgical and epidemiological series (Fernandez et al., 2010; Raappana et al., 2010; Ntali & Wass, 2018). The increasing availability of high-resolution neuroimaging has further increased their detection, with NF-PitNETs now comprising a large proportion of incidentally discovered and surgically treated pituitary tumours (Hefner & Cooper, 2025). Unlike functioning tumours, NF-PitNETs do not produce clinically overt hormone excess and are therefore typically diagnosed at a later stage, most often when they have progressed to macroadenomas causing symptoms of mass effect such as visual impairment and hypopituitarism (Chanson et al., 2018; Ntali & Wass, 2018). Consistent with this delayed presentation, surgical series report that NF-PitNETs account for up to half of all resected pituitary tumours, underscoring their substantial clinical burden.

1.2.1 Oestrogen Receptor Expression in NF-PitNETs

Oestrogen receptors (ERs) have emerged as important regulators of tumour growth, differentiation, and treatment response in several endocrine-related neoplasms. The two [illegible] α [illegible] β [illegible] -activated nuclear transcription factors and exert broad effects on cellular proliferation, differentiation, and apoptosis (Hannen et al., 2019). Both receptors are expressed in normal human pituitary tissue (Shupnik et al., 1998), and earlier studies have reported higher ER expression in NF-PitNETs compared with functioning tumours, particularly in younger patients (Nishioka et al., 2011). In breast cance[illegible] α [illegible] β [illegible] -proliferative role (Treeck et al., 2008). These observations suggest that differential ER expression may influence both tumour biology and therapeutic susceptibility in NF-PitNETs.

At the molecular level, ER signalling intersects with key oncogenic pathways, including MAPK and PI3K/AKT, which are frequently dysregulated in pituitary [illegible] 2 [illegible] 2 [illegible])e proliferation [illegible] α [illegible] and invasion through downstream effectors such as Slug, a transcriptional repressor of E- [illegible] β [illegible] -tumorigenic effects (Zhou et al., 2011). Proteomic studies have further linked ER-related signalling networks to mitochondrial

dysfunction, oxidative stress, and cell cycle dysregulation in pituitary tumours, reinforcing the concept that ERs participate in broader, pathway-level control of tumour behaviour rather than acting in isolation (Wu et al., 2024).

1.2.2 Medical Therapy in NF-PitNETs and Rationale for Tamoxifen

Despite advances in endoscopic transsphenoidal surgery and improvements in perioperative care, residual tumour following surgery remains common, particularly in cases with suprasellar or parasellar extension (Lu et al., 2022). Recurrence or regrowth rates of residual NF-PitNETs have been reported to reach 40–50% in long-term follow-up (Chen et al., 2012; Ratnasingam et al., 2017). Although adjuvant radiotherapy is effective in achieving tumour control, its use is limited by well-recognised long-term complications, including hypopituitarism, neurocognitive impairment, and increased cerebrovascular risk (Ayuk & Stewart, 2009; Minniti et al., 2016). Consequently, management of residual NF-PitNETs continues to rely heavily on surveillance and local therapies, with a clear unmet need for safe, effective, and biologically targeted medical treatments.

In contrast to other pituitary tumour subtypes, NF-PitNETs currently lack approved medical therapy. Trials of dopamine agonists and somatostatin analogues have produced inconsistent and largely disappointing results (Pivonello et al., 2015). More aggressive or experimental approaches, including temozolomide, peptide receptor radionuclide therapy (PRRT), gonadotropin-releasing hormone (GnRH) analogues, and PI3K/mTOR inhibitors, have been explored in selected cases, but their use remains limited to small, heterogeneous cohorts and refractory disease (Hefner & Cooper, 2025). A major obstacle to therapeutic progress is the absence of validated biomarkers to guide patient stratification, predict tumour behaviour, or inform treatment selection. NF-PitNETs are histologically benign but biologically heterogeneous, with some tumours remaining indolent while others exhibit invasive growth, early recurrence, and resistance to conventional therapy (Raverot et al., 2018).

These considerations provide a strong rationale for exploring alternative pharmacological strategies. Drug repurposing has emerged as an attractive and

pragmatic approach, particularly in rare or heterogeneous tumours where conventional drug development is constrained (Pushpakom et al., 2019). Computational approaches, including pathway enrichment analysis and protein–protein interaction network modelling, further support the systematic identification of candidate drugs and mechanistic targets (Corsello et al., 2017). Within this framework, tamoxifen, a selective oestrogen receptor modulator (SERM) widely used in breast cancer, represents a compelling candidate for repurposing in NF-PitNETs.

Tamoxifen acts by competitively binding to oestrogen receptors and modulating downstream transcriptional and non-genomic signalling pathways. Preclinical studies have shown that tamoxifen can induce apoptosis in pituitary tumour cells and alter tumour-associated protein expression profiles (Newton, 1995; Hannen et al., 2019; Lv et al., 2022). Clinically, tamoxifen has been shown to reduce insulin-like growth factor I (IGF-I) levels in acromegalic patients resistant to conventional therapies, and to inhibit tumour growth in experimental models (Stone et al., 2014; Voltan et al., 2023). Other antioestrogenic agents, including fulvestrant and newer selective oestrogen receptor degraders such as AZD9496, have also demonstrated antiproliferative and pro-apoptotic effects in pituitary tumour models (Hannen et al., 2019). Collectively, these findings support the concept that antioestrogen therapy, and tamoxifen in particular, may be repurposed as a rational adjuvant treatment for residual NF-PitNETs, which remain a frequent and clinically challenging cause of postoperative recurrence (Brochier et al., 2010).

1.2.3 Biomarkers and the Author-Defined Four-Domain Framework

Parallel advances in imaging and proteomic technologies have created new opportunities to integrate clinical and molecular data in the assessment of treatment response. MRI-based volumetric analysis provides an objective and reproducible method for quantifying tumour burden and longitudinal changes following therapy (Hussein et al., 2023; Zheng et al., 2024). At the molecular level, proteomic profiling has revealed the complex signalling networks underlying pituitary tumour behaviour, including pathways related to proliferation, inflammation, angiogenesis, and cellular stress responses (Zhan et al., 2016; Wen et al., 2022). However, translating these high-

dimensional molecular data into clinically interpretable and actionable biomarkers remains challenging.

To address this limitation, the present study adopts an author-defined four-domain analytical framework to guide biomarker selection, analysis, and interpretation. This framework conceptualises NF-PitNET pathophysiology and treatment response across four interconnected biological domains: (i) growth and angiogenic signalling, (ii) inflammatory signalling, (iii) cytokine–TNF signalling, and (iv) Wnt modulatory signalling. The framework was developed using a biologically informed, hypothesis-driven approach based on recurring molecular themes identified across published genomic, transcriptomic, proteomic, and translational studies of NF-PitNETs and related pituitary tumours (Zhan et al., 2016; Wen et al., 2022). Growth and angiogenic pathways were included because of their established roles in tumour proliferation, vascular remodelling, and progression, whereas inflammatory and cytokine–TNF pathways were selected because of increasing evidence implicating tumour–microenvironment interactions in pituitary tumour behaviour. Wnt modulatory pathways were incorporated because of emerging data linking aberrant Wnt signalling to pituitary tumour growth, differentiation, and treatment responsiveness. Collectively, these domains were selected a priori to provide a biologically coherent framework capable of integrating heterogeneous molecular signals into a clinically meaningful translational model.

Importantly, this framework was not intended as a definitive biological classification system, but rather as a pragmatic analytical scaffold for investigating pathway-level responses to tamoxifen therapy. Unlike purely data-driven approaches, biomarkers were grouped according to their predominant biological functions before statistical modelling. This strategy was chosen to facilitate mechanistic interpretation and translational relevance within a proof-of-concept study involving a limited sample size. Subsequent multivariate analyses, including exploratory factor analysis, confirmatory factor analysis, and structural modelling, were incorporated to evaluate whether the proposed biological domains had empirical support within the study dataset.

Within this framework, longitudinal serum biomarker profiling was used to capture dynamic biological responses associated with tamoxifen therapy, while tumour oestrogen receptor expression provided a tissue-level anchor for mechanistic interpretation. MRI-based volumetry supplied objective clinical endpoints, and computational bioinformatics and network-based analyses contextualised molecular findings within broader signalling pathways. Despite advances in imaging and molecular profiling, the clinical management of residual NF-PitNETs remains largely empirical, with no validated biomarkers available to guide postoperative risk stratification or targeted medical therapy. In particular, the role of oestrogen receptor signalling as both a therapeutic target and a biomarker axis in residual disease remains insufficiently defined.

This study was therefore designed to address these gaps through a comprehensive, multimodal, and translational research strategy. Rather than focusing on a single dimension of NF-PitNET biology or treatment, this work integrates tumour tissue characterisation through oestrogen receptor profiling, objective assessment of therapeutic response using longitudinal MRI-based volumetry, systematic longitudinal serum biomarker profiling structured around the four-domain framework, and computational analyses to identify tamoxifen-associated genes, pathways, and biological networks. Importantly, the computational component serves as a mechanistic bridge linking tissue receptor biology, circulating biomarker responses, and tumour volumetric outcomes. By integrating clinical outcomes, imaging metrics, tissue-level receptor biology, circulating molecular signals, and in silico pathway interrogation within a unified study design, this thesis provides a comprehensive evaluation of tamoxifen as a therapeutic strategy in residual NF-PitNETs and establishes a translational framework for future biomarker-guided and mechanism-based precision medicine approaches in this challenging tumour subtype.

1.3 PROBLEM STATEMENT

Although histologically benign, NF-PitNETs frequently exhibit clinically aggressive behaviour, including local invasiveness, postoperative persistence, recurrence, and resistance to standard management strategies. Transsphenoidal surgery remains the

cornerstone of treatment; however, complete resection is often precluded by tumour invasiveness and complex parasellar or suprasellar anatomy, resulting in a substantial proportion of patients with residual disease. Tumour regrowth has been reported in up to 40–50% of cases. Although radiotherapy can reduce the risk of progression, its use is limited by significant long-term complications, including hypopituitarism and increased cerebrovascular morbidity. Critically, NF-PitNETs remain the only pituitary tumour subtype without an approved and effective medical therapy, highlighting a major unmet clinical need.

At the biological level, emerging evidence suggests that oestrogen receptor signalling plays an important role in NF-PitNET pathophysiology, particularly through □□□□□□□□□□□□□□□□□□□□□□□□□□□α□□□□□□β□□□□□□□ invasiveness, and cellular behaviour. However, the clinical relevance of tumour oestrogen receptor expression in NF-PitNETs remains insufficiently characterised, and there is currently no robust framework for incorporating ER profiling into postoperative risk stratification or therapeutic decision-making. This represents a critical gap in understanding the molecular determinants of tumour behaviour in this disease.

From a therapeutic perspective, selective oestrogen receptor modulators (SERMs), particularly tamoxifen, have demonstrated antiproliferative and pro-apoptotic effects in preclinical pituitary tumour models, suggesting a plausible role as a repurposed medical therapy for residual NF-PitNETs. Nevertheless, to date, no prospective human studies have systematically evaluated the clinical impact of tamoxifen in NF-PitNETs using objective, quantitative measures of tumour response. In particular, tumour behaviour has not been rigorously assessed using MRI-based volumetric analysis, and the potential modifying effect of tumour oestrogen receptor status on treatment response remains undefined.

At the translational level, NF-PitNETs also lack reliable biochemical or molecular biomarkers of disease activity and treatment response, in contrast to functioning pituitary tumours. This limitation complicates postoperative surveillance, hinders patient stratification, and constrains the development of personalised therapeutic strategies. Moreover, although advances in proteomics and bioinformatics

have revealed complex signalling networks in pituitary tumours, these data have not yet been systematically integrated with imaging outcomes, tissue receptor biology, and longitudinal serum biomarker changes in the context of antioestrogen therapy.

Accordingly, residual NF-PitNETs continue to represent a significant unresolved clinical and scientific challenge. There is a clear need for a comprehensive, integrative approach that combines tumour oestrogen receptor profiling, quantitative MRI-based volumetric assessment, longitudinal serum biomarker analysis, and computational pathway interrogation to evaluate tamoxifen-associated biological and clinical responses and to identify candidate biomarkers that may support mechanism-based, personalised management of this tumour subtype.

1.4 GENERAL OBJECTIVES

To evaluate the therapeutic potential of tamoxifen and identify associated molecular biomarkers in residual NF-PitNETs.

1.5 SPECIFIC OBJECTIVES

1. To determine the immunohistochemical expression patterns of oestrogen [illegible] α [illegible] β [illegible] -PitNET tissue samples.
2. To evaluate the clinical impact of tamoxifen on changes in residual NF-PitNET tumour volume over 12 months.
3. To investigate baseline and longitudinal changes in serum biomarker levels in tamoxifen-treated NF-PitNET patients.
4. To computationally predict and functionally annotate tamoxifen-interacting genes and signalling pathways in NF-PitNETs.

1.6 RESEARCH QUESTIONS

1. [illegible] -PitNET [illegible] α [illegible] tissues?

2. Does tamoxifen therapy result in measurable changes in residual NF-PitNET tumour volume over 12 months?
3. Which serum biomarkers show differential expression before and after tamoxifen treatment?
4. Which genes and signalling pathways are predicted to interact with tamoxifen and contribute to its therapeutic effect in NF-PitNETs?

1.7 RESEARCH HYPOTHESES

1. □ □ α □ □ □ □ β □ □ □ □ □ □ □ □ □ □ □ -PitNET tissue samples. □ □ □ □ □
2. Tamoxifen therapy is associated with measurable changes in residual NF-PitNET tumour volume over 12 months.
3. Tamoxifen treatment modulates specific serum biomarkers in NF-PitNETs.
4. Computational predictions reveal tamoxifen-interacting genes enriched in key tumour-related signalling pathways in NF-PitNETs.

1.8 STUDY JUSTIFICATION

NF-PitNETs are among the most common intracranial tumours and frequently present as macroadenomas due to the absence of clinically overt hormonal hypersecretion. Although transsphenoidal surgery remains the cornerstone of treatment, complete resection is often limited by tumour invasiveness and extension into parasellar or suprasellar structures, resulting in residual disease and reported recurrence or regrowth rates of up to approximately 49%. While radiotherapy may reduce the risk of tumour progression, its use is constrained by recognised long-term complications, including hypopituitarism and cerebrovascular morbidity. Notably, NF-PitNETs remain the only major pituitary tumour subtype without an approved medical therapy, highlighting a substantial unmet clinical need.

From a biological perspective, accumulating evidence suggests that oestrogen receptor signalling contributes to NF-PitNET pathophysiology. The two principal □ α □ □ □ □ □ β □ □ □ □ □ □ □ □ □ □ □ □ □ □

generally [illegible] linked to anti-proliferative and tumour-suppressive functions. Despite these observations, the clinical significance of differential oestrogen receptor expression in NF-PitNETs r[illegible] expression in tumour tissues is therefore necessary to establish a biological foundation for understanding tumour behaviour and exploring potential oestrogen receptor-targeted therapeutic strategies. Accordingly, this study is justified in undertaking detailed [illegible]-PitNET [illegible] tissues as a fundamental first step.

From a therapeutic perspective, tamoxifen, a selective oestrogen receptor modulator (SERM) with a well-established safety profile in other malignancies, is a biologically plausible candidate for therapeutic repurposing in NF-PitNETs. Preclinical studies have shown that tamoxifen can inhibit pituitary tumour growth and modulate tumour-associated protein expression; however, its therapeutic role in NF-PitNETs has not been systematically or prospectively evaluated in humans. Therefore, objective clinical evidence is needed to determine whether tamoxifen may influence tumour growth behaviour in patients with residual disease. This study is justified in evaluating the clinical impact of tamoxifen through a 12-month pilot randomised controlled trial using three-dimensional MRI-based tumour volumetry, which provides an objective and quantitative assessment of tumour response over time.

From a translational and biomarker discovery perspective, NF-PitNETs lack validated biochemical or molecular markers of disease activity and treatment response, unlike functioning pituitary tumours. This limitation hinders postoperative surveillance, patient stratification, and the development of personalised treatment approaches. To address this gap, the present study adopts an author-defined four-domain analytical framework encompassing growth and angiogenic signalling, inflammatory signalling, cytokine–TNF signalling, and Wnt modulatory signalling. Although this framework is not derived from existing clinical classifications, it was developed using a biologically informed, hypothesis-driven approach based on recurring molecular themes reported in the NF-PitNET and pituitary tumour literature. The framework serves as a pragmatic analytical scaffold for organising biomarker selection, interpretation, and integration.

Guided by this framework, the study incorporates longitudinal serum biomarker profiling, including markers of growth and angiogenesis (VEGF, HGF, TGF-α □ □ □ □) □ □ inflammation (IL-6, CD40 Ligand, FGF-basic), cytokine–TNF signalling (TNF-α) □ □ □ □ □ Wnt modulation (DKK1, sFRP1), and relates temporal biomarker changes to treatment allocation and MRI-derived volumetric outcomes.

From an integrative systems biology perspective, computational and bioinformatics analyses are used to contextualise clinical, imaging, tissue, and circulating biomarker findings within broader drug–target–pathway networks. Rather than functioning as an isolated exploratory component, the computational analyses provide mechanistic context for the clinical and molecular findings generated in this study. By identifying tamoxifen-associated genes, molecular targets, and signalling pathways, the in silico analyses facilitate interpretation of tumour receptor expression, serum biomarker responses, and tumour volumetric outcomes within biologically relevant networks. This integrative approach strengthens the translational coherence of the study and supports hypothesis generation regarding potential mechanisms through which tamoxifen may influence residual NF-PitNET behaviour.

In summary, this study is justified by its comprehensive and translational design, which directly addresses important biological, therapeutic, and biomarker-related gaps in the management of residual NF-PitNETs. By integrating tumour receptor profiling, quantitative imaging, longitudinal biomarker assessment, and computational pathway analyses, the study aims to advance understanding of NF-PitNET biology, provide prospective clinical evidence regarding tamoxifen-associated tumour responses, and identify candidate molecular biomarkers that may inform future precision medicine strategies and larger clinical trials in patients with residual NF-PitNETs.

1.9 CONCEPTUAL FRAMEWORK

This study is guided by an integrative conceptual framework that links oestrogen receptor (ER) signalling, tamoxifen intervention, and tumour growth behaviour in NF-PitNETs. In the absence of an established medical therapy for residual NF-PitNETs, the

framework provides a translational model connecting tumour receptor biology, pathway-level molecular regulation, and clinically relevant imaging outcomes.

[illegible] as an important biological characteristic of NF-PitNETs. Tamoxifen, a selective oestrogen receptor modulator capable of crossing the blood–brain barrier, is hypothesised to exert both ER-dependent and ER-independent effects on tumour-associated signalling networks. Central to the framework are four key signalling hubs: [illegible]-catenin. These hubs function β as biologically plausible convergence points linking receptor activity and extracellular signals to downstream cellular processes, including proliferation, survival, angiogenesis, differentiation, and tumour progression. Their inclusion is supported by existing literature and computational network analyses demonstrating their relevance in tumour biology.

To capture the complexity of tumour regulation, four biologically defined signalling domains are incorporated within the framework: the Growth–Angiogenic Domain (HGF, TGF-α [illegible]) [illegible]-6, FGF, CD40), [illegible] the Cytokine–TNF Domain (TNF-α) [illegible] DKK1). These domains represent distinct yet interconnected biological processes that may influence tumour behaviour through shared downstream signalling pathways. Although presented separately for conceptual clarity, substantial crosstalk exists between these domains, and their collective interactions are likely to contribute to overall tumour growth dynamics and treatment responsiveness.

Within this framework, tamoxifen is conceptualised as a system-level modulator that may influence multiple interconnected pathways rather than acting through a single molecular target. The downstream clinical manifestation of these biological effects is reflected in changes in tumour volume, assessed using longitudinal MRI-based volumetry and categorised as tumour shrinkage, stabilisation, or regrowth. Importantly, this framework is intended as a hypothesis-generating model rather than a definitive causal representation of NF-PitNET biology. Serum biomarkers are regarded as

surrogate indicators of pathway activity, while the signalling hubs represent conceptual integration points rather than directly measured biological entities.

The framework was also designed to allow iterative evaluation and refinement through subsequent multivariate analyses. Although the biological domains were defined a priori based on biological plausibility and translational relevance, exploratory factor analysis, confirmatory factor analysis, and structural modelling were incorporated to determine whether the proposed organisation demonstrated statistical and biological coherence within the study cohort. Overall, the framework provides a coherent rationale for integrating tumour receptor profiling, longitudinal biomarker assessment, computational pathway analyses, and imaging outcomes to characterise tamoxifen-associated biological responses in residual NF-PitNETs.

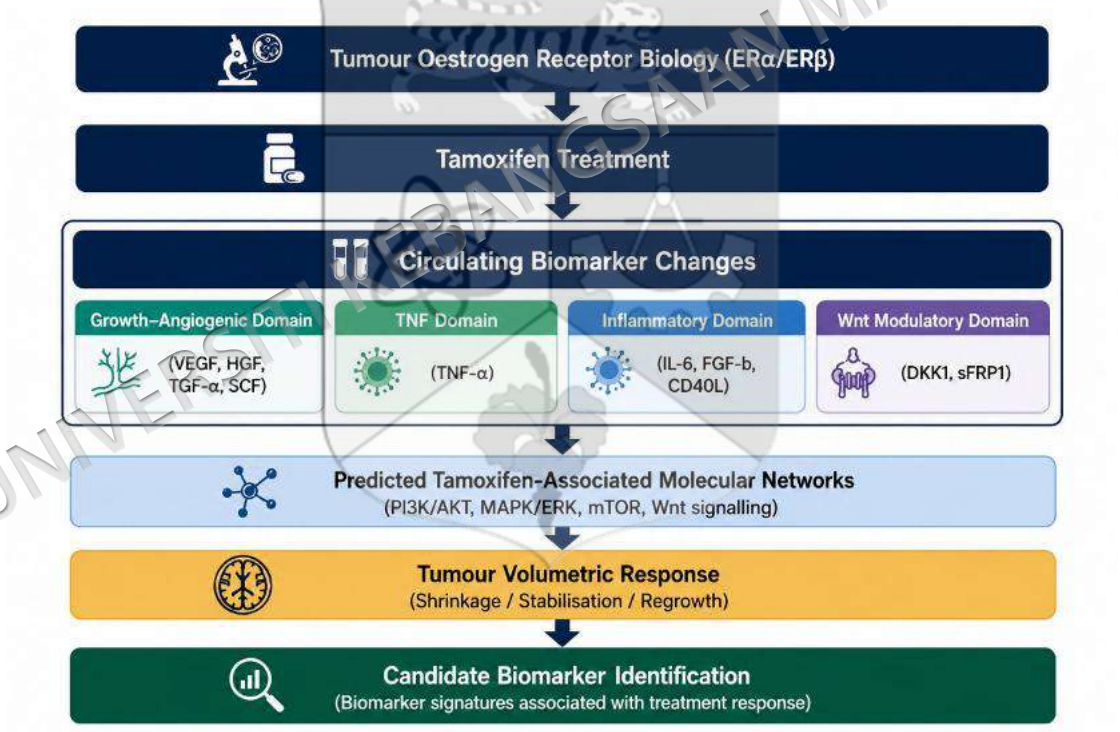

Figure 1.1 Conceptual Framework

1.10 SUMMARY

This chapter established the clinical and scientific context for the present study on residual NF-PitNETs. Although histologically benign, these tumours frequently exhibit

invasive behaviour, incomplete surgical resection, and a high risk of postoperative regrowth. They remain the only pituitary tumour subtype without an approved medical therapy, highlighting a clear unmet clinical need. The chapter outlined the role of oestrogen receptor (ER) signalling in NF-PitNET biology, emphasising the distinct functi[illegible] α [illegible] β [illegible] for tumour receptor profiling. Tamoxifen was introduced as a plausible therapeutic candidate based on its established safety profile and preclinical evidence in pituitary tumour models, with MRI-based tumour volumetry identified as the objective method to assess clinical impact. The importance of biomarkers in monitoring tumour behaviour and treatment response was also introduced, using an author-defined four-domain framework for longitudinal serum profiling, complemented by computational analyses to contextualise molecular and clinical findings. Together, these elements defined the conceptual and methodological foundation of the thesis and set the direction for the subsequent chapters.

CHAPTER II

LITERATURE REVIEW

2.1 OVERVIEW

This chapter provides a comprehensive review of the biological, clinical, and therapeutic foundations relevant to NF-PitNETs and establishes the rationale for the present study. It begins with an overview of the anatomy and physiology of the pituitary gland, including its structural organisation, hormonal functions, and regulation within the hypothalamic–pituitary axis, to provide essential context for pituitary tumour biology.

The chapter then reviews pituitary tumours and their contemporary classification, with particular emphasis on the distinction between functioning and non-functioning tumours, recent updates in the World Health Organization (WHO) classification, and emerging prognostic frameworks. This is followed by a focused discussion on NF-PitNETs, covering their background, epidemiology, natural history, clinical manifestations, subtypes, pathological frameworks, and current concepts in their pathophysiology.

Subsequent sections examine key molecular and cellular pathways implicated in NF-PitNET biology, including growth and angiogenic signalling, inflammatory pathways, the cytokine–TNF–immune checkpoint axis, and Wnt signalling and its modulators. The role of oestrogen receptor signalling in pituitary tumours and NF-PitNETs is then reviewed to provide the biological basis for anti-oestrogen strategies.

The chapter further outlines current treatment modalities for NF-PitNETs, including multidisciplinary and personalised care approaches, surgery, radiotherapy, peptide receptor radionuclide therapy, and emerging medical therapies. This is followed

by a review of selective oestrogen receptor modulators and anti-oestrogen therapies, with an integrative rationale for the potential role of tamoxifen in NF-PitNETs.

Finally, the chapter reviews proposed biomarkers of NF-PitNETs across key biological domains – growth and angiogenic pathways, inflammation, cytokine and TNF signalling, and Wnt-modulating networks – and concludes with a critical appraisal of relevant methodologies and limitations. Collectively, this chapter establishes the conceptual and evidence-based framework that informs the design, objectives, and interpretation of the present study.

2.2 THE ANATOMY AND PHYSIOLOGY OF THE PITUITARY GLAND

[illegible] “ [illegible] interface between the central nervous system and peripheral endocrine organs, coordinating hormonal regulation across multiple body systems (Perez-Castro et al. 2012; Scully & Rosenfeld 2002). Situated within the sella turcica of the sphenoid bone, the gland consists of two structurally and functionally distinct lobes - the anterior pituitary (adenohypophysis) and the posterior pituitary (neurohypophysis) - connected by the pars intermedia and linked to the hypothalamus via the pituitary stalk (Figures 2.1 and 2.2). This arrangement forms the hypothalamic-pituitary neuroendocrine axis, which underpins its central role in physiology and clinical medicine (Hong et al. 2016; Scully & Rosenfeld 2002).

2.2.1 Structural Organisation

The pituitary gland measures approximately 3–9 mm vertically and is encased in dura mater, with the diaphragma sellae forming its superior covering (Chin et al. 2012). Superiorly, the optic chiasm lies 5–10 mm above the gland, while laterally the cavernous sinuses contain cranial nerves III, IV, and VI, as well as branches V1 and V2 of the trigeminal nerve (Chin et al. 2012; Hong et al. 2016). This close anatomical relationship explains why expanding pituitary masses can cause visual field deficits such as bitemporal hemianopia, or cranial nerve palsies presenting as diplopia, ptosis, or facial pain, which occur in 5–17% of pituitary tumour cases (Kim et al. 2007).

The anterior pituitary comprises two-[illegible] specialised hormone-secreting cells arranged in cords and clusters interspersed with sinusoids. The anterior pituitary releases stimulating hormones for the respective glands [illegible] The development and differentiation of the various cell types are primarily initiated by the ventral diencephalon (Scully & Rosenfeld 2002). The anterior lobe of the pituitary gland is divided into three anatomical sections: pars tuberalis, pars intermedia, and pars distalis. The pars distalis is the largest part of the adenohypophysis, accounting for about 80% of its volume (Perez-Castro et al. 2012). Its vascular supply derives from the superior hypophyseal arteries, which establish the hypophysial portal system, allowing efficient delivery of hypothalamic releasing and inhibiting hormones (Cironi et al. 2020; Melmed et al. 2022) (Figure 2.3).

In contrast, the posterior pituitary consists primarily of axonal terminals from hypothalamic neurons and serves as a storage and release site for vasopressin and [illegible] pouch-derived anterior lobe and the neural ectoderm-derived posterior lobe underlies their functional differences (Dubois & ElAmraoui 1995).

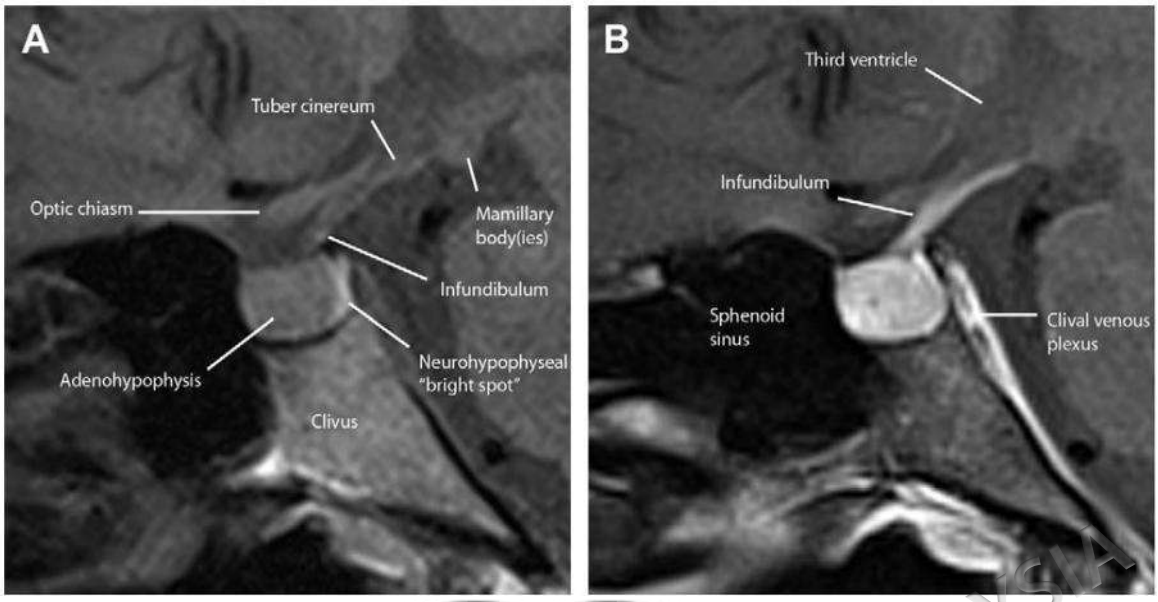

Figure 2.1 Anatomy of pituitary gland

A. Sagittal pre-contrast, fat-saturated T1WI image through the midline sella turcica shows the normal T1 shortening in the neurohypophysis.

B. Post-contrast T1WI image shows the normal enhancement of the pituitary gland, infundibulum, and tuber cinereum region caused by the lack of a blood-brain barrier.

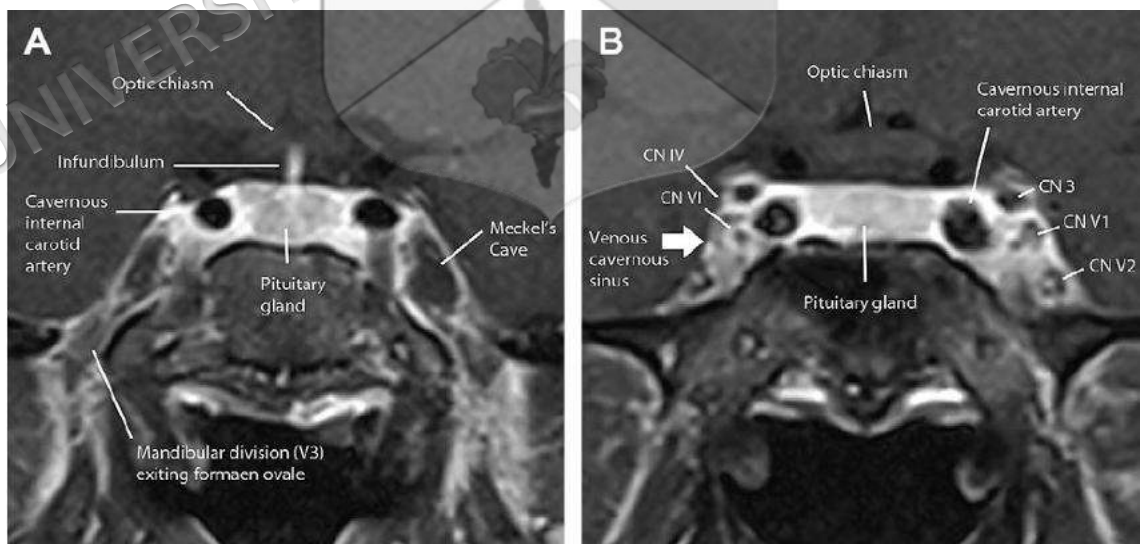

Figure 2.2 Anatomy of pituitary gland

A., B. Coronal post-contrast, fat-saturated T1WI images through the sella turcica show the gland relative to the parasellar cavernous sinuses and suprasellar optic chiasm. The pituitary gland enhances less strongly than the cavernous sinus venous blood.

Figure 2.1 & 2.2 adapted from Chin, B. M., Orlandi, R. R., & Wiggins, R. H., 3rd (2012).

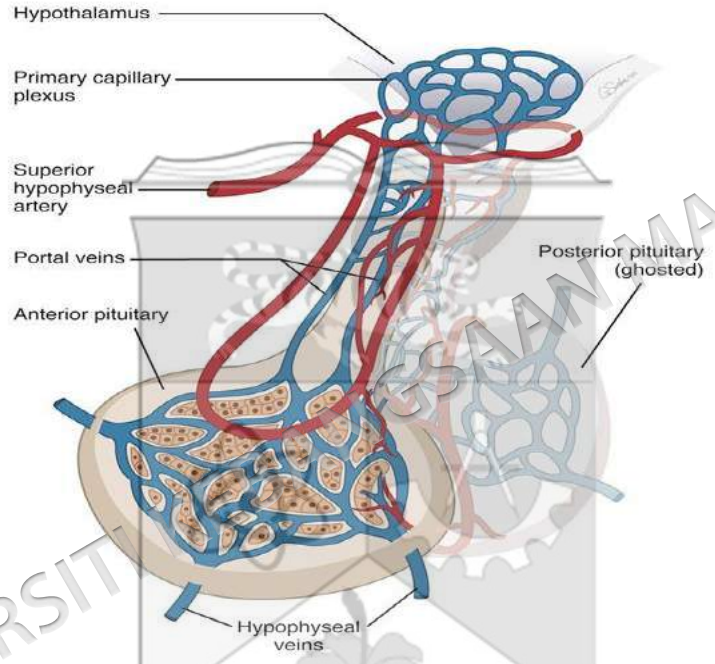

Figure 2.3 Hypothalamic-pituitary vascular and functional relationships (Adapted from(Melmed et al. 2022)

2.2.2 Hormonal Functions

The adenohypophysis consists primarily of five hormone-producing cell types: thyrotropes, lactotropes, corticotropes, somatotropes, and gonadotropes, which respectively secrete thyrotropin, prolactin, ACTH, growth hormone, and gonadotrophins (FSH and LH) (Figure 2.4). These cells produce hormones that regulate thyroid function, lactation, adrenal function, growth, and reproduction. Somatotropes are the major cell type of the anterior pituitary, constituting approximately 50% of the cell population, followed by lactotropes (10–25%), corticotropes (10–20%), thyrotropes

(10%), and gonadotropes (10%) (Yeung et al. 2006). The release of the corresponding hormones by these cells is regulated by hypothalamic hormones, which are supplied via the portal circulatory system. Increasing evidence suggests that these cells play an important role in regulating the function, intercellular communication, and immunoendocrine crosstalk of endocrine pituitary cells (Perez-Castro et al. 2012).

In addition, there is a sixth cell type in the anterior lobe: the non-endocrine, agranular, folliculostellate (FS) cells, which account for about 5–10% of total pituitary cells (Yeung et al. 2006). FS cells comprise about 5–10% of the cells in the anterior pituitary gland (Herkenham 2005). As a mediating cell type, FS cells appear to play an important role in the complex regulation of various endocrine functions of the pituitary gland. Gap junctions between FS cells enable synchronised excitability and long-distance communication throughout the pituitary gland by propagating Ca2+ currents between FS cells (Herkenham 2005). Several studies have also suggested that these cells are capable of trans-differentiation, raising the possibility that they represent a pituitary stem cell population. Furthermore, FS cells are the only cells in the healthy pituitary gland that produce VEGF, as well as other angiogenesis-related substances such as fibroblast growth factor, leukaemia inhibitory factor, and interleukin-6 (Rees et al. 2003). This indicates a key role for FS cells in the regulation of angiogenesis and vascular permeability within the pituitary gland. In addition, FS cells are able to

astrocytes (Ooi et al. 2004). Therefore, a relationship with microglia or astrocyte-like cells is commonly assumed.

Overall, the anterior pituitary is an organ with highly heterogeneous parenchyma, in which the interactions of different endocrine and non-endocrine cell types are regulated in a complex manner.

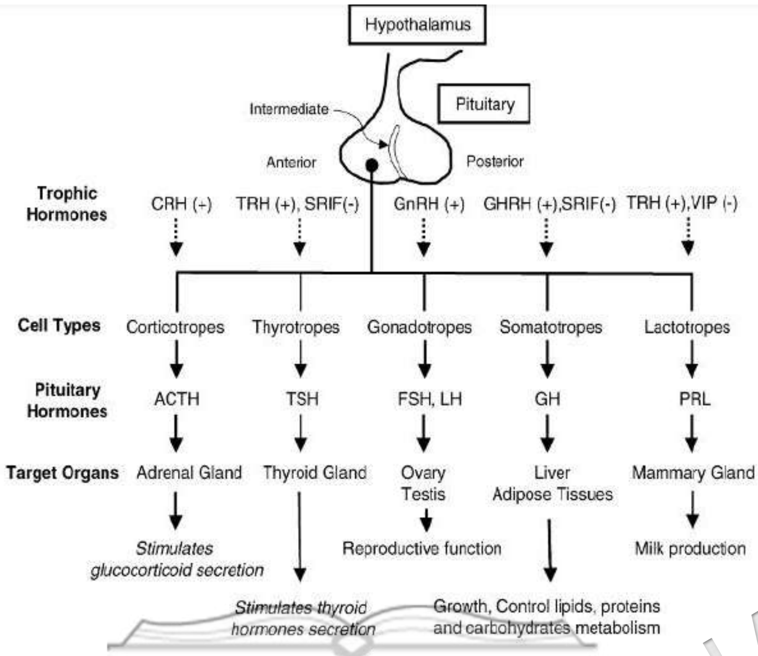

Figure 2.4 Trophic hormones, cell types of the anterior pituitary, and their hormonal secretions. Trophic hormones from the hypothalamus act on specific cell types in the pituitary, causing the release of pituitary hormones which act on target organs to regulate various [illegible] inhibition by the trophic hormones. CRH, corticotropin-releasing hormone; TRH, thyrotropin-releasing hormone; SRIF, somatostatin; GnRH, gonadotropin-releasing hormone; VIP, vasoactive intestinal peptide; GHRH, growth hormone-releasing hormone (Adapted from Ooi GT et al. 2004).

The detailed pathways of adenohypophyseal cytodifferentiation and the transcription factors involved in the development of each hormone-producing cell type are shown in Figure 2.5.

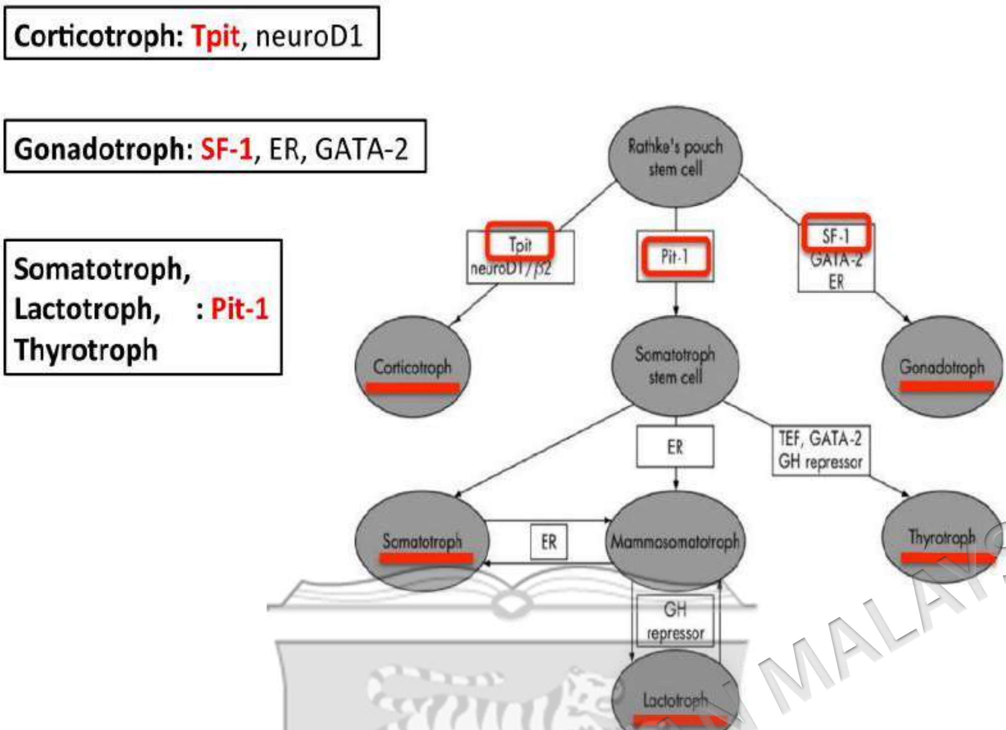

Figure 2.5 Adenohypophyseal lineage and transcription factors (Adapted from Nishioka & Inoshita, 2018)

□ embryogenesis are as follows (Nishioka & Inoshita 2018):

1. Corticotroph cells, determined by the T-box pituitary transcription factor (Tpit);
2. Somatotrophs, mammosomatotrophs, lactotrophs, and thyrotrophs, determined by the pituitary transcription factor (Pit-1);
3. Gonadotrophs, determined by steroidogenic factor-1 (SF-1) and/or GATA-2 in the presence of oe□ □ □ □ □ □ □ □ □ □ □ □ □ □ □ □ α □ □ □ α) □

2.2.3 The Neurohypophysis and the Hypothalamic-Pituitary Axis (HPA)

Although smaller than the anterior lobe, the neurohypophysis plays a central role in neuroendocrine communication. It arises embryologically from the anterior neural crest of the forebrain, differing from the ectodermal origin of the adenohypophysis (Scully & Rosenfeld 2002). Structurally, the neurohypophysis comprises the pars nervosa, the

median eminence of the hypothalamus, and the infundibular stem (Kim et al. 2007). Histologically, it consists mainly of axonal terminals of hypothalamic neurons located in the supraoptic (SON) and paraventricular nuclei (PVN), along with pituicytes and glial cells that modulate hormone secretion (Perez-Castro et al. 2012).

The posterior pituitary functions as a neurohaemal organ. Vasopressin and oxytocin, synthesised in the hypothalamic supraoptic and paraventricular nuclei, are transported along axons and released into the circulation in response to physiological stimuli such as plasma osmolality or uterine contractions (Hong et al. 2016). Vasopressin plays a critical role in water balance, while oxytocin regulates uterine reproductive functions.

2.3 PITUITARY TUMOURS AND CLASSIFICATION

2.3.1 Functioning versus Non-functioning Pituitary Tumours

Pituitary tumours (PTs) are heterogeneous central nervous system lesions that are usually benign and relatively common (Aflorei & Korbonits 2014). Population-level estimates suggest an overall prevalence of approximately 16.7% when both radiological and autopsy data are considered (Ezzat et al. 2004). Reported frequencies vary by method: cancer registries cite approximately 130–230 per 100,000 inhabitants, whereas population studies estimate around 190–280 per million (Daly et al. 2009). PTs are the second most common intracranial neoplasm after meningiomas and are detected in up to 40% of radiological series and approximately 35% of autopsies, highlighting the substantial reservoir of incidental disease (Ezzat et al. 2004). Age and sex patterns also differ. PTs are slightly more common in women and peak between ages 40 and 60 (Aflorei & Korbonits 2014).

Classically, pituitary tumours (PTs) are broadly divided into functioning and non-functioning entities based on hormonal activity (Drange et al. 2000). PTs come to clinical attention due to mass effects from impingement on local structures or manifestations of pituitary hormone excess or insufficiency. These tumours are classified according to their cell type of origin. Each cell type produces specific

hormone products under tightly regulated hypothalamic and peripheral control. The hormone-secreting cells may give rise to functional pituitary tumours that hypersecrete one or more hormones, including PRL, GH, ACTH, and, rarely, FSH, LH, or TSH (Drange et al. 2000). Pituitary tumours with no identifiable clinical hypersecretory syndrome are termed non-functioning pituitary adenomas (NFPA) because the majority of these tumours are, in fact, of gonadotroph cell origin and actually express, albeit inefficiently, FSH, LH, or their free subunits (Solarski et al. 2017). Non-functioning PTs are usually recognised later due to mass effects – headache, bitemporal hemianopsia from optic chiasm compression, and hypopituitarism from gland compromise – often with sizeable tumours at diagnosis and a higher likelihood of invasion, particularly into the cavernous sinus (Chanson & Brochier 2005; Ntali & Wass 2018). A rare form of presentation requiring special attention is pituitary apoplexy, characterised by sudden onset of headache, loss of vision, or hypopituitarism due to intra-tumoural haemorrhage or pituitary infarction (Möller-Goede et al. 2011). It occurs in 2–12% of patients with PTs. In a patient harbouring a PT, it most often occurs in the context of a clinically non-functioning macroadenoma (Möller-Goede et al. 2011). It can occur at any age, but is more frequent between the fifth and sixth decades and is slightly more common in males.

Epidemiology varies across cohorts. In most epidemiological studies, non-functioning PTs are the second most common type of adenoma after prolactinomas when both microadenomas and macroadenomas are considered, but they predominate among macroadenomas (Ntali & Wass 2018). In a population-based series of 471 patients, non-functioning PTs were the most common (43.0%), followed by prolactinomas (39.9%) (Agustsson et al. 2015). Other studies have also reported prolactinomas as the predominant type (Daly et al. 2006; Fernandez et al. 2010). The highest incidence of PTs occurs in the 40–60-year age group (Aflorei & Korbonits 2014). The incidence of PTs depends on tumour type, sex, and race. For example, prolactinomas tend to present earlier than non-functioning PTs, and the incidence of prolactinomas decreases with age (McDowell et al. 2011). Sex distribution also varies by subtype: females predominate in prolactinomas, ACTH-secreting, and TSH-secreting adenomas, whereas non-functioning PTs and GH-secreting tumours are relatively more common in males; with advancing age, the sex gap narrows for most

subtypes except non-functioning PTs (Agustsson et al. 2015; Daly et al. 2006; Mindermann & Wilson 1994).

With respect to local epidemiological data, only one study to date has examined the prevalence of pituitary adenomas in Malaysia. A retrospective study conducted at Kuala Lumpur Hospital between 2006 and 2015 (Yi et al. 2019) included 106 patients with pituitary adenoma who underwent transsphenoidal surgery. Of these, 67 (63.2%) were diagnosed with non-functioning pituitary adenoma, while 39 (36.8%) had functioning pituitary adenoma. In the non-functioning group, 58.2% (n = 39) were men and 41.8% (n = 28) were women, whereas the functioning group comprised 51.3% (n = 20) men and 48.7% (n = 19) women. Although males constituted majority in both groups, there was no statistically significant association between tumour functional status and gender ($p = 0.489$). In contrast, a significant difference in age distribution was observed between the two groups ($p < 0.05$). Approximately 26.9% (n = 18) of patients with non-functioning pituitary adenomas were 50–59 years, while 33.3% (n = 13) of patients with functioning pituitary adenomas were younger than 30 years.

Although most PTs are sporadic (~95%), up to 5% are syndromic or familial. MEN1 is the most frequent hereditary context, but other germline settings include Carney complex (PRKAR1A), familial isolated pituitary adenomas and isolated familial somatotropinoma (AIP), McCune–Albright syndrome (mosaic GNAS), MEN4 (CDKN1B), SDHx-related disease, and DICER1 syndrome (Alrezk et al. 2017; Beckers & Daly 2007; Pepe et al. 2019; Solari et al. 2019; Vasilev et al. 2011). A hereditary origin should be suspected in younger patients, those with multiple endocrine manifestations, or a positive family history (Alrezk et al. 2017; Solari et al. 2019).

The clinical spectrum ranges from asymptomatic incidentalomas to hormonally active or mass-effect–[illegible]) [illegible]“ [illegible] silent (no syndrome) yet biochemically detectable, or completely silent with neither clinical nor biochemical hypersecretion (Mayson & Snyder 2015). Aggressive PTs are defined by radiological invasion and abnormally rapid or clinically relevant growth despite optimal standard therapy (Raverot et al. 2018). Pituitary carcinomas, although

rare, are adenohypophyseal tumours with metastatic activity within or beyond the CNS (Lopes 2017).

Imaging patterns reflect tumour biology and timing of detection. Functioning adenomas tend to be smaller at presentation – often well-circumscribed and intrasellar – whereas non-functioning PTs more commonly exhibit suprasellar extension, optic apparatus compression, and cavernous sinus invasion (Qin et al. 2021).

Molecular mechanisms further stratify disease. Lineage-defining transcription factors (PIT-1, TPIT, SF-1) drive hormonal programmes and influence proliferation in functional adenomas, while in non-functioning pituitary tumours, these factors may indicate lineage without overt hypersecretion, with behaviour dominated by growth dynamics and local effects (Krzentowska et al. 2025b; Nasi-Kordhishti et al. 2025). These differences shape monitoring: functioning tumours are suited to biochemical surveillance and targeted medical therapy (e.g. dopamine agonists, somatostatin analogues), whereas non-functioning pituitary tumours rely on radiological follow-up and volumetry, with transsphenoidal surgery as first-line management and a lower likelihood of gross total resection due to size or invasion (Nishioka et al. 2015; Woo et al. 2024).

Therapeutic pathways therefore diverge. Functioning adenomas typically require multidisciplinary care integrating surgery with subtype-specific medical therapy and, when necessary, radiotherapy (Varlamov et al. 2019). Non-functioning pituitary tumours focus on alleviating mass effect and preserving pituitary function; recurrent or aggressive disease often necessitates vigilant imaging, consideration of re-operation, and adjuvant radiotherapy (Greenman & Stern 2009).

In summary, PTs represent a common and heterogenous group of lesions with epidemiology patterns influenced by ascertainment methods, age, sex, and tumour subtype. Functioning PTs typically present earlier due to overt endocrine syndromes and allow biochemical monitoring, whereas non-functioning PTs often present later with mass effects, are often larger and more invasive, and require imaging-led surveillance and tailored surgery. Familial syndromes account for a significant minority

of cases and should be recognised to facilitate genetic counselling and management. Ongoing advances in endoscopic surgical technique and molecular phenotyping continue to refine risk stratification and support more individualise care across the spectrum of PTs.

Table 2.1 Clinical presentation and hormonal evaluation for pituitary tumours

Pituitary Axis	Clinical Syndrome	Hormonal Evaluation
Lactotroph	Hyperprolactinemia ↓ gynecomastia, impotence, galactorrhea oligomenorrhea/amenorrhea, ↓	>250 µg/L: prolactinoma >500 µg/L: macroprolactinoma <100 µ dilute sample 1:100 PEG precipitation for macroprolactin in-asymptomatic cases
	Hypoprolactinemia -pregnant women: no symptoms breastfeed	hypoprolactinemia
Corticotroph	Syndrome (CS) bruising libido, menstrual irregularity	24H UFC (×2), late-night salivary cortisol (×2), overnight DST (1 mg), 2-day low-dose DST CRH 2 test, DEX-CRH, DDAVP, BPSS
	Secondary Adrenal Insufficiency (SAI) nausea, vomiting, diarrhea	- Basal ACTH: low/normal 8 AM cortisol: >18 µg/dL: excludes SAI <5 µg/dL: confirms SAI … 5–18 µg/dL: stimulation test (e.g., ITT or Synacthen test) required
Somatotroph	Acromegaly / Gigantism ↑ hypertension, etc.	Hyperproduction: - Serum IGF-1 (age- and sex-adjusted) - ↑ → 5 → non-suppression <1 ng/mL (or <0.4 ng/mL ultrasensitive) confirms acromegaly
	GH Deficiency ↑ dyslipidemia, osteopenia delay, hypoglycemia, micropenis	- ≥ - → - -1 + clinical signs + ↓ ≥ 2 diagnosis

…

Gonadotroph	Hyperproduction infertility, galactorrhea hypogonadism	- - ↓ - α- - ↑ - ↓
	Hypogonadism libido	- ↓ - ↓ - ↓
Thyrotroph	Secondary Hyperthyroidism intolerance	- ↑ - ↑ - α- To be … - No suppression with T3, no stimulation with TRH Dynamic test for the confirmatory diagnosis: no response to the T3 suppression test and TRH test
	Secondary Hypothyroidism constipation, dry skin	Hypoproduction Serum TSH: low or normal Serum FT4: low

24H UFC, 24-hour urinary free cortisol; DST, dexamethasone suppression test; DEX-CRH test, dexamethasone suppression corticotrophin releasing hormone test; DDAVP test, desmopressin test; BPSS, bilateral petrosal sinus sampling; ITT, insulin tolerance test; AGHD, adult GH deficiency; 75-g OGTT; 75- -GSU; alpha subunit of glycoprotein hormones (Adapted from Araujo-Castro et al. 2020)

2.3.2 WHO Classification Updates

The classification of pituitary tumours has undergone significant revisions over the past two decades, evolving from a purely histological framework to one that integrates immunohistochemistry (IHC) and transcription factors.

- 2004 WHO (ENDO3): Tumours were defined primarily by histology and hormone immunostaining. Categories included typical adenomas, atypical adenomas (characterised by a high mitotic index, Ki- ≥ % 5 positivity), and carcinomas. However, this approach lacked reproducibility and prognostic accuracy (Lenders et al. 2023).

- 2017 WHO (ENDO4): This revision introduced transcription factors – PIT-1, SF-1, and TPIT – as core markers for lineage assignment. This enabled the [illegible] to silent gonadotroph or corticotroph lineages (Inoshita & Nishioka 2018; [illegible]2[illegible]2[illegible]) [illegible] discontinued, as proliferation markers were considered unreliable in isolation.
- 2021 WHO CNS5: For the first time, pituitary tumours were included in the classification of central nervous system tumours. The nomenclature "[illegible]" [illegible] neuroendocrine nature and spectrum of biological behaviour (Lopes 2025).
- 2022 WHO ENDO5: The latest edition adopted PitNET as the standard term, aligning pituitary tumours with other neuroendocrine neoplasms. Tumours were grouped by transcription factor-defined lineages (PIT-1, SF-1, TPIT, and those without distinct lineage) and the benign ICD-O (/0) code was abandoned, replaced by a malignant (/3) designation. This change generated debate, as many PitNETs behave indolently despite being coded as malignant (Asa et al. 2022).

The 2022 WHO classification als[illegible]"[illegible]" [illegible] more aggressive behaviour and poorer disease-free survival compared to lineage-defined subtypes (Woo et al. 2024). This refinement improves diagnostic accuracy but presents challenges in clinical interpretation, particularly in resource-limited settings where transcription factor panels are not always available. Table 2.2 summarises the major changes in the WHO classifications of endocrine tumours and adenohypophyseal tumours, highlighting controversies for WHO 2022.

Studies confirm the prognostic value of transcription factor-based classification. For example, SF-1 lineage NF-PitNETs generally have a more indolent course than TPIT- or lineage-negative tumours (Woo et al. 2024). However, interpretation of immunohistochemistry is subject to inter-observer variability and antibody limitations.

RNA in situ hybridisation techniques such as RNAscope are being investigated to improve lineage assignment (Monné Rodríguez et al. 2023), while molecular profiling offers additional layers of classification (Whyte et al. 2023).

A major limitation of the current WHO classification of PitNET is its reliance on tumour histotype as the sole prognostic marker, without incorporating a grading or stratification system (Villa et al. 2023). Evidence suggests that the biological determinants of aggressive PitNET are influenced not only by the subtype of the transcription factor, but also by an interplay of various proliferative, radiological, and molecular factors (Woo et al. 2024). The WHO 2022 classification represents an advance in pituitary tumour pathology by standardising diagnosis based on transcription factors; however, controversy remains regarding the rarity of new types, diagnostic reproducibility, global applicability, and uncertain prognostic value. Future editions of the WHO classification could be improved by further integrating clinical, radiological, and pathological classification (Asa et al. 2025).

Table 2.2 Comparison of major changes in the WHO classifications of endocrine tumours and adenohypophyseal tumours with controversies for WHO 2022 (Edited from Villa et al., 2023)

Feature	ENDO3 WHO 2004	ENDO4 WHO 2017	CNS5 WHO 2021	ENDO5 WHO 2022	Controversies / Debated Issues
Nomenclature	Typical adenoma	Adenoma (Subtype)	Pituitary adenoma / pituitary neuroendocrine tumour (PitNET) (Subtype)	Pituitary neuroendocrine tumour (PitNET) (Subtype)	□□□□□□□□□□□“ □□□□□□□” biologically accurate but contentious; □□□□□□□□□□“ □□-O malignant” □ code may cause unnecessary anxiety, affect epidemiology and insurance.
Atypical adenoma	Atypical adenoma	–	–	–	Removal eliminates a poorly reproducible category, but loses a term clinicians used □□□□“-□□□□□” □□□□□□□□□
Carcinoma	Carcinoma	Carcinoma	Carcinoma	Metastatic PitNET (Subtype)	Terminology clarifies rarity of metastasis, □□□□□□□□□□□□□□□□□□□□“ □ discussion leaves grey zone for locally aggressive but non-metastatic tumours.
ICD-O codea	8272/0 Typical adenoma	8272/0 Adenoma	8272/3 Pituitary adenoma / PitNET	8272/3 PitNET	Coding all PitNETs as malignant (/3) is controversial; may not reflect indolent nature of most cases and could distort cancer registry data. □□□□□□□□□
Terminology based on	Hormone secretion	Hormone secretion / pituitary cell lineage	Pituitary cell lineage	Pituitary cell lineage	Exclusive reliance on transcription factor (TF) IHC may overlook tumours with unusual hormone profiles or TF-negative but hormone-positive cases.

□□□□□□□□□

…□ □ □ □ □ □ □ □ □ □ □ □ □

Grading	No grading	No grading	No formal system		Lack of formal grading criticised; some advocate integrated clinico-pathological grading (e.g., Trouillas system) for prognostication.
Staging	No staging	No staging	Dissemination in CSF & MRI/CT/PET		No integration of radiological invasiveness with histopathology, despite evidence of prognostic value.
Proliferation markers	Ki67 cut-off 3% (no mitosis cut-off)	Ki67 (hotspot count): no cut-off; mitosis: no cut-off; (P53)	No grading; Ki67 & mitosis unproven		No agreed cut-offs; subjectivity in “ □ □ □ □ □ □ □ □ ” □□ □ □ □ □ □ □ □ □ standardisation affects reproducibility.
High-risk of recurrence tumours	Atypical adenoma	Invasive, highly proliferative, rapid growth	No staging; invasion unproven	Only accurate histological subtyping	□ □ □ □ □ □ □ □-□□□□“□ □ ”□ □□□ □ □ prognostic value of certain subtypes (e.g., immature PIT1, Crooke cell) still unvalidated.
Subtypes	– Crooke cell adenoma– Silent corticotroph– Lactotroph in men	– Crooke cell adenoma– Silent corticotroph– Acidophil stem cell tumours– Plurihormonal PIT1+ adenoma	Proliferative rate unproven; –	– Crooke cell adenoma– Silent corticotroph– Immature PIT1-lineage– Sparsely granulated somatotroph– Null cell	Recognition of new/rare subtypes (e.g., immature PIT1-lineage, null cell) is applauded for biological precision but criticised for unclear clinical impact and risk of over-classification.

2.3.3 Prognostic Classifications

While the WHO classification defines lineage, it does not incorporate tumour aggressiveness or prognosis. Alternative systems have been proposed to stratify tumours by clinical outcome. Trouillas et al. introduced a clinicopathological model incorporating both radiological invasion and proliferation markers (Ki-67, mitotic index, p53). Tumours are stratified using a five-tier classification:

- Grade 1a: non-invasive, non-proliferative
- Grade 1b: non-invasive, proliferative
- Grade 2a: invasive, non-proliferative
- Grade 2b: invasive, proliferative
- Grade 3: metastatic

This system was validated in over 2,500 patients, showing that grade 2b tumours carried a nearly ninefold higher risk of recurrence compared to grade 1a (Asioli et al. 2019; Lelotte et al. 2018; Raverot et al. 2017; Sahakian et al. 2022; Trouillas et al. 2013). NF-PitNETs classified as 2b have particularly poor long-term outcomes, underscoring the value of integrating invasion and proliferation parameters.

More recently, pangenomic DNA methylation classification has demonstrated that DNA methylation profiling can stratify PitNETs into molecular clusters corresponding to PIT-1, TPIT, and SF-1 lineages, with additional subgroups reflecting aggressiveness (Neou et al. 2020). Methylation patterns not only clarified lineage in previously unclassifiable tumours but also correlated with Ki-67 index and recurrence risk. Importantly, methylation profiling provided superior reproducibility compared to IHC in ambiguous cases. However, critics caution that molecular subgroups should complement rather than replace histopathology, as mixed tumours and technical artefacts remain problematic.

An overarching clinical classification that synthesises clinical presentation, genetic background, biochemical profiles, radiological features, pathological findings, and molecular characteristics remains essential for accurately informing prognosis, therapeutic decision-making, and long-term outcomes in patients with pituitary adenomas. In 2024, the Pituitary Society convened the third Pituitary Adenoma Nomenclature clinical workshop (PANOMEN-3), which proposed an integrated clinicopathological classification framework for pituitary neoplasms aimed at improving prognostic stratification and outcome prediction (Ho et al. 2021). The PANOMEN-3 grading system is calculated at 6 months post-surgery by assigning predefined scores across multiple clinical, biochemical, radiological, pathological, and genetic domains. These include tumour phenotype and secretory activity, degree of hypopituitarism, tumour size, presence of mass effect or invasion, postoperative residual disease, histopathological risk features or high proliferative activity, and the presence of an underlying genetic syndrome. Individual factor scores are summed and then normalised by dividing by the number of assessed risk factors to generate a corrected score. Based on this corrected score, patients are stratified into four grades: [illegible]), [illegible]) [illegible] reflecting progressively increasing biological and clinical risk (Ho et al. 2024).

To date, the PANOMEN-3 classification has not been formally validated in prospective cohort studies. More recently, a multicentre Spanish national cohort study demonstrated a positive association between increasing PANOMEN-3 grades and higher rates of tumour recurrence or progression (Araujo-Castro et al. 2025). In parallel, another study reported outcomes from a large single-centre cohort of 289 patients managed by a dedicated pituitary multidisciplinary team using standardised diagnostic, therapeutic, and follow-up protocols (Chiloiro et al. 2025). Findings from this real-world cohort support the clinical validity of the PANOMEN-3 score, showing a consistent and independent predictive value for recurrence risk and disease-free survival. Collectively, these data indicate that higher PANOMEN-3 grades are associated with a stepwise increase in the likelihood of postoperative residual tumour and subsequent recurrence. This supports the utility of the PANOMEN-3 scoring system in routine clinical practice. By integrating biochemical, pathological, imaging, and clinical parameters into a unified framework, the PANOMEN-3 classification

provides a pragmatic tool to guide personalised follow-up, optimise post-surgical management of residual disease, and inform subsequent treatment strategies.

2.4 NON-FUNCTIONING PITUITARY NEUROENDOCRINE TUMOURS (NF-PITNETS)

2.4.1 Background

NF-PitNETs are clinically significant subsets of pituitary tumours, accounting for approximately 14–54% of all PitNETs (Chen et al. 2012; Ntali & Wass 2018). Unlike functioning adenomas, which are identified through biochemical hypersecretion syndromes, NF-PitNETs do not produce hormone excess at levels sufficient to manifest clinically. The only exception is mild to moderate hyperprolactinaemia, which arises secondarily from pituitary stalk compression rather than autonomous secretion. For this reason, NF-PitNETs often escape early detection and present later in their clinical course, frequently as macroadenomas with suprasellar or parasellar extension (Whyte et al. 2023).

NF-PitNETs exhibit marked biological heterogeneity. While most follow a relatively indolent course, a subset displays aggressive features with rapid growth, local invasion, and early recurrence. Silent corticotroph and plurihormonal PIT-1 lineage tumours, in particular, are associated with greater aggressiveness compared to silent gonadotroph adenomas (Drummond et al. 2019). The variability in behaviour underscores the need to unravel their molecular underpinnings, including genetic, epigenetic, and receptor-mediated mechanisms.

Management of NF-PitNETs includes active surveillance, surgical intervention, and radiotherapy (RT). Surgical resection is the preferred treatment for patients with large tumours or those presenting with symptoms secondary to mass effect (Freda et al. 2011). Current surgical approaches for most NF-PitNETs include endoscopic endonasal surgery (EES) or microscopy-assisted transsphenoidal surgery (MTS), while a transcranial approach is generally reserved for lesions with predominantly suprasellar extension and minimal intrasellar components (de Divitiis et al. 2015). The transsphenoidal route remains the standard of care for tumour resection.

Despite advances in surgical techniques, complete tumour resection is frequently limited by the large size and invasive nature of NF-PitNETs at presentation. Earlier series reported gross total resection (GTR) rates of less than 50%, with postoperative residual tumour carrying a substantial risk of regrowth, affecting approximately 47% of patients, and recurrence rates of 20–25% even after apparently complete resection (Brochier et al. 2010). More recent evidence from a large patient-level meta-analysis involving nearly 4,000 patients has reinforced the prognostic importance of extent of resection, demonstrating significantly inferior progression-free survival following subtotal resection compared with GTR, with long-term progression-free survival reduced by approximately threefold in patients with residual disease (Fong et al. 2023). The same analysis showed that postoperative radiotherapy markedly improves progression-free survival, particularly in patients with subtotal resection, while no significant long-term difference in tumour control was observed between EES and MTS (Fong et al. 2023).

Unlike functioning pituitary tumours, which can be monitored using biochemical markers, NF-PitNETs lack reliable serum indicators of recurrence, making long-term postoperative surveillance heavily dependent on imaging. This limitation, together with the high rates of residual disease and tumour regrowth despite optimal surgery, highlights the ongoing need for robust prognostic biomarkers and the development of effective adjunctive medical therapies to improve long-term disease control.

2.4.2 Epidemiology

Epidemiological studies report a prevalence of clinically relevant NF-PitNETs ranging from 7 to 41 per 100,000 population, though true rates are likely higher due to incidental detection (Ntali & Wass 2018). A recent population-based study from South Korea reported an annual incidence of 3.5 per 100,000 for NF-PitNETs (Oh et al. 2021). NF-PitNETs are the second most common subtype after prolactinomas when both microadenomas and macroadenomas are considered, but predominate among macroadenomas. In many radiological cohorts, NF-PitNETs constitute the majority of pituitary incidentalomas, reflecting their tendency to remain silent until identified on

imaging performed for unrelated reasons (Famini et al. 2011; Freda et al. 2020). In a recent cohort study, nearly half of NF-PitNET cases were detected incidentally, much higher than in older surgical series, which reported incidental detection in less than 20% of cases (Guerreiro et al. 2023).

Incidence peaks between the fourth and eighth decades, with an increasing proportion of cases diagnosed in the elderly. Japanese registry data indicate that up to □ □ % □□ □ □□ □ □ □ □ □ □ □ □ □□ □ □ □ □ □ □ □□ □ □ □ □ □ □ □□ □ □ □ □ □ □ □□ □ □ □ □ □ □ □ -functioning, suggesting □ □ □ ≥ □ 5 age as a risk factor for diagnosis (Kinoshita et al. 2018). Sex distribution varies across studies, with some reporting male predominance and others a more balanced pattern (Castellanos et al. 2022; Fernández-Balsells et al. 2011).

Local data from Malaysia confirm the high frequency of NF-PitNETs. In a Kuala Lumpur hospital series of 106 patients undergoing surgery between 2006 and 2015, 63.2% had NF-PitNETs, most of whom were middle-aged men (Yi et al. 2019). These regional findings are consistent with global epidemiology and highlight the need for country-specific management guidelines.

Familial cases account for about 5% of pituitary tumours. In familial isolated pituitary adenomas (FIPA), NF-PitNETs represent nearly one-fifth of cases, tend to be diagnosed earlier, and are more invasive than sporadic counterparts (Daly et al. 2006; Vasilev et al. 2011). Similarly, in MEN1, PitNETs constitute 15–40% of pituitary lesions (de Laat et al. 2015). These familial associations emphasise genetic predisposition in a subset of PitNETs.

2.4.3 Natural History

The natural history of NF-PitNETs is variable, ranging from stable lesions to progressive invasive tumours. Longitudinal studies of untreated patients suggest that tumour size at diagnosis and female sex are strong predictors of tumour growth (Kim et al. 2025; Lenders et al. 2016). Microadenomas tend to remain stable, although up to 50% growth has been documented in some cohorts (Sam et al. 2015).

Growth kinetics differ between microadenomas and macroadenomas, with annual mean growth rates of approximately 0.4 mm and 1.0 mm, respectively (Sam et al. 2015). Contact with the optic chiasm significantly increases the risk of progression, reflecting the role of anatomical constraints in determining clinical impact. Beyond size, histological subtype also influences behaviour. Silent corticotroph adenomas (SCAs), silent somatotroph adenomas, and plurihormonal PIT-1 lineage tumours are more aggressive than silent gonadotroph adenomas, although the prognostic implications remain under debate (McCormack et al. 2018).

Postoperative recurrence is another hallmark of NF-PitNETs. A meta-analysis from China reported a 12% recurrence rate after complete resection with no residual tumour, compared to 46% in patients with detectable remnants. The mean tumour volume doubling time was 3.4 years, underscoring the importance of long-term imaging surveillance (Chen et al. 2012). Second regrowth rates at 10 years exceeded 45%, even in patients initially disease-free, highlighting the limitations of surgery alone.

Long-term mortality in NF-PitNET patients has been reported as higher than in the general population, mainly due to cardio-cerebrovascular events, infections, and malignancies (Tampourlou et al. 2018). Nevertheless, quality of life can approach normal levels with adequate endocrine replacement therapy and careful follow-up (Ntali et al. 2016). Importantly, tumour phenotype may evolve over time. For example, silent [illegible] with an estimated conversion rate of 3.9% (Righi et al. 2017; Zheng et al. 2020). These findings justify long-term biochemical and radiological monitoring.

2.4.4 Clinical Manifestations

NF-PitNETs typically present with mass effects rather than endocrine hypersecretion, as their hormonal output is biologically inactive or secreted at subclinical levels (Whyte [illegible]2 [illegible]2 [illegible]) [illegible] growth, and degree of compression of adjacent sellar or parasellar structures. Most NF-PitNETs are macroadenomas at diagnosis – exceeding 10 mm in diameter – and are frequently discovered only when visual disturbance or hypopituitarism develops (Drange et al. 2000; Whyte et al. 2023).

NF-PitNETs often have an insidious onset. Visual symptoms are the most common initial complaint, occurring in up to 60–80% of patients at diagnosis (Vargas et al. 2015). The typical pattern is bitemporal hemianopia, caused by suprasellar extension compressing the decussating optic-chiasmal fibres. Involvement of the optic nerves leads to unilateral visual loss, while retrochiasmal spread produces homonymous hemianopia. Advanced chiasmal compression may result in irreversible optic atrophy if decompression is delayed (Shen et al. 2020). Headache is the second most frequent manifestation (Rizzoli et al. 2016). The pain is classically retro-orbital or frontal, resulting from stretching of the diaphragma sellae or invasion of dural and cavernous sinus structures. Although non-specific, chronic headache may precede diagnosis by months or years and should prompt sellar imaging in patients with otherwise unexplained symptoms.

When lateral extension occurs into the cavernous sinus, compression of cranial nerves III, IV, V1, V2, and VI may cause ophthalmoplegia, diplopia, or facial sensory disturbance (Chanson & Brochier 2005). A dramatic but uncommon mode of onset is pituitary apoplexy, defined as acute haemorrhage or infarction within the tumour. Clinically, it presents as sudden, severe headache – □ □ □ □ □ □ □ □ □ □ □ □ □ – □ □ □ “ □ □ accompanied by vomiting, visual loss, or ophthalmoplegia. It occurs in approximately 2–12% of patients with pituitary tumours and is most frequent in large non-functioning macroadenomas in middle-aged men (Möller-Goede et al. 2011). Although apoplexy can occur spontaneously, predisposing factors include major surgery, anticoagulant therapy, head trauma, and dynamic pituitary testing. Prompt high-dose glucocorticoid replacement and surgical decompression are critical to prevent permanent visual or endocrine deficits.

NF-PitNETs compromise normal pituitary function by mechanically compressing residual parenchyma, leading to hypopituitarism in up to two-thirds of cases at presentation (Ntali & Wass 2018). The pattern of hormonal deficiency generally follows the spatial arrangement of pituitary cell types: gonadotropin-secreting cells are most vulnerable, followed sequentially by GH-, TSH-, and ACTH-producing cells. Gonadotropin deficiency presents as menstrual irregularity or amenorrhoea in premenopausal women and decreased libido or erectile dysfunction in men. GH

deficiency contributes to fatigue or reduced exercise tolerance. Central hypothyroidism causes lethargy, cold intolerance, and weight gain, whereas secondary adrenal insufficiency may present with fatigue, anorexia, or hypotension (Ntali & Wass 2018). Mild hyperprolactinaemia (typically < 200 ng/mL) is common, reflecting pituitary stalk compression with interruption of tonic hypothalamic dopaminergic inhibition [illegible] 2 [illegible]) [illegible] “ [illegible] prolactin-[illegible]” secreting adenomas (prolactinomas), which produce markedly higher serum levels and respond to dopamine agonist therapy. Recognising this distinction prevents inappropriate long-term medical therapy.

Chronic hypopituitarism and tumour mass may also cause neurocognitive and psychosocial symptoms. Patients often report memory impairment, reduced concentration, and emotional lability, partly due to endocrine deficits. Large tumours with hypothalamic involvement can disrupt thermoregulation, sleep–wake rhythm, and appetite control, while invasion of the third ventricle may lead to hydrocephalus or altered consciousness in severe cases (van Iersel et al. 2019).

2.4.5 Subtypes and Pathological Frameworks

Advances in immunohistochemistry (IHC) and transcription factor profiling have enabled more precise subclassification of these tumours, which is crucial for prognosis and therapeutic planning. In 2017, members of the International Pituitary Pathology [illegible] “ [illegible] “[illegible]” [illegible] define tumours of adenohypophyseal cells (Asa et al. 2017). The most recent WHO 2022 classification recognises four principal NF-PitNET subtypes based on lineage-specific transcription factors: SF-1 (gonadotroph lineage), TPIT (silent corticotroph lineage), PIT-1 (plurihormonal PIT-1 lineage), and tumours without a distinct lineage (formerly null-cell adenomas) (Table 2.3).

a. Gonadotroph PitNET (SF-1 lineage)

Gonadotroph PitNETs are the most prevalent NF-PitNET subtype, accounting for approximately 50–80% of cases (Manojlovic-Gacic et al. 2018; Woo et al. 2024). These tumours arise from cells expressing steroidogenic factor-1 (SF-1) and often show

- α β polygonal or elongated cells arranged in diffuse, trabecular, or pseudorosette patterns, with eosinophilic cytoplasm and granular chromatin. Electron microscopy reveals abundant rough endoplasmic reticulum and secretory granules measuring 150–300 nm in diameter, features consistent with active glycoprotein synthesis. Clinically, gonadotroph PitNETs usually present as macroadenomas, often exceeding 2–3 cm in diameter, with symptoms dominated by visual field impairment, headache, and hypogonadism. Although non-secretory, man -subunit or FSH levels, but without endocrine hyperfunction. Molecularly, SF-1 activation drives gonadotroph differentiation through cooperation with GATA-2 α (Øystese et al. 2017). The SF-1 lineage is relatively indolent, showing lower recurrence rates and better disease-free survival than other subtypes. Despite this favourable behaviour, a subset displays invasive features, particularly those with increased Ki-67 (> 3%) or p53 overexpression (Di Ieva et al. 2014).

b. PitNETs without distinct lineage

-“ ” hormonal immunoreactivity, has largely been replaced by the WHO 2022 entity “ s any of the” three defining transcription factors – PIT-1, SF-1, or TPIT – and account for approximately 4–5% of NF-PitNETs (Mete et al. 2018). Historically, they were thought to represent undifferentiated adenohypophyseal progenitors; however, molecular re-evaluation has shown that many tumours previously classified as null cells can now be reassigned to a defined lineage using modern immunohistochemical panels and DNA methylation profiling.

True null-cell PitNETs display variable morphology, ranging from uniform chromophobic cells to pleomorphic oncocytic variants. These tumours are often large and invasive, extending into the cavernous or sphenoid sinuses. Clinically, they tend to present with mass effects rather than hormonal dysfunction, yet demonstrate aggressive biological behaviour with high recurrence rates even after gross total resection (Balogun et al. 2015). Invasion and proliferation indices are frequently elevated (Ki-67 > 5%,

strong p53 nuclear staining), consistent with their poorer disease-free survival compared to SF-1 lineage tumours (Almeida et al. 2019).

c. Silent corticotroph PitNETs (TPIT lineage)

The silent corticotroph PitNET is a distinct subtype that expresses TPIT and ACTH but [illegible] ~8% of all NF-PitNETs and is among the most aggressive histological variants (Ben-Shlomo & Cooper 2018). The 2017 World Health Organization (WHO) classification of pituitary adenomas defines corticotroph adenomas as those arising from adenohypophyseal cells of TPIT lineage that express ACTH and other proopiomelanocortin (POMC)-derived peptides (Mete & Lopes 2017). Routine TPIT immunostaining of specimens may help to better identify SCAs (Nishioka et al. 2015). Another distinguishing feature of SCA [illegible] filaments in the cytoplasm of corticotroph cells occur after prolonged exposure to high circulating glucocorticoid levels; as SCAs are non-[illegible] classification also defined two types of SCAs: type I densely granulated SCAs and type II sparsely granulated SCAs (Yavropoulou et al. 2020). POMC mRNA levels in type I SCAs are similar to those found in CD, while levels in type II SCAs are lower. Both types are associated clinically with more aggressive behaviour compared with functional CD adenomas (Mete & Lopes 2017).

Unlike functioning corticotroph tumours, serum cortisol and ACTH levels remain within the normal range; however, subtle hypothalamic–pituitary–adrenal dysregulation may exist. Importantly, silent corticotroph tumours carry a high risk of recurrence, with regrowth rates up to 40–60% at 5 years, even after total excision (Ben-Shlomo & Cooper 2018).

Emerging evidence indicates that transformation from a silent to a functioning corticotroph phenotype can occur postoperatively or after radiotherapy, implying underlying epigenetic plasticity (Righi et al. 2017). DNA methylation and histone modification studies have identified promoter hypermethylation of POMC regulatory regions, which may silence ACTH transcription despite TPIT activation.

d. Silent somatotroph PitNET

Silent somatotroph PitNETs account for approximately 2–4% of all pituitary adenomas (Langlois et al. 2018). Immunohistochemical staining for growth hormone (GH) in these tumours is highly variable, ranging from minimal to strongly positive, but is generally less intense than that seen in clinically functioning somatotroph adenomas associated with acromegaly. More than half of silent somatotroph PitNETs exhibit combined GH and prolactin (PRL) immunoreactivity. In tumours with weak or absent GH staining, nuclear positivity for the transcription factor PIT-1 serves as a useful diagnostic marker, as PIT-1 expression is a consistent feature of all GH-lineage tumours (Langlois et al. 2018).

e. Silent thyrotroph PitNET

Silent thyrotroph PitNETs are exceptionally uncommon, yet are reported more frequently than clinically functioning thyrotropin-secreting adenomas (TSH-omas) (Mete & Lopes 2017). Both silent thyrotroph PitNETs and TSH-omas demonstrate immunoreactivity for TSH-β □□ □ □ □□-subunit□ along with expression of the transcription factors PIT-1 and GATA-2. In addition, these tumours typically show prominent membranous expression of somatostatin receptor subtypes SSTR-2A and SSTR-5 (Yavropoulou et al. 2020).

f. Silent lactotroph PitNET

Silent lactotroph PitNETs are characterised by immunohistochemical expression of PRL, the PIT-1 transcription factor, and ER-α □□ □ □ □ □ □□ □□ □ □ □ □ □2 □ □ □) □ monohormonal silent lactotroph PitNETs are uncommon; most cases occur as clinically silent mixed somatotroph–lactotroph adenomas within PIT-1–positive tumours. Based on ultrastructural features, silent lactotroph PitNETs are further subdivided into sparsely granulated and densely granulated variants (Mete & Lopes 2017).

g. Plurihormonal PIT-1 lineage tumours

PIT-1-positive plurihormonal tumours, formerly designated as silent subtype 3, account for approximately 0.9–1.8% of NF-PitNETs (Lüdecke et al. 2007). These neoplasms

commonly demonstrate immunopositivity for multiple pituitary hormones, including GH, PRL, TSH, a[illegible] α-subunit. Despite this plurihormonal expression, most cases remain clinically non-functioning. Nevertheless, a subset may present with biochemical and clinical hormone excess, resulting in acromegaly, hyperprolactinaemia, or hyperthyroidism (Mete et al. 2016). Retrospective analyses have shown that surgically resected PIT-1-positive plurihormonal tumours are typically macroadenomas and are characterised by aggressive behaviour, invasive growth, and a high propensity for postoperative recurrence (Erickson et al. 2009).

Table 2.3 Classification of pituitary neuroendocrine tumors

PitNET type and subtype	Hormonal IHC	Transcription factors
PIT1 lineage		
Somatotroph tumors		
– Densely granulated	GH, α-subunit	PIT1
– Sparsely granulated	GH	PIT1
Lactotroph tumors		
– Sparsely granulated	PRL	[illegible] α
– Densely granulated	PRL	[illegible] α
Mammosomatotroph tumor	[illegible] α-subunit	[illegible] α
Mixed somatotroph lactotroph	[illegible] α-subunit	[illegible] α
Thyrotroph tumor	β-[illegible] α-subunit	[illegible]
Mature plurihormonal PIT1-lineage tumor	[illegible] β [illegible] α-subunit	[illegible] α [illegible] [a]
Immature PIT1-lineage tumor	[illegible] β α-subunit	[illegible] α
Acidophil stem cell tumor	PRL, GH	[illegible] α
TPIT lineage		
Corticotroph tumors		
– Densely granulated	ACTH and other POMC derivatives	TPIT
– Sparsely granulated	ACTH and other POMC derivatives	TPIT
– [illegible]' [illegible]	ACTH and other POMC derivatives	TPIT
SF1 lineage		
Gonadotroph tumor	[illegible] β [illegible] subunit, or none	[illegible] α [illegible]
No distinct cell lineage		
Plurihormonal tumor	Multiple combinations	Multiple combinations
Null cell	None	None

PitNET, pituitary neuroendocrine tumor; IHC, immunohistochemistry; PIT1, pituitary-specific [illegible] -stimulating hormone; GATA3, GATA-binding protein 3; TPIT, T-box transcription factor; ACTH, adrenocorticotropic hormone; POMC, proopiomelanocortin; SF1, steroidogenic factor 1; FSH, follicle-stimulating hormone; LH, luteinizing hormone.

[a]GATA3 is a paralog of GATA2, and GATA3 immunostaining can detect GATA2-positive cells, which is important for development of gonadotrophs and thyrotrophs (Adapted from Asa et al. 2022)

h. Comparative behaviour and prognostic overview

When subtypes are compared, SF-1 lineage (gonadotroph) tumours have the most favourable prognosis, characterised by slow growth and lower recurrence risk. TPIT lineage (silent corticotroph) and PIT-1 lineage plurihormonal tumours show higher mitotic indices, vascular density, and recurrence rates, consistent with their intermediate-to-aggressive potential. In contrast, tumours without a distinct lineage (null-cell) behave most aggressively, frequently invading adjacent sinuses and showing poor response to adjuvant therapy. A recent observational study (Woo et al. 2024) found that disease-free survival is longest for SF-1 lineage PitNETs, intermediate for TPIT and PIT-1 lineages, and shortest for tumours without lineage differentiation. These findings support the prognostic value of transcription-factor classification and validate the simplification introduced in WHO 2022.

2.4.6 Pathophysiology of NF-PitNETs

a. Background

The pathophysiology of NF-PitNETs reflects a multilayered, network-based biological architecture in which no single mutation is sufficient to drive tumorigenesis. To enable systematic interpretation of a highly fragmented and multidimensional literature, this PhD thesis proposes a conceptual reorganisation of NF-PitNET pathophysiology into four interconnected biological domains. This domain-based framework is defined by the author, does not derive from existing guidelines or textbooks, and is used solely as an analytical construct to support integrative discussion of molecular mechanisms, signalling pathways, and biomarker evidence. Dysregulation across these interconnected systems converges to promote tumour proliferation, invasion, angiogenesis, immune modulation, and postoperative tumour persistence.

b. Growth and angiogenic pathways

Growth dysregulation is a fundamental and unifying mechanism in the pathogenesis of NF-PitNETs. One of the most consistently implicated pathways is the aberrant activation of the phosphoinositide 3-kinase (PI3K)/AKT axis. Activating mutations in PIK3CA enhance downstream AKT signalling, enabling growth factor–independent

proliferation and resistance to apoptotic signals (Lin et al. 2009). However, PI3K/AKT activation alone does not fully explain the marked inter-patient heterogeneity observed in NF-PitNET behaviour, suggesting that it functions within a broader network of cooperating molecular disturbances rather than as a single driver event.

Epigenetic deregulation is a major amplifier of proliferative signalling in NF-PitNETs. Hypermethylation and transcriptional silencing of key tumour suppressors – □ □ □ □ □ □ □ □ □ □□ □ □ □ □ □ □ □ □ □ □□ □ □ □ 2 □ □ – compromise G1–S □□ □ □ □ checkpoint integrity and weaken cell cycle restraint (Hossain et al. 2009; Kober et al. 2018; Zhang et al. 2002, 2003). This pattern supports a model of tumour progression driven predominantly by epigenetic reprogramming and chromatin-level deregulation, rather than by the accumulation of high-impact oncogenic mutations.

Remodelling of the extracellular matrix (ECM) further facilitates tumour expansion, invasion, and angiogenesis. Upregulation of matrix metalloproteinases (MMP1, MMP2, and MMP9), together with osteopontin, promotes basement membrane degradation and stromal infiltration (Feng et al. 2016; Hussaini et al. 2007). Concurrent activation of growth-related mediators such as FGFR4, HMGA1, and MDM2 reinforces proliferative signalling and confers a selective growth advantage through MAPK activation, chromatin remodelling, and p53 degradation, respectively (Mete et al. 2012, 2013; Portovedo et al. 2019; Yao et al. 2017). Importantly, vesicle-mediated communication also contributes to angiogenic signalling; exosomal MMP1 activates protease-activated receptor-1 (PAR-1) on endothelial and stromal cells, highlighting the role of tumour-derived extracellular vesicles in shaping the pro-angiogenic microenvironment.

Alongside protease-driven matrix remodelling, angiogenic signalling is a critical downstream effector of growth-domain dysregulation in NF-PitNETs. Vascular endothelial growth factors (VEGFs) are a family of angiogenic and lymphangiogenic mediators that regulate endothelial cell proliferation, vascular permeability, and neovascularisation, thereby supporting tumour expansion and local invasion (Dai et al. 2021). Elevated VEGF expression has been consistently reported in NF-PitNETs and is associated with invasive behaviour, particularly cavernous sinus invasion, underscoring

its role in tumour–vascular interface remodelling (Cristina et al. 2010; He et al. 2017; Sato et al. 2019; Wang et al. 2014). Comparative analyses further demonstrate that VEGF RNA and protein levels are significantly higher in NF-PitNETs than in normal pituitary tissue; however, VEGF expression does not reliably distinguish non-functioning from functioning PitNETs, indicating that VEGF reflects a shared angiogenic mechanism rather than a lineage-specific biomarker (He et al. 2017; McCabe et al. 2002).

Loss of tumour-suppressive transforming growth factor-β □□□-β□) □□□□□□□□□□□□ further exacerbates invasive behaviour in NF-PitNETs. Reduced expression of TGF-β □ receptor II (TGF-β □□□) □□□□□□□□□□□□□□□□□□□□□□□□□□□□ upregulation of the inhibitory Smad7 collectively attenuate canonical TGF-β □□□□□□ signalling, thereby permitting epithelial–mesenchymal transition (EMT) and enhanced migratory capacity (Gu & Feng 2018; Liu et al. 2016; Zavadil & Böttinger 2005). In parallel, cytoskeletal remodelling driven by EZRIN overexpression increases cell motility, adhesion dynamics, and invasive potential (Chen et al. 2017).

Chromatin-associated regulators and cell-surface receptor systems provide additional layers of proliferative control. The bromodomain protein BRD4 is markedly overexpressed in NF-PitNETs and acts as an epigenetic reader that sustains oncogenic transcriptional programmes. Pharmacological inhibition of BRD4 suppresses c-MYC and BCL2 expression, induces G2/M arrest and apoptosis, and underscores its role as a critical epigenetic dependency (Shi et al. 2020). At the membrane, overexpression of EphB6 correlates with tumour size, suggesting a role in growth regulation (Rubinfeld et al. 2024), while dysregulated G protein–coupled receptor signalling via HTR2B □□□□□□□□□□□□□α □□□□□□□□□γ □□□□□□□□□□□□□□□□□□□□ responsiveness to dopaminergic therapy (Lin et al. 2024).

Canonical cell-cycle regulators are also perturbed in aggressive NF-PitNETs. Increased phosphorylated E2F1, reduced p16 expression, and elevated levels of retinoblastoma protein (Rb) and cyclin D1 collectively promote unchecked G1–S phase transition and are associated with postoperative tumour regrowth (Metin-Armagan et al. 2020). These abnormalities integrate with non-coding RNA–mediated regulatory

networks. For example, activation of the SDF-□α□-134/VEGFA axis enhances VEGFA expression, supporting angiogenesis and invasive growth (Wang et al. 2020), while circVPS13C has been shown to promote tumour cell proliferation and invasiveness through post-transcriptional mechanisms (Zhang et al. 2022).

At the systems level, transcriptomic profiling of non-coding RNAs in NF-PitNETs has shown that dysregulated lncRNA–miRNA–mRNA networks predominantly converge on growth-associated biological processes, including GnRH signalling, cell cycle progression, DNA replication, genome maintenance pathways, and intercellular junction regulation (Ghafouri-Fard et al. 2022). These findings reinforce the concept of NF-PitNETs as tumours driven by sustained proliferative signalling.

Consistent with this framework, public NFPA microarray analyses have demonstrated marked divergence from normal pituitary tissue, with reproducible alterations in CACNA2D4, CXCR4, KLF8, and PITX2 (Taniguchi-Ponciano et al. 2020). Collectively, these changes reflect convergent disruption of calcium-dependent growth control, stemness-associated transcriptional programmes, and chemokine-mediated growth–immune cross-talk, further consolidating the central role of growth and angiogenic dysregulation in NF-PitNET pathophysiology.

c. Inflammatory pathways

Inflammation in NF-PitNETs is subtle, immune-cold, and tumour-permissive rather than overtly inflammatory. A pivotal pathway is the IL-6R/JAK2/STAT3/MMP9 axis, particularly active in null-cell adenomas, where it drives ECM degradation and proliferation (Feng et al. 2016). This pathway exemplifies how inflammatory signalling directly contributes to tumour aggressiveness rather than representing a reactive immune response.

NF-PitNETs exhibit pronounced immune dysfunction rather than immune activation. Immune escape is promoted by upregulation of ARG2 and SEMA3A and downregulation of HLA-B, which impairs antigen presentation and supports tumour

survival (Richardson et al. 2017). This places NF-PitNETs within the immune-cold phenotype typical of non-immunogenic tumours.

Aggressive NF-PitNETs display a distinctly immune-cold microenvironment that enables silent tumour progression. These tumours are characterised by increased diminished immune surveillance (Han et al. 2020). Elevated IL-10 further suppresses remodelling and invasion (Huang et al. 2021; Lin et al. 2022). Collectively, these features establish a permissive, immunosuppressive niche that supports tumour growth and helps explain the limited responsiveness of NF-PitNETs to immunotherapeutic strategies.

d. Cytokine–TNF–Immune Checkpoint Axis

Cytokines constitute a distinct yet interconnected domain in NF-PitNET biology. TNF- and stromal remodelling (Zhao et al. 2021). Although less extensively studied than IL-6, TNF- –inflammatory network rather than strictly under classical inflammation.

Immune checkpoint pathways, notably PD-1/PD-L1, are upregulated in aggressive tumours and reflect cytokine-driven immune exhaustion (Wang et al. 2018). However, the low immunogenicity and low mutational burden of NF-PitNETs limit the clinical utility of checkpoint blockade, except in select high-expression subsets.

e. Wnt Signalling and Wnt Modulators

-catenin signalling dysregulation is one of the most consistently reported molecular abnormalities in NF-PitNETs. Early transcriptomic studies by Moreno et al. demonstrated altered expression of several key regulatory genes, including SFRP1, TLE2, PITX2, NOTCH3, and DLK1, in NFPAs, implicating disruption of Wnt pathway control in tumour progression (Moreno et al. 2005). Subsequent work has shown that epigenetic silencing or repression of extracellular Wnt antagonists, such as sFRP2,

[illegible] β-catenin, thereby facilitating its cytoplasmic accumulation and nuclear translocation (Song et al. 2018; Wu et al. 2016). [illegible] β-catenin activates canonical proliferative targets, including c-MYC, which contributes to sustained tumour growth and cellular transformation (Liu et al. 2017). Consistent with this, invasive tumours exhibit [illegible] β-catenin at Ser552, linking heightened Wnt pathway activity to tumour aggressiveness and recurrence risk (Rai et al. 2022).

Beyond these canonical mechanisms, Wnt4, a secreted glycoprotein involved in cellular proliferation and differentiation, has also been implicated in pituitary tumour biology. Weiping Li et al. (2014) reported that the Wnt4 pathway is dysregulated in most pituitary adenomas and that its overactivation may paradoxically inhibit tumour [illegible] β-catenin were found to be [illegible] overexpressed in the majority of pituitary adenomas. Functional experiments by Zhao [illegible] β-catenin regulates the AKT and STAT3 pathways and upregulates MMP-2/9, cyclin D1, and CDK4, thereby promoting cellular proliferation and invasiveness in pituitary adenoma models (Zhao et al. 2015).

[illegible] β-catenin signalling also contribute to NF-[illegible] PitNET pathobiology. The proto-oncogene c-MYC plays a central role in tumour growth, cellular transformation (Formosa et al. 2012). In NF-[illegible] β-catenin and c-MYC have been proposed as useful immunohistochemical markers of invasiveness, although validation in larger cohorts is required before they can be adopted for prognostic stratification (Liu et al. 2017). Another important downstream target is pituitary homeobox 2 (PITX2), which is essential for pituitary development and differentiation. Acunzo et al. (2011) demonstrated that Wnt-induced PITX2 expression may contribute to the development of gonadotroph adenomas and NFPAs by promoting anti-apoptotic mechanisms.

Importantly, Wnt dysregulation in NF-PitNETs occurs at multiple biological levels, including epigenetic silencing, transcriptional alteration, and post-transcriptional regulation, rather than through a single dominant genetic lesion (Wu et al. 2016; Song et al. 2018). Systems-level analyses indicate that Wnt signalling is extensively

interconnected with other oncogenic pathways, including PI3K/AKT, MAPK, Hippo, EMT, VEGF, JAK–STAT, ErbB, TGF-β (Hosseinkhan et al. 2022). Such pathway crosstalk is a recognised feature of many malignancies and has also been demonstrated in pituitary adenomas. For example, SOX2 was shown to promote pituitary adenoma cell proliferation by mediating crosstalk between the Wnt and Sonic hedgehog (Shh) pathways, further underscoring the integrative role of Wnt signalling within the tumour regulatory network (Tang et al. 2019).

From a regulatory perspective, endogenous inhibitors of Wnt signalling are classically divided into two major groups. The first group comprises secreted Wnt antagonists, including the SFRP family, WIF1, and Cerberus, which suppress both canonical and non-canonical Wnt signalling by directly binding Wnt ligands and preventing their interaction with Frizzled (FZD) receptor complexes (Elston & Clifton-Bligh 2010). The second group consists primarily of the Dickkopf (DKK) family, which inhibits canonical Wnt signalling by binding to the LRP5/6 co-receptors, thereby disrupting receptor complex formation and downstream signal propagation (Bao et al. 2012). The DKK family may also influence non-canonical signalling (Wang et al. 2023).

The secreted frizzled-related protein (SFRP) family consists of five members (SFRP1–SFRP5). Although SFRPs are downstream targets of Wnt signalling, they function as negative feedback regulators and act as tumour suppressors in several malignancies (Baharudin et al. 2020). In pituitary adenomas, Wu et al. first reported that SFRP4 promoter hypermethylation is increased in invasive tumours, leading to reduced SFRP4 expression (Wu et al. 2015). In a follow-up study, the same group demonstrated that SFRP2 suppresses tumour growth and invasion by modulating Wnt signalling, and that its expression is inversely associated with NFPA aggressiveness (Wu et al. 2016). Collectively, these findings support a tumour-suppressive role for SFRP2 and SFRP4 in pituitary adenomas and suggest their potential utility as biomarkers of tumour aggressiveness and prognosis.

Another key extracellular antagonist, Wnt inhibitory factor 1 (WIF1), is a critical regulator of Wnt signalling that directly binds Wnt proteins and prevents

activation of the receptor signalling complex (Kerekes et al. 2021). Song et al. (2018) reported that downregulation of WIF1 and SFRP4 is inversely associated with NFPA aggressiveness, and demonstrated that miR-137 modulates NFPA invasion by affecting WIF1 promoter methylation and Wnt pathway activity (53). Subsequently, Zhu et al. (2018) showed that WIF1 and TGF-β [illegible] proliferation and recurrence in NFPA. In parallel, Cheng developed a clinical prediction model based on 295 NFPA samples and identified WIF1, TGF-β [illegible] 2 [illegible] tumour age, and tumour volume as significant predictors of recurrence (Cheng et al. 2019). Taken together, these data position WIF1 as a central inhibitory checkpoint of Wnt signalling in pituitary adenomas and a promising biomarker for tumour behaviour.

More recently, increasing attention has been directed towards the role of non-coding RNAs (ncRNAs) as modulators of Wnt signalling in pituitary tumours. Song et al. (2018) demonstrated that miR-137 regulates Wnt signalling via modulation of WIF1 methylation in NFPA. Conversely, some ncRNAs appear to activate Wnt signalling and promote tumour progression. Shen et al. (2019) showed that miR-543 enhances pituitary adenoma invasion and inhibits apoptosis by downregulating Smad7 and activating the Wnt pathway.

[illegible] -catenin signalling in [illegible] NF-PitNETs functions less as a primary oncogenic driver and more as a downstream integrator and amplifier of diverse upstream oncogenic inputs, including growth factor signalling, epigenetic dysregulation, and inflammatory cues.

Table 2.4 summarises core molecular mechanisms underlying NF-PitNET pathophysiology.

Table 2.4 Pathophysiological Mechanisms of NF-PitNETs According to Molecular Domains

Category	Key Molecular Drivers / Mechanisms	Functional Role in NF-PitNET Biology
Growth / Angiogenic	PI3K/AKT pathway activation (genetic or post-translational)	Growth-factor–independent proliferation and survival
	$p18^{INK4C}$ loss	□ □ □ □ □ □ □ □ □ □ □ □ □ □ □ □ □ □ □ cell-cycle progression
	TGF-β □ □ □ □ ↓ □ □ □ □ □ □ ↓ □	Attenuation of tumour-suppressive TGF-β □ □ □ □ □ □ □ □ □ □ □ □ □ □
	EZRIN overexpression	Cytoskeletal plasticity, cell motility, invasion
	ZAC1 downregulation	Reduced apoptosis and growth restraint
	MMP1 / MMP2 / MMP9 upregulation	□ □ □ □ □ □ □ □ □ □ □ □ □ □ □ □ → angiogenesis
	FGFR4 activation	MAPK-mediated tumour proliferation
	Osteopontin upregulation	Pro-angiogenic ECM signalling
	HMGA1 / HMGA2 overexpression	□ □ □ □ □ □ □ □ □ □ □ □ □ □ □ □ □ □ □ aggressiveness
	MDM2 elevation	□ 5 □ □ □ □ □ □ □ □ □ □ □ □ □ □ advantage
	Exosomal MMP1	Paracrine PAR-1–mediated angiogenesis
	□ □ □ □ 2 □ □ □ □ □ □ □ □ □	Epigenetic silencing of tumour-suppressor pathways
	miRNA dysregulation (miR-181, miR-598, miR-128a, etc.)	Post-transcriptional control of EMT and proliferation
	Non-coding RNA–mediated dysregulation of GnRH signalling, DNA replication, DNA repair (mismatch and nucleotide excision repair), tight and gap junction pathways, and N-glycan biosynthesis	Promotes pituitary tumour cell proliferation, genome maintenance, endocrine growth signalling, and loss of growth restraint, contributing to tumour expansion and invasiveness
	CACNA2D4, KLF8, PITX2, CXCR4 dysregulation (microarray-based transcriptomic signature)	Convergent disruption of calcium-dependent growth control, stemness-associated transcriptional programmes, and chemokine-mediated growth–immune cross-talk promoting tumour proliferation and invasiveness
Inflammation	IL-6R / JAK2 / STAT3 / MMP9 axis	Proliferation, invasion, ECM remodelling
	ARG2, SEMA3A upregulation	Immune suppression and tumour immune escape
	HLA-B loss	Impaired antigen presentation
Cytokine / TNF / Immune checkpoint	TNF-NF-κ □ □ □ □ □ □ □ □ □ □ □	Supports EMT, angiogenesis, tumour survival
	PD-1 / PD-L1 upregulation	Immune checkpoint–mediated T-cell suppression
Wnt Pathways	sFRP2 / sFRP4 / WIF1 downregulation	□ □ □ □ □ □ □ □ □ □ □ □ □ □ □ □ □ -catenin activation
	□ □ □ □ -catenin β accumulation	Transcription of c-MYC and proliferative genes

2.5 OESTROGEN RECEPTOR SIGNALLING IN PITUITARY TUMOURS AND NF-PITNETS

-estradiol, E2) is a key regulator of pituitary physiology, influencing the synthesis and secretion of LH, FSH, and PRL through activation of ERs (Turgeon & Waring 2000). Two principal nuclear ER isoforms are

These receptors function as ligand-activated transcription factors and mediate the genomic actions of oestrogen, while rapid non-genomic signalling is partly mediated by membrane-associated ERs and the G protein–coupled oestrogen receptor (GPER) (Camilletti et al. 2019). In pituitary cells, ER-dependent signalling affects multiple downstream pathways, including the MAPK and PI3K/Akt cascades, as well as cytoskeletal organisation, ion channel regulation, and cellular metabolism (Clarke 2002; Yamakawa & Arita 2004).

oliferative actions of proliferation and promoting differentiation (Hall & McDonnell 1999; Shupnik et al. 1998). Experimental studies in animal models further support more restricted actions, such as induction of progesterone receptor (PR) expression and modulation of gonadotroph cell populations (Sánchez-Criado et al. 2004). Targeted n (Gieske et al. 2008).

-regulatory receptor in specific cellular contexts.

In the context of pituitary tumours, ER expression shows marked heterogeneity is highest in PRL-secreting tumours, whereas gonadotroph tumours exhibit intermediate levels, and GH-secreting tum -negative (Chaidarun et

gonadotroph tumours and is less frequently detected in prolactinomas (Chaidarun et al. 1998). These findings indicate that the re varies substantially across pituitary tumour lineages.

Within NF-PitNETs specifically, immunohistochemical studies have consistently shown that gonadotroph and null-cell tumours exhibit the highest nuclear immunorea been reported to be higher in macroadenomas than in microadenomas, suggesting a potential associa also examined the relationship between ER expression and invasiveness. Zhou et al. 2) invasive NF-PitNETs compared with non-invasive tumours, implying that the balance influence invasive behaviour. However, other studies have reported differing patterns, with non-invasive tumours in lesions (Manoranjan et al. 2010). These discrepancies highlight the complexity of ER signalling in NF-PitNETs and suggest that receptor context, co-regulators, and downstream pathways are likely to modulate the biological effects of ER activation.

The interaction between ER signalling and cell adhesion pathways provides further mechanistic insight into tumour invasiveness. Loss of E-cadherin is a recognised feature of aggressive pituitary adenomas (Zhou et al. 2013), and ER pathways have been shown to regulate E-cadherin expression in epithelial systems (Helguero et al. 2008). In NF- -cadherin and Slug expression, -cadherin levels (Zhou et al. 2011). -cadherin showed the opposite pattern, being positively –E-cadherin axis, thereby contributing to differential invasive potential in NF-PitNETs.

From a prognostic per[illegible] α [illegible] particularly in male patients with NF-PitNETs. Øystese et al. (2017) demonstrated that [illegible] α [illegible] ially in younger men, predicts a higher risk of repeat [illegible] with somatostatin receptor subtype 2 (SSTR2) levels, consistent with earlier observations in breast cancer models suggesting that oestrogens may regulate SSTR2 [illegible]-dependent mechanisms (Kimura et al. 2008). These findings [illegible] α [illegible] functionally linked to tumour behaviour and therapeutic responsiveness.

At the cellular level, oestrogen plays a central role in regulating gonadotroph proliferation, differentiation, and survival. Oestrogen stimulates basal and GnRH-induced secretion of LH, FSH, and PRL, sensitises gonadotrophs to GnRH by increasing GnRH receptor expression, and modulates secretory granule mobilisation and the pool of responsive gonadotroph cells (Haydar Ali Tajuddin et al. 2020). These effects are mediated through both classical genomic mechanisms – via nuclear ER dimerisation and transcriptional regulation – and rapid non-genomic pathways involving membrane-associated ERs and GPER, with downstream activation of c-Src, MAPK, PI3K/Akt, cAMP, and calcium signalling. In addition, oestrogen influences apoptotic turnover of gonadotrophs across the oestrous cycle, with suppression of apoptosis during periods of high GnRH and oestrogen exposure, thereby maintaining the functional gonadotroph population (Yin & Arita 2002).

A particularly important molecular link between oestrogen signalling and pituitary tumorigenesis is the pituitary tumour transforming gene (PTTG). Oestrogen was the first identified inducer of PTTG expression, and increased PTTG levels stimulate fibroblast growth factor 2 (FGF2) and vascular endothelial growth factor (VEGF) production, thereby promoting tumour growth, invasion, and angiogenesis (Trott et al. 2019). Overexpression of PTTG is sufficient to drive cellular transformation and tumour development. In NF-PitNETs, PTTG expression has been reported in nearly all cases in some series, with higher levels associated with tumour regrowth (Noh et al. 2009), although other studies have found high prevalence without a consistent

association with invasiveness or hormonal expression (Ramírez et al. 2012). Nevertheless, these findings support a biologically plausible pathway linking oestrogen–ER signalling to proliferative and angiogenic programmes in NF-PitNETs.

[illegible] differentially expressed across NF-PitNET subtypes, are linked to tumour size, invasiveness, and prognosis, and regulate key pathways involved in proliferation, [illegible] α [illegible] pituitary oestrogen action and a potential biomarker of aggressive behaviour in selected patient groups. However, despite these advances, existing studies remain heterogeneous in methodology and clinical endpoints, and ER status has not yet been systematically integrated with longitudinal tumour behaviour or therapeutic response in NF-PitNETs. This gap provides a strong biological and clinical rationale for the present study to [illegible] α [illegible] β [illegible]-PitNETs and to [illegible] relate these findings to tumour dynamics and treatment response in subsequent analyses.

Table 2.5 Chronological Summary of ER Gene (ESR1/ESR2) and protein (□ □/α□ □)β Expressions in NF-PitNET Subtypes

Year	Study	NF Cohort (n)	NF Subtypes Included	Method	□ □ α □□ □□ □ □ □ □□ □	□ □ β □□ □□ □ □ □ □□ □	Key Clinical / Biological Associations
1994	Friend et al.	Included non-functioning adenomas (within mixed PA cohort)	Gonadotroph, null cell among others	RNase protection assay, molecular ER analysis	ER (ESR1) mRNA detected predominantly in gonadotroph lineage; weak/absent in corticotroph and pure GH tumours; null-cell variably positive	□ □ β □□ □ □ □□ □ □ □ - □ □ β □□ □ □)	Early molecular evidence that ER gene expression is lineage-dependent, favouring gonadotroph/NF lineages
1995	Zafar et al.	Mixed cohort including NF □ □ □ □ □ □ adenomas)	Gonadotroph, null cell, oncocytoma, others	RT-PCR, in situ hybridisation, IHC, ligand-binding	ESR1 mRNA present in all gonadotroph, null-cell and oncocytoma tumours; ER protein detectable only in a minority (mainly PRL and some gonadotroph)	□ □ β □□ □ □ □□ □ □ □ - ER era)	Establishes lineage-specific ER gene expression with variable protein detectability
1997	Chaidarun et al.	10 clinically non-functioning (within 40 PAs)	Gonadotroph, null cell	RT-PCR, Southern blot	Wild-type ESR1 mRNA in ~57% of gonadotroph tumours; absent in null-cell tumours; tumour-specific ESR1 splice variants mainly in gonadotroph tumours	Not the main focus	Demonstrates tumour- and lineage-specific ESR1 expression and splice variants
1998	Chaidarun et al.	10 clinically non-functioning (within 38 PAs)	Gonadotroph, null cell	RT-PCR + functional assays	ESR1 mRNA restricted to lactotroph/gonadotroph lineages; not detected in pure null-cell tumours	ESR2 mRNA detected in 100% of null-cell tumours and ~29% of gonadotroph tumours	□ □ □ □ □ □ □ □ □□ □ may mediate estrogen □ □ □ □ □ □ □ □ □ □ - negative lineages
2004	Pereira-Lima et al.	42 non-functioning (within 158 PAs)	Mixed non-functioning	IHC	□ □ α □ □ □ □ □ □ □ □ □ □ (~5.7%); higher in invasive macroadenomas vs microadenomas	Not assessed	Early IHC suggests low □ □ α □ □ □ □ □ size/invasion more relevant than subtype □ □ □□ □ □□ □ □ □

…□ □ □ □ □ □ □ □ □ □ □ □ □

2008	Burdman et al.	26 non-secreting	Non-secreting adenomas	IHC (clone 1D5)	□ □ □ □ □ □ 2 □ □ □ □ □	Not assessed	Highlights early methodological limitations and inter-study heterogeneity
2010	Manoranjan et al.	NF within 75 adenomas	Gonadotroph (FSH/LH), null cell, silent corticotroph I–III, ACTH	□ □ □ □ □ □ □ □ α □ □ β □	□ □ □ □ □ □ □ □ α □ □ □ β & null cell; lowest in silent corticotroph & ACTH; higher in macroadenomas	□ □ □ □ □ □ □ □ gonadotroph & null cell (and PRL); lowest in ACTH & silent corticotroph; no significant size/invasion correlation	Establishes subtype-□ □ □ □ □ □ □ □ □ distribution; suggests □ □ β □ □ □ □ □ □ □ lineage/differentiation
2011	Nishioka et al.	59 NFomas	Non-functioning adenomas	RT-qPCR	ESR1 mRNA higher in NFomas than GH adenomas; correlates with SSTR subtypes (esp. <50 years)	Not separated by subtype	Links ESR1 to somatostatin receptor networks (therapeutic relevance)
2011	Zhou et al.	41 NFPA	Mixed NFPA	IHC, RT-PCR, Western blot	□ □ □ □ □ □ □ □ □ □ □ □ □ □ invasive tumours; correlates positively with Slug	Lower □ □ β □ □ □ □ 2 invasive tumours; correlates positively with E-cadherin	Shows opposing roles □ □ □ □ □ α □ □ □ □ □ invasion (Slug/E-cadherin axis)
2016	Gao et al.	197 NFPA (within 289 PAs)	Predominantly NFPA; compared with GH- and PRL-secreting tumours	Tissue microarray □ □ □ □ □ □ □ □ □ α	□ □ □ □ □ □ □ □ □ □ □ expression in ~80% of NFPA; higher prevalence than in PRL- and GH-secreting tumours; no clear association with tumour size or recurrence	Not assessed	Demonstrates high □ □ □ □ □ □ □ □ □ □ □ NFPA, supporting biological relevance of ER signalling and therapeutic targeting in non-functioning tumours
2017	Øystese et al.	145 NFPA (IHC), 106 (RT-qPCR)	Predominantly gonadotroph; also null-cell	IHC (IRS) + RT-qPCR	□ □ □ □ □ □ □ □ □ □ □ □ □ ESR1 predict earlier/higher □ □ □ □ □ □ □ □ □ □ □ □ correlates with SSTR2 in males	Not primary focus	First large study showing sex-dependent prognostic value of □ □ α □ □ □ □ □ □ □

□ □ □ □ □ □ □ □

…continuation

2019	Sosa et al.	Experimental models	Pituitary tumour cells	Immunofluorescence, Western blot, signalling assays	□ □ □ □ □ □ □ □ □ □ □ α ı ERK1/2 and promotes proliferation	Not focus	Mechanistic support □ □ □ □ -driven growth signalling
2020	Hattori et al.	20 pure, treatment-naïve NFPA	NFPA only	RT-dPCR + IHC (validated antibodies)	□ 2 □ □ □ β □ □ □ high, ~50% very low/absent); correlates with GREB1	very low/faint at mRNA and protein level	Highlights molecular heterogeneity and □ □ □ □ □ □ □ □ □ □ □ detection

2.6 TREATMENT MODALITIES FOR NF-PITNETS

2.6.1 Multidisciplinary and Personalised Care Approach

Unlike functioning adenomas, effective medical therapies for NF-PitNETs are lacking; therefore, current management relies on active surveillance, surgery, and radiotherapy. Transsphenoidal surgery is recommended as first-line treatment for large tumours causing visual impairment or mass effect, while primary radiotherapy is reserved for selected inoperable cases or patients unfit for surgery (Freda et al. 2011; Loeffler & Shih 2011).

A risk-stratified approach guides clinical decision-making based on symptoms, tumour size, pituitary function, visual field status, and MRI features (Table 2.6). Symptomatic patients, particularly those with visual field (VF) defects or hormonal deficiencies, are usually referred for surgery. Postoperative management depends on residual tumour burden and histological risk, with low-risk cases managed by surveillance and hormonal replacement, and high-risk cases considered for adjuvant radiotherapy or further therapies. For macroadenomas, MRI invasiveness, visual function, and endocrine status further refine management, while incidental microadenomas are typically followed with interval MRI.

The management of NF-PitNETs requires a multidisciplinary approach because of their heterogeneous biological behaviour, variable risks of progression, and potential for long-term endocrine, neurological, and visual complications. Contemporary consensus recommends that patients with pituitary tumours are managed through specialised multidisciplinary pituitary teams comprising endocrinologists, pituitary neurosurgeons, neuroradiologists, neuropathologists, radiation oncologists, and ophthalmologists. Such collaborative care facilitates accurate diagnosis, coordinated treatment planning, longitudinal surveillance, and timely intervention when tumour progression or treatment-related complications occur.

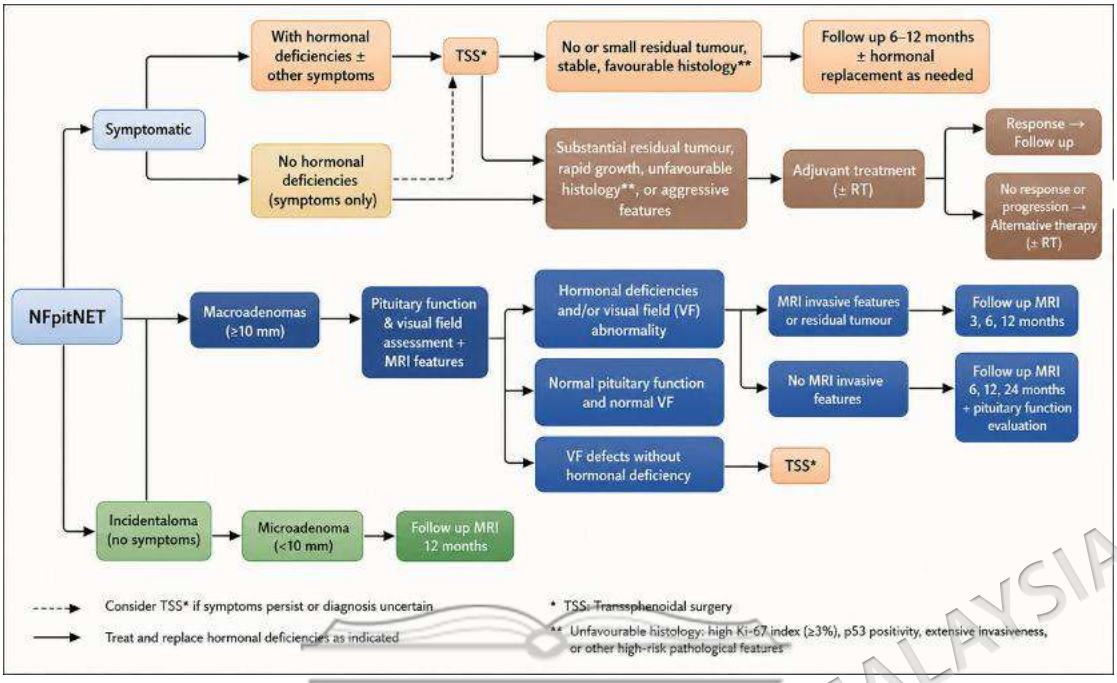

Figure 2.6 Management of NF-PitNETs algorithm

VF, visual field defects; TSS, transsphenoidal surgery; RT, radiotherapy; TMZ, temozolomide

(Edited from Yavropoulou et al. 2020)

This management algorithm was adapted and modified from the review by Yavropoulou et al. (2020). The original figure was revised to improve clarity, update terminology, and better reflect current clinical practice. Modifications include refinement of the diagnostic and treatment pathways, incorporation of contemporary concepts in postoperative management, and revision of imaging surveillance recommendations based on the latest international consensus guideline on pituitary incidentalomas published by Fleseriu et al. (2025). The decision pathways were reorganised to better reflect real-world clinical practice by integrating pituitary hormonal assessment, visual field evaluation, and MRI findings into the initial assessment. The postoperative management pathway was also updated by distinguishing patients with stable, minimal residual tumour from those with substantial residual disease or aggressive pathological features, and by replacing the simplified radiotherapy pathway with a broader adjuvant treatment approach that better reflects contemporary multidisciplinary care.

Although the 2025 Pituitary Society International Consensus Statement was developed primarily for conservatively managed pituitary incidentalomas, many of its

surveillance principles are applicable to patients with residual NF-PitNETs following surgery (Fleseriu et al. 2025). The consensus recommends dedicated pituitary MRI using standardised thin-section contrast-enhanced imaging protocols and advocates risk-adapted surveillance rather than fixed follow-up schedules. In the absence of tumour progression, repeat MRI is recommended after 2–3 years for microadenomas, after 1 year for macroadenomas locat□ □ □ ≥ 5 □□ □ □□ □ □ □ □□ □ □ □□ □ □ □–12□□ □ □ □ □ months for macroadenomas situated <5 mm from the optic chiasm. Subsequent imaging intervals should be individualised according to tumour growth kinetics, patient age, tumour consistency (solid versus cystic), T2-weighted MRI characteristics, pituitary □ □ □ □ □ □□ □ □ □ □ □ □ □ □ □ □□ □ □ □□ □ □ □ □ □ □ □ □□ □ □□ □ □ □ □□ □ □ □ □□ □ □ □ □□ □ from the optic chiasm may subsequently undergo surveillance every 2–3 years, whereas stable or slowly enlarging macroadenomas located <5 mm from the optic chiasm generally require MRI every 1–2 years. Enlarging or invasive tumours, particularly those with cavernous sinus extension, warrant closer radiological surveillance and multidisciplinary reassessment to determine the need for further intervention. Regular endocrine evaluation should accompany imaging surveillance because new pituitary hormone deficiencies may develop despite radiological stability.

Despite these evidence-based recommendations, surveillance of residual NF-PitNETs continues to rely predominantly on anatomical imaging and endocrine assessment. However, tumour size alone does not reliably predict biological behaviour. While many residual tumours remain stable for prolonged periods, others demonstrate progressive growth despite similar radiological characteristics. This variability highlights the limitations of morphology-based surveillance and has driven increasing interest in complementary biological markers capable of refining individual risk stratification and predicting treatment response.

Recent advances in precision medicine have expanded opportunities to integrate clinicopathological characteristics with circulating biomarkers, molecular profiling, radiomics, and artificial intelligence-assisted MRI analysis. Automated tumour segmentation, volumetric growth modelling, and radiomic feature extraction may improve prediction of tumour progression beyond conventional imaging. Within this evolving framework, the present study extends current surveillance strategies by

integrating longitudinal MRI volumetry with circulating biomarker profiles, composite biological indices, and computational pathway analysis. These complementary biological approaches have the potential to improve prediction of tumour behaviour and identify patients most likely to benefit from tamoxifen, thereby supporting a more personalised approach to postoperative surveillance and treatment.

Although most NF-PitNETs follow an indolent clinical course, a small subset exhibits aggressive behaviour characterised by rapid tumour progression, repeated recurrence despite surgery and radiotherapy, radiological invasiveness, or resistance to conventional treatment. For these uncommon tumours, the 2025 European Society of Endocrinology Clinical Practice Guideline for Aggressive Pituitary Tumours and Pituitary Carcinomas recommends management within specialised multidisciplinary centres, incorporating comprehensive pathological assessment (including Ki-67 labelling index, mitotic count, and p53 immunoreactivity), consideration of molecular profiling where available, intensified MRI surveillance, and timely discussion of repeat surgery, radiotherapy, or systemic therapies when standard treatment has failed (Raverot et al. 2025). These recommendations emphasise dynamic risk assessment and personalised management for the minority of patients whose tumours demonstrate aggressive biological behaviour, complementing the broader surveillance principles recommended for the majority of residual NF-PitNETs.

2.6.2 Surgical Management

Surgery remains the cornerstone of treatment for symptomatic NF-PitNETs, particularly when there are visual field deficits, cranial nerve dysfunction, or radiological evidence of optic chiasm compression and tumour apoplexy. These clinical scenarios require timely operative intervention to prevent irreversible neuro-ophthalmic damage. In contrast, small and asymptomatic incidentalomas may be managed conservatively with interval MRI and endocrine monitoring, as many remain stable or even regress spontaneously over time (Freda et al. 2011). The decision to pursue surgical therapy therefore requires a comprehensive assessment that integrates tumour size, anatomical invasion, patient comorbidities, and surgeon expertise.

The transsphenoidal approach, especially the modern endoscopic endonasal technique, has become the gold standard for most NF-PitNETs. Compared with the traditional microscopic method, endoscopy offers panoramic visualisation, enhanced illumination, and angled optics, improving access to suprasellar and parasellar extensions while reducing surgical morbidity (Juthani et al. 2021). Advances such as intraoperative navigation systems, high-definition 4K endoscopy, and vascularised nasoseptal flap reconstruction have further refined surgical precision and significantly reduced postoperative cerebrospinal fluid (CSF) leak rates to below 5% (Song et al. 2022). Endoscopic-assisted resections are also associated with faster postoperative recovery and shorter hospital stays (Goshtasbi et al. 2021). Although the transsphenoidal approach is preferred, transcranial surgery remains necessary in select cases, particularly for giant tumours, lesions with extensive lateral extension beyond the cavernous sinus, or fibrous tumours where endonasal dissection is limited.

The extent of tumour resection is a major determinant of long-term outcome. Gross-total resection (GTR) is achieved in only 60–73% of macroadenomas, with cavernous sinus invasion (Knosp grades 3–4) posing the greatest challenge to complete removal (Ajlan et al. 2017; Yu et al. 2018). When residual tumour remains, nearly half of patients experience regrowth within 10 years (Batista et al. 2018), whereas recurrence following true GTR occurs in approximately 8% (McClure et al. 2024). Neuro-ophthalmic recovery following decompression is generally favourable, with 68% of patients demonstrating improvement in visual field defects, while 5% deteriorate (Muskens et al. 2017). Factors associated with better visual outcomes include smaller tumour size, shorter duration of visual symptoms, and absence of optic atrophy.

In contrast, restoration of normal pituitary endocrine function following surgery remains unpredictable, based on recent meta-analyses (Pedersen et al. 2022). In a multicentre study, approximately 10% of patients developed new postoperative hormonal deficiencies that frequently necessitate long-term hormone replacement therapy. Fully endoscopic pituitary surgery was associated with improvement in pituitary function in a meaningful subset of patients, with recovery of adrenal function being the most commonly observed endocrine improvement (Little et al. 2020). While no definitive predictors of postoperative glandular recovery were identified, larger

tumour size and cavernous sinus invasion were significant predictors of newly acquired hypopituitarism.

Multiple predictors of surgical success have been identified. Radiological features such as cavernous sinus invasion or sphenoid sinus extension significantly reduce the likelihood of gross total resection (GTR) (Hwang et al. 2016), while tumour consistency also plays a critical role; fibrous tumours are notoriously difficult to resect completely (Chen et al. 2020). Histopathology provides additional prognostic insight, with silent corticotroph (TPIT-lineage) and plurihormonal PIT-1 lineage tumours demonstrating higher recurrence rates than gonadotroph-derived tumours (Manojlovic-Gacic et al. 2018).

Surgical morbidity varies depending on tumour characteristics and the complexity of the procedure. The overall rate of complications ranges from 8% to 26% and includes transient diabetes insipidus, CSF leaks, meningitis, and new hypopituitarism (Namvar et al. 2023). Although the mortality rate remains very low (<1%), long-term follow-up is essential due to the potential for delayed recurrence, evolving endocrine dysfunction, and the risk of future interventions. As the experience of the surgeon affects the complication rate, a centre performing more than 25 transsphenoidal operations for pituitary adenomas per year provides a high likelihood of safe transsphenoidal surgery (Honegger & Grimm 2018).

Overall, surgical management of NF-PitNETs has evolved considerably with the advent of endoscopic techniques, advanced imaging guidance, and improved reconstruction methods. Nonetheless, tumour invasiveness, histological subtype, and proliferative activity remain major barriers to achieving durable disease control, underscoring the need for postoperative surveillance and consideration of adjunctive therapies in selected high-risk patients.

2.6.3 Radiotherapy

Radiotherapy remains a central therapeutic option in the management of NF-PitNETs, particularly for patients with residual, recurrent, or surgically inoperable disease. In these cases, radiotherapy acts as an essential adjunct by inducing double-stranded DNA

damage, mitotic arrest, and cellular senescence, ultimately achieving durable long-term tumour control (Wang et al. 2018a).

Two major radiotherapy modalities are commonly used: fractionated external-beam radiotherapy (EBRT) and stereotactic radiosurgery (SRS), each selected according to tumour size, anatomical constraints, and proximity to critical neurovascular structures. Traditional EBRT delivers a cumulative dose of 45–55 Gy across 25–28 fractions over five to six weeks (Sheehan et al. 2012). Long-term observational data consistently report 10-year progression-free survival (PFS) rates of 85–95%, with measurable tumour shrinkage in up to 90% of patients (Sheehan et al. 2012). These outcomes support EBRT as a reliable option for large or invasive remnants, particularly when the tumour abuts the optic chiasm or cannot safely be treated with single-dose radiosurgery.

However, EBRT has a well-recognised profile of delayed toxicities. Hypopituitarism is the most common long-term complication, affecting 50–80% of patients within 10 years due to radiation injury to normal pituitary and hypothalamic tissue (Fernandez et al. 2009). Other late adverse effects, although less common, include cognitive changes, radiation-induced vasculopathy, optic neuropathy, and, very rarely, secondary neoplasms (Sattler et al. 2015). These risks are particularly relevant in younger patients, highlighting the importance of careful risk–benefit evaluation.

In contrast, stereotactic radiosurgery (SRS)—including Gamma Knife, CyberKnife, and linear accelerator (linac)-based systems – delivers a highly focused, high-dose radiation beam in a single session with sub-millimetre precision. This approach is most suitable for small (< 3 cm), well-circumscribed tumours located at a safe distance from the optic apparatus. Long-term studies demonstrate 10-year local control rates of up to 90–95%, with a relatively favourable toxicity profile, mainly new-onset hypopituitarism (Sheehan et al. 2013). Optic neuropathy is rare when dose constraints are observed. For lesions close to critical structures, fractionated stereotactic radiotherapy (FSRT) offers a hybrid solution, delivering smaller doses over several fractions to minimise optic toxicity while maintaining high efficacy (Kopp et al. 2012).

The decision to initiate radiotherapy is influenced by tumour behaviour, radiological characteristics, and pathological aggressiveness. Radiotherapy is generally indicated for residual invasive macroadenomas, particularly those with cavernous sinus extension where complete resection is rarely achievable; for documented regrowth of residual tissue during surveillance; and for aggressive tumours. The optimal timing of radiotherapy remains debated (Chanson et al. 2019). Some centres favour early adjuvant radiotherapy immediately after surgery to minimise the risk of recurrence in high-risk remnants, while others adopt a deferred approach, reserving treatment for radiologically confirmed progression, thereby reducing unnecessary exposure and long-term endocrine morbidity (Goyal-Honavar et al. 2025). The absence of randomised controlled trials comparing these strategies means that decisions are best made through multidisciplinary consensus, incorporating neurosurgical, endocrine, and radiation oncology perspectives.

Overall, radiotherapy – whether delivered as conventional EBRT or as precision stereotactic techniques – provides excellent long-term tumour control in NF-PitNETs and remains indispensable when surgical cure is not feasible. Advances in radiation planning, targeting accuracy, and fractionation strategies have progressively reduced morbidity while maintaining high efficacy (Hemaidia et al. 2024).

2.6.4 Peptide Receptor Radionuclide Therapy (PRRT)

PRRT is an internal radiotherapeutic approach that delivers targeted radiation to tumour cells expressing specific peptide receptors using gamma-emitting radiopharmaceuticals. Although primarily established for the management of neuroendocrine tumours, PRRT has also been investigated as a therapeutic option for aggressive pituitary tumours resistant to conventional treatments. Various pituitary tumour subtypes express somatostatin receptors and can accumulate radiolabelled somatostatin analogues, such as 68Ga-DOTATATE. In its 2018 clinical practice guidelines, the European Society of Endocrinology recognised PRRT as a potential alternative therapy for aggressive pituitary tumours refractory to standard treatments, including temozolomide (Raverot et al. 2018). However, published studies to date have

involved small patient cohorts, with considerable heterogeneity in administered radionuclides and dosing regimens (Maclean et al. 2014).

2.6.5 Emerging Medical Therapies

Medical therapy for NF-PitNETs has historically been limited by the absence of a dominant hormonal driver and the heterogeneous expression of actionable molecular targets. However, advances in tumour biology, receptor profiling, and molecular genetics have gradually expanded the range of potential pharmacological strategies. Current approaches include dopamine agonists, somatostatin analogues, cytotoxic chemotherapy, targeted molecular therapies, immunotherapies, and other biologically driven experimental treatments. Although none of these options is currently established as first-line therapy for typical NF-PitNETs, they are increasingly used in the management of residual, recurrent, or aggressive disease.

To date, no medical therapies have been formally recommended in treatment guidelines, although cabergoline and somatostatin analogues can improve visual symptoms and induce tumour shrinkage in approximately 20–40% of tumours (Batista et al. 2019; Colao et al. 2008). Dopamine agonists (DAs) were among the earliest pharmacological agents investigated in NF-PitNETs because dopamine D2 receptor (D2R) expression can be demonstrated in a subset of these tumours. Cabergoline and bromocriptine achieve tumour stabilisation in a proportion of patients, although clinically meaningful tumour shrinkage remains uncommon (Colao et al. 2008; Greenman et al. 2016; Iglesias et al. 2022). Among these agents, cabergoline is generally preferred because of its higher receptor affinity, longer half-life, and more favourable tolerability profile. Importantly, therapeutic responsiveness does not appear to correlate with the degree of D2R expression, as shown in a randomised clinical trial (Batista et al. 2019). However, the available studies are limited by small sample sizes, predominantly retrospective designs, and methodological heterogeneity. Dopamine agonists are therefore typically reserved for selected patients with significant postoperative residual disease or tumours not suitable for surgery or radiotherapy.

Somatostatin analogues (SSAs), including octreotide and lanreotide, have also been evaluated based on their affinity for somatostatin receptor subtypes, particularly

SSTR2 and SSTR5 (Colao et al. 2010). Aggressive NF-PitNETs frequently exhibit low SSTR2 expression, which likely explains their limited responsiveness to first-generation SSAs. Some gonadotroph tumours expressing SSTR3 or SSTR5 may show partial responses, although supporting evidence remains largely anecdotal. A case–control study assessed long-acting octreotide (octreotide LAR) in patients with residual tumours demonstrating positive uptake on somatostatin receptor scintigraphy and reported tumour stabilisation in 81% of treated patients compared with 47% in the control group over a mean follow-up of 37 months (Fusco et al. 2012). However, treatment did not result in tumour volume reduction, improvement in visual field defects, or recovery of pituitary function. To date, no clinical studies have specifically examined pasireotide in NF-PitNETs, and available in vitro data have produced inconsistent results (Ibáñez-Costa et al. 2016).

For aggressive or malignant pituitary tumours, temozolomide (TMZ) is the established systemic agent, achieving radiological response rates of approximately 30–40%, particularly in tumours with low O-6-methylguanine-DNA methyltransferase (MGMT) immunoexpression (McCormack et al. 2018). Nevertheless, recurrence following TMZ withdrawal is common, and more than half of initial responders eventually develop resistance (Losa et al. 2016). In parallel, a range of targeted therapies has been explored, including anti-angiogenic agents such as bevacizumab (Dai et al. 2021), epidermal growth factor receptor inhibitors (gefitinib, erlotinib), and mTOR inhibitors such as everolimus, with variable success in case reports and small series (Ilie et al. 2019). Activation of the PI3K/AKT/mTOR pathway, often associated with PIK3CA mutations, provides a rationale for PI3K inhibitors (e.g. alpelisib) and mTOR inhibitors (Dai et al. 2013; Zatelli et al. 2010). Similarly, dysregulation of MAPK signalling suggests potential benefit from MEK inhibitors such as trametinib, although clinical evidence remains preliminary (Serioli et al. 2023).

Immunotherapy has also emerged as a potential option in selected cases. A small subset of mismatch repair–deficient or hypermutated PitNETs has shown responsiveness to immune checkpoint inhibitors targeting PD-1 or PD-L1, such as nivolumab and pembrolizumab (Voellger et al. 2022). However, the low tumour mutational burden in most PitNETs, the rarity of immunogenic cases, and the risk of

immune-related endocrinopathies limit broad applicability. Ongoing studies aim to identify predictive biomarkers for immunotherapeutic benefit.

Additional experimental and epigenetic strategies are being explored. Dopamine–somatostatin chimeric molecules, such as TBR-760, offer dual dopamine and somatostatin receptor targeting and have shown promising activity in preclinical models of dopamine agonist-resistant prolactinomas (Florio et al. 2008). However, there are currently no published clinical studies evaluating TBR-760 in NF-PitNETs, and its potential role in the management of these tumours has yet to be established. Epigenetic therapies, including DNA methyltransferase inhibitors and histone deacetylase inhibitors, have demonstrated tumour-suppressive effects in preclinical models (Shariq & Lines 2019)□ □□ □ □ □ □ □ □ □ □□ □ □ □ □-catenin pathway□ □□ □ □ □□ □ suggests potential roles for Wnt pathway inhibitors or epigenetic modulators aimed at restoring pathway homeostasis. Bromodomain-containing protein 4 (BRD4), a key transcriptional regulator involved in cell cycle control, has also emerged as a novel target. Shi et al. (2020) reported that BRD4 expression is significantly increased in PitNETs compared with normal pituitary tissue and that treatment with the selective BRD4 inhibitor ZBC-260 markedly suppressed proliferation and reduced expression of oncogenic drivers such as c-Myc and B-cell lymphoma-2, despite no significant differences in BRD4 levels among NF-PitNET subtypes.

Collectively, these developments highlight a paradigm shift towards precision medicine approaches guided by tumour lineage, receptor expression, molecular alterations, and immunological features (Voellger et al. 2021). However, despite these advances, effective and durable medical therapies for typical NF-PitNETs remain limited, particularly for patients with residual or progressive disease.

2.7 SELECTIVE OESTROGEN RECEPTOR MODULATOR (SERM) AND ANTI-OESTROGEN IN PITUITARY TUMOURS

There has been sustained interest in anti-oestrogen-based treatments because it is well established that oestrogen signalling plays a key role in the pathogenesis of pituitary adenomas (Gao et al. 2017). Importantly, the relative levels of oestrogen receptor alpha □ □ □ α) □□ □ □ □□ □ □□□□□□□□□□ □ □□□□□ □ □ β) □□ □ □ □□ □□ □ □ □ □ □ □ □ □

pharmacological actions of anti-oestrogens (Paterni et al. 2014). This concept is particularly relevant in NF-PitNETs, in which ER expression is heterogeneous and subtype-dependent, suggesting that modulation of oestrogen signalling could have differential biological and therapeutic effects.

Selective oestrogen receptor modulators (SERMs) are a group of non-steroidal, chemically diverse compounds characterised by tissue-specific modulation of oestrogen receptor signalling. Depending on the cellular context, SERMs can act as oestrogen agonists in some tissues and as oestrogen antagonists in others. Clinically, SERMs are approved for several indications, including breast cancer treatment, prevention and treatment of postmenopausal osteoporosis, and the management of acromegaly (Stone et al. 2014). The first SERM, tamoxifen (TAM), was developed in the 1970s, followed by raloxifene, clomifene, and bazedoxifene (Komm & Mirkin 2014).

Among SERMs, the triphenylethylene compound tamoxifen was the first to demonstrate mixed agonist and antagonist activities at the pituitary gland. In cultured

therefore been postulated to show greater -positive tumours (Esslimani-

responses (Hall & McDonnell 1999b). Support for direct anti-tumour effects of oestrogen receptor modulation in pituitary neoplasia is provided by in vitro studies in pituitary adenoma cell lines representing corticotroph, somatotroph, and lactotroph lineages, rather than non-functioning tumours. In these models, several SERMs (including bazedoxifene, clomifene, and raloxifene) significantly reduced cell viability, induced apoptosis, and suppressed migratory and invasive behaviour, with associated modulation of ERK and p53 signalling pathways (Hannen et al. 2019). In addition to their direct effects on pituitary tumour cells, oestrogens and SERMs exert clinically relevant systemic endocrine actions, particularly on the growth hormone (GH)–insulin-like growth factor 1 (IGF-1) axis (Balili & Barkan 2014). Both oestrogens and SERMs have been shown to significantly reduce circulating IGF-1 production, acting predominantly through impairment of GH signalling at the peripheral (hepatic) level, rather than by suppressing GH secretion itself. On this basis, their use in patients with

persistent acromegaly after surgery or in those unsuitable for surgery has been proposed as a viable therapeutic option. Moreover, the adoption of SERMs or oestrogens as add-on therapy to standard treatments for acromegaly has been shown to improve biochemical disease control (Voltan et al. 2023). Although these data are not derived from NF-PitNET models, they provide important proof-of-principle evidence that oestrogen receptor blockade can exert biologically meaningful anti-tumour effects in pituitary-derived cells.

Fulvestrant is a non-□ □ □ □ □ □ □ □ □ “ □ □ □ □ ” □□ □ □ □ □ □ □ □ □ □ □ □ □ □ □ offer advantages over tamoxifen derivatives, which retain partial agonist activity in the pituitary. Fulvestrant appears to downregulate oestrogen receptor expression and block ER-mediated gene transcription (Nathan & Schmid 2017). In experimental settings, fulvestrant has been shown to inhibit pituitary adenoma growth both in vivo and in vitro through induction of apoptosis (Gao et al. 2017). Additionally, fulvestrant reduces pituitary tumour-transforming gene (PTTG) expression in human pituitary tumours in vitro, further supporting a role for selective anti-oestrogen strategies in pituitary tumour therapy (Heaney et al. 2002). While these findings cannot be directly extrapolated to non-functioning tumours, they reinforce the biological plausibility of targeting oestrogen receptor signalling in pituitary neoplasia and highlight the relative paucity of NF-PitNET–specific functional data.

2.7.1 Integrative Rationale for Tamoxifen in NF-PitNETs

Taken together, the limited efficacy of existing medical therapies in NF-PitNETs, the central role of oestrogen signalling in pituitary tumour biology, and the importance of □ □ □ □□ □ α □ □ □ β □□ □ □ □ □ □ □ □ -oestrogen pharmacology provide a□ □ □ compelling rationale for exploring oestrogen receptor modulation as a therapeutic strategy in this tumour subtype.

Experimental studies also provide biological support for investigating tamoxifen in pituitary tumours. In vitro studies using pituitary tumour cell models have shown that tamoxifen inhibits tumour cell proliferation, induces apoptosis, and modulates oestrogen receptor-mediated signalling pathways involved in cell cycle regulation and tumour growth (Heaney et al. 2002; Lv et al., 2022). However, most

available evidence has been derived from functioning pituitary tumour models or established pituitary cell lines, while direct experimental data in NF-PitNETs remain limited. Consequently, the current study was designed to translate these preclinical observations into a clinical setting by assessing whether tamoxifen produces measurable radiological and molecular effects in patients with residual NF-PitNETs.

Tamoxifen is particularly attractive because of its unique pituitary-relevant pharmacological profile, including its ability to cross the blood–brain barrier and its isoform-selective actions. Tamoxifen is a selective oestrogen receptor modulator (SERM) widely used for the treatment and prevention of breast cancer. It was first synthesised in 1962 and subsequently developed as an effective anticancer agent (Quirke 2017). Clinically, its benefit is greatest in patients with oestrogen receptor–positive tumours, in whom therapeutic responses are consistently superior (Brufsky & Dickler 2018). The defining feature of tamoxifen is its tissue-selective oestrogen agonist and antagonist activity. Tamoxifen is widely distributed in the body, with N-desmethyl-tamoxifen as the principal circulating metabolite. The elimination half-life of tamoxifen is approximately 5–7 days, while its active metabolite has a longer half-life of around 14 days, supporting sustained pharmacological effects during chronic therapy (Jordan 2003).

Tamoxifen is generally well tolerated, but long-term use is associated with a recognised increase in endometrial cancer risk, particularly in postmenopausal women. In the ATLAS trial, continuation of tamoxifen to 10 years (versus stopping at 5 years) increased the incidence of endometrial cancer, with a relative risk of 1.74 (Davies et al. 2013). The cumulative risk during years 5–14 was 3.1% in the continuation group compared with 1.6% in controls, with a small absolute increase in mortality of 0.2%. The excess risk was largely confined to postmenopausal women, with minimal risk observed in premenopausal patients. ATLAS also reported an increased risk of pulmonary embolism (relative risk 1.87), no significant increase in stroke, and a modest reduction in ischaemic heart disease. Importantly, the absolute mortality from endometrial cancer was much lower than its incidence, and the overall survival benefits of tamoxifen in ER-positive disease substantially outweighed these risks (Davies et al. 2013). In the context of potential use beyond breast cancer, these data emphasise the

need for careful patient selection and gynaecological surveillance during prolonged therapy, particularly in postmenopausal women, while recognising that the absolute uterine cancer risk remains small.

From a translational perspective, practical considerations further favour tamoxifen. Bazedoxifene, another SERM capable of crossing the blood–brain barrier, represents a potential alternative but is substantially more expensive, limiting its feasibility for long-term or widespread use. Although fulvestrant has demonstrated robust in vitro antitumour activity in pituitary tumour models, its parenteral (injectable) formulation may present challenges for patient acceptance and long-term treatment adherence. In contrast, tamoxifen is orally administered, widely available, and comparatively inexpensive, making it a more feasible and scalable option for therapeutic repurposing in patients with NF-PitNETs. These considerations together justify tamoxifen as a rational, accessible, and clinically pragmatic candidate for targeting oestrogen receptor signalling in NF-PitNETs, particularly in the setting of residual or progressive disease where established options remain limited.

2.8 BIOMARKERS OF NF-PITNETS

2.8.1 Growth and Angiogenic Pathways

Dysregulation of growth- and angiogenesis-related signalling is one of the most consistently validated molecular domains underlying aggressive behaviour in NF-PitNETs, with the strongest and most comprehensive evidence from gonadotroph tumours. Proteomic profiling has shown that residual gonadotroph NF-PitNETs requiring postoperative reintervention display extensive enrichment of translational machinery, ROBO signalling, and mRNA metabolic processes, involving more than 500 differentially expressed proteins associated with unfavourable clinical outcomes (Hallén et al. 2024). These alterations converge on sustained activation of the PI3K–AKT signalling axis, supported by integrated phosphoproteomic–transcriptomic analyses identifying AKT1 and TSC2 as central regulatory hubs driving tumour growth and progression (Liu et al. 2020). In line with this, reduced SF-1 labelling in gonadotroph tumours correlates with early recurrence and is accompanied by upregulation of stemness-associated markers SOX2 and GFRA3, reinforcing the

concept that PI3K–AKT pathway activation and cellular dedifferentiation programmes are core biological drivers of tumour progression (Hickman et al. 2021).

Multi-omics modelling further refines this growth-promoting landscape by identifying reduced expression of neuroendocrine regulators GALR1 and PENK as hallmarks of invasive behaviour, supporting the notion that loss of neuromodulatory restraint facilitates tumour expansion and spread (Wu et al. 2025). Collectively, these findings indicate that growth-domain dysregulation in NF-PitNETs is not solely proliferative but reflects broader reprogramming of neuroendocrine identity and signalling control.

A complementary set of proliferation-associated biomarkers strengthens the prognostic significance of this domain. Nuclear pEGFR-T693 is significantly enriched in recurrent gonadotroph tumours and serves as an independent predictor of recurrence, highlighting aberrant EGFR activation as a clinically meaningful growth signal (Rai et al. 2021). MCM7, a key regulator of DNA replication licensing, has emerged as one of the most robust indicators of postsurgical progression, with overexpression strongly correlating with the Ki-67 index and mitotic activity in clinically unstable tumours (Hallén et al. 2021). Collectively, MCM7, Ki-67, mitotic count, pEGFR-T693, and PI3K–AKT-associated effectors form a 2.6 biomarker panel for stratifying growth-related recurrence risk in NF-PitNETs. However, these biomarkers have largely been evaluated individually or in retrospective cohorts, and their performance as an integrated biomarker panel has yet to be validated prospectively before they can be adopted for routine clinical risk stratification.

Recent evidence further refines interpretation of the proliferation axis by emphasising coordinated cell-cycle checkpoint dysregulation rather than isolated proliferative indices. Comparative analyses of Ki-67, cyclin D1, and p53 across transcription-factor-defined PitNET subtypes have shown that these markers collectively reflect altered cell-cycle control (Krzentowska et al. 2025a). Ki-67 primarily indicates proliferative activity with limited standalone prognostic value, whereas cyclin D1 overexpression signifies enhanced G1–S phase transition, particularly in hormonally inactive tumours. p53 acts as a modulatory tumour

suppressor whose biological relevance becomes apparent mainly in combinatorial assessments. Notably, the concurrence of high cyclin D1 expression with reduced p53 expression identifies a subset of uniformly invasive tumours, underscoring the superior discriminative power of integrated growth-domain biomarker assessment compared with single-marker evaluation (Krzentowska et al. 2025a).

Beyond canonical proliferation signalling, growth and angiogenic behaviour in NF-PitNETs are further shaped by epithelial–mesenchymal transition (EMT)-associated and microenvironment-modulating factors. Upregulation of SNAI1, SNAI2, Vimentin, and KLK10—initially characterised in invasive corticotroph tumours (Gil et al. 2023)—is relevant in this context due to their roles in cytoskeletal remodelling, tumour expansion, and extracellular matrix (ECM)-mediated invasion. These EMT regulators enhance cellular motility, promote proliferative plasticity, and establish a microenvironment permissive to angiogenesis and sustained growth. Notably, nuclear localisation of E-cadherin and its adaptor KLHL14 in highly invasive tumours reflects intracellular relocalisation rather than loss of adhesion protein, and is associated with shorter progression-free intervals (Berardinelli et al. 2024). In parallel, the stemness-associated protein S100B contributes to adhesion restructuring and cellular dedifferentiation, further supporting its role as an auxiliary marker of invasive growth potential in NF-PitNETs.

Additional regulatory complexity in this domain is introduced by modulators of the EGFR–STAT3 axis. Long non-coding RNAs EGFR-AS1, LINC00240, and SNHG12, which regulate EGFR–STAT3 signalling and are significantly downregulated in invasive NF-PitNETs, influence proliferative transcriptional programmes and growth-factor responsiveness (Esmaeili Motlagh et al. 2024). Their dysregulation suggests lineage-independent enhancement of tumour growth capacity through altered post-transcriptional control.

Exosomal microRNAs further reinforce the growth–angiogenic phenotype. Exosomal miR-151a-5p, miR-652-3p_R+1, and miR-1180-3p are consistently associated with invasive NF-PitNET behaviour and modulate pathways governing cell adhesion, cytoskeletal organisation, and proliferative signalling (Lyu et al. 2021).

Through vesicle-mediated intercellular communication, these microRNAs support angiogenic processes and amplify tumour expansion via paracrine and autocrine signalling loops.

Growth-associated dysregulation is also evident in null-cell and mixed-lineage tumours. Large-scale acetylome analyses have identified down-acetylation of 296 proteins involved in metabolic regulation, translation, oxidative stress responses, and cell adhesion, implicating epigenetically mediated metabolic rewiring as a driver of tumour expansion (Wen et al. 2021). Null-cell tumours also demonstrate alterations in checkpoint regulators, including E2F1, p16, pE2F1-S364, and CHEK2, consistent with impaired senescence control and sustained proliferative capacity (Metin-Armagan et al. 2020). In contrast, conventional proliferation and angiogenesis markers such as Ki-67, Bcl-2, CD34/CD105, and VEGF-A do not reliably discriminate invasive from non-invasive phenotypes (Ghadir et al. 2020), underscoring the superior prognostic value of integrative, multi-omics-derived biomarkers.

Extracellular matrix remodelling constitutes an additional growth-enabling mechanism in this context. Null-[illegible] MMP alongside downregulation of TIMP1, forming a hypoxia-driven proteolytic axis that promotes invasive growth independently of classical EMT pathways (Yu et al. 2025). Similarly, proteases such as CTSK, MMP2, and MMP9 correlate strongly with sphenoid sinus and cavernous sinus invasion, highlighting the close association between ECM degradation, tumour expansion, and anatomical spread (Liu et al. 2022). Exosomal MMP1 (exo-MMP1), a consistent feature of invasive NF-PitNETs, further promotes angiogenesis and tumour cell migration via PAR-1-mediated signalling, directly linking vesicle-associated proteolysis to tumour progression (Ren et al. 2022). The protease-dominant signature described by Ren Yuan and colleagues further indicates that liquid-biopsy interpretation must account for matrix-remodelling activity, which can elevate certain RNAs or proteins irrespective of tumour lineage, necessitating subtype-inclusive analytical strategies (Ren et al. 2022).

Epigenetic dysregulation further integrates into this growth–angiogenic framework. DNA methylation analyses identified 605 differentially methylated CpG

sites across 389 genes in tumours requiring reintervention compared with radiologically stable gonadotroph NF-PitNETs, implicating epigenetic control as a determinant of postoperative progression (Hallén et al. 2024). Tissue-level profiling demonstrated that hypomethylation of NUP93 and LGALS1 strongly predicts the need for reintervention, supporting the lineage-independent prognostic utility of DNA methylation markers (Hallén et al. 2022). In parallel, exosomal miRNA profiling identified hsa-miR-486-5p as the strongest diagnostic and prognostic circulating marker, with expression changes correlating with longitudinal progression risk, offering a feasible non-invasive surveillance tool for gonadotroph populations frequently managed conservatively (Lyu et al. 2021).

Finally, transcriptomic systems-level analyses reinforce the integrative nature of growth-domain dysregulation. A three-way interaction model associated tumour invasiveness with biological processes involving mRNA processing and spindle organisation, nominating Nkx3-1 and Fech as switch genes governing invasive states (Khayer et al. 2021). Moreover, a 21-transcript mRNA classifier achieved high accuracy in identifying invasive tumours, supported by protein-level validation of INSM1 and HSPA2 and exploratory detection of exosomal RNA, underscoring the feasibility of integrating liquid-biopsy approaches in mixed-lineage NF-PitNETs (Bao et al. 2021).

Collectively, growth and angiogenic biomarkers – including PI3K–AKT-associated effectors, coordinated proliferation and cell-cycle regulators, EMT-associated proteins, EGFR–STAT3-modulating long non-coding RNAs, exosomal microRNAs, ECM-remodelling proteases, and epigenetic signatures – form a dominant and integrative molecular domain that underpins NF-PitNET expansion, invasiveness, and aggressive clinical behaviour across tumour lineages.

2.8.2 Inflammation

Inflammation in NF-PitNET is shaped by interactions between tumour cells and the surrounding immune microenvironment. In unclassified and mixed-lineage NF-PitNETs, an eight-gene immune–invasion classifier demonstrated strong predictive accuracy for invasive behaviour, highlighting the contribution of inflammatory gene

activation and immune infiltration to tumour progression (Wu et al. 2023). These findings underscore the role of inflammation-associated transcriptional signatures as determinants of clinical behaviour across tumour subtypes.

Alterations in inflammatory cell death pathways further reinforce the significance of inflammation in tumour biology. Reduced expression of the necroptotic mediators RIP3K and MLKL was associated with increased tumour size and invasion, suggesting that suppression of necroptosis may facilitate tumour survival and expansion (Khamseh et al. 2022). This attenuation of inflammatory programmed cell death reflects a mechanism through which NF-PitNETs may persist within an immune-modulated microenvironment.

Collectively, inflammation-driven signalling in NF-PitNETs encompasses immune infiltration patterns, suppression of inflammatory cell death pathways, and coordinated immune–proliferative transcriptional networks.

2.8.3 Cytokine and TNF Axis

Epigenetic and post-transcriptional mechanisms further refine cytokine and TNF signalling in NF-PitNETs. Dysregulation of long non-coding RNAs associated with STAT3-mediated transcription has been identified in invasive tumours, highlighting an additional regulatory layer controlling cytokine responsiveness and downstream transcriptional programmes (Esmaeili Motlagh et al. 2024). These lncRNA alterations suggest that cytokine-driven gene networks may be epigenetically reprogrammed to enhance tumour adaptability, immune crosstalk, and invasive capacity.

Endocrine–immune interaction constitutes an additional modulatory component of this axis. Endocrine receptor profiling has demonstrated a bimodal pattern of ESR1 expression with functional correlation to GREB1, indicating transcriptionally active oestrogen signalling even within mixed NF-PitNET populations (Hattori et al. 2020). This finding suggests convergence between hormone-responsive pathways and cytokine-regulated transcriptional networks, reinforcing the role of cytokine–growth crosstalk in shaping tumour behaviour.

Systemic corroboration of cytokine-axis dysregulation is provided by circulating non-coding RNA profiles. Serum studies have consistently reported downregulation of candidate tumour-suppressive microRNAs, including miR-26b, miR-138, miR-206, and let-7e, which are known to restrain cytokine-responsive and invasion-related transcriptional programmes (Zhang et al. 2021). Suppression of these circulating miRNAs parallels tissue-level activation of growth and invasion networks, indicating that cytokine/TNF-axis perturbations extend beyond the local tumour microenvironment. Their detectability in circulation supports their potential utility as minimally invasive biomarkers of aggressive behaviour and post-surgical progression risk (Zhang et al. 2021).

Collectively, these findings establish the cytokine and TNF axis as a coherent and biologically relevant biomarker domain in NF-PitNETs. Through coordinated chemokine receptor signalling, cytokine-responsive lncRNA dysregulation, endocrine–immune crosstalk, and circulating microRNA alterations, this domain integrates immune activity with tumour growth dynamics and contributes to invasion, progression, and recurrence risk.

Within this immunologically active landscape, PD-L1 serves as a complementary biomarker reflecting tumour–microenvironment interaction rather than classical cytokine signalling alone. In the study by Krzentowska et al. (2025), PD-L1 expression (tumour proportio□ □□ □ □ □ □ ≥ □ %) □□ □ □ □□ □ □ □ □ □ □ □□ □ □□ □ □ □ □ higher prevalence in gonadotroph, corticotroph, and particularly null-cell tumours. Its strongest diagnostic utility was observed in null-cell adenomas, suggesting that less-differentiated tumours may preferentially engage immune checkpoint mechanisms as part of immune-evasive and aggressive growth programmes. Although PD-L1 did not reach statistical significance as an independent predictor of invasiveness, it showed the highest odds ratio for invasive behaviour among evaluated biomarkers, supporting its role as a microenvironment-linked growth and immune-modulatory marker rather than a standalone inflammatory indicator (Krzentowska et al. 2025a).

2.8.4 Wnt Pathway and Wnt-Modulatory Networks

Dysregulation of Wnt signalling has emerged as a reproducible and biologically coherent feature across NF-[illegible]-catenin–centred β mechanisms occupying a [illegible]-catenin at Ser552 has been strongly associated with tumour invasion and postoperative recurrence, providing a robust phospho-signature of canonical Wnt pathway activation (Rai et al. 2022). This modification reflects functional cross-talk between AKT and Wnt signalling cascades, [illegible]-catenin stabilisation β, nuclear translocation, and transcriptional activation of growth- and invasion-related gene programmes. Collectively, these findings position β-catenin as a key transcriptional integrator linking proliferative signalling with invasive tumour behaviour.

Beyond direct pathway activation, epigenetic disruption of Wnt-modulatory circuits further contributes to NF-PitNET progression. Genome-wide DNA methylation profiling has identified hypermethylation of GABRA1 as a highly discriminative marker of aggressive behaviour and postsurgical progression (Hallén et al. 2022). Although GABRA1 is classically associated with GABAergic neurotransmission, its relevance in NF-PitNETs lies in its epigenetic silencing and functional clustering with extracellular Wnt antagonists, including sFRP2, sFRP4, and WIF1. This coordinated [illegible]-catenin activity and [illegible] transcriptional reprogramming associated with invasion and recurrence. These observations underscore the importance of chromatin-level and transcriptional modulation of Wnt-regulatory networks in determining postoperative tumour behaviour.

Circulating Wnt-related microRNAs provide an additional, minimally invasive layer of evidence supporting Wnt pathway involvement in NF-PitNET aggressiveness. Exosomal miR-93-3p, miR-574-5p, and miR-134 are significantly altered in NF-PitNETs and are known regulators of Wnt-driven transcriptional outputs, cytoskeletal organisation, and proliferative signalling (Lyu et al. 2021). Their consistent modulation in patient serum reinforces their potential utility as liquid biopsy biomarkers for

monitoring Wnt pathway activity and predicting invasive potential, particularly in tumours managed with postoperative surveillance.

Collectively, Wnt pathway and Wnt-modulatory markers define an integrated mechanistic framework underpinning invasive and recurrent NF-PitNET biology. □□□□□□□□ β-catenin activation, epigenetic reprogramming of Wnt inhibitory networks, and systemic dissemination of Wnt-related microRNA signals, this domain represents a core molecular axis driving transcriptional plasticity, tumour expansion, and postsurgical recurrence. Although multiple signalling systems contribute to NF-PitNET biology, only a subset of these perturbations translate into measurable biomarkers suitable for diagnostic, prognostic, or monitoring purposes.

Current discoveries, including circulating proteins, exosomal components, tissue markers, methylation signatures, and microRNAs, are summarised in Table 2.6.

Table 2.6 Summary of biomarkers in NF-PitNETs

Domain	Biomarker Category	Specific Biomarkers	Clinical / Translational Relevance
Growth / Angiogenic Pathways	Core growth signalling (multi-omics)	AKT1, TSC2; hub group: SPARCL1, IGFBP5, SCG3	Central growth-state regulators repeatedly associated with aggressive behaviour
	Lineage & dedifferentiation markers	SF-1 □↓) □□□□2 □	Loss of differentiation and stemness enrichment; linked to early recurrence
	Neuroendocrine restraint / neurosignalling	GALR1, PENK	Loss associated with invasive growth and reduced neuroendocrine differentiation
	EGFR signalling	pEGFR-T693	Independent predictor of postoperative recurrence
	Replication & proliferation	MCM7, Ki-67, mitotic count	Robust indicators of postsurgical progression; MCM7 among the strongest
	Cell-cycle checkpoints	Cyclin D1, p53	Combinatorial patterns □□□□□□□□□□↑ □□ uniformly invasive tumours
	EMT & cytoskeletal remodelling	SNAI1, SNAI2, Vimentin, KLK10	Promote invasion, motility, and angiogenic permissiveness
	Adhesion / junction remodelling	KLHL14, nuclear E-cadherin; E-/N-cadherin distribution	Reflect adhesion plasticity and invasive phenotype

□□□□□□□□

…□ □ □ □ □ □ □ [

	Receptor-linked growth markers	SSTR2, EphB6, HTR2B	Associated with tumour size, growth signalling, or invasive phenotype
	Switch-gene / invasive-state regulators	Nkx3-1, Fech	Govern transcriptional transitions between non-invasive and invasive states
	EGFR–STAT3-modulating lncRNAs	EGFR-AS1, LINC00240, SNHG12	Post-transcriptional regulation of growth-factor responsiveness
	Exosomal growth-related miRNAs	miR-151a-5p, miR-652-3p_R+1, miR-1180-3p, miR-486-5p	High-performance liquid-biopsy markers of invasive growth and angiogenesis
	Epigenetic & metabolic rewiring	Hypo-acetylated protein panel (296 proteins)	Metabolic reprogramming linked to tumour expansion
	Senescence & checkpoint escape	E2F1, p16, pE2F1-S364, CHEK2	Impaired senescence and sustained proliferative capacity
	Hypoxia & ECM remodelling	□ □ □ □ □ α □ □ -MMP, □ □ □ □ □ □ □ ↓)	EMT-independent invasive growth
	Proteases (tissue / exosomal)	CTSK, MMP2, MMP9, exosomal MMP1	Strong correlation with cavernous/sphenoid sinus invasion
	Epigenetic growth modulators	NUP93 (hypomethylated), LGALS1 (hypomethylated)	Growth- and angiogenesis-linked predictors of progression and reintervention
	Multi-marker classifiers	21-transcript invasive classifier (INSM1, HSPA2); 605-CpG / 389-gene methylation signature	High diagnostic accuracy for invasion and postoperative risk
Inflammation	Immune–invasion transcriptional programmes	Eight-gene immune–invasion classifier	Predicts invasive behaviour in unclassified/mixed-lineage NF-PitNETs
	Necroptosis pathway suppression	□ □ □ □ □ □ □ ↓) □ □ □	Suppression associated with increased tumour size and invasion
Cytokine / TNF Axis	TNF-associated signatures	TNF-linked transcriptomic profiles	Enriched in invasive NF-PitNETs
	Chemokine receptors	CXCR4	Mediates immune-cell recruitment and stromal activation
	STAT3-associated regulatory lncRNAs	STAT3-linked lncRNA network	Epigenetic modulation of cytokine responsiveness
	Cytokine-linked transcription factors	KLF8, PITX2	Interface cytokine signalling, stemness, and invasion
	Estrogen–cytokine crosstalk modulators	ESR1, GREB1	Context-dependent modulation of growth–cytokine signalling

□ □ □ □ □ □ □ □ □

...continuation

	Circulating cytokine-linked miRNAs	miR-26b, miR-138, miR-206, let-□ □ □ ↓)	Minimally invasive biomarkers of cytokine-driven aggressiveness
	Immune checkpoint markers	PD-□ □ □ □ □ □ ≥ □ %)	Tumour–microenvironment interaction; subtype discrimination; trend-level association with invasiveness
Wnt Pathway / Wnt-Modulatory Networks	Canonical Wnt activation	Nuclear β-catenin; phospho-β-catenin (Ser552)	Strongly associated with invasion and postoperative recurrence
	Epigenetic Wnt antagonists / modulators	sFRP2, sFRP4, WIF1; GABRA1 (hypermethylated)	Loss of extracellular Wnt inhibition; highly reproducible invasion markers
	Exosomal Wnt-related miRNAs	miR-93-3p, miR-574-5p, miR-134	Liquid-biopsy indicators of Wnt-driven invasion and cytoskeletal regulation

*TPS – tumour proportion score

2.9 COMPUTATIONAL AND NETWORK PHARMACOLOGY APPROACHES

2.9.1 Rationale for Computational Approaches in Tumour Biology

Tumour biology is increasingly recognised as a complex, multi-layered process driven by interconnected signalling networks rather than isolated molecular events. In pituitary tumours, growth, invasiveness, and treatment response are influenced by the dynamic interplay between growth factor signalling, angiogenic pathways, inflammatory mediators, and intracellular kinase cascades (Haydar Ali Tajuddin et al. 2025). Traditional single-target or single-biomarker approaches are often insufficient to capture this biological complexity (Di Mauro et al. 2025). Recent integrative multi-omics analyses have shown that NF-PitNET pathogenesis is driven by coordinated pathway-network alterations rather than isolated molecular changes, supporting a systems-level, multi-marker analytical strategy for biomarker discovery and therapeutic interpretation (Wen et al. 2022).

In this context, systems biology and computational modelling have emerged as important complementary strategies to experimental and clinical research (Wang et al. 2015). These approaches enable the integration of large-scale biological data, facilitate hypothesis generation, and allow exploration of network-level mechanisms underlying drug action and disease behaviour. Rather than focusing solely on one receptor or

pathway, computational methods aim to characterise how multiple targets and signalling modules interact to shape phenotypic outcomes, which is particularly relevant for tumours with heterogeneous molecular drivers such as NF-PitNETs.

2.9.2 Network Pharmacology and Drug Repurposing in Oncology

Network pharmacology applies systems biology principles to pharmacology by modelling drugs, targets, and pathways as interconnected networks. This approach is particularly suited to complex diseases such as cancer, where effective therapies often act by modulating multiple targets rather than a single molecular node. In oncology, network-based methods are increasingly used to investigate drug mechanisms, predict off-target effects, identify synergistic pathways, and support drug repurposing strategies (Li & Kar 2025).

Drug repurposing, the identification of new therapeutic indications for existing drugs, offers several advantages, including reduced development time, lower cost, and established safety profiles (Kulkarni et al. 2023). For rare or clinically challenging tumours such as NF-PitNETs, where effective medical therapies are limited, repurposing strategies are especially appealing. Tamoxifen, a selective oestrogen receptor modulator (SERM) with established clinical use in breast cancer, is a candidate for this approach. Although its classical mechanism involves modulation of oestrogen receptor signalling, accumulating evidence indicates that tamoxifen also affects multiple non-classical pathways, including PI3K/AKT, MAPK/ERK, and apoptosis-related signalling cascades (Rouhimoghadam et al. 2018). Network pharmacology offers a conceptual and analytical framework to systematically explore these multi-target effects and link them to tumour-relevant biological processes.

2.9.3 In Silico Target Prediction, Protein–Protein Interaction Networks, and Pathway Enrichment

Contemporary computational workflows in network pharmacology typically integrate several key components. In silico target prediction tools, such as ligand-based or structure-based algorithms, identify putative protein targets of a given compound based on chemical similarity, pharmacophore matching, or known bioactivity profiles. These

predicted targets can then be mapped onto protein–protein interaction (PPI) networks to visualise and analyse their functional interrelationships within the cellular context.

PPI network analysis enables the identification of highly connected nodes, or “[illegible]” [illegible] is, and disease pathogenesis (Guo et al. 2021). In parallel, pathway enrichment analysis using curated databases such as the Kyoto Encyclopaedia of Genes and Genomes (KEGG) groups target genes into biologically meaningful pathways, facilitating interpretation at the systems level (García-Campos et al. 2015). Together, these approaches shift the analytical focus from individual genes to coordinated signalling modules, which is more consistent with the known biology of tumour progression and therapeutic response.

In endocrine and neuro-oncological research, such integrative in silico strategies have been increasingly applied to explore molecular mechanisms, identify candidate biomarkers, and prioritise pathways for experimental validation (Feng et al. 2023b; Meng et al. 2023). Although these methods are inherently hypothesis-generating, they provide a rational, data-driven means of contextualising experimental and clinical observations within broader signalling networks.

2.9.4 Relevance to NF-PitNETs and Translational Research

NF-PitNETs are characterised by significant biological heterogeneity and a lack of effective medical treatment options for residual or recurrent disease. Although advances in molecular pathology and biomarker research have improved understanding of their pathogenesis, translating these insights into targeted therapies remains limited. In this context, a network-based computational approach offers several advantages. First, it enables the integration of diverse molecular signals – such as growth, angiogenic, inflammatory, and kinase-driven pathways – into a unified analytical framework. Second, it facilitates the identification of key signalling hubs and pathway clusters that may underlie tumour behaviour and therapeutic response. Third, it provides mechanistic context for clinical and biomarker findings, thereby strengthening the biological plausibility of observed treatment effects.

In a translational study design combining immunohistochemistry, clinical imaging outcomes, serum biomarker profiling, and computational modelling, network pharmacology serves as an important bridge between molecular data and clinical phenotypes. Specifically, in the context of tamoxifen therapy for NF-PitNETs, computational analysis can predict relevant targets, highlight convergent signalling pathways such as PI3K/AKT and MAPK, and identify central hub genes that may mediate growth and angiogenic modulation. This integrative perspective supports a shift from a single-receptor view of tamoxifen action towards a multi-pathway, systems-level interpretation.

2.10 REVIEW OF METHODOLOGY AND LIMITATIONS

NF-PitNETs are clinically heterogeneous lesions with unpredictable postoperative behaviour, especially in patients with residual disease. Biologically, a substantial body of literature has focused on tumour phenotyping using histopathology and molecular markers, including proliferative indices and ER expression. The finding that a proportion of NF-PitNETs express ERs has provided a mechanistic rationale for implicating oestrogen signalling in pituitary tumour biology and for considering endocrine modulation as a potential therapeutic strategy.

Building on this biological foundation, anti-oestrogen approaches, including tamoxifen and related agents, have been investigated primarily in cell lines and in vitro or experimental models of pituitary tumours. These studies have shown that oestrogen receptor modulation can influence tumour cell proliferation, signalling pathways, and interactions with developmental pathways such as Wnt signalling. However, despite this preclinical rationale, there have been no prospective clinical trials evaluating tamoxifen in patients with NF-PitNETs, and human evidence remains limited to indirect or extrapolated observations from other pituitary tumour subtypes and experimental systems.

In parallel, considerable effort has been devoted to identifying biomarkers that reflect tumour biology, aggressiveness, and risk of progression in NF-PitNETs. This literature is dominated by tissue-based markers derived from surgical specimens, including ER expression, proliferation markers, growth factor signalling components,

inflammatory mediators, and elements of Wnt and other developmental pathways. More recently, interest has emerged in circulating biomarkers as minimally invasive tools for disease monitoring, although such studies remain scarce in NF-PitNETs and are typically limited by small sample sizes and cross-sectional designs.

More recently, bioinformatics and network-based approaches have been applied to pituitary tumour research, enabling the exploration of pathway enrichment, protein–protein interaction networks, and multi-target drug–gene relationships. These studies highlight the complexity of signalling crosstalk involving oestrogen receptors, growth and angiogenic pathways, inflammatory and cytokine networks, and Wnt modulators. However, in NF-PitNETs, such analyses remain largely disconnected from longitudinal clinical data and have not been incorporated into prospective therapeutic studies, limiting their translational impact.

Across these layers of evidence – from receptor biology, to preclinical therapeutic models, biomarker discovery, and finally bioinformatics modelling – several limitations are evident. The literature is predominantly cross-sectional and retrospective, providing static snapshots of a disease that is inherently dynamic. Clinical endpoints are often crude or dichotomised, and molecular studies are frequently siloed, with limited integration between tissue biology, circulating markers, imaging dynamics, and therapeutic response. Moreover, analytical strategies have generally relied on single-marker or single-pathway approaches, despite clear evidence of network-level biological interactions.

These limitations have important translational consequences. Despite strong biological and preclinical justification for targeting oestrogen signalling in NF-PitNETs, there is currently no clinical trial evidence to define the therapeutic impact of tamoxifen in this setting, nor any integrated framework linking ER status, downstream molecular pathways, and longitudinal tumour behaviour in patients. Similarly, there are no validated biomarker or systems-level models to guide postoperative surveillance, predict residual tumour growth, or stratify patients for medical therapy. As a result, clinical management remains largely reactive and empirical rather than mechanism-informed or predictive.

Therefore, computational results should be considered complementary to, rather than a substitute for, experimental and clinical data. Their main value lies in guiding interpretation, prioritising targets and pathways, and providing a coherent mechanistic framework that can be tested and refined through laboratory and clinical investigation. In the context of NF-PitNETs, where tissue access and large clinical cohorts are limited, such integrative approaches offer a pragmatic and scientifically grounded strategy to advance mechanistic understanding and therapeutic exploration.

Taken together, the literature reveals a central gap: the absence of a prospective, integrative, and translational clinical framework that connects tumour receptor biology, preclinical therapeutic rationale, quantitative imaging dynamics, longitudinal biomarker profiles, and systems-level pathway analysis to treatment response and disease behaviour in NF-PitNETs. While mechanistic and experimental data are increasingly sophisticated, they have not yet been translated into patient-level, longitudinal, intervention-based evidence. Figure 2.6 summarises the progression of the literature review from established knowledge in NF-PitNETs and prevailing methodological approaches, through key conceptual and methodological limitations and their translational consequences, to the identification of a central unmet need. This funnel culminates in the rationale for an integrative, longitudinal, multi-domain framework linking tumour tissue biology, quantitative imaging, circulating biomarkers, and multivariate analysis.

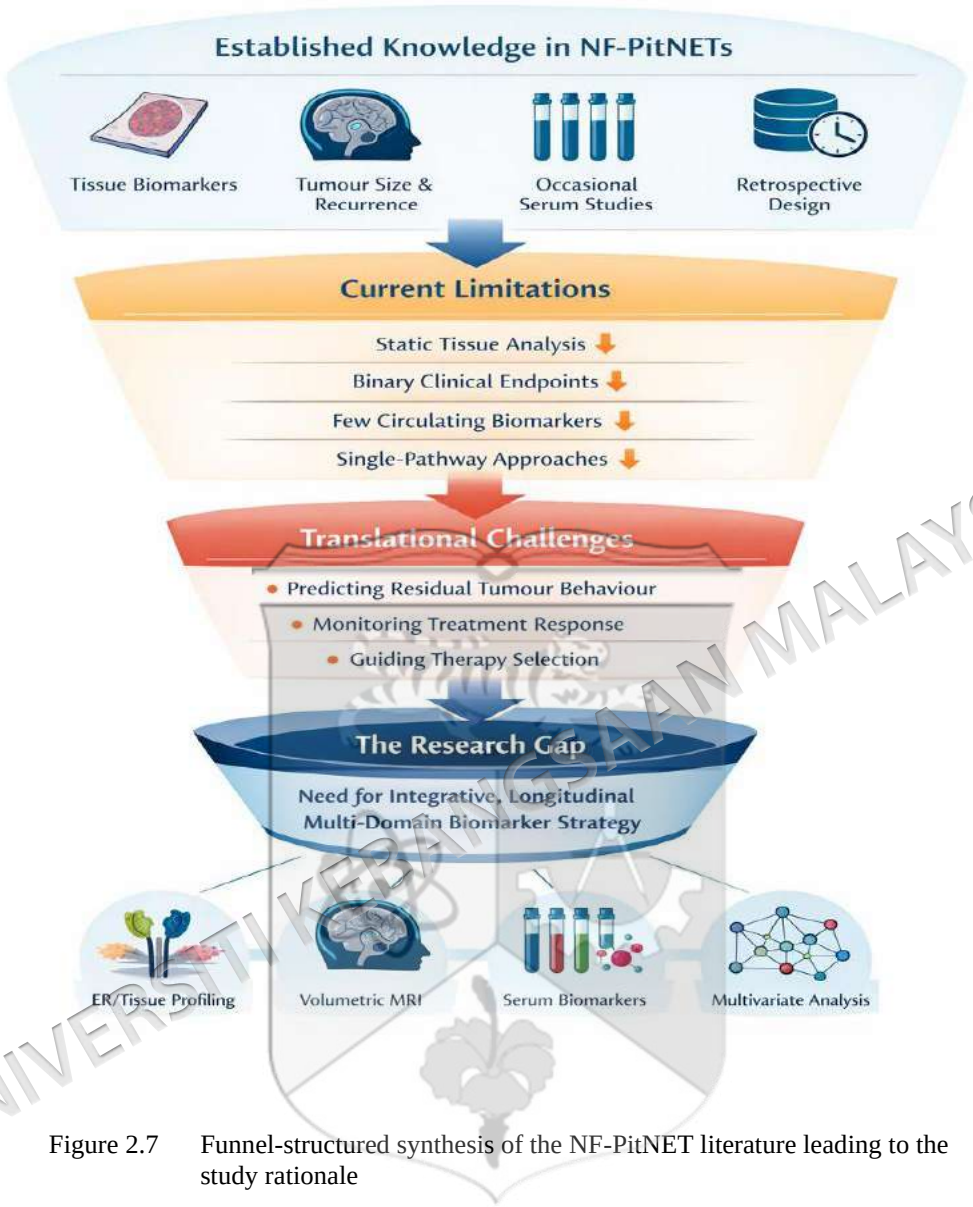

Figure 2.7 Funnel-structured synthesis of the NF-PitNET literature leading to the study rationale

2.11 SUMMARY

This chapter critically reviewed the biological, pathological, and clinical foundations of NF-PitNETs to establish the scientific rationale the present study. It commenced with an overview of normal pituitary gland anatomy and physiology, providing the structural and functional context necessary to understand tumour development. This was followed by a comprehensive discussion of pituitary tumours and their classifications, incorporating recent updates from the WHO, and the contemporary prognostic framework.

The chapter then examined NF-PitNETs in detail, including their epidemiology, natural history, clinical presentation, histopathological subtypes, and underlying pathophysiological mechanisms. Particular emphasis was placed on key molecular pathways implicated in tumour growth and progression, including proliferative and angiogenic signalling networks, inflammatory cascades, the cytokine-TNF immune checkpoint axis, and Wnt signalling and its regulatory modulators. The role of oestrogen receptor signalling in pituitary tumorigenesis was also explored, providing a mechanistic basis for therapeutic modulation through anti-oestrogen strategies.

Current management paradigms were synthesised, highlighting the importance of multidisciplinary care and reviewing established and emerging treatment modalities, including surgery, radiotherapy, peptide receptor radionuclide therapy, and evolving systemic therapies. A focused evaluation of selective oestrogen receptor modulators was undertaken, with specific attention to the biological and translational rationale for tamoxifen in NF-PitNETs.

Next, candidate biomarkers spanning proliferative, angiogenic, inflammatory, immune-regulatory and hormonal domains were reviewed, alongside computational and network-based approaches as complementary tools to integrate molecular data, including in silico target prediction, protein–protein interaction analysis, and pathway enrichment. Finally, methodological considerations and recognised limitations in the existing literature were highlighted. Collectively, this chapter integrated current evidence, identified critical knowledge gaps, and defined the conceptual and translational framework that underpins the subsequent chapters of this thesis.

CHAPTER III

METHODOLOGY

3.1 OVERVIEW

This chapter outlines the methodological framework used to investigate the therapeutic and mechanistic role of tamoxifen in residual NF-PitNETs. Given the rarity and biological heterogeneity of NF-PitNETs, the study was designed as a translational, proof-of-concept investigation integrating laboratory-based tissue analysis, a pilot clinical trial, serum biomarker profiling, and in silico bioinformatics analyses. This integrative strategy was chosen to balance scientific rigour with feasibility in a rare-disease context, while enabling both clinical and mechanistic questions to be addressed within a single coherent framework.

Figure 3.1 summarizes the methodology which comprises four interlinked components: (i) immunohistochemical characterisation of archival NF-PitNET tissues; (ii) a 12-month, open-label, randomised pilot trial comparing tamoxifen with active surveillance; (iii) serum biomarker profiling using multiplex immunoassays and ELISA within a predefined, domain-based framework; and (iv) in silico target prediction, pathway enrichment, and protein–protein interaction network analyses.

The chapter details the study design, study population, sample size and power considerations, research instruments, laboratory procedures, imaging procedure, bioinformatics workflow, statistical analyses, and ethical considerations. This structured and transparent approach ensures methodological coherence and reproducibility, providing a robust foundation for interpreting the results presented in subsequent chapters.

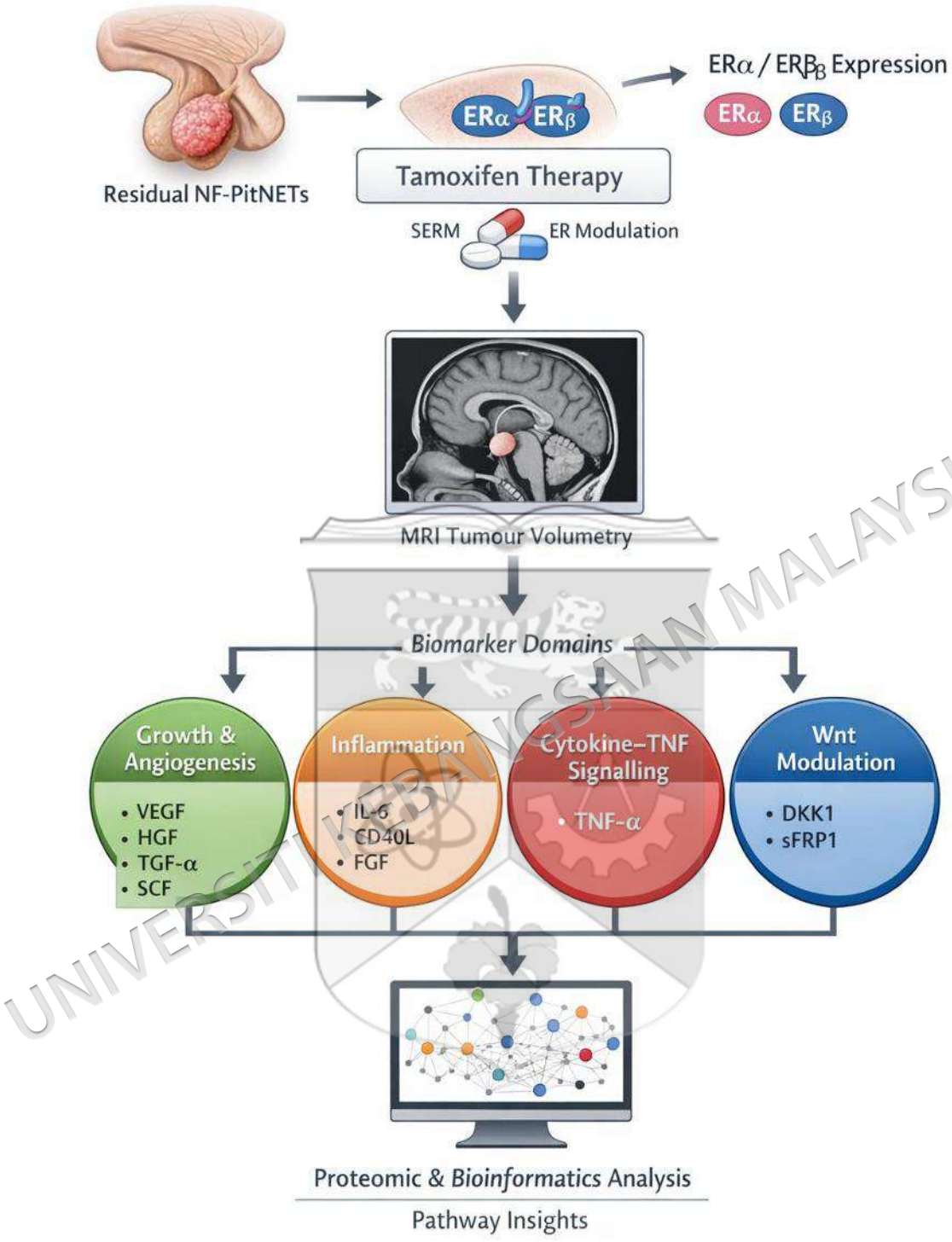

Figure 3.1 Methodology flowchart

3.2 STUDY DESIGN

This study was designed as a translational, proof-of-concept investigation integrating tissue-based laboratory analyses, a clinical intervention, and complementary molecular and computational bioinformatic approaches to evaluate the therapeutic potential of tamoxifen in residual NF-PitNETs, while simultaneously exploring associated molecular and biomarker changes.

The design addressed each study objective with a dedicated methodological component. For the first objective, archival formalin-fixed, paraffin-embedded NF-[illegible] expression, along with proliferative markers (Ki-67, p53, and mitotic counts), were evaluated to define receptor prevalence and tumour behaviour. Semi-quantitative H-[illegible] pathological characterisation. This component established the biological rationale for targeting oestrogen receptor signalling.

The second objective was addressed through a prospective, randomised, open-label pilot clinical trial comparing tamoxifen with active surveillance in patients with residual NF-PitNETs following surgery. Participants were randomised in a 1:1 ratio and followed for 12 months. Serial magnetic resonance imaging (MRI) with blinded volumetric assessment quantified tumour response over time, providing an objective measure of treatment effect.

To achieve the third objective, longitudinal serum samples were collected at predefined time points and analysed using multiplex immunoassays and enzyme-linked immunosorbent assay (ELISA). Biomarkers were selected to represent four predefined biological domains: growth/angiogenic, inflammatory, cytokine–TNF, and Wnt modulatory pathways. Changes in biomarker profiles were analysed in relation to treatment allocation and MRI-defined tumour outcomes.

This final objective was addressed using in silico bioinformatics analyses to predict tamoxifen-interacting genes and enriched signalling pathways. These findings were integrated with the serum biomarker domains and clinical outcomes to provide a

systems-[illegible] of action in NF-[illegible] PitNETs.

Collectively, this objective-driven, multi-tiered design links tissue biology, clinical efficacy, circulating biomarkers, and molecular pathway analysis, providing a coherent translational framework for investigating tamoxifen therapy in a rare tumour setting.

3.3 STUDY POPULATION

Participants were recruited from two high-volume referral centres in Malaysia: the Endocrine Clinic at Hospital Canselor Tuanku Muhriz (HCTM) and the Neurosurgery Clinic at Hospital Kuala Lumpur (HKL). Both centres serve as national referral hubs for pituitary disorders, ensuring access to a diverse and representative patient population. Recruitment was conducted by a single recruiter, who performed all screening of medical records and imaging archives to identify eligible patients. Written informed consent was obtained from all participants, and ethical approval was secured before the study commenced.

Eligible participants were adults aged 18 years or older with a confirmed diagnosis of NF-PitNET who had undergone transsphenoidal surgery at least one year before study entry and had radiological evidence of residual tumour on a postoperative MRI performed at least three months after surgery. To confirm that the lesion represented persistent residual disease rather than tumour regrowth, all participants underwent review of interval MRI surveillance. If the most recent MRI had been performed more than six months before enrolment, a repeat MRI was obtained before study entry. Only patients with persistent residual tumour showing stable size on the pre-enrolment MRI were eligible for inclusion. Patients with radiological evidence of tumour progression were not enrolled. Patients who had undergone repeat surgery within the preceding six months were also eligible, provided persistent postoperative residual tumour was demonstrated following the most recent surgery and remained stable on the pre-enrolment MRI. The diagnosis of NF-PitNET was based on: (1) MRI evidence of a pituitary lesion with or without compressive symptoms; (2) absence of clinical features of anterior pituitary hormone hypersecretion; (3) normal or subnormal

biochemical levels of growth hormone (GH), insulin-like growth factor-1 (IGF-1), thyroid-stimulating hormone (TSH), thyroid hormones, and adrenocorticotropic hormone (ACTH); and (4) postoperative histopathological confirmation of a pituitary adenoma.

Exclusion criteria were defined to minimise confounding influences on tumour biology and to ensure treatment safety. Patients were excluded if they had a history of malignancy, had received pituitary radiotherapy or radiosurgery, had been treated with dopamine agonists within the preceding six months, or had unstable compression of the optic chiasm. Additional exclusions included uncontrolled diabetes melli[illegible] ≥ [illegible] 10%), advanced chronic kidney disease (eGFR < 30 mL/min/1.73 m²), hepatic dysfunction (Child–Pugh class B or C), advanced cardiac insufficiency (left ventricular ejection fraction < 40% or New York Heart Association class III–IV), and significant psychiatric illness requiring antipsychotic or antidepressant therapy. Female patients who were pregnant, breastfeeding, had a history of oophorectomy, or had received recent hormone replacement therapy were also excluded to avoid hormonal confounding. Any condition deemed by the investigators to interfere with study conduct or interpretation was grounds for exclusion.

3.4 SAMPLE SIZE AND POWER CALCULATION

3.4.1 Sample Size for First and Second Objectives

The initial sample size estimation was based on a previous clinical study by Greenman et al. (2016), which evaluated dopamine agonist therapy in patients with NF-PitNETs. In that study, tumour volume reduction was observed in 37% of treated patients, compared with no measurable tumour reduction in the control group. Using these proportions as reference values, the sample size calculation for a dichotomous outcome was performed using PS Power and Sample Size software (version 3.1.2). Assuming a [illegible] $_0$) [illegible] f 0.37, a total of [illegible] 20 participants per group was estimated to provide 80% statistical power at a two-sided α [illegible] 5 [illegible] sample size for the clinical trial was set at 50 participants. Accordingly, for the initial phase of the study, 50 archived tumour tissue samples were retrieved for

immunohistochemical analysis of oestrogen receptor expression and proliferative markers.

The required sample size based on the primary clinical endpoint – defined as binary responder status – was subsequently re-evaluated following a pre-specified interim analysis. Responder status was defined as radiologically measurable tumour shrinkage on MRI at 6 months. Interim analysis of the first 16 participants (8 in the tamoxifen arm and 8 in the control arm) demonstrated tumour shrinkage in 3 participants (37.5%) receiving tamoxifen, compared with no responders (0%) in the [illegible] ($p = 0.046$). [illegible]

Assuming these observed proportions approximate the true underlying [illegible] 5 [illegible] -arm parallel) [illegible] design with equal allocation, a two-[illegible] α [illegible] was calculated using the standard formula for comparing two independent proportions:

[illegible] α 2) × √ (2 − β) × √ ([illegible] − [illegible]) [illegible] [illegible] − [illegible])))

where:

[illegible] [illegible]) 2 [illegible] 5 [illegible]) 2 [illegible] 5 [illegible]

[illegible] − α 2) [illegible] [illegible] α [illegible] 5) [illegible]

[illegible] − β) [illegible] [illegible] % [illegible])

Substituting the values:

[illegible] 5 5 2) [illegible] [illegible]) ²

$= (1.082 + 0.407)^2 / (0.375)^2$

$= (1.489)^2 / 0.1406$

= 2.217 / 0.1406

= 15.8

Based on anticipated effect size and feasibility considerations inherent to a rare disease setting, the required sample size was estimated at 16 participants per arm, corresponding to a total of 32 participants to achieve 80% statistical power at a 5% significance level. Accordingly, 32 participants (16 per arm) were recruited. However, 12 participants were subsequently excluded from the final analysis. Exclusions were primarily attributable to logistical disruptions during the COVID-19 pandemic, including inability to attend scheduled follow-up MRI scans and clinical assessments, tumour re-enlargement necessitating early surgical re-intervention before completion of the planned 12-month follow-up, and interrupted treatment protocols. Consequently, a final evaluable cohort of 20 participants (10 per arm) completed the full treatment and imaging protocol.

Given the resulting evaluable sample size of 20 participants (10 per arm), the study was analysed and interpreted as an external pilot randomised trial rather than a definitive efficacy trial. In this context, the primary objectives were to assess feasibility, characterise tumour volumetric trajectories, and obtain preliminary estimates of outcome variability and effect direction to inform the design of a future adequately powered study. Formal hypothesis testing was therefore considered exploratory.

Methodological guidance for pilot trials indicates that when a moderate to large treatment effect is considered plausible, a sample size of approximately 10 participants per arm is sufficient to provide stable preliminary estimates of key design parameters while remaining feasible and proportionate (Kunselman 2024; Whitehead et al. 2016). In light of the observed interim response rates and the practical constraints imposed by attrition, the final cohort of 10 participants per group is considered appropriate for this hypothesis-generating pilot study, while recognising that confirmatory conclusions will require a larger, fully powered trial.

3.4.2 Sample Size for Third Objective

The secondary endpoint of the study was to determine the differentially expressed serum proteins following tamoxifen treatment. The statistical framework for biomarker analysis was based on paired t-test methodology, appropriate for evaluating within-subject changes before and after intervention. Sample size requirements were estimated using the University of Maryland calculator (https://sph.umd.edu/department/epib/sample-size-calculation-completely-randomized-treatment-control-designs).

For paired biomarker comparisons, the sample size per group was estimated using the standard formula for paired t-tests:

$$n = ((Z(1-\alpha\ 2)\ -\beta)\ \delta\ \sigma))^2$$

Where:

$Z1-\alpha\ 2$ -

$Z1-\beta$

δ -change of 1.0, corresponding to a two-fold change), σ 0.7 from log-transformed data).

Substituting these values:

$$n = ((1.96 + 0.84) / (1.\ ))^2\ 2\ )^2 \approx$$

= 0.05.

Analyses were conducted on ten paired patients overall. This tiered strategy ensured that exploratory biomarker findings were contextualised within clinically

defined response categories, while recognising the hypothesis-generating nature of the study.

3.4.3 Study Power

Based on the observed responder rates in the evaluable cohort—40% (4/10) in the tamoxifen group versus 0% (0/10) in the control group – the recalculated statistical power of the study was approximately 73% at a two-□ □ □ □ □ □ α □□ □ □ □ □ □□ □□ □ □ 5 □ □□ is slightly below the conventional 80% threshold, this level of power is considered acceptable for a pilot clinical trial. Consistent with CONSORT-pilot recommendations (Hopewell et al. 2025), the findings are interpreted as preliminary and hypothesis-generating, providing essential estimates of effect size, variability, and feasibility parameters to guide the design of future adequately powered confirmatory trials.

3.5 OUTCOME MEASURES

3.5.1 Primary Outcome Measures

This study defined two primary outcome measures reflecting its biological and clinical objectives. The primary tissue-based outcome was the immunohistochemical □ □ □ □ □ □ □ □ □ □ □ □ □ □ □ □ □ □ □ α □□ □ □ -PitNET β specimens, evaluated by the intensity of nuclear staining and quantified using the H-score method for both receptors (HSCOREA and HSCOREB). This measure characterised tumour ER expression and supported subsequent analyses of its relationship with clinical and molecular measures associated with tamoxifen therapy. The primary clinical outcome was tumour volumetric response, assessed by final tumour volume at 12 months ($T2VOL_2$) and tumour shrinkage. All volumetric measurements provided a quantitative assessment of treatment-related changes in residual NF-PitNET burden.

3.5.2 Secondary Outcome Measures

Secondary outcome measures addressed the translational biomarker aims of the study and provided mechanistic context for the primary outcomes. These included longitudinal changes in circulating serum biomarkers representing growth–angiogenic, inflammatory, cytokine–tumour necrosis factor, and Wnt-modulatory pathways,

measured at two time points (before and after tamoxifen therapy) in the intervention group. Additionally, secondary outcomes included the association between individual biomarkers and multivariate biomarker profiles with tumour volumetric response, as well as the derivation of composite biomarker indices and latent pathway axes using multivariate modelling approaches.

3.6 STUDY VARIABLES

Table 3.1 summarises all continuous variables used in the study. Each variable is classified according to its analytical role (outcome, predictor, or covariate) to clarify its use in subsequent statistical models. Table 3.2 presents all categorical variables included in the study. Variables are grouped by clinical and analytical relevance and are defined according to their symbols or abbreviations used for statistical analysis.

Table 3.1 Continuous Study Variables

Category	Variable	Definition / Measurement	Analytical Role
Primary clinical outcome	Final tumour volume ($T2VOL_2$)	MRI-derived tumour volume at 12 months	Dependent
Primary predictor	Baseline tumour volume ($T0VOL_2$)	MRI-derived baseline volume	Covariate
	Interim tumour volume ($T1VOL_2$)	MRI-derived tumour volume at 6 months follow-up	Covariate
	Absolute change in	$T2VOL_2 -$	Covariate
	Percentage change in	Δ	Covariate
Primary tissue outcomes	α-score (HSOREA)	Nuclear H-score (0–300)	Dependent / Covariate
	β-score (HSCOREB)	Nuclear H-score (0–300)	Dependent / Covariate
Secondary molecular outcomes	Individual serum biomarkers (pre and post)	VEGF, HGF, TGF-α, CD40L, FGF, TNF-α, sFRP1	Dependent
	Composite Biomarker Indices (CBIs)	Z-score–derived domain indices	Dependent
Clinical parameter	Postop duration	Months from last surgery to enrolment	Covariate
	Baseline pituitary hormones	GH, IGF-1, ACTH, cortisol, TSH, free T4, PRL, LH, FSH	Covariates
Molecular parameter	Change of individual serum biomarkers (Δ)	VEGF, HGF, TGF-α, CD40L, FGF, TNF-α, sFRP1	Covariates
	CBI combined cohort and CBI post tamoxifen	Z-score–derived domain indices	Covariates

Table 3.1 Categorical Study Variables

Category	Variable	Definition / Categories	Analytical Role
Primary clinical outcomes	Tumour response category	Shrinkage / Stabilisation / Regrowth	Dependent
Primary predictor	Study arm	Tamoxifen / Active surveillance	Independent
Primary tissue outcomes	□ □ α □ □ □ □ □ □ □ □	Positive / Negative	Dependent
	□ □ β □ □ □ □ □ □ □ □	Positive / Negative	Dependent
Secondary tissue outcome	p53 mutation	Positive / Negative	Covariate
	Ki-67	<3% / >3%	Covariate
	Mitotic count	Positive / Negative	Covariate
Demographic	Age	Years at diagnosis and enrolment	Covariate
	Race	Malay or Chinese	Covariate
Clinical parameters	Repeat surgery	Present / Absent	Covariate
	Pituitary apoplexy	Present / Absent	Covariate
	Cranial nerve palsy	Present / Absent	Covariate
	Pre or post-op hormonal replacement	Present / Absent	Covariate
	Extrasellar extension	Present / Absent	Covariate

3.7 IMMUNOHISTOCHEMISTRY (IHC)

Formalin-fixed, paraffin-embedded (FFPE) tumour specimens obtained from surgical resections of NF-PitNETs were processed in the histopathology laboratories of HCTM and HKL. Representative tumour blocks were selected after routine diagnostic histopathological review. Tissue blocks were sectioned at approximately 3 µm thickness using a rotary microtome and mounted on adhesive glass slides (Platinum Pro White, Matsunami, Japan). The slides were air-dried at room temperature overnight and then incubated on a hot plate at 62°C for 1 hour to ensure optimal tissue adhesion.

For diagnostic confirmation and tumour subtyping, immunohistochemical staining for anterior pituitary hormones, including ACTH, GH, PRL, FSH, LH, and TSH, was performed at the Histopathology Laboratory, HKL, according to routine diagnostic protocols. These results were used to exclude functioning pituitary tumours and to support the classification of cases as non-functioning PitNETs based on the absence of clinically significant hormone hypersecretion and the immunophenotypic profile.

Following diagnostic confirmation, routine haematoxylin and eosin (H&E) staining was performed on representative sections for histomorphological evaluation. Sections were deparaffinised, rehydrated through graded alcohols, stained with haematoxylin followed by eosin, dehydrated, cleared in xylene, and mounted with a permanent mounting medium. Mitotic figures were assessed on H&E-stained sections by light microscopy in areas of highest tumour cellularity and mitotic ac“ ”) -power fields (HPF) (Trouillas et al. 2013). This evaluation complemented the Ki-67 and p53 immunohistochemical indices in the overall assessment of tumour proliferative activity and biological behaviour.

-67, and p53 was performed on 50 selected NF-PitNET samples at the HCTM Histopathology Laboratory. Whole tissue sections from FFPE blocks were used to allow comprehensive assessment of intratumoural heterogeneity. Immunohistochemical staining was carried out using the Abcam Mouse and Rabbit Specific HRP/DAB IHC Detection Kit – Micro- were diluted to ’ working solution. The DAB substrate working solution was prepared by diluting the 5 ×

Deparaffinisation and antigen retrieval were performed using a Decloaking) cooling at room temperature for 30 minutes and rinsing under running tap water. Endogenous peroxidase activity was blocked with Abcam Peroxidase-Blocking Reagent for 10 minutes, followed by washing. Slides were then incubated with the respective primary antibodies for 30 minutes at room temperature, followed by washing. Sections were subsequently incubated with the mouse specifying reagent (complement) for 10 minutes, washed, and then incubated with goat anti-rabbit HRP conjugate for 30 minutes at room temperature.

Antigen–antibody complexes were visualised using 1× DAB-containing substrate working solution for 7 minutes, producing a brown precipitate at sites of antigen localisation. The sections were then counterstained with haematoxylin, dehydrated through graded alcohol solutions (80%, 90%, 100%, 100%), cleared in xylene, and mounted with a xylene-based permanent mounting medium.

The primary antibodies used were mouse monoclonal anti-Ki-67 (clone MIB-1, ready-to-use), mouse monoclonal anti-p53 (clone DO-7, ready-to-use), mouse monoclonal anti-[illegible]β [illegible]β [illegible]5 5 [illegible]-[illegible]α[illegible]) [illegible] (clone EP1, ready-to-use). Appropriate antigen retrieval buffers were applied according to antibody specifications, including high-[illegible] solution for Ki-[illegible]α-[illegible]

Appropriate positive and negative controls were included in each staining run to ensure technical validity and reproducibility. Normal tonsil tissue, ovarian carcinoma, gallbladder carcinoma, and breast carcinoma tissues were used as positive controls for Ki-[illegible]5 [illegible]β [illegible]α [illegible] by omission of the primary antibody to assess non-specific staining and background signal.

Evaluation of ER expression was limited to nuclear staining, following [illegible]α [illegible] Cytoplasmic and membranous staining patterns were not quantified. Semi-quantitative analysis was performed using the Histo-score (H-score) method (Manoranjan et al. 2010; Rai et al. 2020). Staining intensity was graded on a four-tier ordinal scale (0 = no staining, 1 = weak, 2 = moderate, 3 = strong). The H-score was calculated as the sum of the percentage of stained tumour cell nuclei multiplied by the corresponding intensity score, yielding a continuous score from 0 to 300. Only moderate to strong staining (scale 2 or 3) was considered immunopositive, whereas weak staining (scale 1) or absence of staining was considered immunonegative.

Tumour proliferative and invasive behaviour was characterised using the clinicopathological classification proposed by Trouillas et al. (2013), which integrates

the Ki-67 labelling index, mitotic count, p53 immunopositivity, and histopathological evidence of invasion (cavernous sinus, sphenoidal sinus, or dura mater). For Ki-67 assessment, immunostained slides were first examined at low magnification to identify the hotspot (the area showing the highest density of positively stained tumour cell nuclei). Within this hotspot, tumour cell nuclei were counted in 10 consecutive HPF (×400 magnification), with approximately 5,000 nuclei evaluated per tumour. The Ki-67 labelling index was calculated as the percentage of positively stained tumour nuclei within the hotspot. Mitotic activity was recorded as the absolute number of mitoses per 10 HPF. Proliferation was considered present when at least two of the following three criteria were met: Ki-□ □ □□ □ □ □ □ □ □ □ □ □□ □ □ □ □ ≥ □ % HPF, and p53 □ □ □□ □ □ positivity (>10 strongly positive nuclei per 10 HPF).

All immunostained slides were evaluated by an experienced neuropathologist blinded to clinical data and treatment allocation to minimise observer bias and ensure objectivity and reproducibility of the assessments.

3.8 PILOT CLINICAL TRIAL

Clinical and demographic data were collected prospectively using standardised case report forms (Appendix). Variables included age, sex, clinical presentation, surgical history, and anterior pituitary hormonal profiles.

Randomisation for the clinical trial was stratified by sex and age to ensure balanced groups. The intervention group received tamoxifen orally at 20 mg daily for the first month, increasing to 40 mg daily thereafter, for a total duration of 12 months (Balili & Barkan 2014). Adherence to tamoxifen was monitored by pill counts, and adverse events were systematically documented at each visit. The control group underwent active surveillance according to routine clinical care (Batista et al. 2019). All patients were monitored every three months for clinical status, laboratory investigations, and treatment tolerance.

3.9 MRI-BASED TUMOUR VOLUMETRY

Radiological monitoring of residual tumour volume was performed at baseline (T0) and at 6 (T1) and 12 months (T2) after study entry using gadolinium-enhanced T1-weighted magnetic resonance imaging (MRI) acquired on a 1.5 Tesla Philips Ingenia scanner at the Department of Radiology, HKL. The baseline MRI used for study enrolment was required to have been performed at least six months after the most recent transsphenoidal surgery. If the most recent MRI had been obtained more than six months before enrolment, a repeat MRI was performed before study entry. This ensured that transient postoperative changes had resolved and that volumetric assessment reflected persistent residual tumour rather than postoperative surgical changes. Residual tumour margins were manually delineated on every contiguous 3-mm coronal slice containing tumour using Horos software (Møller et al. 2020). The software automatically reconstructed the segmented regions into a three-dimensional model and calculated total tumour volume (cm^3) by summing the segmented areas across all segmented slices. To minimise observer bias, all volumetric measurements were performed independently by a single neuroradiologist blinded to treatment allocation. Each MRI examination was segmented on three separate occasions, and the average tumour volume was used for statistical analysis.

Treatment outcomes were categorised as tumour s□ □ □ □ □ □ □ □ ≥ 2 5 % □ □ □ □ □ □ □ □) □ □ □ □ □ □ □ □ □ □ □ □ □ □ □ □ □ □ □ 2 5 % □ □ □ □ □) □ □ □ □ □ □ tumour volume (Batista et al. 2019). This classification enabled objective evaluation of treatment efficacy while accounting for expected variability in MRI-based volumetric measurements. Tumour invasiveness was defined radiologically as Knosp grade 3 or 4 (Araujo-Castro et al. 2021). In addition to these categorical outcomes, continuous tumour volumes at baseline (T0), 6 months (T1), and 12 months (T2) were analysed to characterise longitudinal changes in tumour size.

3.10 SERUM BIOMARKER PROFILING

3.10.1 Selection of serum biomarkers and domain-based framework

Given the biological heterogeneity of NF-PitNETs, a structured approach to serum biomarker analysis was adopted. This pilot study used a translational, hypothesis-generating strategy, with biomarker selection based on biological relevance across related signalling pathways.

Serum biomarkers were organised using an author-defined, domain-based framework developed as an analytical tool to group analytes according to their dominant functional roles. The domains do not represent established diagnostic categories but were pre-specified to support hypothesis-driven and integrative analysis. Analyte selection was also informed by analytical feasibility, serum stability, and the reliability of multiplex immunoassay and ELISA measurements. Selected biomarkers were grouped into four biological domains representing key signalling axes relevant to NF-PitNET biology, and this structure guided downstream analyses:

a. Domain 1 – Growth and angiogenic

Analytes: Hepatocyte growth factor (HGF), transforming growth factor-α □□ □-α)□ □ □ vascular endothelial growth factor (VEGF) and stem cell factor c-kit (SCF)

This domain represents growth factor-driven and angiogenic signalling involved in tumour proliferation, stromal interaction, and vascular development. HGF, TGF-α □ □ VEGF, and SCF have been implicated in pituitary tumour growth and angiogenesis through effects on cellular proliferation, vascularisation, and tissue remodelling (Hou et al. 2010; La Rosa et al. 2008; Leker et al. 2009; Lohrer et al. 2001). These mediators were therefore grouped to capture mitogenic and angiogenic activity.

b. Domain 2 – Inflammatory

Analytes: Basic Fibroblast growth factor (FGF), interleukin-6 (IL-6) and CD40 ligand (CD40L)

This domain reflects inflammatory and immune–stromal signalling within the tumour microenvironment. Interleukin-6 was selected as a central pro-inflammatory cytokine, while CD40 ligand represents immune activation and immune–stromal crosstalk. Although CD40 is a member of the TNF receptor superfamily, CD40–CD40L signalling has been shown to directly induce IL-6 gene transcription via TRAF2- and NF-κ -dependent pathways, supporting the grouping of CD40 ligand with IL-6 within the inflammatory domain (Mann et al. 2002). Although FGF is classically categorised as a growth factor, evidence indicates that FGF-related signalling via FGFR plays a regulatory role in inflammatory responses, including modulation of IL-6 and immune activation markers, supporting its inclusion within the inflammatory domain in the present analytical framework (Cheng et al. 2019; Cox et al. 2013).

c. Domain 3 – Cytokine–TNF-α

Analyte: Tumour necrosis factor-α (TNF-α)

TNF-α and its ability to act independently across inflammatory, immune, and apoptotic signalling pathways (Gough & Myles 2020). Evidence from pituitary tumour studies indicates that TNF-α -dependent mechanisms, including effects on cellular invasion, hormone regulation, and tissue remodelling (Wu et al. 2024; Xiao et al. 2011). Its separation as an individual domain enabled targeted evaluation of TNF-α-specific signalling within the analytical framework.

d. Domain 4 – Wnt modulatory

Analytes: Secreted frizzled-related protein 1 (sFRP1) and Dickkopf-related protein 1 (DKK1)

-catenin signalling, rather than direct proliferative effects. Regulation of Wnt activity is mediated by secreted inhibitory proteins, which are broadly grouped into two main families: secreted frizzled-related proteins (sFRPs) and Dickkopf (DKK) proteins (Song et al. 2018). Accordingly, sFRP1

and DKK1 were selected to represent control of Wnt signalling intensity and homeostasis.

Collectively, these four biological domains were defined a priori to provide a structured framework for integrating biomarkers and their associated biological functions into pathway-level analyses. This domain-based framework was developed to facilitate interpretation of complex biomarker interactions, reduce dimensionality, and minimise reliance on isolated single-marker analyses. Rather than representing fixed biological classifications, the proposed domains served as an initial conceptual framework that was subsequently evaluated and refined using multivariate models. This integrative approach enabled both biologically informed and data-driven characterisation of treatment-associated biomarker responses.

3.10.2 Blood Sampling and Storage

Serum samples were collected at baseline from both study groups for comparative analyses. A second blood sample was obtained from the intervention group after 12 months of tamoxifen therapy.

Ten millilitres of peripheral venous blood were collected using plain tubes under standard aseptic conditions. Samples were allowed to clot at room temperature (25–28 °C) for 20–30 minutes before centrifugation at 3,000 × g for 10 minutes at 2–4 °C. After centrifugation, serum was carefully separated to minimise cellular contamination and ns. Samples with visible lipaemia were clarified by repeat centrifugation for 10 minutes at 2–4 °C, after which the clarified supernatant was transferred into a new tube. Haemolysed samples were excluded to reduce analytical interference. The separated serum was 5 (Figure 3.2) at the Endocrine Unit, Clinical Examination Laboratory, HCTM until analysis (Figure 3.4). All samples were labelled with unique serial numbers to ensure blinding during downstream analyses (Figure 3.3).

Figure 3.2 Freezer at −80 °C

Figure 3.3 Sample storage and labelling

Figure 3.4 Endocrine Unit, Clinical Examination Laboratory, HCTM

3.10.3 Multiplex Immunoassay

Serum concentrations of VEGF, IL-6, TNF-α CD40L, HGF, TGF-α EGF, and SCF were quantified using a multiplex bead-based immunoassay (Human Tumour Biomarker Luminex® Performance Assay; R&D Systems, USA) (Figure 3.5) at the Prima Nexus Laboratory, Puchong.

The assay uses fluorescent microspheres coated with analyte-specific capture antibodies. Target proteins in serum bind to the beads and are then detected using biotinylated detection antibodies and streptavidin-phycoerythrin (Figure 3.6). Fluorescent signals proportional to analyte concentration were acquired using a Luminex® 200 detection system (Luminex Corporation, USA) (Figure 3.7).

a. Plate layout and sample loading

All assays were performed in a 96-[illegible] recommended plate layout. Each plate included a complete calibration curve and internal quality controls. Six serially diluted standards (Std1–Std6) were loaded in

duplicate to generate standard curves, along with duplicate blank wells for background signal correction.

Patient serum samples were dispensed into designated wells at volumes of 70–100 µL per well. Duplicate measurements were performed where applicable to enhance analytical precision. A standardised plate layout was applied consistently across all assay runs to ensure inter-assay comparability.

To preserve protein integrity, repeated freeze–thaw cycles were avoided. In accordance with the PrimePlex protocol, 140–200 µL of serum per assay kit was prepared for each participant. Where samples were analysed across multiple multiplex panels, aliquot volumes were increased proportionally.

b. Assay workflow

All reagents, including standards, internal controls, and antibody-immobilised bead [illegible] and reagent loading, antibody-coated beads were added to each well. Plates were sealed, protected from light, and incubated for 2 hours at room temperature with continuous agitation at 600 rpm (Figure 3.7).

After incubation, plates were washed to remove unbound material, and biotinylated detection antibodies were added. Following a further incubation and wash step, streptavidin-phycoerythrin was added to enable fluorescent signal generation. Plates were then washed Plates were then washed three times using a magnetic plate washer, and beads were resuspended in reading buffer before data acquisition using the Luminex® 200 system (Figure 3.8 & Figure 3.9).

c. Data processing and quantification

Analyte concentrations were calculated from standard curves generated using five-parameter logistic regression. Biomarkers were grouped into predefined biological domains during statistical analysis to aid biological interpretation.

d. Quality control measures

To minimise pre-analytical and analytical variability, stringent quality control measures were implemented. These included standardised clotting and centrifugation procedures, exclusion of haemolysed sam[illegible] minimal freeze–thaw cycles, and inclusion of duplicate standards and blank controls on each assay plate. These measures ensured reliable and reproducible quantification of circulating proteins, including low-abundance cytokines.

Figure 3.5 Human Tumour Biomarker Luminex® Performance Assay Kit

Figure 3.6 Multiplex immunoassay kit

Figure 3.7 Luminex® 200 System (Luminex Corporation, USA)

Figure 3.8 Assay workflow

The complete sample set was analysed using the Luminex® 200 platform with a magnetic bead-based multiplex immunoassay. This approach enables simultaneous detection and quantification of multiple biomarkers in a single assay, improving analytical efficiency and sample utilisation.

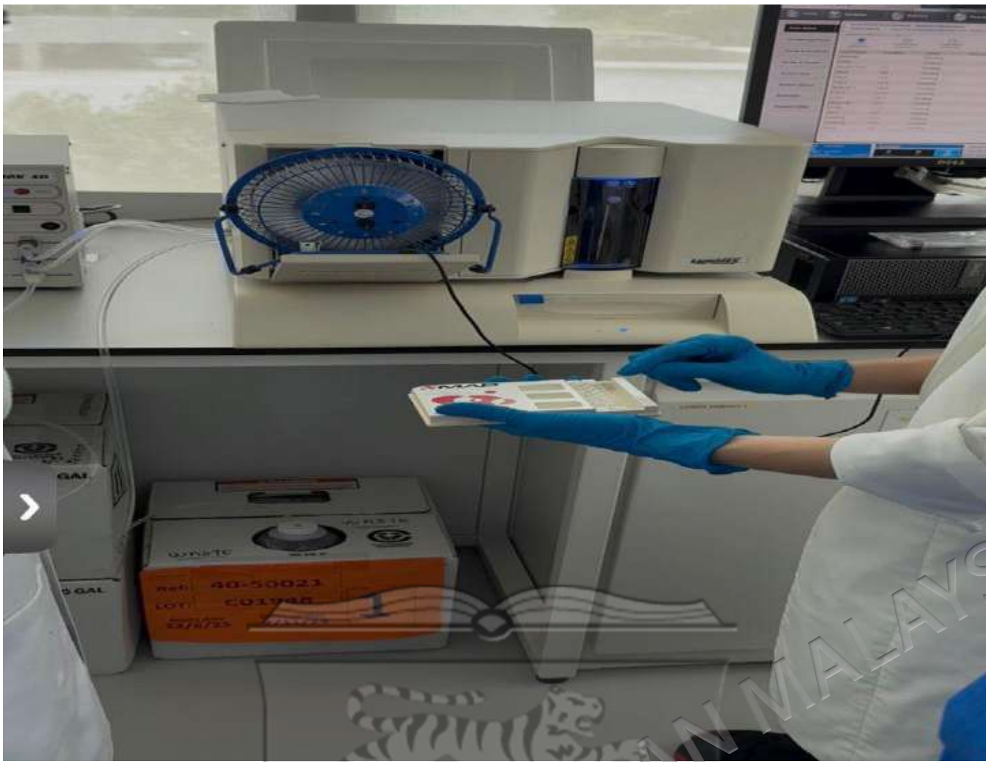

Figure 3.9 Calibration and verification in progress before the multiplex run to ensure optimal instrument performance and data accuracy

3.10.4 Enzyme-Linked Immunosorbent Assay (ELISA)

For Wnt pathway-specific validation, serum levels of DKK1 and sFRP1 were measured using commercial pre-coated ELISA kits (R&D Systems). Sandwich ELISA formats were used for both analytes.

[illegible] μ [illegible] into the designated wells of a pre-coated micro-ELISA plate, followed by incubation for 90 minutes at 37 °C. After incubation, the contents of the wells were removed, and 100 μ [illegible] incubated for a further 1 hour at 37 °C. The wells were then washed three times with wash buffer to remove unbound components.

[illegible] μ [illegible] (HRP) conjugate working [illegible] solution was added to each well and incubated for 30 minutes at 37 °C, after which the [illegible]

added to each well and incubated for 15 minutes at 37 °C in the dark to allow colour □ □ □ □ □ □ □ □ □ □ □ □ □□ □ □ □□ □ □ □ □ □ □ □ □□ □ □ □□ □ □ □ □ □ □ □□ □ □□ □ □ absorbance was measured at 450 nm using a microplate reader.

For data analysis, duplicate optical density (OD) readings for each standard and sample were averaged, and background correction was performed by subtracting the mean OD of the zero standard. A four-parameter logistic (4-PL) standard curve was generated by plotting standard concentrations against corresponding OD values on a log–log scale. Sample concentrations were interpolated from the standard curve and adjusted for dilution factors where applicable. Coefficients of variation (CV%) were calculated, and values below 20% were considered acceptable in accordance with bioanalytical validation guidelines.

Figure 3.10 shows the BIOBASE microplate reader connected to a laptop computer for instrument control, data acquisition, and analysis of ELISA measurements. Figure 3.11 shows the preparation area for ELISA, including commercial assay kits (Elabscience), reagents, microcentrifuge tubes, pipettes, and basic laboratory equipment used for handling samples and reagents prior to plate-based measurement.

Figure 3.10 Laboratory Setup for ELISA Data Acquisition and Analysis

Figure 3.11 ELISA Reagents and Bench Setup for Serum Biomarker Analysis

Table 3.2 Specific analytes, domains and analytical methods

Analyte	Domain	Analytical Method
VEGF	Angiogenic & Growth	Multiplex immunoassay
TGF-α	Angiogenic & Growth	Multiplex immunoassay
SCF	Angiogenic & Growth	Multiplex immunoassay
HGF	Angiogenic & Growth	Multiplex immunoassay
IL-6	Inflammation	Multiplex immunoassay
CD40L	Inflammation	Multiplex immunoassay
FGF-b	Inflammation	Multiplex immunoassay
TNF-α	Cytokine–TNF Axis	Multiplex immunoassay
DKK1	Wnt Signalling	ELISA
sFRP1	Wnt Signalling	ELISA

3.11 BIOINFORMATICS

3.11.1 Construction of the Tamoxifen–Target Gene Network

To identify potential molecular targets of tamoxifen, an in silico target prediction approach was used with SwissTargetPrediction, which estimates likely biological targets based on combined two-dimensional and three-dimensional chemical similarity to known ligands. The SMILES (Simplified Molecular Input Line Entry System) representation of tamoxifen was used as input for target prediction. Predicted targets with a probability score greater than 0.1 were selected to ensure biological relevance. This strategy enabled the identification of candidate genes with a high likelihood of interacting with tamoxifen.

3.11.2 Functional and Pathway Enrichment

Functional enrichment analysis of the predicted target genes was conducted using the Database for Annotation, Visualization and Integrated Discovery (DAVID; version 6.8). This analysis identified significantly enriched pathways within the Kyoto Encyclopedia of Genes and Genomes (KEGG). In parallel, Gene Ontology (GO) enrichment was assessed to characterise target genes according to cellular components (CC), molecular functions (MF), and biological processes (BP).

3.11.3 Protein–Protein Interaction Network Construction

A protein–protein interaction (PPI) network was constructed for the predicted target genes using interaction data retrieved from the STRING database (version 11.0). This

approach facilitated the identification of functional and physical interactions among the target proteins. The resulting interaction data were imported into Cytoscape (version 3.9.1) for network visualisation and downstream analysis. To identify key hub proteins within the network, the cytoHubba plugin was used to rank nodes based on multiple centrality metrics, allowing prioritisation of highly connected and potentially influential proteins within the tamoxifen-associated network.

3.12 STATISTICAL ANALYSES

3.12.1 Overview of Analytical Framework

□ □ □ □□ □ □ □ □ □ □ □ □ □ □ □ □□ □ □ □ □ □ □ □□ □ □ □ □□ □ □ □ □□ □ □ □ □ □ □ □ □□ □ □ □□ □ □

objectives using descriptive, inferential, multivariate, and computational approaches. Conventional statistical analyses were performed using SPSS version 25.0 (IBM Corp., Armonk, NY, USA). Partial least squares structural equation modelling (PLS-SEM) was conducted using SmartPLS version 4 (SmartPLS GmbH, Boenningstedt, Germany) to evaluate multivariate relationships among latent constructs and observed variables. Complementary in silico and network-based analyses were performed using SMILES-based target prediction, DAVID, STRING, and Cytoscape to support pathway-level interpretation and systems-level integration of findings. For pathway enrichment analyses, *p*-values were adjusted for multiple testing using the Benjamini–Hochberg false discovery rate procedure.

3.12.2 Data Pre-Processing

Raw data from IHC, MRI-based tumour volumetry, multiplex immunoassays, and ELISA were systematically screened before statistical analysis. Initial checks focused on data completeness, internal consistency, distributional properties, and homogeneity of variance to ensure analytical validity. Outliers were identified by graphical inspection with boxplots and confirmed using standardised Z-score thresholds (±3.0). Extreme values were reviewed for clinical plausibility and assay performance before any exclusion. Continuous variables were assessed for normality using both the Shapiro–Wilk and Kolmogorov–Smirnov tests.

For serum biomarker analyses, multiplex immunoassay data underwent additional quality control procedures. Analytes with concentrations below the lower limit of detection were assigned values equal to the minimum detectable concentration. Samples and analytes with excessive variability or poor assay performance were flagged based on coefficient of variation (CV) thresholds, in accordance with manufacturer recommendations. Duplicate measurements were averaged for downstream analysis.

3.12.3 Descriptive Analyses

Descriptive statistics were used to characterise the study cohort. Continuous variables were presented as mean ± standard deviation (SD) or median with interquartile range (IQR), depending on data distribution. Categorical variables were summarised as frequencies and percentages.

3.12.4 Inferential Analyses

a. Baseline profiles

Group comparability at baseline between the tamoxifen and control arms was assessed using the chi-square test, independent samples t-test, or Mann-Whitney U test, as appropriate. This includes demographic profile, baseline endocrine function, and clinical, histopathological, radiological, biomarkers and ER expressions and H-scores.

b. Primary outcome analyses

Primary outcome analysis followed a stepwise framework, focusing first on continuous tumour volumetric outcomes and then on categorical treatment response. To control for baseline differences and interim tumour dynamics, analysis of covariance (ANCOVA) was used to evaluate 12-month tumour volume, adjusting for baseline and 6-month measurements. Longitudinal changes in tumour volume were examined using repeated-measures ANOVA (RM-ANOVA) with Mauchly's test of sphericity applied ($\geq$ 5 time points); when the assumption was not violated, sphericity-assumed results were reported, and when violated ($p < 0.05$), Greenhouse–Geisser-corrected degrees of

freedom were applied. Within-group changes in the tamoxifen arm were assessed using paired-sample t-tests or the Wilcoxon signed-rank test, as appropriate.

Treatment response was categorised a priori based on longitudinal MRI-derived tumour volume changes into three groups: tumour shrinkage, stabilisation, and regrowth, using predefined percentage change thresholds relative to baseline (see Section 3.8). Tumour volume metrics within each response group were summarised as means and standard deviations. Between-group differences in final tumour volume [illegible] 2 [illegible] $_2$) [illegible] Δ [illegible] cha[illegible] %Δ [illegible]) [illegible]-way omnibus ANOVA. Where the omnibus [illegible]’ [illegible] applied to identify specific pairwise group differences (shrinkage vs stabilisation, shrinkage vs regrowth, and stabilisation vs regrowth). All tests were two-sided, with statistical significance set at $p < 0.05$. In addition, subgroup analyses were conducted within the tamoxifen-treated cohort to determine whether volumetric outcomes (shrinkage and stabilisation) differed between response categories, using independent-samples t-tests.

Correlations between tumour volumetric parameters and clinical variables were [illegible]’ -stage approach: first, with [illegible] baseline tumour volume to identify correlates of initial tumour burden; second, with final tumour volume to explore potential predictors of treatment-associated tumour behaviour.

Predictors of final tumour volume were explored using regression modelling [illegible] 2 [illegible] the dependent variable. Candidate predictors were first screened using simple linear regression, and variables with $p < 0.200$ were retained for multivariable modelling. Multiple linear regression was then performed using both Enter and Stepwise methods, with final model selection based on checks of assumptions (multicollinearity, residual normality, homoscedasticity, and independence of errors). Results were reported using regression coefficients and adjusted R^2, and interpreted in the clinical and biological context.

For binary outcome analysis, tumour shrinkage was specified as the dependent variable. Simple logistic regression was used to screen candidate predictors, including clinical and volumetric variables, baseline and post-treatment serum biomarkers, and composite biomarker indices. Results were expressed as odds ratios with 95% confidence intervals and p-values, and model fit was summarised using Cox & Snell R^2 and Nagelkerke R^2. Variables with $p < 0.200$ were considered for subsequent multivariable logistic regression, with appropriate checks for model assumptions and sparse data.

c. Secondary outcome analyses

Secondary outcome analyses focused on serum biomarkers to evaluate their associations with tumour behaviour and treatment response using a structured, stepwise analytical framework. First, baseline comparability between the tamoxifen and control groups was assessed to confirm biochemical equivalence before intervention. Baseline concentrations of the ten serum biomarkers were compared between groups using independent-samples t-tests or Mann–Whitney U tests, as appropriate based on data distribution.

Second, longitudinal within-group analyses were performed in the tamoxifen cohort to identify treatment-associated changes across biomarkers representing the growth–angiogenic, inflammatory, cytokine–TNF, and Wnt-modulatory pathways. Paired-samples t-tests or Wilcoxon signed-rank tests were applied according to distributional assumptions. To account for multiple comparisons, the Benjamini–Hochberg false discovery rate (BH-FDR) correction was applied to all inferential p-values, with $q \leq$ □□ □ □ 5 □□ □ □ □ □ □ □ □ □ □ □ □□ □ □ □ □ □ □ □ □ □ □ □ □□ □ □ □ paired analyses (10,000 resamples) were conducted to obtain robust estimates of within-subject changes in serum biomarkers following tamoxifen therapy.

Third, correlation analyses were conducted to examine associations between serum biomarker levels and tumour volume at baseline and at final follow-up, enabling exploration of relationships between circulating biomarkers and tumour burden over time. Finally, regression-based analyses were applied to evaluate the predictive value of individual serum biomarkers for final tumour volume and tumour shrinkage.

d. Bootstrapped analyses

For the paired serum biomarker analyses, bootstrapping was used as a resampling strategy to improve the stability of statistical estimates given the limited sample size (n = 20). Estimates were recalculated over 10,000 bootstrap iterations to generate empirical sampling distributions and bias-corrected 95% confidence intervals (Kostanek et al. 2024). The concordance of effect estimates across parametric, non-parametric, and bootstrapped analyses indicated internal consistency and supported the robustness of the serum biomarker analytical framework.

3.12.5 Multivariate Analyses

a. Exploratory Factor Analysis (EFA)

Exploratory factor analysis (EFA) was conducted to identify latent structures within the serum biomarker datasets and to examine biomarker clustering patterns across different treatment phases. EFA was performed in three predefined subsections: (i) pre-treatment biomarkers, (ii) post-treatment biomarkers, and (iii) pre–□ □ □ □ □□ □ □ □ □ □ □□ Δ) □□ □ □ □ allowing characterisation of baseline biological organisation, treatment-associated reorganisation, and treatment-related biological responses.

Prior to factor extraction, data suitability was assessed using the Kaiser–Meyer–□ □ □ □ □ □□ □ □ □) □□ □ □ □ □ □ □ □ □□ □ □□ □ □ □ □ □ □ □ □□ □ □ □ □ □ □ □□ □ □ □ □ □ □ □□ □ □ □ values ranged from 0.49 to 0.56, indicating acceptable adequacy for analysis (Kaiser 1974)□ □□ □ □ □ □ □ □ □ ’ □ □□ □ □ □ □ □□ □ □ □ □□ □ □ □ □ $p \leq 0.001$), □ □ □ □□ □ □ confirming that the correlation matrices were appropriate for factor extraction (Bartlett 1954).

Factors were extracted using principal component analysis, with the number of retained components determined by the Kaiser criterion (eigenvalues > 1.0). Factors were ordered by descending eigenvalues, and cumulative variance explained was examined to ensure adequate data representation. Variables were assigned to factors □ □ □ □ □ □□ □ □□ □ □ □ □ □□ □ □ □ □ □ □ □□ □ □ □ □ □ □ □ □□ □ □ □ □ □ □ □□ □ □ □ □ □ □□ □ □ □ □

meaningful. Negative loadings were interpreted as inverse associations with the latent factor.

To assess the robustness of the factor solutions in the context of a pilot sample size, bootstrap resampling was performed, and the consistency of factor loadings and directional stability across iterations was evaluated. Analyses were also repeated using z-score standardised biomarker values to confirm the scale independence of the factor structure. Factor labels were assigned post hoc, based on the dominant biomarkers loading onto each factor, to facilitate biological interpretation. EFA was used as a dimensionality reduction approach to identify biologically coherent biomarker domains and to inform subsequent multivariate analyses.

b. Confirmatory Factor Analysis (CFA)

Single-factor measurement models were evaluated using confirmatory factor analysis (CFA) to assess indicator reliability, internal consistency, and convergent validity for the five Composite Biomarker Indices (CBIs) (Table 3.2). Standard thresholds were [illegible] ≥ [illegible]’ [illegible] α ≥ [illegible] 0.50) to establish measurement adequacy before structural modelling (Hair et al. 2022). Validated CBIs were then incorporated into a Partial Least Squares Structural Equation Model (PLS-SEM) using SmartPLS v4, with significance assessed by bootstrapping (5,000 resamples; bias-corrected 95% confidence intervals) to ensure robust inference in this small-sample study.

To enable pathway-level interpretation and reduce dimensionality, CBIs were constructed by aggregating biologically related biomarkers into coherent domains identified through EFA and supported by biological plausibility (Table 3.4). All biomarker variables were standardised to Z-scores (Appendix A21) to account for differences in measurement scales before index construction. For domains comprising multiple biomarkers, each CBI was calculated as the arithmetic mean of the constituent standardised biomarkers.

Five CBIs were defined: CBI-1 (Growth/Angiogenic Axis), comprising HGF, VEGF, TGF-α [illegible]-2 (Inflammatory/FGF Axis), comprising FGF, IL-6 and

CD40L; CBI-3 (Wnt Modulator Axis), comprising sFRP1 and DKK1; CBI-4 (Cytokine/TNF-α □□ □ □ □ □) □ □□ □ □ □ □ □ □ □ □ □ □ □ □ □ -α □□ □□ □ □ □□ -α □□□□□□□□□□□□□□□□ □ □ the sole biomarker within this biological domain; and CBI-5 (ER Signalling Axis), comprising standardised H-sc□ □ □ □ □□ □ □□ □ α □□ □ □ □□ □ β □ □□ □ □ □ - □ □ □ □ □□ treatment CBI measurement models were evaluated using the corresponding standardised biomarker values. Together, these CBIs provided a structured, biologically interpretable representation of key signalling domains, enabling multivariate modelling at the pathway rather than the individual biomarker level.

Table 3.3 Construction of Composite Biomarker Indices (CBIs) and Their Biological Domains

Index	Constituent Biomarkers (Z-scores)	Pathway Representation	Formula
CBI-1 (Growth / Angiogenic Axis)	HGF, VEGF, TGF-α □ □□ □ □	Proliferation and angiogenesis	(zHGF + zVEGF + zTGF-α □□ □□ □ □ □)
CBI-2 (Inflammatory / FGF Axis)	FGF, IL-6, CD40L	Cytokine-driven repair	(zFGF + zIL-6 + zCD40)/3
CBI-3 (Wnt Modulator Axis)	SFRP1, DKK1	Canonical Wnt inhibition	(zSFRP1 + zDKK1)/2
CBI-4 (Cytokine / TNF-α □ Axis)	TNF-α	Inflammatory activation	zTNF-α
CBI-5 (ER Signalling)	□ □ α □ □□ □ β (H-score)	Oestrogen receptor context	□ □ □ □□α □□□□β) □

c. Partial Least Squares Structural Equation Modelling (PLS-SEM)

Following EFA, CBIs were constructed to summarise pathway-level activity and reduce dimensionality among correlated biomarkers by using Confirmatory Factor Analysis (CFA). These indices were analysed using Partial Least Squares Structural Equation Modelling (PLS-SEM) in SmartPLS v4 to evaluate their combined influence on treatment response, defined as post-treatment tumour volume change. Model estimation used bootstrapping with 5,000 resamples to obtain robust significance estimates.

Interpretation of the PLS-SEM followed established variance-based SEM guidelines and proceeded in two stages: evaluation of the measurement model and assessment of the structural model. Convergent validity of the measurement model was

alpha values above 0.70, composite reliability values above 0.70, and average variance extracted (AVE) values exceeding 0.50. These criteria indicate adequate internal consistency and convergence of indicators within each construct.

The structural model was interpreted based on the magnitude, direction, and statistical significance of path coefficients obtained through non-parametric bootstrapping. Coefficients of determination (R^2) were used to assess the proportion of variance explained in the outcome variable. Path coefficients with bootstrapped confidence intervals not crossing zero were considered statistically significant. The pre-defined hierarchical CBI model is shown in Figure 3.12. This model represents the a priori analytical framework developed from EFA and biological rationale, prior to estimating the measurement and structural models using hierarchical PLS-SEM.

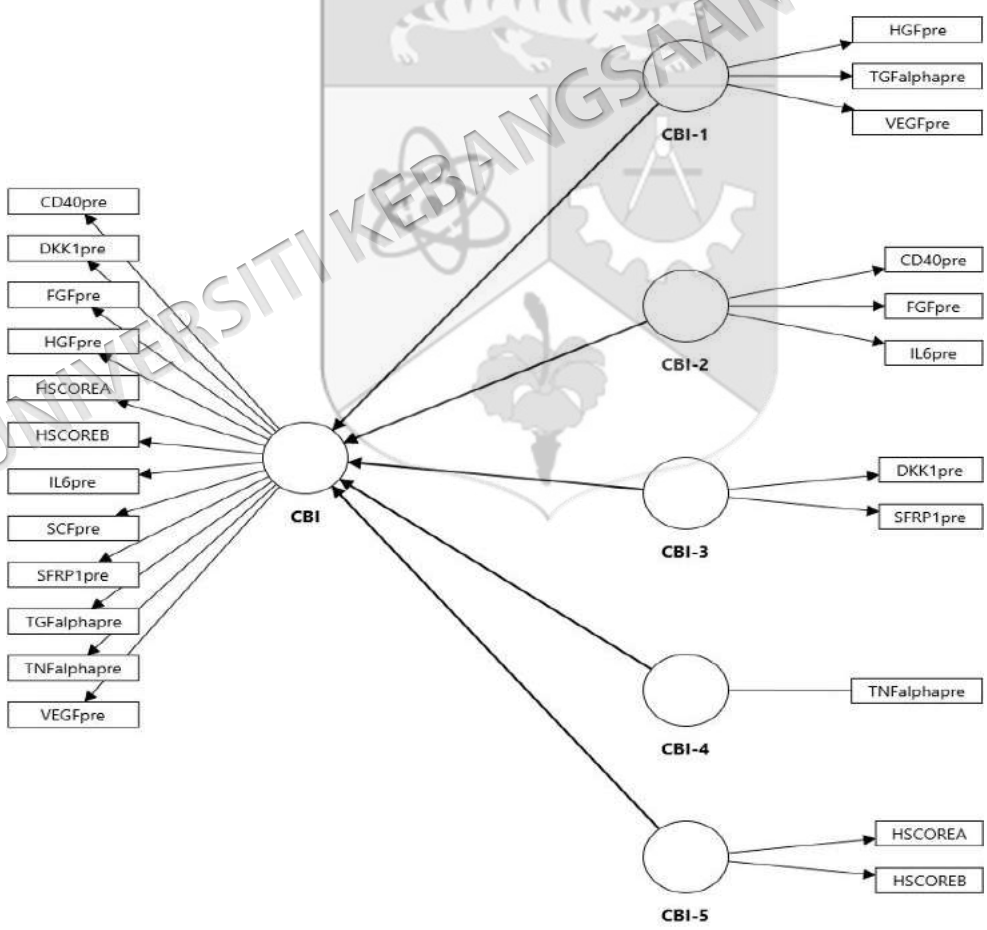

Figure 3.12 Original hierarchical Composite Biomarker Index (CBI) model specification based on baseline biomarker domains.

3.12.6 Computational Analyses

For the *in silico* analyses, statistical procedures were applied primarily at the pathway enrichment stage. Predicted tamoxifen-associated target genes were identified from publicly available pharmacological databases and subjected to Gene Ontology (GO) and Kyoto Encyclopedia of Genes and Genomes (KEGG) pathway enrichment analyses using the DAVID platform. As the analysis was designed to investigate the potential molecular mechanisms of tamoxifen rather than NF-PitNET-specific molecular networks, enrichment was performed on predicted tamoxifen-associated targets without restricting the analysis to disease-specific transcriptomic or proteomic datasets. Enrichment significance was evaluated using over-representation testing against the human genome background. To control for multiple comparisons across pathways and functional categories, *p*-values were adjusted using the Benjamini–Hochberg false discovery rate (FDR) method. Pathways and functional terms with an FDR-adjusted *q*-value < 0.05 were considered statistically significant and retained for biological interpretation.

Protein–protein interaction (PPI) networks were constructed using STRING and visualised in Cytoscape. Network topology was analysed using standard centrality metrics, including degree, betweenness centrality, and closeness centrality, to prioritise hub genes and key network regulators. These network analyses were descriptive and ranking-based rather than inferential; no formal hypothesis testing was applied to network topology measures. Hub genes were therefore identified based on their relative topological importance within the predicted tamoxifen-associated interaction network rather than on statistical significance.

3.12.7 Data Completeness and Handling of Missing Values

Tumour volumetric measurements were obtained a[illegible] $_0$) [illegible] 2 [illegible] $_2$) [illegible]-[illegible] $_1$) [illegible] unavailable due to disruptions in scheduled MRI appointments during the COVID-19 movement control period. These missing observations accounted for less than 10% of all longitudinal data points and were considered missing at random. Longitudinal analyses were conducted using a General Linear Model with Repeated Measures

(GLM-RM), which permits inclusion of participants with partially observed follow-up data by using all available observations rather than enforcing complete-case exclusion. This approach preserved statistical power and minimised bias associated with unnecessary listwise deletion. Consequently, overall temporal trends in tumour volume could be reliably estimated despite limited missing intermediate measurements.

3.12.8 Data Quality and Validity

To ensure analytical consistency, all volumetric and biomarker measurements underwent predefined quality-control procedures before statistical analysis. For MRI volumetry, tumour volumes were manually delineated, and each tumour volume was measured three times by the same blinded radiologist. The mean of the three measurements was used as the final volume estimate at each time point to minimise intra-observer variability and measurement noise.

Serum biomarker analyses were performed using multiplex immunoassays and ELISA. Each assay plate included duplicate wells for all samples, as well as internal standards and positive and negative controls. For each biomarker, the mean of duplicate measurements was used for analysis to reduce random within-assay variability and provide a stable central estimate. Analytical precision was assessed using the percentage difference between duplicates and □ considered acceptable for intra-assay reproducibility. As all samples were analysed within a single assay batch, inter-assay variability was not estimated.

3.13 ETHICAL CONSIDERATIONS

The study was conducted in accordance with the Declaration of Helsinki and Malaysian national guidelines for biomedical research. Ethical approval was granted by the Universiti Kebangsaan Malaysia Research Ethics Committee (JEP-2019-055) and the Malaysian Medical Research and Ethics Committee (MREC; NMRR-18-3778-45144) (see Appendix J). Written informed consent was obtained from all participants before enrolment. Data confidentiality was strictly maintained, and participants were informed of their right to withdraw at any stage without consequence to their medical care.

Table 3.4 Summary of Specific Research Objectives, Variables and Statistical Analyses

Specific Objective	Outcome / Dependent Variables	Independent / Predictor Variables	Statistical / Analytical Methods
1. To determine the immunohistochemical expression [illegible] α [illegible] NF-PitNET tissue samples.	[illegible] α [illegible] β [illegible] [illegible] α -score (HSCOREA); [illegible] β -score (HSCOREB)	Study arm	Descriptive analyses; Chi-square test, [illegible]' Independent t-test, Mann-Whitney U test
2. To evaluate the clinical impact of tamoxifen on changes in residual NF-PitNET tumour volume.	T0VOL$_2$, T1VOL$_2$, T2VOL$_2$, Δ [illegible] and %Δ [illegible]; Tumour response categories;	Study arm; Demographic, clinical, radiological, endocrinological variables; HSCOREA; HSCOREB; T0VOL$_2$	ANCOVA; repeated-measures GLM; paired t-test; [illegible]' [illegible]-way ANOVA with LSD post-hoc testing; [illegible]' [illegible] ple and multiple linear regressions, simple logistic regression
3. To investigate baseline and longitudinal changes in serum biomarker levels in tamoxifen-treated NF-PitNET patients.	Baseline biomarkers, post-treatment biomarkers, and total change in biomarkers; latent biomarker constructs; tumour shrinkage; T2VOL$_2$	Time (pre versus post); tumour response categories; Composite biomarker indices (CBI); T0VOL$_2$, T2VOL$_2$	Independent t-test / Mann–Whitney U test; paired t-test / Wilcoxon signed-rank test; Benjamini–Hochberg (BH-FDR) correction; Spearman correlation; Simple and Multiple linear regression; Simple logistic regression; EFA; PLS-SEM; bootstrapped paired analysis
4. To computationally predict and functionally annotate tamoxifen-interacting genes and signalling pathways in NF-PitNETs.	Enriched KEGG pathways; hub genes; network topology metrics	Predicted tamoxifen target genes	False discovery rate (FDR) correction; protein–protein interaction network construction; descriptive network topology analysis

3.14 SUMMARY

This chapter outlined a translational, proof-of-concept methodology to evaluate both the therapeutic and mechanistic effects of tamoxifen in residual NF-PitNETs using a three-tiered design. The study integrated immunohistochemical profiling, a 12-month pilot randomised clinical trial with MRI-based tumour volumetry as the primary outcome, serum biomarker analysis, and complementary bioinformatics approaches. Immunohistochemistry established the biological plausibility of oestrogen receptor targeting, while the open-label trial compared tamoxifen with active surveillance using blinded volumetric assessment. Longitudinal serum biomarkers were analysed by multiplex immunoassays and ELISA within a domain-based framework. Statistical analyses combined descriptive, inferential, and multivariate methods with bootstrapping and false discovery rate correction to address sample size constraints. In silico target prediction, pathway enrichment, and network analyses contextualised the clinical and biomarker findings within established molecular signalling frameworks. Overall, this integrative framework provided a robust, hypothesis-generating study to inform future confirmatory studies and therapeutic development in NF-PitNETs.

CHAPTER IV

RESULTS AND DISCUSSION

4.1 STUDY COHORT

A total of 96 patients with NF-PitNETs who underwent surgery between 2017 and 2019 and attended post-operative follow up were initially identified. Sixteen patients were excluded at the screening stage due to incomplete or missing data, leaving 80 patients screened for eligibility. Of these, 50 patients consented to tissue retrieval for histopathological studies. After eligibility assessment, 40 patients were excluded for predefined reasons: absence of residual tumour (n = 24), prior radiotherapy (n = 6), history of malignancy (n = 2), poorly controlled diabetes mellitus on insulin (n = 3), poor cardiac function (n = 3), and current use of antipsychotic medication (n = 2). The remaining 40 patients fulfilled the eligibility criteria and were invited to participate. Eight patients declined participation, while the remaining 32 provided written informed consent for both tumour tissue analysis and enrolment in the clinical trial. These 32 [illegible] years) and sex (male vs female).

Sixteen patients were allocated to the tamoxifen treatment arm and sixteen to the active surveillance (control) arm. During follow-up, 12 participants (six in each arm) were excluded from the per-protocol analysis. Reasons for exclusion were inability to attend follow-up visits because of COVID-19 movement control restrictions or logistical issues (n = 5); documented tumour regrowth requiring urgent repeat surgical intervention (n = 2, both in the control arm); identification of giant pituitary adenomas during the prespecified interim analysis (n = 3; two in the tamoxifen arm and one in the [illegible] and/or tumour volume approaching or exceeding 10 cm³) (Gaia et al. 2022) with

extreme volumetric outliers that were considered likely to disproportionately influence the analyses; and non-adherence to the protocol (n = 2).

Consequently, 20 patients (10 in each arm) completed the study and were included in the final per protocol analysis. The detailed participant flow is summarised in the CONSORT diagram in the Appendix B. All participants in the intervention group completed the study protocol without experiencing major adverse effects (see Appendix H and I).

4.2 BASELINE PROFILES

At baseline, demographic, clinical, endocrinological, radiological, histopathological, and molecular characteristics were comparable between groups (see Appendix A2 and A3).

4.2.1 Demographic Profile

The mean age at diagnosis did not differ significantly between groups, indicating age balance at study entry (Table 4.1). Median age at enrolment was similar between groups: 57.0 years (IQR 44.0–63.25) in the control arm and 52.0 years (IQR 45.5–61.5) in the tamoxifen arm (p = 0.733) (Table 4.2). Gender distribution was identical in both arms, with equal proportions of male and female patients. Racial composition showed a predominance of Malay ethnicity in both groups, with a small but comparable representation of Chinese patients (see Appendix A4).

4.2.2 Clinical Features and Endocrine Function

Clinical presentations did not differ significantly. Headache occurred at similar frequencies, and visual disturbance – a common manifestation of suprasellar compression – was observed in nearly all patients in both groups. Cranial nerve involvement was rare overall and appeared only in the control group (10%), but the difference was not statistically significant. This low incidence is consistent with typical presentations of NF-PitNETs, in which cranial neuropathies are less common than optic chiasm compression. Repeat surgical intervention was common in both groups,

occurring in 50% of patients in the control arm and 40% in the tamoxifen arm, with no statistically significant difference between groups (see Appendix A4).

Endocrine dysfunction was also comparable at baseline. The proportions of patients with hypocortisolism, hypogonadism, and hypothyroidism were similar across groups, although hypothyroidism was slightly more frequent in the control arm. Panhypopituitarism occurred only in the control group but did not reach statistical significance due to the small sample size. Pre-operative and post-operative hormonal replacement therapies, including hydrocortisone, thyroxine, and testosterone, were similarly distributed between study arms (see Appendix A4). The post-operative duration prior to enrolment was also similar between groups. The median post-operative interval was 24 months (IQR 15.75–24.25) in the control group and 27 months (IQR 15.0–42.25) in the tamoxifen group, with no statistically significant difference (p = 0.648) (Table 4.2).

4.2.3 Radiological Features

All participants had invasive tumours prior to surgical intervention, with baseline tumour volumes exceeding 1.0 cm³, consistent with the definition of macroadenomas. Baseline radiological characteristics were highly comparable between the control and tamoxifen-treated groups. Suprasellar extension was present in all patients in both groups, reflecting the typical superior growth pattern of large NF-PitNETs. Parasellar involvement was also frequently observed and did not differ significantly between groups. Infrasellar extension was identified only in the tamoxifen group (20%); however, this difference did not reach statistical significance (see Appendix A4).

Baseline tumour volume (□ □ □ □ □ $_2$) □□ □ □ □□ □ □ □ □ □ □ □□ □ □ □ □ □ □ □□ □ □ baseline tumour volume was 2.24 ± 1.31 cm³ in the control group and 1.90 ± 1.54 cm³ in the tamoxifen group, with no statistically significant difference between groups (p = 0.602) (Table 4.1).

4.2.4 Histological Features

Histopathological subtypes were similarly distributed between the two treatment arms. Null cell adenomas and silent gonadotroph tumours comprised the majority of cases. Although silent corticotroph and plurihormonal tumours were observed only in the control group, this difference was not statistically significant (see Appendix A4). None of the specimens met the criteria for proliferative tumours, as all showed a Ki-67 index of less than 3%, with no significant p53 expression and no increased mitotic activity. Accordingly, all tumours were classified as invasive but non-proliferative, corresponding to group 2a in the prognostic classification proposed by Trouillas et al. (2013).

Table 4.1 Baseline Continuous Variables with Normal Distribution Compared Between Control and Tamoxifen Groups Using Independent t-test

Variable	Control Mean (SD)	Tamoxifen Mean (SD)	Mean Diff	t-stat	*p*-value
Age at diagnosis	49.40 (11.21)	48.30 (9.87)	1.10	0.23	0.818
Baseline tumour v[illegible]	2.24 (1.31)	1.90 (1.54)	0.34	0.53	0.602
[illegible] β H-score	94.50 (127.55)	88.00 (115.26)	6.50	0.12	0.906

Normality assumptions was fulfilled

Table 4.2 Baseline Continuous Variables with Non-normal Distribution Compared Between Control and Tamoxifen Groups Using Mann-Whitney U Test

Variable	Control Median (IQR:Q1-Q3)	Tamoxifen Median (IQR:Q1-Q3)	U-test	*p*-value
Age at enrolment	57.0 (44.0–63.25)	52.0 (45.5–61.5)	45.50	0.733
[illegible] α -score	0.00 (0.00–1.25)	0.00 (0.00–0.00)	46.00	0.627
Post-op duration (months)	24 (15.75–24.25)	27 (15.0–42.25)	44.00	0.648

4.3 IMMUNOHISTOCHEMICAL EXPRESSION OF OESTROGEN RECEPTORS IN NF-PITNETS

Out of 50 NF-[illegible] α [illegible] cases (18%) showing positive nuclear immunostaining and a mean H-score of 99.4 ± 2 [illegible] β [illegible] 34 of 50 cases (68%) displaying positive immunostaining and a higher mean H-score

[illegible] 2 [illegible] 5 [illegible] β [illegible] NF-PitNET cohort.

In the clinical trial cohort (n = 20), baseline immunohistochemical analysis also [illegible] α [illegible] α [illegible] %) [illegible] expression was more frequent, detected in 6 of 10 patients (60%) in the control group [illegible] %) [illegible] e trial cohort, and no significant differences in receptor positivity were observed between groups at baseline (see Appendix A4).

Quantitative assessment using the H-score further supported these findings. [illegible] α [illegible] -score of 0.00 (IQR 0.00–1.25) in the control group and 0.00 (IQR 0.00–0.00) in the tamoxifen group, with no significant difference between groups (p = 0.627) (Table 4.2). Similarly, [illegible] β -scores were comparable between groups, with mean values of 94.50 ± 127.55 in the control group and 88.00 ± 115.26 in the tamoxifen group (p = 0.906). The large standard deviations indicate substantial inter-[illegible] expression across the cohort (Table 4.1). Representative NF-PitNET tissue sections [illegible] Figure 4.1.

(a)

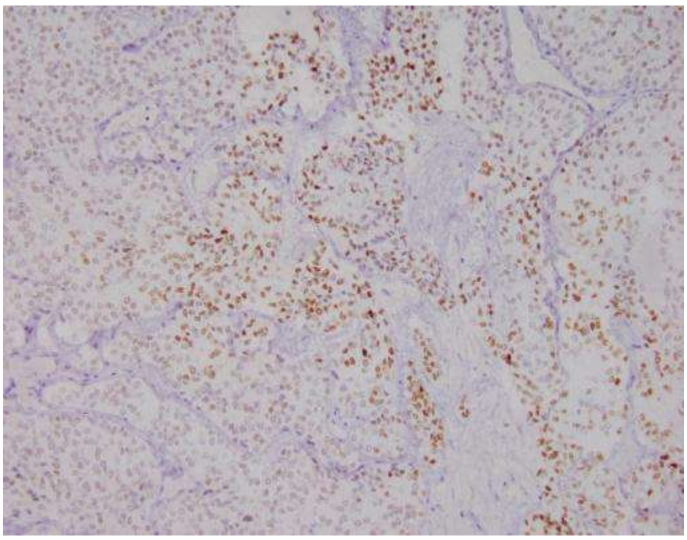

(b)

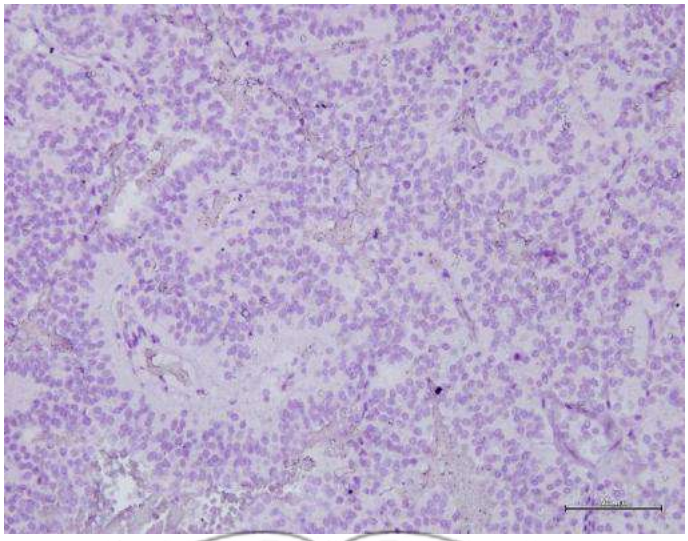

(c)

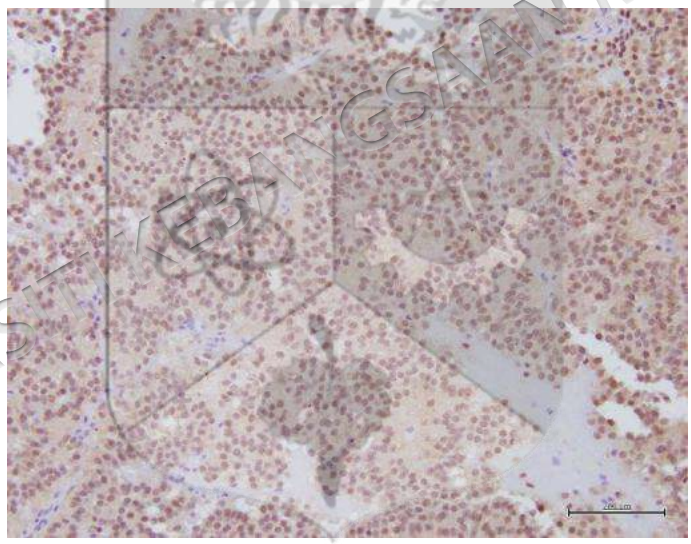

(d)

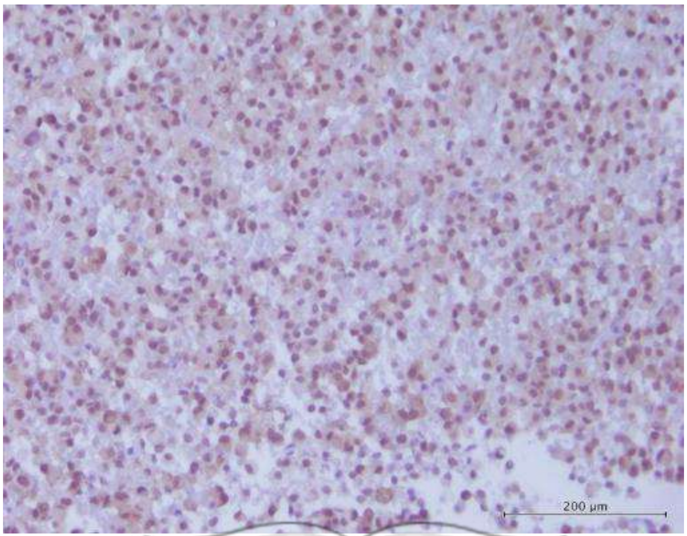

(e)

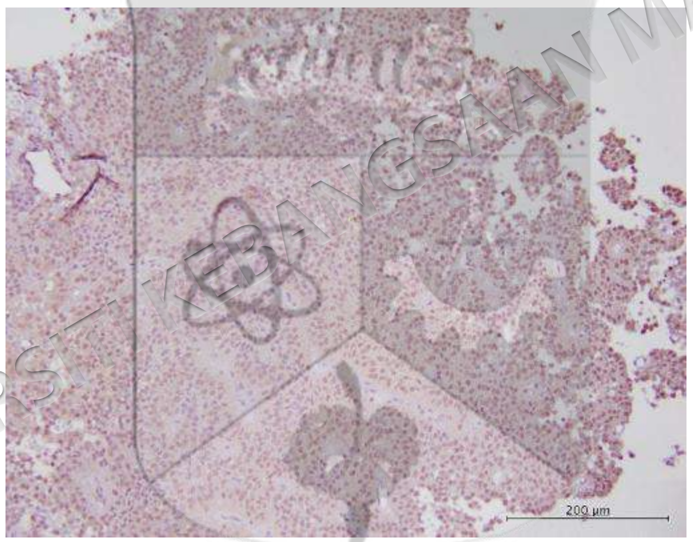

Figure 4.1 Representative immunohistochemical staining patterns of oestrogen receptors in NF-PitNET tissue sections

a) α
b) staining. α
c) β
d) β
e) β)

All Images were taken at ×200 magnification (Adapted from Haydar Ali Tajuddin, A et al. 2025)

4.4 CLINICAL IMPACT OF TAMOXIFEN ON TUMOUR VOLUMES

4.4.1 Continuous Tumour Volumetric Outcomes

-month tumour volume
-month tumour volume between the tamoxifen and control groups (F(1,16) = 2.643, *p* = 0.142). The adjusted (marginal) mean tumour volume at 12 months was 1.861 cm³ for the tamoxifen group and 2.395 cm³ for the control group, indicating a numerically lower adjusted mean in the tamoxifen arm, although this difference did not reach statistical significance.

T2VOL (F = 7.238, *p* = , η² =) in the outcome. In co covariate in the model (F = 2.909, *p* = , η² = 5)

Overall, these findings indicate that although the tamoxifen group had a lower adjusted mean 12-month tumour volume, the between-group difference was not statistically significant after adjustment, and baseline tumour volume remained the main determinant of final tumour volume.

Table 4.3 Analysis usted for Baseline and Interim Tumour Volumes Using ANCOVA

Variable	*n*	Mean (SD)	Adjusted Mean (Marginal Mean)	F (1,16)	*p*-value	
Control	10	2.600 (1.543)	2.395	2.643	0.124	0.142
Tamoxifen	10	1.656 (1.270)	1.861			
Covariates						
				7.238	0.016*	0.311
				2.909	0.107	0.154

Normality assumptions were fulfilled
*Significant, p < 0.05

Tumour volume did not show a statistically significant overall change across the three time points (T_0, T_1 and T_2) (F(2,36) = 2.889, *p* = 0.069). There was also no evidence of a differential temporal pattern between the tamoxifen and control groups

(F(2,36) = 1.44, $p = 0.249$), indicating that tumour volume trajectories over time were broadly similar in both groups.

Planned contrasts indicated a significant change in tumour volume between baseline and 6 months ($p = 0.044$), whereas the change between 6 and 12 months was not statistically significant ($p = 0.078$). Consistent with these findings, between-group comparisons at individual time points showed no significant differences in tumour volume at baseline ($p = 0.602$), 6 months ($p = 0.566$), or 12 months ($p = 0.153$).

Overall, these results indicate that, in this pilot cohort, there was no statistically significant overall time effect or between-group difference in tumour volume, although a modest short-term change was observed between baseline and 6 months.

Within the tamoxifen-treated group, tumour volume showed a statistically significant reduction over 12 months, decreasing from 1.90 cm^3 at baseline to 1.66 cm^3 at follow-[illegible] $p = 0.045$).[illegible] – [illegible] 2 This finding suggests a small but measurable reduction in tumour volume in patients receiving tamoxifen over the study period.

Table 4.4 Longitudinal Tumour Volume by Study Arm Using Repeated-Measures General Linear Model (RM-GLM)

Tumour Volume : F (2,36)= 2.888; $p = 0.069$[a]		
		Mean (SD)
For Control	[illegible]	2.24 (1.31)
	[illegible]	2.76 (1.40)
	[illegible] 2 [illegible]	2.60 (1.54)
For Tamoxifen	[illegible]	1.90 (1.54)
	[illegible]	2.19 (1.18)
	[illegible] 2 [illegible]	1.66 (1.27)
Within-subject contrasts (RM-GLM):		
Baseline vs 6 months: $p = 0.044$*[b]		
6 months vs 12 months: $p = 0.078$[b]		
Time x Study Arm: F (2,36) = 1.44; $p = 0.249$[a]		

Tumour Volume at Baseline	Mean (SD)	T-Stats (df)	*p*-value
For Control	2.24 (1.31)	0.531 (18)	0.602[c]
For Tamoxifen	1.90 (1.54)		
Tumour Volume at 6 months			
For Control	2.76 (1.40)	0.592 (18)	0.566[c]
For Tamoxifen	2.19 (1.18)		

[illegible]

…[illegible]

Tumour Volume at 12 months			
For Control	2.60 (1.54)	1.494 (18)	0.153[c]
For Tamoxifen	1.66 (1.27)		

*Significant at $p < 0.05$

a: RM-[illegible] p = 0.920). [illegible]

b: Planned within-subject contrasts from repeated-measures GLM.

[c] Independent-samples t-test between study arms at each time point.

Table 4.5 Within-Group Comparison of Tumour Volume Before and After Tamoxifen Treatment Using Paired t-test

Variable	**Mean (Pre, cm^3)**	**Mean (Post, cm^3)**	**Mean Diff (Post – Pre)**	t	**df**	p
Tumour Volume (T_0 vs T_2)	1.90	1.66	−0.24	−2.32	9	0.045*

*Significant at $p < 0.05$

Figure 4.2 illustrates the distribution of tumour volumes at T0, T1, and T2 for the control and tamoxifen-treated groups. Although the tamoxifen group had a numerically lower median baseline tumour volume than the control group, baseline tumour volumes did not differ significantly between groups (Table 4.1; $p = 0.602$). As participants were allocated using block randomisation without stratification by tumour volume, this numerical difference most likely reflects random variation associated with the small pilot sample. In the control group, tumour volumes generally remained stable or increased over time. Median tumour volume increased from baseline to interim follow-up and remained elevated at final follow-up, with relatively wide interquartile ranges at all time points, indicating substantial inter-individual variability. Several [illegible] consistent with tumour growth in a subset of cases.

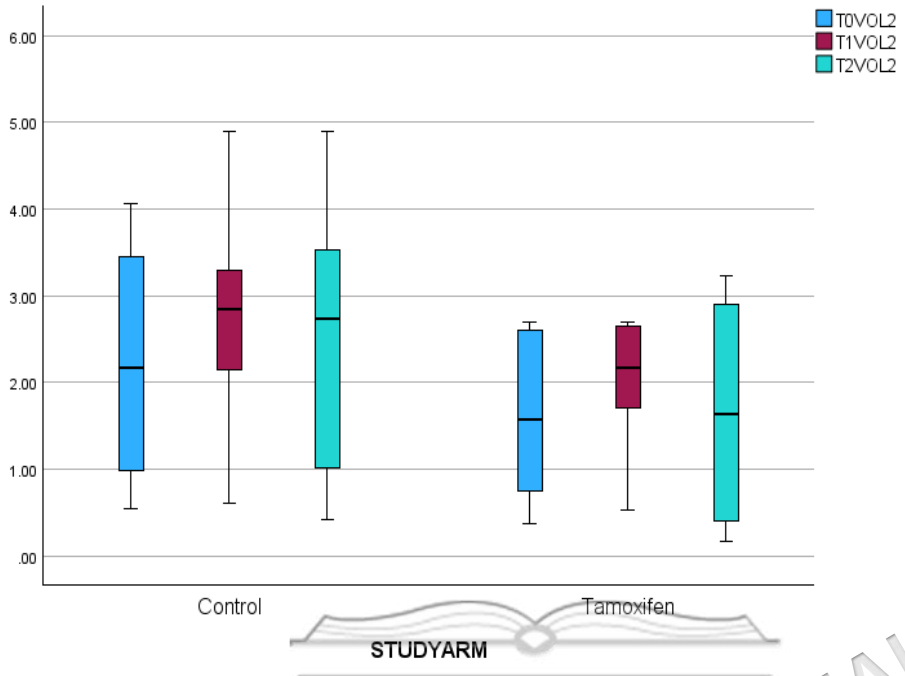

Figure 4.2 Longitudinal Changes in Tumour Volume Across Study Arms (T_0, T_1, and T_2)

In contrast, the tamoxifen group displayed a different volumetric trajectory. Median tumour volume increased modestly from baseline to interim follow-up but declined at T2. The distribution at final follow-up shifted downward relative to both baseline and interim measurements, with lower medians and reduced upper ranges compared with the control group. This pattern suggests a tendency towards tumour stabilisation or reduction in tamoxifen-treated patients.

Figure 4.3 shows the estimated mean tumour volumes at three time points for the control and tamoxifen-treated groups. At T_0, the mean tumour volume was slightly higher in the control group than in the tamoxifen group. From T_0 to T_1, both groups showed an increase in mean tumour volume, with a more pronounced rise in the control group. Between T_1 and T_2, the groups followed different trajectories. In the control group, mean tumour volume remained elevated with only a modest decline, while the tamoxifen group showed a marked reduction in mean tumour volume at T_2.

Overall, the plot shows a non-parallel pattern of change over time between the groups, with the greatest separation at the final follow-up. These visual trends are consistent with the repeated-measures GLM analysis, which found a significant within-subject contrast between T_0 and T_1, and a non-significant but directional reduction between T_1 and T_2.

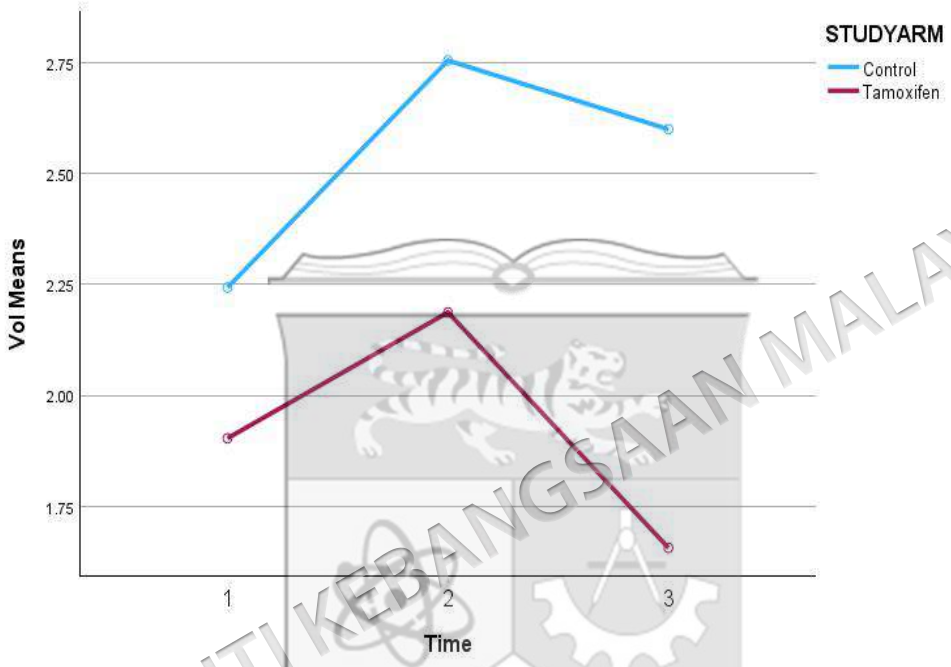

Figure 4.3 Estimated Marginal Means of Tumour Volume Over Time Points by Treatment Group

Figure 4.4 presents representative images from the tamoxifen-treated cohort, demonstrating the greatest tumour volumetric reduction, with a decrease of up to 87% from the original residual tumour volume over the 12-month follow-up period. At baseline, coronal contrast-enhanced T1-weighted MRI showed a well-defined residual sellar–suprasellar mass with clear contrast enhancement (Figure 4.4A(i), 4.4B(i)). At 6 months of treatment, repeat MRI demonstrated a visible reduction in tumour size in both coronal and sagittal planes, with a decrease in maximal tumour dimensions and overall enhancing tumour bulk (Figure 4.4A(ii), 4.4B(ii)). By 12 months, further tumour shrinkage was observed, with a marked reduction in residual tumour volume and a corresponding decrease in contrast-enhancing tissue (Figure 4.4A(iii), 4.4B(iii)). This

serial imaging progression highlights a sustained and progressive volumetric response to tamoxifen therapy over one year, as assessed by three-dimensional MRI-based tumour segmentation. Among all treated patients, this case showed the greatest relative tumour volume reduction and is therefore presented as a representative example of maximal radiological response within the intervention

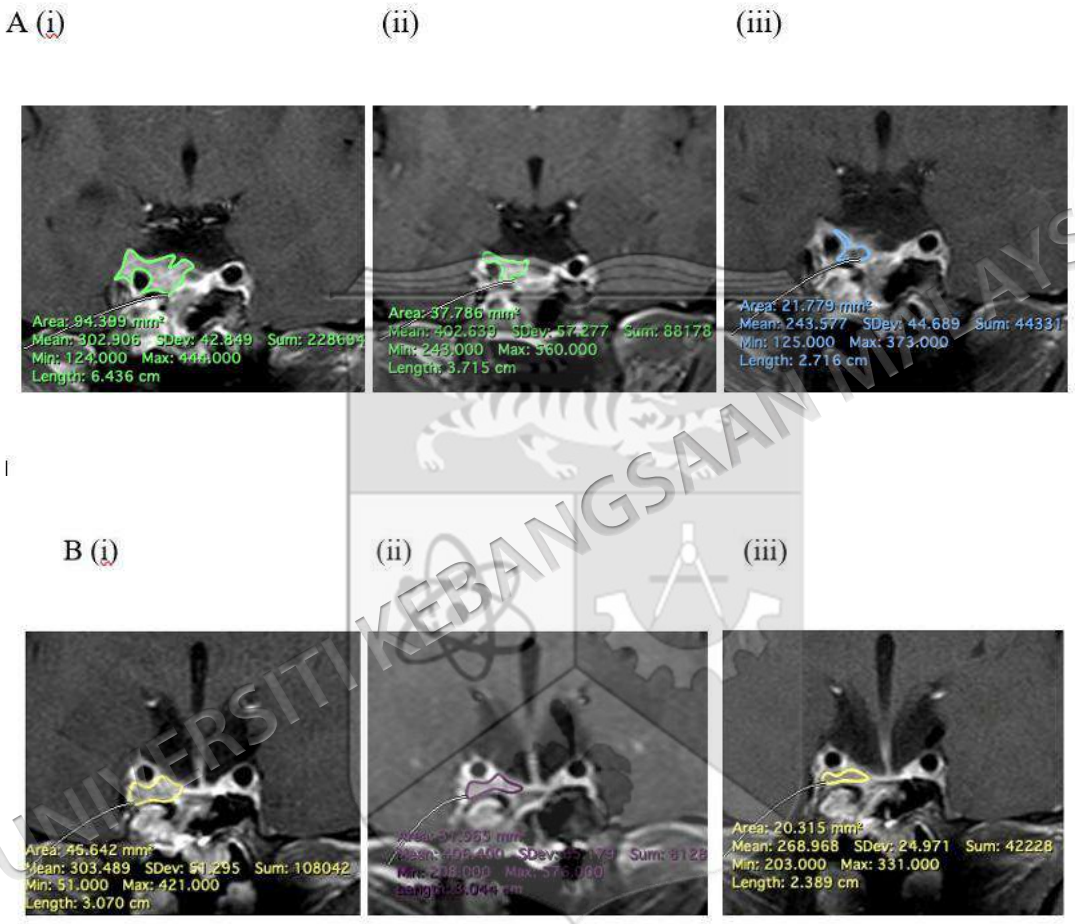

Figure 4.4 Representative MRI images of a patient who was treated with tamoxifen and whose tumour volume had shrunk the most

(Adapted from Haydar Ali Tajuddin, A et al.2025)

(A) Coronal contrasted T1-weighted MR images obtained at T_0 (i) at T_1 (ii) & at T_2 (iii)

(B) Coronal contrasted T1-weighted MR images obtained at T_0 (i) at T_1 (ii) & at T_2 (iii)

4.4.2 Categorical Treatment Outcomes

Treatment outcome categories differed significantly between the control and tamoxifen-treated groups (Table 4.6). Tumour shrinkage was observed only in the tamoxifen group, occurring in 4 of 10 patients (40%), while no patients in the control group achieved a comparable reduction in tumour volume; this difference was statistically significant (p = 0.014). Tumour stabilisation was the most frequent outcome in both groups, observed in 80% of control patients and 60% of tamoxifen-treated patients. In contrast, tumour regrowth occurred only in the control group, affecting 2 patients (20%), and was not observed among patients receiving tamoxifen.

Table 4.6 [illegible] Exact Test

Treatment Outcome	Control (n = 10)	Tamoxifen (n = 10)	*p*-value
Shrinkage	0 (0%)	4 (40%)	0.014*
Stabilisation	8 (80%)	6 (60%)	
Regrowth	2 (20%)	0 (0%)	

*Significant, $p < 0.05$

Volumetric outcomes differed significantly across response categories when [illegible] 2 [illegible] $_2$ [illegible] Δ [illegible] 7). At follow-up, %Δ patients in the [illegible] shrinkage category had the lowest mean tumour volume (1.08 ± 1.44 cm³), compared with those in the stabilisation (2.13 ± 1.25 cm³) and regrowth (4.21 ± 0.96 cm³) categories. One-way ANOVA showed a statistically significant difference in $T2VOL_2$ across outcome groups (F (2, 17) = 4.062, p = 0.036).

[illegible] Δ [illegible]

[illegible] the stabilisation group showed minimal net change (0.13 ± 0.22 cm³). In contrast, the regrowth group had a substantial mean increase in tumour volume (1.53 ± 0.64 cm³). These differences were highly significant (F (2,17) = 18.625, p = 0.001).

[illegible] %Δ [illegible] me groups (F (2,17) = [illegible] 21.675, p [illegible]) [illegible] ± 25.67%, while the stabilisation group showed minimal change (5.77% ± 11.26%). Patients with tumour regrowth had a marked increase in tumour volume, with a mean

percentage increase of 77.88% ± 70.52%. Wide confidence intervals in the regrowth category reflect the small number of patients in this subgroup.

Table 4.7 Comparison of Final Tumour Volume and Volumetric Change Across Treatment Response Categories Using One-way ANOVA

Variable	Outcome	*n*	Mean (SD)	F-stat (2,17)	*p*-value
Final tumour volume	Shrinkage	4	1.08 (1.44)	4.062	0.036*
	Stabilisation	14	2.13 (1.25)		
	Regrowth	2	4.21 (0.96)		
Absolute volume change	Shrinkage	4	− 5	18.625	0.001*
	Stabilisation	14	0.13 (0.22)		
	Regrowth	2	1.53 (0.64)		
Percentage tumour volume change	Shrinkage	4	− 5 (25.67)	21.675	0.001*
	Stabilisation	14	5.77 (11.26)		
	Regrowth	2	77.88 (70.52)		

Normality assumptions were fulfilled
*Significant, $p < 0.05$

Post hoc pairwise comparisons showed significant differences in volumetric outcomes across tumour response categories (Table 4.8) 2 shrinkage group had lower mean final volumes compared with those in the regrowth $p = 0.011$) and compared with the stabilisation cm³, $p = 0.281$). A significant difference was also observed between the stabilisation and regrowth groups, with the regrowth group exhibiting substantially higher final $p = 0.044$). − 2 ³

Δ comparisons. Tumour shrinkage was associated with a significantly greater reduction $p = 0.001$) and $p < 0.001$). The stabilisation group also differed $p = 0.001$).

Similarly % Δ tumour shrinkage showed significantly greater percentage reductions compared with $p = 0.001$) and the regrowth group (mean difference − 2 $p < 0.001$). A significant difference was also

[illegible] p [illegible] = 0.001).

Table 4.8 Post-Hoc Pairwise Comparisons of MRI-Based Volumetric Outcomes Across Tumour Response Categories

Group Comparison	Mean Difference	*p*-value
Dependent Variable: Final Tumour Volume (T2VOL$_2$, cm^3)		
Shrinkage vs Stabilisation	–1.05	0.281
Shrinkage vs Regrowth	–3.13	0.011*
Stabilisation vs Regrowth	–2.08	0.044*
Outcome Measure Group Comparison	Mean Difference	*p*-value
Dependent Variable: [illegible] Δ [illegible]		
Shrinkage vs Stabilisation	–1.08	0.001*
Shrinkage vs Regrowth	–2.48	<0.001*
Stabilisation vs Regrowth	–1.39	0.001*
Outcome Measure Group Comparison	Mean Difference	*p*-value
Dependent Variable: [illegible] %Δ		
Shrinkage vs Stabilisation	–54.29%	0.001*
Shrinkage vs Regrowth	–126.40%	<0.001*
Stabilisation vs Regrowth	–72.11%	0.001*

Normality assumptions were fulfilled
Least Significant Difference (LSD) following one-way ANOVA
*Significant, $p < 0.05$

4.4.3 Subgroup Analyses

As expected from response classification, volumetric outcomes differed significantly between the two subgroups (Table 4.9). The shrinkage group showed a markedly greater [illegible] 5 [illegible] %) [illegible] – [illegible]) [illegible] p = 5 0.001). Absolute volume change also differed significantly, with a [illegible] – [illegible] 5 [illegible] ^{3} [illegible] 2 2 [illegible] ^{3}) [illegible] 5 % [illegible] – 2 [illegible]) – p = 2 0.018).

No significant differences were observed between subgroups for demographic, baseline clinical, or radiological variables, including age, age at diagnosis, post- [illegible] (all p ≥ 0.05, see Appendix A11). [illegible] 2 [illegible] -scores did not differ significantly between groups.

Table 4.9 Subgroup Analysis Comparing Tumour Shrinkage and Stabilisation in Tamoxifen-Treated Patients Using Independent t-test

Variable	Shrinkage (n=4) Mean (SD)	Stabilisation (n=6) Mean (SD)	Mean Difference	t-stat (8)	*p*-value
Percentage volume change (%Δ)	–48.53 (25.67)	+11.65 (7.30)	–60.17	–5.57	0.001*
Absolute volume change (Δ)	–0.95 (0.97)	+0.22 (0.18)	–1.17	–2.97	0.018*

*Significant, $p < 0.05$

4.4.4 Correlations with Tumour Volumes

[illegible] $r = 0.855$ for both, $p = 0.002$), indicating high temporal stability of tumour burden in untreated patients. In the tamoxifen-treated group, baseline tumour volume also remained strongly correlated with 12-month tumour volume ($r = 0.855$, $p = 0.002$), suggesting that initial tumour size continued to be an important determinant of longer-term tumour burden despite treatment. However, the association between baseline and 6-month tumour volume in the tamoxifen group was weaker and not statistically significant ($r = 0.590$, $p = 0.073$), implying greater short-term variability in tumour volume during the early treatment period.

No significant correlations were observed between baseline tumour volume and other clinical or demographic variables, including age, age at diagnosis, post-operative duration, volumetric change indices, or oestrogen receptor expression (all $p > 0.05$). This indicates that, within this cohort, baseline tumour size was the main correlate of subsequent tumour volume, whereas other measured clinical and biological factors did not show detectable associations. Full correlation results are provided in Appendix A12.

[illegible] $r = 0.855$, $p = 0.002$) and [illegible] ($r = 0.927$, $p < 0.001$). This pattern indicates marked

temporal stability in tumour size among untreated patients, with tumour burden at diagnosis and at interim follow-up closely predicting final tumour volume.

In contrast, in the tamoxifen-[illegible] 2 [illegible]$_2$ [illegible] [illegible] (r = 0.748, p = 0.013), while no significant correlation was observed with T0VOL$_2$, %Δ [illegible] or other clinical or molecular variables. This suggests that, under tamoxifen treatment, early on-treatment tumour status rather than baseline tumour burden was more closely related to final tumour volume, consistent with greater short-term variability in tumour behaviour following treatment initiation.

No other variables showed statistically significant associations with final tumour volume in either group (all $p > 0.05$; see Appendix A12 and A13), indicating that, within this cohort, preceding tumour volume was the dominant correlate of long-term tumour burden, particularly in the control group.

4.5 SERUM BIOMARKER PROFILES AND LONGITUDINAL CHANGES

All serum biomarkers were measured in duplicate and generally showed acceptable intra-assay precision. For the multiplex immunoassays, most measurements had C[illegible] ≤ [illegible] 20%; however, HGF, SCF/c-kit ligand, and TGF-α [illegible] (>20%) in a subset of samples, particularly at low concentrations near the lower limit of quantification, while CD40 Ligand, VEGF, IL-6, TNF-α [illegible] 2 [illegible] occasionally showed high CV values (Appendix E and F). The ELISA-based measurements (SFRP1 and DKK1) showed good duplicate agreement with acceptable intra-assay variability, indicating stable assay performance for these analytes. Accordingly, values with higher analytical variability were interpreted with caution.

4.5.1 Baseline Serum Biomarker Profiles

At baseline, none of the measured serum biomarkers showed statistically significant differences between the two study arms (all $p > 0.05$). Baseline concentrations of VEGF, HGF, FGF, TGF-α [illegible] -α [illegible] -6, DKK1, and sFRP1 were comparable between groups (Appendix A5 and A6). This baseline comparability indicates that the two groups were biochemically well balanced prior to intervention, reducing the

likelihood that subsequent between-group differences in biomarker trajectories or clinical outcomes could be attributed to pre-existing differences in circulating biomarker profiles.

4.5.2 Longitudinal Changes in Biomarkers Following Tamoxifen Therapy

Baseline serum biomarker levels did not differ significantly among the three treatment outcome groups (all $p > 0.05$; Appendix A8), indicating that no baseline biomarker distinguished between shrinkage, stabilisation, and regrowth categories. Although numerical differences were observed across groups, the wide confidence intervals and small subgroup sizes suggest limited statistical power to detect between-group differences at baseline.

Longitudinal serum biomarker analyses were conducted in the tamoxifen-treated group only, as the primary objective of this component was to evaluate biomarker changes associated with tamoxifen therapy. Baseline biomarker measurements were obtained in both study arms to establish pre-treatment comparability, whereas serial biomarker measurements were prioritised in the intervention group because of budgetary constraints.

Among biomarkers with normally distributed change scores, TNF-α [illegible] only marker to show a statistically significant pre–post change following tamoxifen therapy (Table 4.10). Mean TNF-α [illegible] 2 [illegible] baseline to 27.53 ± 18.06 pg/mL at follow-up, corresponding to a mean difference of − 5 [illegible] ($t = 2.34$, $p = 0.044$). In contrast, TGF-α [illegible] -significant [illegible] L, $p = 0.665$), IL-6 showed a non-significant increase (mean difference +5.60 pg/mL, $p = 0.359$), and DKK1 showed a non-[illegible] $p = 0.560$). Thus, within this [illegible] subset of biomarkers, only TNF-α [illegible] ly significant longitudinal change following tamoxifen treatment.

For biomarkers with non-normally distributed change scores, no statistically significant pre–post differences were observed (all $p > 0.05$; Appendix A16). Specifically, CD40L, HGF, and SCF showed more negative than positive ranks, but

these shifts did not reach statistical significance. FGF and VEGF demonstrated near-symmetrical distributions of positive and negative ranks, whereas sFRP1 showed more positive than negative ranks; however, none of these patterns reached statistical significance.

After adjustment for multiple comparisons using the Benjamini–Hochberg false discovery rate procedure ($q = 0.05$), none of the biomarker pre–post changes remained statistically significant (Appendix A17). Although TNF-α □□ □ □ □ □ □ □□ □□ □ □ □ □ □ significant reduction ($p = 0.044$), this association did not remain significant after FDR correction and should therefore be interpreted cautiously.

Overall, these findings suggest that tamoxifen therapy was associated with a reduction in circulating TNF-α □□ □ □ □ □ □ □ □□ □ □ □□ □ □□ □ □ □ □ □ □□ □ □ □ □ circulating biomarkers did not demonstrate consistent longitudinal changes. Baseline serum biomarker profiles were also not significantly associated with subsequent volumetric treatment response within the limitations of this pilot study.

Table 4.10 Longitudinal Changes in Normally Distributed Serum Biomarkers (Pre- vs Post-Treatment) Using Paired t-test

	Mean (SD)			
Variable	**Pre Mean (pg/ml)**	**Post Mean (pg/ml)**	***t*-stat**	***p*-value**
TNF-α	42.64 (11.54)	27.53 (18.06)	2.34	0.044*
TGF-α	5.76 (3.89)	5.21 (2.00)	0.45	0.665
IL-6	68.51 (18.36)	74.11 (25.71)	-0.97	0.359
DKK1	3740.60 (1876.45)	3309.60 (2449.73)	0.61	0.560

Assumption normality was fulfilled
*Significant, $p < 0.05$

4.5.3 Bootstrapped Paired Analyses

Bootstrapped analyses indicated statistically significant pre–post changes across all assessed serum biomarkers, with all bootstrapped $p < 0.001$ and 95% confidence intervals not crossing zero. Three biomarkers – DKK1, HGF, and TGF-α – showed significant increases following treatment (Table 4.11). In contrast, the remaining biomarkers showed significant decreases over time. These included CD40L, VEGF, TNF-α □ □□ 1, SCF, IL-6, and FGF.

Collectively, these bootstrapped results suggest consistent and directionally coherent biomarker modulation over the study period, with robust evidence of change across all measured markers. The narrow confidence intervals indicate high internal consistency of the estimated changes within this cohort. However, given the small sample size and the contrast with conventional parametric and non-parametric analyses, these findings should be interpreted as supportive sensitivity analyses that reinforce the presence and direction of within-subject changes rather than as definitive confirmatory evidence.

Table 4.11 Bootstrapped Paired Analysis of Pre–Post Changes in Serum Biomarkers Following Tamoxifen Therapy in NF-PitNET Patients

Biomarker	Trend	Mean Change (Pre–Post) (pg/ml)	Bootstrapped 95% CI (Lower–Upper)	Bootstrapped *p*-value
DKK1	Increasing	+431.00	+389.17 to +472.83	0.001*
HGF	Increasing	+237.28	+220.70 to +253.87	0.001*
TGF-α	Increasing	+0.55	+0.48 to +0.62	0.001*
CD40L	Decreasing	− □ 5 □ □ 2	− □ □ □ □ □ □ □ □ □ □ □ □ □	0.001*
VEGF	Decreasing	− □ 2 □ □ □	− □ 2 □ □ □ □ □ □ □ □ □ □	0.001*
TNF-α	Decreasing	− 2 5 □ □ □	− 2 5 □ □ □ □ □ □ □ □ 2	0.001*
sFRP1	Decreasing	− □ □ □ □ □	− □ □ □ □ □ 2 □ □ □ □ □	0.001*
SCF	Decreasing	− 5 □ □ □	− □ □ □ □ □ □ □ □ 5 □	0.001*
IL-6	Decreasing	− 5 □ □ □	− 5 □ □ □ □ □ □ □ 5 □	0.001*
FGF	Decreasing	− □ □ □ □	− □ □ □ □ □ □ □ □ □ □	0.001*

4.5.4 Correlation Between Serum Biomarkers and Tumour Volumes

In the control group, no baseline biomarker showed a significant correlation with $T0VOL_2$ or $T2VOL_2$ (all $p > 0.05$), with correlation coefficients ranging from weak to moderate and showing no consistent directional pattern (see Appendix A12). Similarly, in the tamoxifen-treated group, no baseline biomarker was significantly associated with $T0VOL_2$ or $T2VOL_2$ (all $p > 0.05$; see Appendix A13). Although moderate inverse trends were observed for CD40L and DKK1 at baseline, and for sFRP1 and TNF-α □ □ □ 12 months, these did not reach statistical significance. Overall, baseline biomarker profiles were not significantly associated with residual tumour volume in either group.

In the tamoxifen-treated cohort, no post treatment biomarkers showed a significant monotonic correlation with $T2VOL_2$ (all $p > 0.05$). Several markers, including DKK1, sFRP1, VEGF, and TNF-α □ reached statistical significance.

□ □ □ □ □□ □ □ □ □ □ □□ □ □□ □ □ □ □□ □ □ □ □ □ □ □ □□ Δ) □□ □ □ □ outcomes (T0VOL$_2$, T1VOL$_2$, T2VOL$_2$□ □Δ □ □ □%Δ□□□□□□□) □ □□ □ □ □ □□ □ □ □ □ □ □ not significant, consistent with biological heterogeneity and the limited sample size (see □ □ □ □ □ □ □ □ □□ □ □) □ □□ □ □ □□ □ □ □ □ □ □ □ □ □ □□ □ □ □ □□ □ □ □ □ □ □ □ T1VOL$_2$ (r □ = □ □ p 2 □□ □ □ □ □) □ □□ □ □ □Δ □ □ □□ □ □ □ □ □ □ atively with T1VOL$_2$ (r = − □ □ □ p ≅ 0.006), indicating that greater reductions in these markers were associated with smaller tumour volumes at 6 months. No significant associations were found for these markers with T0VOL$_2$, T2VOL$_2$, or other markers of volume change.

All other biomarkers showed no significant correlations with any volumetric outcome (all $p > 0.05$), although some moderate, non-significant trends were observed □ Δ □-α □□ □ □ □ □$_2$ □ □ □ □ Δ □ □ □ %Δ □□ □□.

Overall, within this pilot cohort, only changes in SCF and sFRP1 were significantly associated with tumour volume at 6 months, while no biomarker showed a robust association with baseline volume, 12-month volume, or overall volumetric change. Significant inverse correlations were observed between changes in SCF and □ □ □ □ □ □□ □ □ □□ □ □ □ □$_2$ □ □□ □ □ □ □ □ □ □ □ □□ □ □ □ □□ □ □ □ □ □ □□ associated with smaller tumour volumes during the early phase of treatment. However, these associations were not seen at □2 □ □ □ $_2$ □ □□ □ □ □ □ □ □ □□ relationship □□ □ □ □ □ between early biomarker modulation and tumour volumetric response.

4.6 PREDICTORS OF TUMOUR VOLUMETRIC OUTCOMES

4.6.1 Predictors of Final Tumour Volume

Of all variables tested in the univariable linear regression analyses, %Δ □ □□ was the only continuous predictor to show a statistically significant association with T2VOL$_2$ (B = □ □ □ 2 □ □β t □= 2.45, p = 0.025) (see Appendix A18). This indicates that a greater percentage change in tumour volume was associated with a higher residual tumour volume at 12 months. This model explained approximately 25% of the variance in T2VOL$_2$ ($R^2 = 0.25$; adjusted $R^2 = 0.21$), representing a moderate effect size for a single predictor in this pilot cohort.

In contrast, Δ[illegible] was not significantly associated with $T2VOL_2$ ($p = 0.140$), suggesting that percentage change is a more informative descriptor of residual tumour burden than absolute change in this dataset.

[illegible] α [illegible] - [illegible] β treatment serum biomarkers, including the composite biomarker indices, showed significant associations with $T2VOL_2$ (all $p > 0.05$). Although several post-treatment markers (CD40post, DKK1post, SFRP1post, IL6post) demonstrated moderate standardised coefficients, their confidence intervals crossed zero and did not reach statistical significance, indicating at most weak or unstable trends.

For categorical response variables, tumour regrowth was a significant predictor of $T2VOL_2$ [illegible] 2 [illegible] *t* β 2.37, $p = 0.029$), indicating that patients classified as having regrowth had significantly larger residual tumour volumes at 12 months. This model accounted for approximately 24% of the variance in $T2VOL_2$ ($R^2 = 0.24$; adjusted $R^2 = 0.20$). In contrast, shrinkage and stabilisation were not significant predictors.

Study arm (tamoxifen vs control) was not significantly associated with $T2VOL_2$ in univariable analysis ($p = 0.153$), suggesting that treatment allocation alone did not explain variability in 12-month residual volume when considered in isolation.

No evidence of multicollinearity was observed (all tolerance = 1.00; VIF = 1.00), confirming that the univariable estimates are statistically stable.

Overall, the simple regression analyses indicate that radiological progression metrics – particularly percentage volume change and regrowth status – are the only variables that show meaningful unadjusted associations with $T2VOL_2$, whereas individual biomarkers and ER expression do not demonstrate significant predictive value in this pilot cohort.

In the multivariable model, both %Δ[illegible] and DKK1post remained statistically significant independent determinants of $T2VOL_2$. %Δ[illegible] showed a strong positive

association with $T2VOL_2$ [illegible] t = 3.50, p = 0.010), indicating that greater relative tumour volume change was independently associated with larger residual tumour volume at 12 months. Conversely, DKK1post showed a strong inverse association with $T2VOL_2$ [illegible] ≈ [illegible] β [illegible] − [illegible] p = 0.010), indicating that higher post-treatment DKK1 levels were independently associated with smaller residual tumour volumes at 12 months. This suggests a potential protective or growth-suppressive association of DKK1 within the Wnt-modulatory pathway in the treated group.

This model explained a substantial proportion of variance in $T2VOL_2$ (R^2 = 0.72; adjusted R^2 = 0.63), indicating strong explanatory performance for a two-predictor model in this pilot dataset. Collinearity diagnostics were acceptable (tolerance = 0.83; VIF = 1.20), confirming that the two predictors contributed independent information to the model (Table 4.12, see Appendix A19).

Table 4.12 Analysis of Univariate Predictors of Final Tumour Volume Using Multiple Linear Regression

Predictor	Unstandardised B	*t*-stat	*p*-value	95% CI	VIF
(Constant)	3.34	6.78	<0.001	2.18, 4.51	-
%Δ [illegible]	0.03	3.50	0.010*	0.01, 0.05	1.20
DKK1post	0.00	− [illegible] 5	0.010*	0.00, 0.00	1.20

Dependent variable: $T2VOL_2$
Multiple Linear regression was applied; R^2 = 0.72; Adjusted R^2 = 0.63
Overall model F (2, 7) = 9.00, p = 0.011
CI=Confidence Interval; VIF= Variance Inflation Factor
*Significant, $p < 0.05$

4.6.2 Predictors of Tumour Shrinkage

Binary logistic regression was conducted to identify clinical, radiological, histological, and biomarker predictors of tumour shrinkage. None of the variables tested showed a statistically significant association with the likelihood of shrinkage (all $p > 0.05$) (see Appendix A20). For all variables, the odds ratios [Exp(B)] were close to 1.0, and the 95% confidence intervals included unity, indicating no meaningful increase or decrease in the odds of shrinkage associated with these factors.

The pseudo-R^2 val[illegible] −0.11; [illegible] −0.16), demonstrating that each model explained little to no

variance in the probability of shrinkage. This suggests that, within this pilot cohort, shrinkage is a weakly predictable outcome when using single clinical or biomarker variables.

Overall, these findings indicate that no single baseline or post-treatment biomarker, ER expression measure, or clinical variable independently predicts tumour shrinkage in this dataset. This likely reflects a combination of biological heterogeneity, small sample size, and the complex, multifactorial nature of treatment response in NF-PitNETs. The results support the broader conclusion that single-marker models are insufficient and that continuous volumetric outcomes or multivariate or pathway-level approaches are more informative for capturing treatment effects in this disease.

4.7 MULTIVARIATE MODELLING OF BIOMARKER DOMAINS IN RELATION TO TUMOUR VOLUME AND TREATMENT RESPONSE

4.7.1 Exploratory Factor Analysis (EFA)

a. Z-Score–Standardised pre-treatment biomarkers

Four components with eigenvalues greater than 1.0 were extracted from the pre-treatment serum biomarker dataset, collectively explaining 81.96% of the total variance (Table 4.13) (see Appendix A22). The first component accounted for 36.02% of the variance and was characterised by strong positive loadings for HGF, TGF-α □ □□ □ □ □ □ □ and SCF. The second component explained 21.83% of the variance and comprised high positive loadings for FGF and IL-6, with an inverse loading for CD40L. The third component accounted for 13.68% of the variance and was dominated by sFRP1. The fourth component explained 10.43% of the variance and was characterised by TNF-α □ □ Together, these four components accounted for the majority of variability in pre-treatment biomarker expression. Z-score standardisation reproduced the same four-component structure with strengthened and consistent loadings, indicating that the factor solution was stable and not dependent on measurement scale. All components demonstrated minimal bias (< 0.05) and consistent directional loadings across resampled datasets, confirming the robustness of the factor structure.

Table 4.13 Baseline Serum Biomarkers Identifying Latent Biochemical Axes Using Exploratory Factor Analysis

Component	Variable	Factor Loading	Eigenvalue	% Variance Explained	Cumulative %
Factor 1 – Growth / Angiogenic Axis	HGF	0.94	3.60	36.02	36.02
	TGF-α	0.91			
	VEGF	0.83			
	SCF	0.66			
Factor 2 – Inflammatory / FGF Axis	CD40L	–0.81	2.18	21.83	57.85
	FGF	0.81			
	IL-6	0.79			
Factor 3 – Wnt Modulator Axis	SFRP1	0.75	1.37	13.68	71.53
	DKK1	0.73			
Factor 4 – Cytokine / TNF-α	TNF-α	0.69	1.04	10.43	81.96

Extraction Method: Principal Component | *Rotation Method:* Varimax with Kaiser Normalisation | Convergence after 7 iterations.

b. Z-Score–Standardised post-treatment biomarkers

EFA of post-treatment serum biomarkers identified three components with eigenvalues greater than 1.0, collectively explaining 86.06% of the total variance (Table 4.14). The first component accounted for 53.48% of the variance and showed strong positive loadings across a broad range of biomarkers, including CD40L, HGF, SCF, TGF-α TNF-α component was interpreted as a global treatment-responsive axis, reflecting coordinated systemic biomarker modulation following tamoxifen therapy.

The second component explained 18.85% of the variance and was characterised by high loadings IL-6 and FGF, consistent with a residual inflammatory and growth factor–related axis persisting after treatment. The third component accounted for 13.73% of the variance and was dominated by sFRP1, representing a distinct Wnt modulatory axis that remained separable from other post-treatment biomarker domains. Together, these three components captured the majority of post-treatment biomarker variability, indicating a more consolidated factor structure compared with the pre-treatment dataset.

Table 4.14 Post-Treatment Serum Biomarkers Identifying Treatment-Responsive Latent Axes Using Exploratory Factor Analysis

Component	Variable	Factor Loading	Eigenvalue	% Variance Explained	Cumulative %
Factor 1 – Global Treatment-Responsive Axis	CD40L	0.90	5.35	53.48	53.48
	HGF	0.74			
	SCF	0.77			
	TGF-α	0.84			
	TNF-α	0.92			
	VEGF	0.98			
	DKK1	0.75			
Factor 2 – Residual Inflammatory / FGF Axis	FGF	0.62	1.89	18.85	72.34
	IL-6	0.92			
Factor 3 – Wnt Modulatory Axis	SFRP1	0.96	1.37	13.73	86.06

c. Z-Score Standardised Change of Biomarker Scores

EFA of pre– Δ) than 1.0, collectively explaining 95.98% of the total variance in treatment-induced biomarker changes (Table 4.15). The first component accounted for 47.35% of the variance -α Δ coordinated modulation of key growth factor pathways in response to tamoxifen therapy.

The second component explained 19.47% of the variance and showed high -α Δ Δ Δ angiogenic shift axis. The third component accounted for 16.19% of the variance and - Δ Δ consistent with a cytokine and stromal adjustment axis. The fourth component explained 12.98% of the variance and was Δ -specific response axis.

Overall, the change-score EFA revealed a highly structured pattern of coordinated biomarker dynamics following tamoxifen therapy, with clear separation of growth factor–driven, inflammatory–angiogenic, cytokine–stromal, and Wnt-specific response domains.

Table 4.15 Pre–Post Change Scores Identifying Latent Treatment-Response Axes Using Exploratory Factor Analysis

Component	Variable	Factor Loading	Eigenvalue	% Variance Explained	Cumulative %
Factor 1 – Core Treatment Effect Axis	Δ [illegible]	0.97	5.21	47.35	47.35
	Δ [illegible]-α	0.68			
	Δ [illegible]	0.77			
Factor 2 – Inflammatory / Angiogenic Shift Axis	Δ [illegible]L [illegible]	0.68	2.14	19.47	66.82
	Δ [illegible]-α	0.94			
	Δ [illegible]	0.90			
	Δ [illegible]	0.83			
Factor 3 – Cytokine / Stromal Adjustment Axis	Δ [illegible]-6	0.87	1.78	16.19	83.01
	Δ [illegible]	0.74			
Factor 4 – Wnt-Specific Response Axis	Δ [illegible]	0.95	1.43	12.98	95.98

4.7.2 Confirmatory Factor Analysis (CFA)

a. Measurement model in the combined cohort

To confirm the latent biomarker domains identified by EFA, a hierarchical confirmatory factor analysis was conducted using partial least squares structural equation modelling (PLS-SEM). The hierarchical Composite Biomarker Index (CBI) comprised five predefined lower-order constructs representing the Growth/Angiogenic Axis (CBI-1), Inflammatory Axis (CBI-2), Wnt Modulator Axis (CBI-3), Cytokine/TNF-α [illegible]-4), and ER Signalling Axis (CBI-5).

The overall measurement model for the combined cohort is illustrated in Figure 4.5. The combined cohort model demonstrated satisfactory convergence for the Growth/Angiogenic Axis (CBI-1), whereas the remaining lower-order constructs showed limited measurement stability. Standardised outer loadings for CBI-1 were high, with HGFpre, TGF-α [illegible] and 0.910, respectively (Table 4.16). In contrast, CBI-2, CBI-3, CBI-4, and CBI-5 were represented only by their strongest individual indicators (CD40L, DKK1, TNF-α [illegible] α [illegible]) [illegible] the heterogeneous combined cohort. Consequently, the Growth/Angiogenic Axis demonstrated the most robust measurement properties among the predefined biological domains.

The reflective measurement model for CBI-1 demonstrated excellent convergent validity and indicator reliability. All factor loadings exceeded 0.70, with TGF-α □ □ □ □□ □ □ □ □ □ □ □□ □ □ □□ □ □ □ □ □ □ □□ □ □ □ □ □ □□ □ □ □ □ □) □ VEGFpre (0.910). Composite reliability and average variance extracted also met recommended thresholds, supporting the validity of CBI-1 as the most stable lower-order construct within the combined cohort.

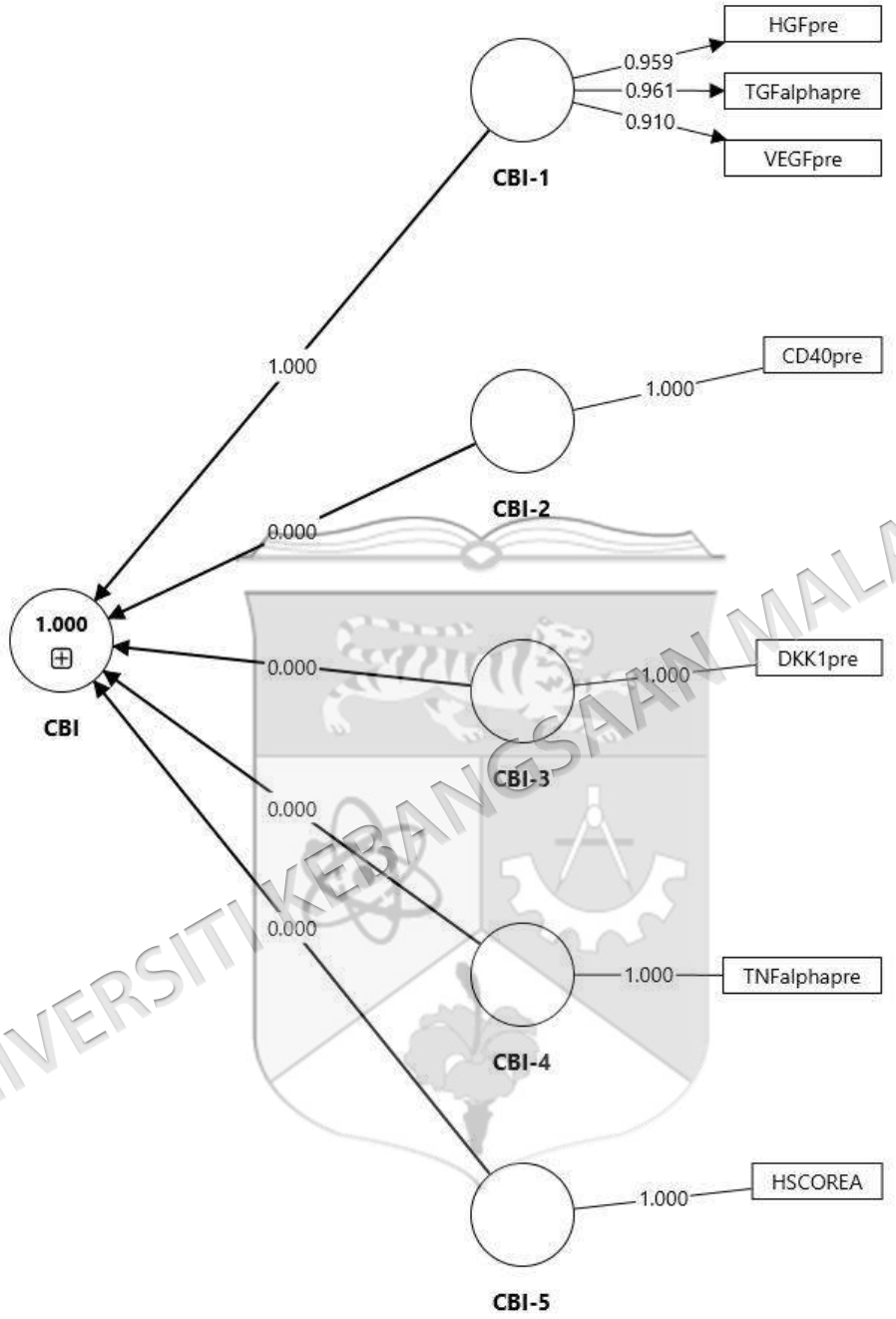

Figure 4.5 Hierarchical PLS-SEM measurement model of the Composite Biomarker Index (CBI) in the combined cohort

Table 4.16 Measurement Model Results for the CBI Construct in the Combined Cohort

Construct	Item	Loading > 0.7	Cronbach's alpha	Composite reliability	AVE	R^2
CBI	VEGFpre	0.91	0.938	0.96	0.89	1
	HGFpre	0.959				
	TGF-α □ □ □	0.961				
CBI-1	HGFpre	0.959	0.938	0.96	0.89	
	TGF-α □ □ □	0.961				
	VEGFpre	0.91				

b. Measurement model in the intervention cohort

The hierarchical PLS-SEM measurement model for the intervention (post-tamoxifen) cohort is presented in Figure 4.6. All five predefined CBIs were incorporated into the hierarchical model. The estimated path coefficients showed that the Growth/Angiogenic Axis (CBI-1) contributed most strongly to the higher-ord□ □ □ □ □ β □ = 0.511), followed by CBI-2 □ β □ □ □ 2 -5 □)β□□□□□□2 -2 □)β□□□□□□□□□□ □ □) □ □ CBI-□ □ β □ □ □ □ □ 2) □ constituted the dominant biological domain within the post-tamoxifen biomarker network.

Given the dominant contribution of CBI-1 within the hierarchical model, a focused confirmatory measurement model was subsequently evaluated to further examine the measurement properties of the Growth/Angiogenic Axis (Figure 4.7), with the corresponding results summarised in Table 4.17. The standardised path coefficient between CBI-1 and the higher-order CBI was 0.879, indicating a strong positive association. Bootstrapping (5,000 resamples) confirmed this relationship to be highly significant (t = 970.333, p < 0.001), with excellent estimation stability (SD = 0.001).

The focused confirmatory model showed that CBI-1 explained 77.3% of the variance in the higher-order Composite Biomarker Index (R^2 = 0.773), with a very large effect size (f^2 = 3.405). The Growth/Angiogenic construct also demonstrated robust measurement characteristics, with HGFpost, TGF-α □ standardised outer loadings of 0.849, 0.816, and 0.906, respectively. Collectively, these findings confirm that the Growth/Angiogenic Axis was the most stable and influential

lower-order construct within the intervention cohort, supporting its role as the principal biological domain within the hierarchical Composite Biomarker Index framework.

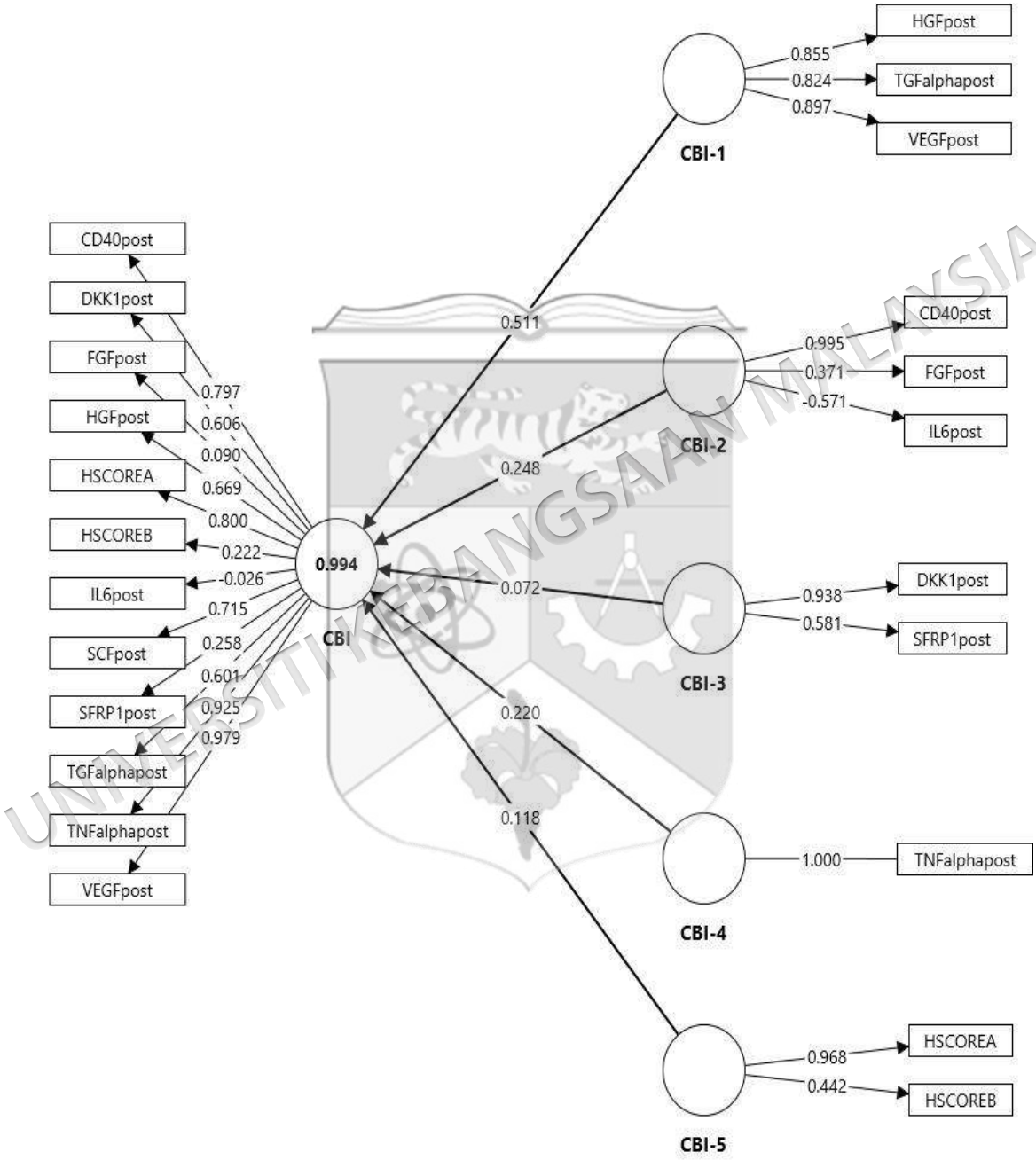

Figure 4.6 Hierarchical PLS-SEM measurement model of the Composite Biomarker Index (CBI) in the post-tamoxifen intervention cohort.

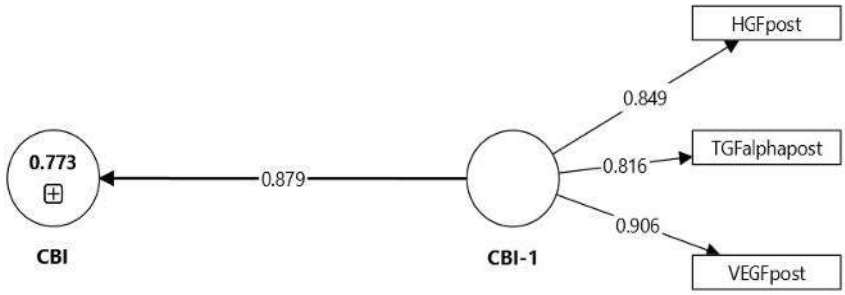

Figure 9.7 Confirmatory PLS-SEM measurement model of the Growth/Angiogenic Axis (CBI-1) in the post-tamoxifen intervention cohort.

Table 9.1 Measurement properties of the Growth/Angiogenic Axis (CBI-1) in the post-tamoxifen intervention cohort.

Construct	Item	Loading > 0.7	□ □ □ □ □ □ alpha	Composite reliability	AVE	R^2	f^2
CBI-1	HGFpost	0.849	0.958	0.979	0.960	0.773	3.405
	TGF-α □ □ □	0.816					
	VEGFpost	0.906					

4.8 COMPUTATIONAL MECHANISTIC VALIDATION

4.8.1 Tamoxifen-Target Interaction Network

Using an interaction probability threshold greater than 0.10, a total of 109 tamoxifen-associated targets were identified (Figure 4.8). Several prominent genes were highlighted, including CHRM2, OPRD1, CHRM3, CHRM1, CHRM4, CHRNA7, NPY2R, CHRM5, HTR2B, HTR2C, and ADRA1D, which are primarily involved in neuroendocrine and neurotransmitter-related signalling pathways.

The predicted targets encompassed a wide range of functional classes, including G protein-coupled receptors (Families A and B), enzymes, kinases, nuclear receptors, ligand-gated ion channels, transporters, oxidoreductases, and proteases, among others. The overall distribution of these functional categories is shown in Figure 4.9, illustrating the broad molecular spectrum of proteins potentially modulated by tamoxifen.

4.8.2 Functional Enrichment Analysis of Tamoxifen-Associated Genes

Functional enrichment analysis showed that the predicted target genes were significantly enriched in pathways related to neurotransmission, intracellular signalling, and cancer biology (see Table A23 Appendix). The most significantly enriched pathways were Neuroactive ligand–receptor interaction (hsa04080), Calcium signalling pathway (hsa04020), and cAMP signalling pathway (hsa04024), all of which are central to neuroendocrine communication and signal transduction.

Other significantly enriched pathways included Cellular senescence (hsa04218), Pathways in cancer (hsa05200), and Cholinergic synapse (hsa04725), as well as cancer-related pathways such as Small cell lung cancer (hsa05222) and Prostate cancer (hsa05215), indicating broader oncogenic relevance of these targets.

The Neuroactive ligand–receptor interaction pathway comprised 42 genes and was the most significantly enriched pathway (fold enrichment = 10.32415; FDR = 1.58 × □□ □ see Figure A3 Appendix). Key genes in this pathway included CHRM2, OPRD1, CHRM3, HTR2A, DRD1, ADRA1A, OPRM1, and HTR2C, highlighting a strong over-representation of neurotransmitter and hormone receptor signalling components among the predicted tamoxifen targets.

The Cholinergic synapse pathway was also significantly enriched (10 genes; □ □ □ □ □□ □ □ □ □ □ □ □ □ □ □ □□ □□ □ □ □ □ see Figure A4 Appendix). This × □□ □ pathway included genes such as CHRM2, ACHE, CHRM3, AKT2, CHRNA7, and FYN, supporting a role for acetylcholine-mediated synaptic and downstream signalling processes in the tamoxifen-associated network.

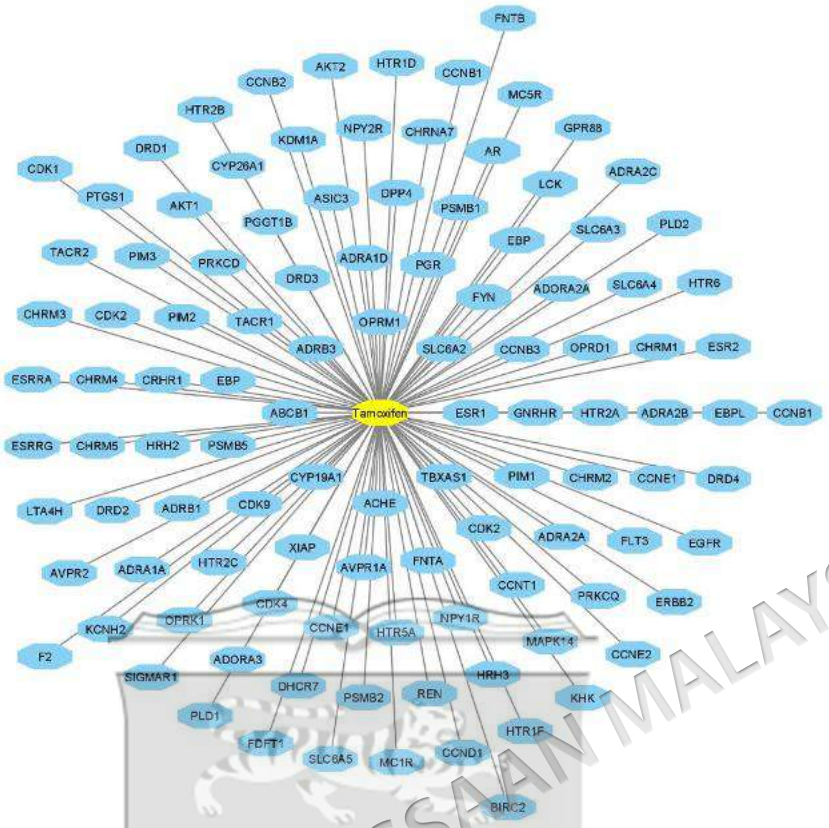

Figure 9.8 Tamoxifen associated Interaction Network Based on SwitchTarget Prediction

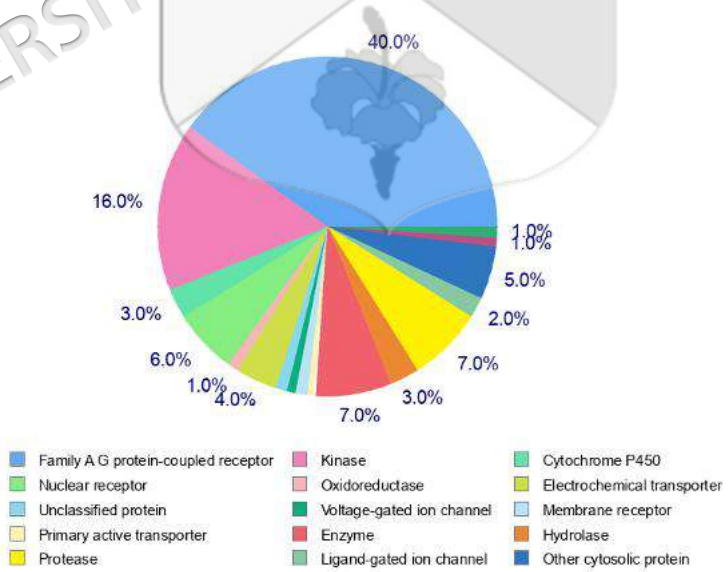

Figure 9.9 Target Class Distribution of the identified target classes based on their functional roles in the signaling network associated with Tamoxifen

Gene Ontology (GO) enrichment analysis further showed that the predicted targets were predominantly associated with G protein-coupled receptor signalling, chemical synaptic transmission, and adenylate cyclase-related signalling processes (Figure 4.10). At the cellular level, these genes were mainly localised to the plasma membrane, dendrites, and synapses, while molecular function analysis highlighted neurotransmitter receptor activity, serotonin receptor activity, and ligand binding, consistent with a receptor-centric signalling profile.

4.8.3 Protein–protein interaction (PPI) network and Hub Gene Identification

Protein–protein interaction analysis identified a network of 89 interacting genes (Figure 4.11). This network represents a coordinated signalling system that may underlie tamoxifen-related biological effects.

Hub analysis identified the top central genes as AKT1, ESR1, SLC6A4, DRD2, EGFR, SLC6A3, OPRM1, CRHR1, HTR2C, SLC6A2, HTR2A, DRD1, ERBB2, ADRA2A, ESR2, MAPK14, CHRM2, ADRA2B, DRD4, and CDKN1B (Figure 4.12). These genes occupy key regulatory positions within the network and are involved in pathways governing cell survival, proliferation, growth factor signalling, oestrogen signalling, and neurotransmitter transmission.

Notably, AKT1 and MAPK14 are central components of survival and stress-response pathways; ESR1 and ESR2 are direct mediators of oestrogen signalling; and EGFR and ERBB2 are major growth factor receptors. The presence of multiple dopamine, serotonin, and transporter-related genes (such as DRD1, DRD2, and SLC6A4) further underscores the strong neuroendocrine and receptor-driven character of the tamoxifen-associated network.

Collectively, the computational analyses show that tamoxifen is predicted to interact with a broad, receptor-rich signalling network dominated by neuroactive ligand–receptor interactions, calcium and cAMP signalling, and cancer-related pathways. The enrichment of neurotransmitter and hormone receptor pathways, along with the identification of key hub genes such as AKT1, MAPK14, ESR1, ESR2, EGFR, and ERBB2, supports a model in which tamoxifen acts through multi-pathway

modulation rather than a single linear target. This systems-level network structure aligns with the complex biological behaviour of NF-PitNETs and provides a mechanistic framework linking oestrogen receptor modulation, growth factor signalling, and neuroendocrine receptor pathways to the clinical and biomarker responses observed in this study.

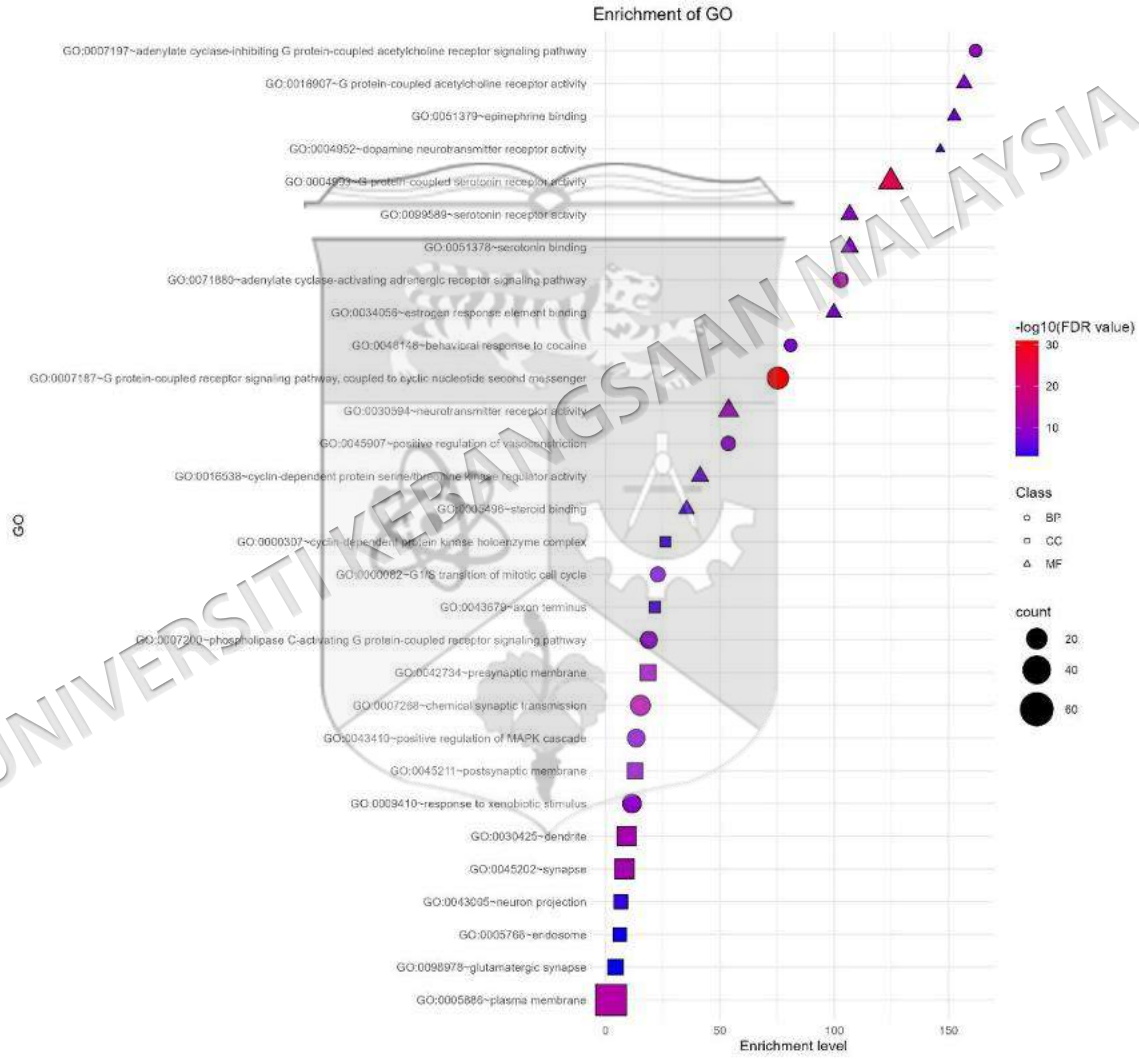

Figure 9.10 Top 10 Biological Processes (BP), Cellular Components (CC), and Molecular Functions (MF) Identified for Targeted Genes (Adapted from Haydar Ali Tajuddin, A et al, 2025)

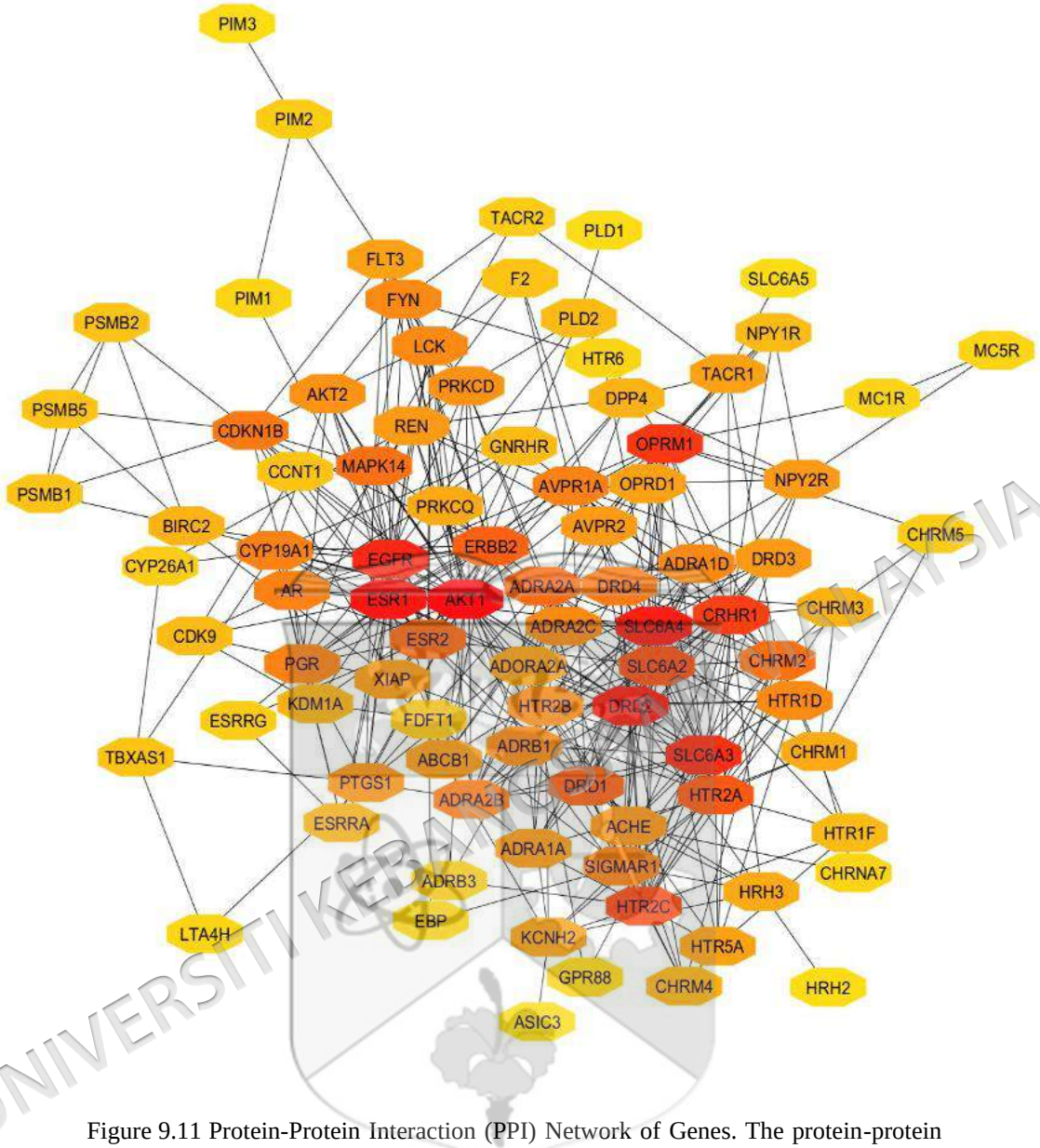

Figure 9.11 Protein-Protein Interaction (PPI) Network of Genes. The protein-protein interaction (PPI) network of 89 genes identified through a string-based PPI analysis. These genes are involved in the signaling pathways associated with Tamoxifen. The red node indicated the more degree of interaction than yellow (Adapted from Haydar Ali Tajuddin, A et al, 2025)

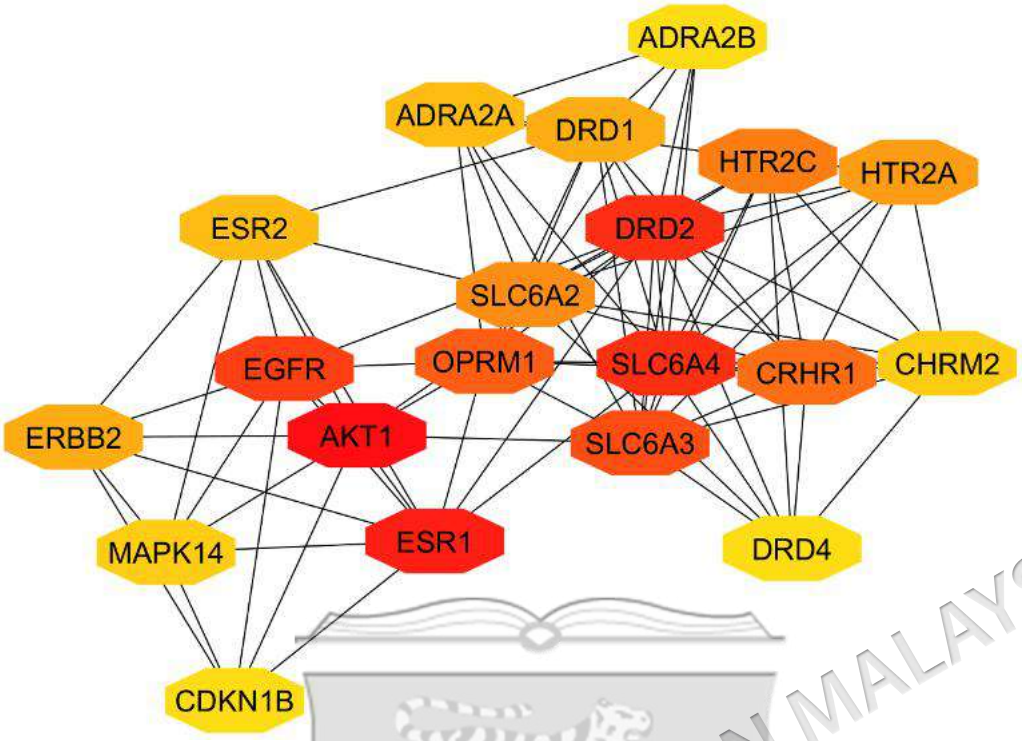

Figure 9.12 The top hub genes identified from the protein-protein interaction (PPI) network of genes. These hub genes represent the central nodes in the interaction network and are likely to play key roles in mediating the signaling pathways associated with tamoxifen. The red node indicated the more degree of interaction than yellow (Adapted from Haydar Ali Tajuddin, A et al, 2025)

Table 9.2 Summary of Research Findings

No.	Research Objective	Research Question	Analyses Used	Key Findings
1	To determine the immunohistochemical expression patterns of oestrogen [illegible] α primary NF-PitNET tissue samples.	What are the expression patterns of [illegible] α [illegible] primary NF-PitNET tissues?	Immunohistochemistry (H-[illegible]) [illegible] exact test, independent t-test, Mann–Whitney U test	[illegible] α [illegible] % [illegible] α [illegible] β [illegible] marked inter-individual variability. No significant differences [illegible] α [illegible] β [illegible] and tamoxifen groups.
2	To evaluate the clinical impact of tamoxifen on changes in residual NF-PitNET tumour volume.	Does tamoxifen therapy result in measurable changes in residual NF-PitNET tumour volume over 12 months?	ANCOVA, RM-GLM, paired t-test, one-way ANOVA with LSD post-[illegible] exact test, Spearman correlation, linear and logistic regressions	ANCOVA showed a moderate but non-significant adjusted between-group effect. Repeated-measures GLM indicated that neither the overall time effect nor the time-by-treatment interaction reached statistical significance, although the longitudinal trend favoured the tamoxifen arm. On continuous analyses, paired testing demonstrated a modest but statistically significant reduction in tumour volume over 12 months within the tamoxifen group. Across response categories, final tumour volume and volume-change indices differed significantly and remained robust on bootstrapping. Categorical response analysis showed that tumour shrinkage occurred exclusively in the tamoxifen group (40%), with no shrinkage observed in controls.
3	To investigate baseline and longitudinal changes in serum biomarker levels in tamoxifen-treated NF-PitNET patients.	Which serum biomarkers show differential expression before and after tamoxifen treatment?	Independent t-test, Mann–Whitney U test, paired t-test, Wilcoxon signed-rank test, Benjamini–Hochberg FDR, bootstrapped paired analysis, Spearman correlation, linear and logistic regressions, Exploratory Factor Analysis (EFA), Confirmatory Factor Analysis (CFA), Partial Least Squares Structural Equation Modelling (PLS-SEM)	Baseline biomarker levels did not differ significantly between groups. Conventional paired analyses showed a decrease in TNF-α [illegible] significant after FDR adjustment. In multiple linear regression, post-treatment DKK1 emerged as an independent inverse predictor of final tumour volume. Bootstrapped analyses demonstrated consistent directional changes across biomarkers. Multivariate modelling identified a dominant latent Growth/Angiogenic axis, primarily driven by HGF, VEGF, and TGF-α [illegible] intervention cohort.

[illegible]

…□ □ □ □ □ □ □ □ □ □ □ □ □ □				
4	To computationally predict and functionally annotate tamoxifen-interacting genes and signalling pathways in NF-PitNETs.	Which genes and signalling pathways are predicted to interact with tamoxifen and contribute to its therapeutic effect in NF-PitNETs?	Computational target prediction, pathway enrichment analysis, protein–protein interaction network analysis, hub-gene ranking	Computational analyses implicated key signalling networks, particularly PI3K/AKT and MAPK-related pathways, and identified central hub genes (including AKT1, MAPK14, ESR1, and DRD2). These findings provide mechanistic support for the observed modulation of growth–angiogenic signalling associated with tamoxifen treatment.

4.9 INTEGRATED DISCUSSION

4.9.1 Clinical Evidence Supporting Tamoxifen as a Potential Therapeutic Strategy for Residual NF-PitNETs

Residual NF-PitNETs remain a therapeutic challenge because no established medical therapy has consistently been shown to prevent postoperative tumour progression. Current management therefore relies largely on serial MRI surveillance, with repeat surgery or radiotherapy reserved for progressive, symptomatic, or anatomically threatening disease (Dekkers et al. 2008; Ntali & Wass 2018; Molitch 2017). Within this context, the present study evaluated whether tamoxifen could modify the clinical behaviour of residual NF-PitNETs and whether the observed volumetric changes were biologically plausible within an endocrine-responsive tumour framework.

A central requirement for valid interpretation of treatment effects in interventional studies is demonstrable baseline equivalence between study arms. In this cohort, the tamoxifen and control groups were well matched across key demographic, clinical, radiological, and molecular variables, thereby strengthening the internal validity of treatment comparisons. The absence of significant differences in age at diagnosis, age at enrolment, sex distribution, and major presenting symptoms is particularly relevant. In NF-PitNETs, age influences tumour proliferative potential, endocrine reserve, and long-term recurrence patterns, while the symptom profile often reflects tumour size and invasiveness at presentation. By achieving equivalence in these variables, the study reduces the risk that differences in longitudinal tumour behaviour were confounded by intrinsic host or disease factors.

Radiologically, comparable tumour volumes and patterns of suprasellar and parasellar extension indicate a similar postoperative disease burden. Baseline tumour size is a recognised determinant of regrowth risk and response to adjuvant intervention; thus volumetric equivalence is critical (Ratnasingam et al. 2017) for attributing subsequent changes to pharmacological exposure rather than initial tumour mass. Although baseline tumour volume did not differ statistically between groups, the modest sample size limits the interpretation of non-significant comparisons.

Consequently, a small imbalance in baseline tumour burden cannot be completely excluded as a contributor to subsequent tumour behaviour. Comparable rates of repeat surgery further reinforce baseline biological parity. In the context of NF-PitNETs, reoperation frequently reflects invasive growth, incomplete resectability, or aggressive regrowth kinetics (Hefner & Cooper 2025). The balanced distribution of this surrogate marker of aggressiveness across arms supports the interpretation that intrinsic tumour biology was broadly equivalent at study entry.

Interpretation of treatment response should also take tumour heterogeneity into account. The contemporary WHO classification recognises that PitNETs comprise multiple transcription factor-defined lineages with distinct biological behaviour and potentially different therapeutic responsiveness. However, this study was initiated before the widespread implementation of WHO lineage- and transcription factor-based classification in routine pathological practice in Malaysia. Consequently, lineage and transcription factor expression were not systematically evaluated. This does not invalidate the findings but should temper their interpretation, as lineage-specific tumours may differ in growth potential, receptor biology and response to endocrine manipulation (Lenders et al. 2023).

Another limitation in the interpretation of treatment response relates to the classification of NF-PitNETs. The relatively high proportion of tumours classified as null-cell adenomas should be interpreted cautiously because, under the current WHO classification, many tumours previously designated as null-cell adenomas are reclassified following transcription factor immunohistochemistry as gonadotroph tumours, tumours without distinct cell lineage or tumours with mixed or atypical transcription factor expression. As transcription factor immunohistochemistry was not available during the conduct of this study, some tumours classified as null-cell adenomas may not represent true null-cell tumours. This limitation should be considered when interpreting the biological heterogeneity of the study cohort and highlights an important priority for future validation studies. Although silent corticotroph and plurihormonal tumours were randomised to the control group only, the present study was not powered to evaluate treatment effects by tumour subtype. Consequently, it cannot be determined whether tumour progression seen exclusively in

the control group reflects differences in intrinsic subtype biology, random variation arising from the small sample size or a true treatment effect. Importantly, overall baseline clinical and radiological characteristics were comparable between study arms, supporting internal validity, although a potential contribution of subtype-specific behaviour cannot be excluded and warrants investigation in larger studies.

In addition, menopausal status was not directly recorded or analysed in this [illegible] as a pragmatic surrogate, reflecting the approximate mean age of natural menopause and aiming to reduce imbalance in endogenous hormonal status between treatment arms. This design feature partially addresses the potential influence of menopausal status on tamoxifen pharmacodynamics, although chronological age cannot fully capture individual variability in ovarian function, hypogonadism or circulating oestrogen exposure.

Immunohistochemical assessment in this study was limited to the nuclear localisation o[illegible] α [illegible] β [illegible] (Manoranjan et al. 2010). However, accumulating evidence indicates that oestrogen signalling in pituitary tumours also involves membrane-[illegible] α [illegible] protein-coupled oestrogen receptor (GPER), which mediate rapid non-genomic signalling through pathways such as ERK1/2 (Kelly & Levin 2001; Levin & Hammes 2016; Sosa et al. 2019). These receptors have been identified in pituitary tissue and may influence cellular proliferation independently of nuclear ER signalling. Consequently, nuclear receptor expression alone may not fully capture the complexity of endocrine responsiveness in NF-PitNETs, underscoring the importance of future studies that incorporate membrane-associated ER signalling and GPER biology.

[illegible] β [illegible] validation studies have demonstrated considerable variability among commercially [illegible] β [illegible] specificity (Andersson et al. 2017; Birgersson et al. 2022). In the present study, initial [illegible] β 2 [illegible] -specific staining, [illegible] necessitating rep[illegible] β 5 5 [illegible]) [illegible]

malignancies, pituitary-specific validation remains limited. Consequently, antibody-dependent variability should be considered when interpreting the prevalence and biologica [illegible] β [illegible]

Tamoxifen exhibits differential activity towards ER isoforms, acting [illegible] α [illegible] β [illegible]) [illegible] β [illegible] responsiveness. Supporting this concept, Madeira et al. (2013) demonstrated that breast [illegible] α [illegible] erβ suppression of proliferation following tamoxifen therapy than tumours dominated by either receptor [illegible] α [illegible] β [illegible] β [illegible] lance as a potential predictor of tamoxifen responsiveness in NF-PitNETs.

[illegible] -negative tumours. A recent case report demonstrated significant tumour regression w [illegible] -positive, p53-mutant, triple-negative breast cancer patient with brain metastases, resulting in a marked reduction in [illegible] and mutant p53 within cancer cells (Scarpetti et al. 2023). These data provide direct [illegible] -dependent sensitivity to anti-oestrogen therapy. Applied to NF-PitNETs, the receptor profile observed in the present study, charac [illegible] β expression, defines a biological context plausibly permissive to tamoxifen responsiveness. The observation that tumour shrinkage occurred exclusively in the tamoxifen-treated group is therefore biologically coherent within this receptor [illegible] -scores and volumetric response categories indicates that receptor abundance alone is unlikely to fully explain inter-individual variability in therapeutic outcome. This is consistent with a model in which isoform composition, receptor localisation, co-regulator interactions and downstream pathway engagement are critical determinants of endocrine responsiveness. Overall, these findings suggest that oestrogen receptor expression,

□ □ □ □ □ □ □ □ □ □ □ □ □ □ β □ □ □ □ □ □ □ -PitNETs and may provide a plausible biological basis for exploring anti-oestrogen therapy in this context (Pérez et al. 2015). At the same time, they underscore the multidimensional nature of oestrogen signalling and reinforce the hypothesis-generating rationale for an integrative analytic approach that combines receptor profiling, volumetric outcomes and pathway-level biomarker analyses. Such multidimensional evaluation may ultimately refine patient selection and optimise therapeutic targeting in residual or recurrent NF-PitNETs.

The divergence between treatment arms supports the interpretation that tamoxifen may exert a disease-modifying effect rather than simply reflecting random variation in tumour growth. Tumour shrinkage occurred exclusively in the tamoxifen group (40%), whereas tumour progression was observed only in the control group (20%) ($p = 0.014$). Nevertheless, these findings should be interpreted within the recognised natural history of residual NF-PitNETs. Contemporary Pituitary Society consensus guidelines emphasise that conservatively managed residual pituitary tumours exhibit heterogeneous behaviour, with many remaining stable for prolonged periods, some enlarging, and a small proportion demonstrating spontaneous regression during follow-up (Fleseriu et al. 2025). Consequently, tumour stability alone cannot be regarded as definitive evidence of treatment efficacy in a proof-of-concept study.

This inherent biological variability has also complicated the interpretation of previous medical therapies. A recent systematic review and meta-analysis of five studies evaluating cabergoline concluded that its ability to induce tumour shrinkage in NF-PitNETs was limited, although approximately half of patients achieved prevention of postoperative tumour progression with a low frequency of adverse events (Botelho et al. 2022). Similarly, studies of somatostatin receptor ligands have generally demonstrated modest or inconsistent effects on tumour growth, reflecting the heterogeneous expression of somatostatin receptor subtypes among NF-PitNETs. Although direct comparison is constrained by differences in patient populations, follow-up duration, imaging methodology, and response definitions, the absence of tumour regrowth together with volumetric tumour shrinkage in 40% of tamoxifen-treated patients compares favourably with the reported natural history of residual NF-PitNETs and previously investigated medical therapies. Furthermore, the concordance between

the clinical, biomarker, and computational findings supports the interpretation that the observed tumour responses are unlikely to be explained by natural history alone. Collectively, these findings provide preliminary evidence that tamoxifen may represent a promising endocrine-based therapeutic strategy for selected patients with residual NF-PitNETs and warrants evaluation in larger prospective comparative studies.

Importantly, the response thresholds used in the present study were not arbitrarily selected but were chosen to maximise clinical discrimination between biologically distinct tumour behaviours. A cut-off of 25% change in tumour volume was adopted to classify tumour shrinkage, stability, and progression, consistent with previous volumetric studies showing that this threshold reliably distinguishes meaningful biological change from expected measurement variability in pituitary tumours. A volumetric threshold of approximately 25% provided strong discrimination between clinically relevant outcome groups and improved identification of tumours showing true progression compared with minor fluctuations attributable to imaging variability or measurement error. Consequently, although spontaneous stability is recognised in the natural history of residual NF-PitNETs, the use of a predefined 25% volumetric threshold in the present study increased confidence that the observed response categories represented biologically meaningful differences in tumour behaviour rather than random variation. This is further supported by the clear separation in volumetric trajectories between the shrinkage, stable disease, and regrowth groups, together with the alignment of these clinical outcomes with the accompanying biomarker and computational findings.

An important temporal observation was that both groups showed tumour enlargement from baseline to six months, followed by divergence between six and twelve months. This early parallel increase suggests that tamoxifen did not produce an immediate cytotoxic effect and that the first six months may reflect intrinsic NF-PitNET behaviour or measurement variability inherent in volumetric assessment of irregular residual lesions. The subsequent reduction in tumour volume in the tamoxifen group is biologically compatible with the pharmacology of selective oestrogen receptor modulation. Unlike cytotoxic therapy, tamoxifen is expected to act gradually through transcriptional regulation and downstream pathway modulation involving proliferation,

angiogenesis, apoptosis, and tumour–stromal interaction. Thus, the delayed divergence at twelve months may represent the cumulative anatomical manifestation of earlier biological reprogramming rather than an immediate antitumour effect. In the management of NF-PitNETs, long-term disease stabilisation is often regarded as a clinically meaningful outcome. In this context, the observation of true volumetric regression in a subset of treated patients is particularly notable. Although the absolute scale of volume change in this cohort is relatively modest, it remains biologically and clinically relevant given the typically slow yet persistent growth of these tumours. Collectively, these observations support the conclusion that tamoxifen can induce not only tumour stabilisation but also genuine tumour regression in selected individuals. Quantitative analyses of both absolute and percentage volume change confirmed that these response categories represent distinct clinical phenotypes. Patients with tumour shrinkage showed the greatest reductions in volume, those with stabilisation exhibited minimal change, and those with regrowth demonstrated substantial increases in tumour size. Dynamic measures of change provided superior discrimination compared with single time-point measurements, underscoring their value in a slowly evolving and heterogeneous disease such as NF-PitNET.

Pharmacologically, tamoxifen and its active metabolite, 4-hydroxy-tamoxifen, can cross the blood–brain barrier (Lien et al. 1991; Novick et al. 2020) and compete [illegible] α [illegible] β [illegible] -protein-coupled [illegible] oestrogen receptor GPER1 (Long et al. 2017). Although tamoxifen itself has approximately 20–25-[illegible] α [illegible] hydroxylated metabolite shows near-[illegible] α [illegible] higher affinity fo[illegible] β [illegible]) [illegible] endogenous oestrogen at the receptor level. Beyond receptor-mediated actions, tamoxifen also exerts oestrogen receptor–independent effects. It directly inhibits the dopamine transporter even in the presence of ER antagonists (Mikelman et al. 2017b, 2018) and inhibits protein kinase C (PKC) (Mikelman et al. 2017a). Demonstration of PKC inhibition in purified enzyme systems indicates that this effect is not solely oestrogen receptor–mediated. Functionally, tamoxifen acts as either an oestrogen antagonist or agonist in a context-dependent manner, influenced by tissue type, receptor expression, and co-regulatory proteins (Martinkovich et al. 2014). While its actions are

well characterised in peripheral tissues, its central nervous system effects are less well defined (Novick et al. 2020). Available data indicate that tamoxifen can act as a GPER1 agonist in the brain, reproducing certain rapid, non-genomic effects of estradiol, particularly in hypothalamic pathways (Long et al. 2017). In the presence of estradiol, tamoxifen generally exerts anti- -mediated -driven behaviours (Lund et al. 2005; Sá et al. 2016), whereas under oestrogen-deprived conditions it shows oestrogen-like actions, -dependent oxytocin receptor expression and cognitive performance (Patisaul et al. 2003; Velázquez-Zamora et al. 2012). This pattern is consistent with the profile of a partial agonist, in which net activity depends on endogenous ligand levels. Accordingly, we postulated that patients with NF-PitNETs, in whom hypogonadism is common, may exhibit a physiological state of oestrogen deficiency. The patient with the greatest tumour shrinkage had experienced premature menopause for approximately five years and had not received hormone replacement therapy (Amalina et al. 2024), suggesting that the endogenous hormonal milieu may influence treatment responsiveness. This interpretation is supported by recent evidence from breast cancer showing that the long-term benefit of tamoxifen varies according to menopausal status, highlighting the importance of the hormonal environment in determining endocrine responsiveness (Johansson et al. 2025).

Taken together, the clinical findings support tamoxifen as a biologically plausible therapeutic strategy for selected patients with residual NF-PitNETs. The balanced baseline characteristics reduce the likelihood of major confounding, while the pattern of early parallel tumour enlargement followed by delayed divergence is consistent with a therapy that acts through gradual biological modulation rather than immediate cytotoxicity. The receptor and pharmacological data further support this interpretation but also indicate that oestrogen receptor expression alone cannot fully explain response. These observations provide the clinical foundation for the next section, which examines whether tamoxifen-associated tumour behaviour is accompanied by coordinated systemic biomarker changes and whether these changes support the concept of tamoxifen as a systems-level biological modulator.

4.9.2 Biological Evidence Supporting Coordinated Systems-level Modulation by Tamoxifen

The favourable tumour volumetric responses described in the previous section provide clinical evidence that tamoxifen may modify tumour behaviour in residual NF-PitNETs. However, radiological changes alone offer limited insight into the biological processes underlying treatment responsiveness. Tumour growth reflects the cumulative effects of multiple interconnected molecular events involving cellular proliferation, angiogenesis, inflammatory signalling, apoptosis, extracellular matrix remodelling and tumour–host interactions. Consequently, understanding tamoxifen-associated tumour response requires assessment of the accompanying biological changes rather than reliance on volumetric outcomes alone. The present study therefore examined longitudinal changes in a predefined panel of circulating biomarkers selected to represent key biological pathways implicated in pituitary tumour biology and the known pharmacological actions of tamoxifen.

Unlike proteomic discovery studies, the present investigation adopted a hypothesis-driven translational approach. Candidate biomarkers were selected a priori, based on existing evidence linking them to oestrogen signalling, angiogenesis, inflammatory regulation, growth factor activity, cytokine signalling and Wnt pathway modulation in pituitary tumour biology. This approach enabled the prospective evaluation of biologically plausible circulating markers within a randomised clinical trial while maintaining mechanistic relevance. The intention was not merely to identify a single predictive biomarker but to determine whether coordinated biological responses across multiple interconnected pathways more accurately reflected tamoxifen-associated tumour modulation.

Overall, longitudinal changes in individual serum biomarkers were modest and heterogeneous. Only TNF-α □□ wed a statistically significant reduction following tamoxifen therapy before correction for multiple testing, while most biomarkers did not demonstrate significant independent longitudinal changes. These findings should not be interpreted as evidence that tamoxifen lacks biological activity. Rather, they are biologically consistent with the recognised heterogeneity and slow growth kinetics of NF-PitNETs. Unlike rapidly proliferating malignancies, residual NF-PitNETs

demonstrate relatively indolent behaviour, so circulating proteins are unlikely to function as direct surrogates of tumour burden. Furthermore, serum biomarkers represent downstream manifestations of multiple interacting signalling pathways and are influenced by tumour biology, host immune responses, endocrine status, angiogenesis, stromal interactions and systemic physiological variability. Consequently, individual biomarkers are unlikely to capture the complexity of treatment-associated biological responses in isolation.

Despite the limited discriminatory performance of most individual biomarkers, several biologically meaningful associations emerged. Among the ten candidate biomarkers evaluated, post-treatment DKK1 was identified as an independent predictor of final tumour volume, with higher post-treatment DKK1 concentrations associated with smaller residual tumours. Wnt signalling is a fundamental pathway in development and tissue homeostasis and is frequently dysregulated in cancer, including pituitary tumorigenesis (Wang et al. 2023). DKK1, a □□□□□□□□□□□□□□-catenin □□□□□□□□□ signalling, was initially characterised as a tumour suppressor, but its biological role is now recognised as highly context-dependent, varying with tumour type, pathway wiring, and the tumour microenvironment (Kagey & He 2017). Depending on these factors, DKK1 may restrain or promote tumour progression through canonical and non-canonical Wnt pathways, as well as through interactions with PI3K/Akt signalling and immune components (Kim et al. 2012). Accordingly, the association between DKK1 and tumour volume in this study should not be interpreted as evidence that DKK1 alone determines response, but rather as a systemic readout of Wnt pathway engagement within a broader, interconnected signalling network influenced by tamoxifen.

The significant inverse correlation between sFRP1 and interim tumour volume supports the involvement of Wnt pathway modulation during the early phase of tamoxifen therapy. Together with the early change-score association observed for SCF, these findings suggest that early volumetric tumour changes may reflect initial modulation of Wnt-regulatory and growth factor signalling pathways. The absence of similar associations at 12 months may indicate that these biomarkers primarily capture early pharmacodynamic responses, with subsequent tumour behaviour influenced by more complex biological adaptation and inter-individual variability over time. This

temporal pattern is biologically consistent with evidence that anti-oestrogen therapies interact with both canonical and non-canonical Wnt signalling pathways and modulate growth factor networks involved in tumour proliferation and remodelling. Although sFRP1 and SCF were associated with early tumour response, DKK1 emerged as the biomarker most strongly associated with final tumour volume, suggesting that different components of the Wnt signalling network may contribute to distinct phases of the treatment response.

Beyond individual markers, exploratory factor analysis identified coherent latent axes representing growth–angiogenic, inflammatory, cytokine–stromal, and Wnt-modulatory domains across baseline, post-treatment, and change-score datasets. The reorganisation of these axes following tamoxifen therapy indicates coordinated, pathway-level modulation rather than isolated biomarker effects. Building on this structure, a CBI representing the growth–angiogenic axis demonstrated excellent reliability and convergent validity, with HGF, TGF-α [illegible] consistently in both the combined cohort and the tamoxifen-treated subgroup. The hierarchical specification of the final measurement model reflects a technical requirement for model identification rather than a causal biological hierarchy, and its primary contribution is to demonstrate measurement quality and construct validity.

Conceptually, this integrative biomarker framework explains why individual circulating markers showed inconsistent associations with tumour volume, whereas pathway-level constructs provide a more stable and biologically meaningful representation of treatment-related molecular modulation. In a heterogeneous disease such as NF-PitNET, aggregating correlated biomarkers into latent constructs reduces noise, enhances signal stability, and aligns statistical modelling with underlying biological organisation. By integrating volumetric outcomes with latent biomarker domains, this study advances a system-level framework for understanding endocrine responsiveness in NF-PitNETs and lays the groundwork for future precision-based biomarker stratification. These findings also clarify the relationship between the biomarker analyses and the subsequent computational investigations presented in this thesis. The biomarker framework was derived empirically from longitudinal clinical observations rather than predefined through computational modelling, and the latent

biological domains therefore emerged directly from patient-derived data. An important mechanistic question subsequently arises: do these clinically derived biological domains correspond to recognised molecular signalling networks? The following section addresses this question by integrating the empirical biomarker findings with independent computational analyses. Rather than constructing the biological framework, the in silico analyses provide mechanistic validation that the coordinated biomarker responses observed clinically converge with established signalling pathways known to regulate pituitary tumour biology.

4.9.3 Integrated Molecular Mechanisms Underlying Tamoxifen Responsiveness in NF-PitNETs

The convergence between the in vivo biomarker findings and the in silico analyses provides an integrated systems-level framework that supports the biological plausibility of tamoxifen action in NF-PitNETs. Importantly, the computational analyses were not intended to define the biomarker framework a priori, but rather to determine whether the empirically derived biomarker domains identified in patients were supported by established tamoxifen-associated molecular networks. Bioinformatics enrichment demonstrated significant involvement of tamoxifen-interacting genes in the PI3K/AKT, □ □ □ □ □ □ □ □ □ □□ □ □ □ □-catenin □signalling β pathways, all of which are recognised regulators of tumour proliferation, survival, metabolism, angiogenesis and cellular adaptation in pituitary tumours (Derwich et al. 2023). The concordance between these computationally enriched pathways and the observed biomarker domains, particularly the Growth/Angiogenic and Wnt-modulatory axes, provides independent mechanistic support for the biological relevance of the CBI. This complementary integration of patient-derived biomarker data with computational pathway analysis strengthens the translational interpretation of the findings and establishes a coherent mechanistic link between Objectives 3 and 4.

In this study, the selected biomarkers are best interpreted within interrelated signalling axes that reflect both NF-PitNET biology and the pleiotropic pharmacology of tamoxifen. Beyond its role as an oestrogen receptor antagonist, tamoxifen modulates a broad molecular network: computational analysis identified 109 associated genes spanning neurotransmitter and hormone receptors, GPCRs, ion channels, kinases, and

oxidoreductases, with strong enrichment in neuroactive ligand–receptor interactions (FD□ □□ □□ □ 5 □ □ − 2 □) □ □□ □ □□ □ □ □ □□ □ □□ □ □ □ □ □ □□ □ □ □□ □ □ □ □□ pituitary function (Zemková & Stojilkovic 2018). This is consistent with transcriptomic data linking these pathways to invasiveness and metabolic reprogramming in NF-PitNETs (Feng et al. 2023a). Within this framework, DKK1 and sFRP1 define a Wnt-modulatory axis and align with their associations with final and interim tumour volume, respectively, supporting a role for Wnt pathway modulation in both early and longer-term tumour dynamics. The growth–angiogenic axis (HGF, SCF, TGF-α □ □□ □ □ □) □ converges on the PI3K/AKT–MAPK/ERK–mTOR network, providing a rationale for their aggregation into a latent construct; notably, tamoxifen-modulated genes such as AKT1 and MAPK14 map directly onto these pathways and regulate apoptosis and survival in pituitary tumour cells (Derwich et al. 2023).

In parallel, IL-6 and TNF-α □□ □ □ □ □ □ □ □ □ □□ □ □□ □ □ □ □ □ □ □ □ □ □ □ □ □ interfaces with PI3K/AKT and MAPK signalling, consistent with a role in tumour–host interactions rather than direct surrogacy of tumour mass. The identification of dopaminergic and serotonergic genes (DRD1, DRD2, DRD4, SLC6A2/3/4) suggests a neurotransmitter regulatory axis that may influence treatment responsiveness, as supported by evidence that tamoxifen inhibits the dopamine transporter (Mikelman et al. 2018). Additional hub genes such as EGFR and ERBB2 link oestrogen receptor modulation to growth factor pathways involved in tumour growth and resistance (Vamvoukaki et al. 2023), while the tumour suppressor CDKN1B represents another antiproliferative axis influenced by tamoxifen, with loss of $p27^{KIP1}$ expression reported in aggressive pituitary adenomas (Sav et al. 2012). Other neuroendocrine receptors, including OPRM1, CRHR1, CHRM2, and ADRA2A/B, further illustrate the complexity of receptor-level signalling in PitNETs and the broad pharmacological scope of tamoxifen (Taghavi et al. 2023). Collectively, this network-level view explains why individual circulating biomarkers show weak and inconsistent associations with tumour volume and supports pathway-level or latent construct modelling over single-marker analyses. Importantly, these computational findings were not used to derive the biomarker domains, but rather to determine whether the empirically identified biomarker constructs converged on recognised molecular pathways relevant to pituitary

tumour biology. The close agreement between the two approaches provides independent mechanistic support for the biological framework proposed in this study.

The convergence between the computational analyses and the empirically derived biomarker domains is further reinforced by multivariate modelling of serum biomarkers. The identification of structured latent domains, particularly the growth–angiogenic axis, and their reorganisation following tamoxifen therapy indicates that treatment is associated with coordinated shifts in interconnected signalling networks. Rather than reflecting suppression of a single dominant effector molecule, these patterns suggest that tamoxifen induces a reweighting of tumour-supportive signalling modules, including pathways governing proliferation, vascular support, and stromal interaction.

Among the computationally identified signalling hubs, EGFR-associated signalling is particularly noteworthy, as it provides a mechanistic bridge between oestrogen receptor biology and growth factor-mediated proliferation. Cross-talk between ER and EGFR signalling has been extensively described in endocrine-responsive malignancies, where activation of receptor tyrosine kinase pathways can alter endocrine sensitivity and contribute to therapeutic resistance (Vamvoukaki et al. 2023). A similar mechanism may operate in NF-PitNETs, whereby tamoxifen affects not only classical oestrogen receptor signalling but also downstream growth factor pathways that regulate tumour proliferation and angiogenesis. Within this framework, ER signalling should be regarded as the biological entry point for tamoxifen action, whereas PI3K/AKT and MAPK function as central integrative hubs through which multiple extracellular stimuli converge to determine tumour behaviour. This interpretation is also consistent with the clinical findings of the present study, in which receptor expression alone was insufficient to explain treatment response, whereas pathway-level biological constructs provided substantially greater discriminatory power.

This interpretation is strongly supported by experimental and translational evidence. Preclinical studies have shown that tamoxifen suppresses pituitary adenoma cell proliferation and migration, induces apoptosis, and inhibits tumour growth, accompanied by downregulation of PI3K/AKT signalling, modulation of apoptotic

regulators, and reprogramming of the tumour microenvironment (Lv et al. 2022). In addition, broader mechanistic analyses have shown that tamoxifen influences multiple signalling nodes involved in angiogenesis, invasion, apoptosis, and drug resistance, including suppression of VEGF and basic FGF, modulation of TGF-β □ □ □ □ □ □ □ □ □ □ □ □ interference with protein kinase C and multidrug resistance pathways (Bogush et al. 2012). Together, these data support the concept that tamoxifen acts as a polyvalent, network-modulating agent. Within this systems framework, the clinical and biomarker findings of the present study can be interpreted as in vivo reflections of network-level pathway modulation. The limited robustness of single circulating biomarkers, contrasted with the clearer structure observed in multivariate models, is consistent with a therapy that exerts distributed effects across multiple interconnected pathways.

Taken together, these findings indicate that the principal biological effect of tamoxifen in NF-PitNETs is unlikely to result from direct inhibition of a single receptor or downstream effector. Instead, tamoxifen appears to induce progressive reorganisation of interconnected signalling networks centred on PI3K/AKT and MAPK activation. This systems-level interpretation provides a coherent mechanistic explanation for the latent biomarker constructs and establishes a molecular framework within which additional signalling pathways, including calcium signalling, cAMP signalling, dopaminergic regulation and Wnt modulation, collectively influence therapeutic responsiveness. Importantly, the convergence of computational prediction, experimental evidence, patient-derived biomarker profiles and clinical volumetric responses substantially strengthens the biological plausibility of tamoxifen as a systems-level modulator of NF-PitNET biology.

4.9.4 Integrated Model of Tamoxifen Response in NF-PitNETs

Although definitive predictive factors cannot be established from this proof-of-concept study, the present findings support the biologically plausible hypothesis that patients with low-volume residual NF-PitNETs, favourable oestrogen receptor profiles, and favourable Wnt-related biomarker signatures may derive greater benefit from tamoxifen therapy. This hypothesis requires prospective validation before clinical implementation.

The proposed mechanistic model (Figure 4.13) summarises the integration of the clinical, molecular, and computational findings generated throughout this study. At its core, the model demonstrates convergence of two complementary biological domains identified empirically from patient-derived data. The Growth–Angiogenic Biomarker Domain, represented by HGF, TGF-α [illegible] ugh [illegible] growth factor receptors onto the PI3K/AKT–MAPK signalling network that regulates tumour proliferation, angiogenesis, cellular survival, and remodelling. In parallel, the Wnt-modulatory domain, represented by DKK1 and sFRP1, provides an additional regulatory axis that interacts with these downstream signalling pathways. Integration of these domains with computationally identified hub genes, including AKT1, MAPK14, EGFR and ESR1, supports the concept that tamoxifen influences NF-PitNET biology through coordinated network modulation rather than isolated inhibition of individual receptors or signalling molecules.

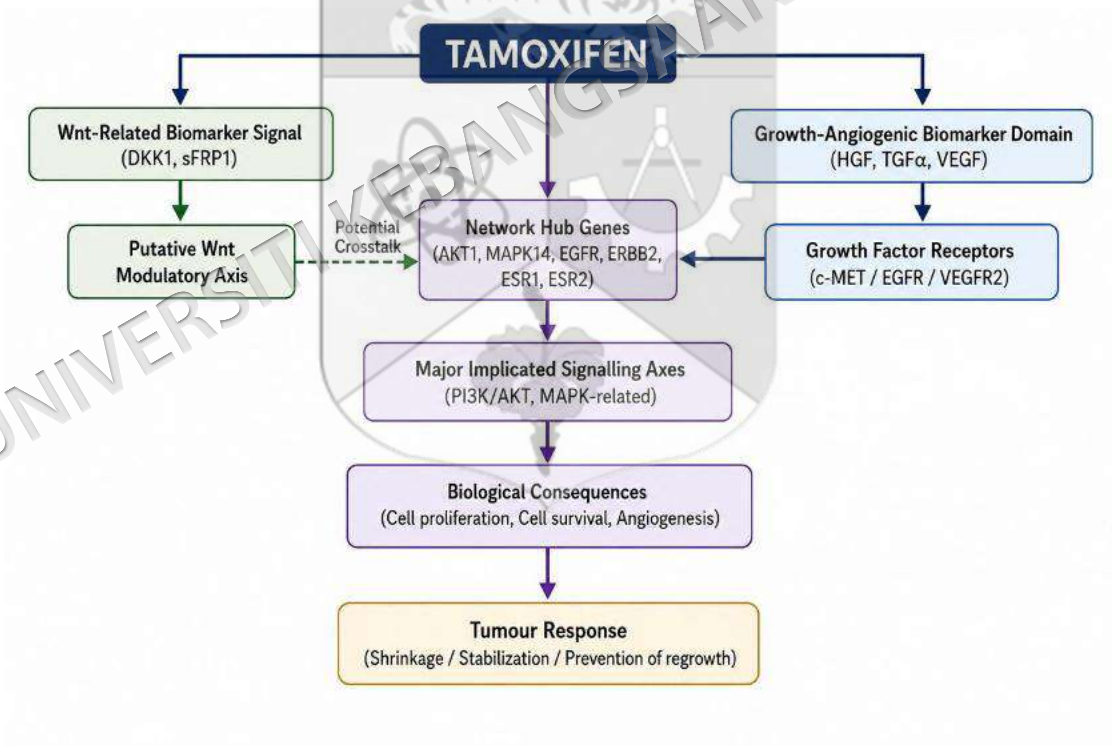

Figure 4.13 Proposed integrated mechanistic model of tamoxifen action in residual NF-PitNET

[illegible] biologically plausible endocrine-responsive environment within many NF-PitNETs. [illegible] α [illegible]

present study, its recognised role as the principal target of tamoxifen suggests that future α β more comprehensive understanding of endocrine responsiveness. Nevertheless, the absence of a direct associati β indicates that receptor abundance is unlikely to be the sole determinant of therapeutic responsiveness. Instead, the present findings support a multidimensional model in which receptor localisation, E α β downstream signalling activity, co-regulatory proteins, and broader pathway interactions collectively determine biological sensitivity to tamoxifen. Consequently, β lex endocrine-responsive phenotype rather than an independent predictive biomarker.

At the clinical level, the divergence in tumour growth trajectories between treatment groups suggests that tamoxifen modifies tumour growth behaviour in a subset of patients. However, the variable magnitude of response observed among treated individuals also reflects the inherent biological heterogeneity of NF-PitNETs. Although the present study demonstrated the biological plausibility of tamoxifen therapy, several factors that may influence endocrine responsiveness – including transcription factor-defined tumour lineage, menopausal status, and additional aspects of oestrogen receptor – were not evaluated. α β Consequently, the relative contribution of these factors to inter-individual variability in treatment response remains uncertain and should be addressed in future validation studies.

At the molecular level, the serum biomarker analyses demonstrate that treatment-associated biological responses are distributed across interconnected signalling pathways rather than concentrated within a single circulating protein. This systems-level organisation explains why isolated biomarkers showed limited and inconsistent associations with tumour volume, whereas multivariate modelling identified biologically coherent latent domains with substantially greater stability and interpretability. Within this framework, DKK1 emerged as an independent biomarker associated with final tumour volume, suggesting sustained modulation of the Wnt signalling network, while the Growth–Angiogenic construct comprising HGF, TGF-α and VEGF captured coordinated regulation of tumour-supportive growth factor

signalling. Rather than functioning independently, these complementary domains define an integrated molecular signature that reflects pathway-level biological adaptation during tamoxifen therapy.

Conceptually, the proposed model provides a mechanistic explanation for the heterogeneous clinical responses observed in this study. In a biologically diverse tumour such as an NF-PitNET, therapeutic responsiveness is unlikely to result from uniform suppression of a single molecular target. Instead, tamoxifen appears to exert distributed effects across multiple interacting signalling pathways, leading to progressive reorganisation of tumour-supportive biological networks. This systems-level interpretation is reinforced by the concordance between longitudinal biomarker analyses and independent computational pathway enrichment, which together provide complementary evidence that the clinically derived biomarker domains converge on recognised molecular mechanisms relevant to pituitary tumour biology.

Importantly, the integrated model proposed in this study should be regarded as a translational framework rather than a definitive biological pathway. The computational analyses provide mechanistic support for the observed clinical and biomarker findings but do not establish direct causal relationships. Similarly, although DKK1 and the Growth–Angiogenic biomarker construct emerged as the most informative molecular features within this cohort, these observations require validation in larger, independent cohorts incorporating contemporary transcription factor-based PitNET classification, comprehensive endocrine phenotyping, and tissue-level molecular profiling. Such studies will be essential to determine whether distinct molecular or lineage-defined subgroups exhibit differential responsiveness to tamoxifen.

In relation to the study objectives, these findings fulfil the overall aim of evaluating the therapeutic potential of tamoxifen in residual NF-PitNETs, while addressing the specific objective of identifying molecular biomarkers associated with treatment response. This study does not propose a single definitive biomarker. Rather, it establishes a putative systems-level biomarker framework comprising three complementary components: (i) oestrogen receptor expression in NF-PitNETs as the

tissue-level biological basis for endocrine responsiveness; (ii) DKK1 as a representative circulating Wnt-regulatory biomarker; and (iii) a reproducible growth–angiogenic signalling module represented by HGF, TGF-α computational and clinical findings, these complementary components provide a biologically grounded framework for biomarker-guided patient stratification and establish a conceptual foundation for future precision endocrine therapy in residual NF-PitNETs.

CHAPTER V

CONCLUSION

5.1 KEY FINDINGS AND THEIR IMPLICATIONS

This study evaluated the therapeutic potential of tamoxifen in NF-PitNETs and examined molecular correlates of treatment response using a multimodal translational framework integrating tumour oestrogen receptor profiling, longitudinal MRI volumetry, circulating serum biomarkers, and computational pathway analyses. This integrative approach reflects the biological heterogeneity of NF-PitNETs and is based on the premise that therapeutic effects in these tumours are more plausibly mediated through coordinated pathway-level modulation than isolated molecular or clinical factors.

For the first specific objective, immunohistochemical analysis demonstrated that a substantial proportion of NF-PitNETs express oestrogen receptors, with a predominant □ □ □ □ □ □ □ □ β □ establishes a biological credible rationale for endocrine modulation using selective oestrogen receptor modulators such as tamoxifen. However, the marked inter-tumour variability in receptor expression and distribution underscores the intrinsic heterogeneity of NF-PitNETs and indicates that receptor status alone is insufficient to predict therapeutic responsiveness. Clinically, this suggests that while ER expression supports the plausibility, it should be interpreted within a broader molecular and signalling context rather than used as the sole stratification criterion.

For the second specific objective, longitudinal MRI-based volumetric assessment over 12 months revealed a clinically meaningful divergence in tumour behaviour growth trajectories between treated and control groups. Tumour shrinkage occurred exclusively in the tamoxifen-treated cohort, whereas tumour regrowth was confined to the control group. Although tumour stabilisation remained the most frequent

overall outcome, the absence of regrowth and the presence of true volumetric regression in treated patients supports the conclusion that tamoxifen can alter tumour growth dynamics rather than merely delay progression. The convergence of results across complementary analytical approaches strengthens the robustness of this finding. In clinical setting where medical options for residual NF-PitNETs remains limited, these data suggest that tamoxifen may serve as a disease-modifying adjunct in selected patients.

For the third specific objective, baseline serum biomarkers profile spanning growth, angiogenic, inflammatory, cytokine, and Wnt-modulatory pathways showed no significant baseline differences between groups, confirming biochemical comparability prior to intervention. Following treatment, changes in individual biomarkers were modest and heterogeneous, and no single analyte demonstrated consistent predictive utility. This reinforces the limitation of single biomarker approaches in biologically complex tumours. In contrast, multivariate modelling identified coordinated shifts across biologically coherent domains, supporting the view that treatment-related molecular effects are more accurately represented at the pathway or axis level. These findings support the conceptual and practical value of composite, systems-based biomarker models for monitoring therapeutic effects in heterogeneous tumours.

For the fourth specific objective, computational analyses revealed enrichment of tamoxifen-interacting targets within neuroactive ligand–receptor interactions, calcium and cyclic AMP signalling, and key oncogenic pathways including PI3K/AKT and ERK/MAPK. Considered alongside the clinical and biomarker findings, these results provide a coherent mechanistic framework linking oestrogen receptor modulation by tamoxifen to downstream growth, survival, inflammatory, and Wnt-related signalling networks known to influence NF-PitNET behaviour. The convergence of in silico predictions with in vivo molecular and clinical observations strengthens the biological plausibility of the observed therapeutic effects and supports a network-based interpretation of tamoxifen action.

Collectively, these findings demonstrate that tamoxifen can favourably alter tumour growth trajectories in a subset of patients with residual NF-PitNETs and that

treatment response is best conceptualized as coordinated pathway-level molecular recalibration rather than suppression of isolated targets. The key implication for future research and clinical practice is that biomarker-guided management in NF-PitNETs will likely require multivariate, systems-level frameworks to achieve meaningful precision in patient stratification and treatment monitoring.

5.1 STUDY CONTRIBUTIONS

This thesis makes several substantive and original contributions to the field of NF-PitNETs by advancing both conceptual understanding and methodological approaches across histopathological, clinical, molecular, and computational levels.

First, beyond descriptive reporting [illegible] α [illegible] β [illegible] offers a conceptual reframing of oestrogen receptor biology in NF-PitNETs. By embedding receptor profiling within a broader discussion of receptor isoforms, subcellular localisation, and downstream signalling context, the study moves the field from a static, receptor-abundance model towards a functionally integrated view of oestrogen signalling. This shifts the interpretive focus [illegible] " [illegible] " [illegible] " [illegible] " [illegible] modulation in pituitary tumours.

Second, at the clinical-translational level, this thesis introduces a prospective, volumetry-based framework for evaluating medical therapy in residual NF-PitNETs. The use of longitudinal quantitative MRI volumetry offers a sensitive and reproducible method for detecting subtle changes in tumour growth kinetics, providing a methodological template for future interventional studies in slow-growing neuroendocrine tumours.

Third, at the molecular level, this study represents one of the earliest structured, provides one of the first structured, longitudinal serum biomarker profiling efforts in tamoxifen-treated NF-PitNETs. Importantly, biomarker evaluation was approached from a systems-perspective, recognizing circulating proteins as tumour–host signalling networks rather than isolated indicators. This conceptual orientation aligns biomarker

analysis with the established biological complexity of NF-PitNETs and advances the methodological sophistication of translational endocrine research.

Fourth, the thesis introduces and validates a multivariate, latent-construct approach to interpreting systemic molecular responses to therapy. By integrating exploratory and confirmatory factor analyses with clinical and biomarker data, the thesis demonstrates how pathway-level structure can be extracted from heterogeneous molecular measurements and used to generate biologically coherent signalling axes. This provides a transferable analytical framework applicable to other endocrine or neuro-oncological contexts characterised by complex, multivariate biology.

Finally, and most importantly, this work presents a novel integrative protein profiling paradigm for treatment response in NF-PitNETs. Rather than identifying a single predictive biomarker, the study delineates a pathway-informed, multicomponent molecular signature that combines a regulatory pathway node (DKK1, reflecting Wnt pathway engagement) with a reproducible growth–angiogenic signalling module (HGF, TGF-α □ □□ □ □ □) □ □□ □ □ transition from descriptive biomarker cataloguing to mechanistically anchored, systems-based model of therapeutic monitoring and stratification in pituitary tumours.

Overall, these contributions position the present thesis as a translational and methodological bridge linking receptor biology, quantitative imaging, circulating biomarkers and computational pathway modelling. It establishes a foundation for future development of biomarker-guided, precision-oriented endocrine therapy in NF-PitNETs and provides a conceptual and methodological platform upon which larger validation studies and future stratified clinical trials can be built.

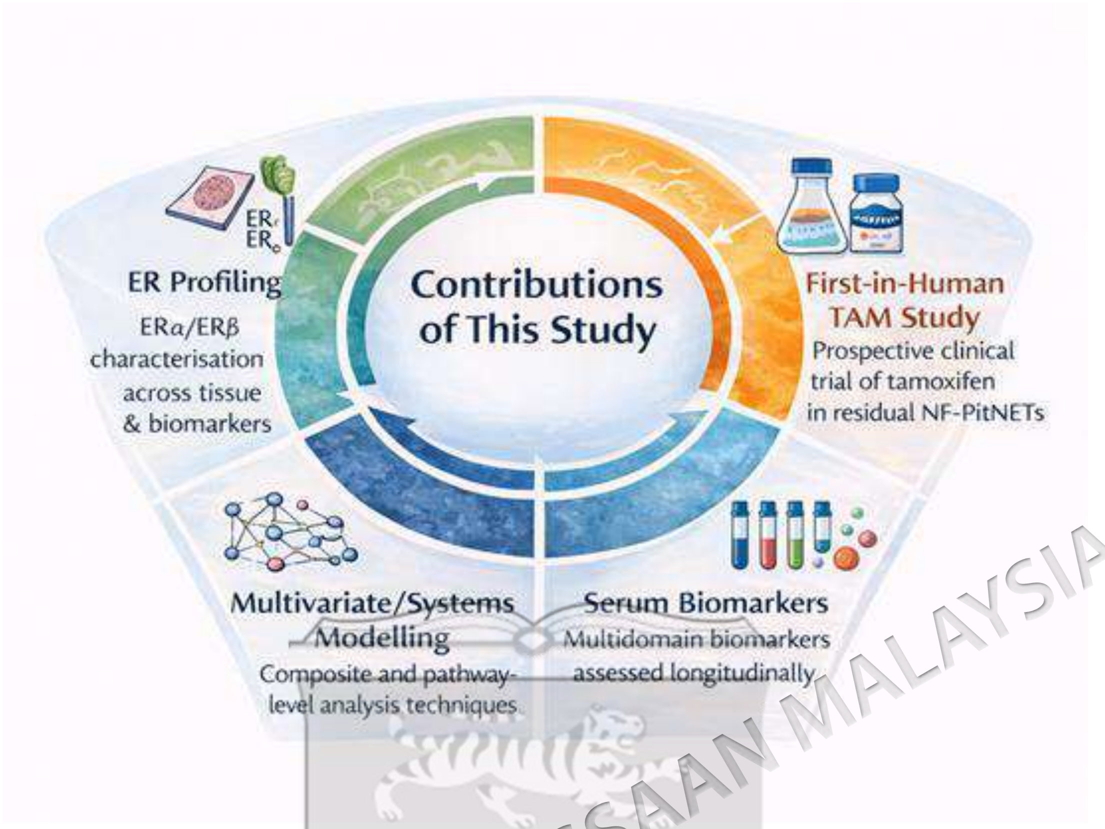

Figure 5.1 Conceptual overview of the key contributions of the present study in NF-PitNETs

Figure 5.1 summarises the four integrated pillars of the present study: (i) [illegible]-PitNET tissues to establish biological plausibility; (ii) prospective clinical evaluation in patients with residual NF-PitNETs to translate preclinical rationale into patient-level evidence; (iii) longitudinal serum biomarker profiling across multiple biological domains to capture dynamic molecular changes over time; and (iv) multivariate and systems-level modelling to integrate pathway interactions and derive composite biological signatures. Together, these components illustrate a unified translational framework linking tumour biology, clinical intervention, molecular dynamics, and advanced analytical strategies.

5.2 STRENGTH

This study possesses several important strengths that enhance the credibility, coherence, and translational value of its findings.

First, it adopts a genuinely integrated, multimodal design, combining longitudinal MRI-based tumour volumetry, immunohistochemical profiling of oestrogen receptors, circulating serum biomarker analysis, multivariate statistical modelling, and bioinformatic pathway enrichment. This comprehensive approach enables the research question to be addressed from complementary clinical, molecular, and computational perspectives, moving beyond single-endpoint or single-method studies that often fail to capture the complexity of NF-PitNET biology.

Second, the use of quantitative, three-dimensional MRI volumetry as the primary clinical outcome represents a major methodological strength. Volumetric assessment provides a more sensitive and objective measure of tumour behaviour than categorical or diameter-based measures, particularly in a disease characterised by slow growth and heterogeneous response patterns, thereby strengthening the clinical relevance of the findings. This approach enhances both precision and translational relevance.

Third, although circulating serum biomarkers are known to exhibit biological and analytical variability, they remain the most practical and clinically feasible modality for longitudinal monitoring, as blood sampling is minimally invasive, repeatable, cost-effective, and easily integrated into routine clinical care. To mitigate variability, this study employed careful a priori biomarker selection, restricting the panel to well-established markers that have been repeatedly reported in the literature and shown to be reliably measurable and relatively stable in serum. This strategy, together with standardised sample handling, duplicate measurements, and quality control procedures, was designed to improve measurement consistency and interpretability. While individual biomarkers still showed heterogeneous changes, the identification of coordinated, pathway-level patterns through multivariate modelling supports the value of serum biomarkers when analysed at the construct level rather than as isolated signals.

Fourth, the study deliberately moves beyond a single-biomarker paradigm by applying multivariate and construct-based approaches, including exploratory and confirmatory factor analysis and the development of a Composite Biomarker Index (CBI). This strategy aligns well with contemporary systems-biology thinking and the

known biological complexity of pituitary tumours, where coordinated pathway activity is more informative than isolated molecular markers. The demonstration of coherent latent biomarker axes and a robust growth–angiogenic construct provides a biologically meaningful framework for interpreting molecular modulation under tamoxifen therapy.

Finally, the statistical strategy enhances analytical robustness. The use of bootstrapped inference, effect size estimation, and multiple complementary statistical models reflects a rigorous and transparent analytical strategy tailored to small-sample, exploratory translational research. Together with the integration of bioinformatic pathway enrichment, which strengthens biological plausibility by linking clinical and biomarker findings to established signalling hubs (PI3K/AKT, ERK/MAPK, mTOR, □ □ □ □ □ □ □ -catenin), this study successfully fulfils its pilot objectives by demonstrating feasibility, detecting early therapeutic signals, and generating testable hypotheses for future confirmatory trials.

5.3 LIMITATIONS

Several limitations warrant consideration. First, the small pilot sample size limits statistical power, increases the risk of type II error, and precludes definitive subgroup or predictive analyses. Accordingly, this study was designed as exploratory and hypothesis-generating, with emphasis on effect sizes, signal direction, and estimation of outcome variability to inform a future definitive trial. Although covariance adjustment and repeated-measures modelling were used to improve precision, all findings should be interpreted as preliminary.

Second, attrition, largely related to disruptions during the COVID-19 pandemic, further reduced the effective sample size and may have introduced selection bias related to follow-up completion.

Third, circulating serum biomarkers represent systemic proxies rather than direct measures of intratumoural signalling. Serum levels may be influenced by host-related factors, and downstream transcription factors recommended in contemporary WHO frameworks were not assessed by immunohistochemistry. These constraints

likely contributed to weak or inconsistent signals in single-marker analyses and underscore the need for integrated pathway-level and tissue-based validation.

Fourth, although MRI volumetry provided a more sensitive assessment of tumour change than conventional linear measurements, several methodological limitations remain. Tumour segmentation and volume assessment were performed by a single experienced neuroradiologist, who was blinded to treatment allocation. Each tumour was measured three times, and the mean of the three measurements was used to reduce intra-observer variability. However, because only one neuroradiologist performed the assessments, inter-radiologist variability and inter-rater reliability could not be evaluated. In addition, pre-surgical tumour growth rate was not analysed because serial preoperative MRI examinations obtained at standardised intervals were not consistently available across the cohort. Although enrolment criteria required confirmation of stable postoperative residual disease and excluded patients with established regrowth at screening, the absence of pre-surgical growth-rate data limits assessment of whether intrinsic tumour kinetics influenced subsequent residual tumour behaviour or apparent response to tamoxifen.

Fifth, while bootstrapping and multivariate modelling enhance internal consistency in small samples, they cannot compensate for limited population representation. Thus, the estimates primarily reflect internal robustness rather than assured external generalisability. Exploratory factor analysis was additionally constrained by moderate sampling adequacy and domain imbalance.

Sixth, the 12-month follow-up and discrete assessment time points may not fully capture longer-term tumour kinetics or delayed treatment effects in a slowly progressive disease.

Finally, computational and network pharmacology analyses are inherently inferential. In silico predictions depend on database completeness and simplify complex biological systems; therefore, they provide mechanistic coherence but not direct proof of pathway activation or suppression.

Overall, this study should be regarded as a proof-of-concept investigation. Despite its limitations, it demonstrates feasibility, identifies biologically plausible therapeutic signals, and generates testable hypotheses that justify larger, adequately powered, and mechanistically integrated future studies in residual NF-PitNETs.

5.4 FUTURE DIRECTIONS

5.4.1 Prospective Validation and External Generalisability

Future research should prioritise prospective validation of these findings in larger, multicentre cohorts to enhance statistical power, external validity and precision of effect estimates. Multicentre recruitment would better capture the clinical and biological heterogeneity of NF-PitNETs while reducing centre-specific bias. Confirmation of tumour stabilisation and shrinkage under tamoxifen therapy, together with replication of the Composite Biomarker Index and latent pathway axes, is essential. As the present study identified a putative biomarker profile based primarily on circulating proteins, prospective validation should also incorporate tissue-level immunohistochemical assessment of the selected candidate biomarkers, particularly DKK1, sFRP1, HGF, TGF-α [illegible] available. Correlating tissue expression with circulating biomarker concentrations, volumetric response and clinical outcomes would provide important biological validation of the proposed systems-level biomarker signature and clarify whether serum alterations reflect intratumoural pathway activity. Additionally, the use of both conventional parametric methods and Bayesian approaches would enable more robust and transparent inference in the context of relatively small and clinically heterogeneous populations.

To strengthen interpretability and address antibody-related uncertainty, future studies should i[illegible]β[illegible] approaches at transcript and protein levels. At the mRNA level, quantitative PCR (qPCR) or RNA sequencing could be used to measure ESR2 expression and assess [illegible]β[illegible] should also incorporate molecular characterisation of the ESR1 gene, which encodes [illegible]α[illegible]

additional predictive information beyond protein immunohistochemistry alone. □ □ □ □ □ □ □ □ □ □ □□ □ □ □ □□ □ □ □ □□ □ α □ □ □ β □□ □ □ -defined tumour lineage and pathway-level molecular profiling may facilitate identification of endocrine-responsive NF-PitNET subgroups and improve prediction of tamoxifen responsiveness. At the protein level, Western blotting with rigorously validated antibodies and appropriate positive and negative controls could help confirm expected molecular weight bands and reduce the risk of cross-reactivity. In addition, targeted proteomic approaches, such as mass spectrometry-□ □ □ □ □ □□ □ □ □ □-specific □ □□ □ □□ □ peptides (e.g. LC-MS/MS or parallel reaction monitoring), would provide high-□ □ □ □ □ □ □ □ □ □ □ □□ □ □ □ □ □ □ □ □ □ □ □ □ □ □ □ □ □ β □□ □ □ □ □ □ □ □ □ □ □ betw□ □ □ □□ □ □ □ □ □ □ □ □ □□ □ □ □ □□ □ □□ □ □ □ □ □ □ □ □ □□ □ □ □ □ variants and their variable antibody recognition. Together, these multimodal tissue, transcriptomic and proteomic approaches would improve confidence that immunohistochemical staining reflects true receptor expression, facilitate inter-study comparability and provide a more robust foundation for linking molecular profiles with tumour behaviour, biomarker signatures and therapeutic response in NF-PitNETs.

5.4.2 Longer-Term Follow-up and Longitudinal Modelling

Extended follow-up (3 to 5 years) is necessary to evaluate durability of treatment control effects and differentiate sustained from delayed progression. Extended observation would also allow more accurate characterisation of tumour growth trajectories over time. Where possible, more frequent and standardised imaging time points should be included to support longitudinal modelling using appropriate mixed-effects or growth-curve methods. This would provide a more realistic representation of the dynamic behaviour of residual NF-PitNETs under endocrine modulation.

5.4.3 Integration of Tissue-Based and Circulating Biomarkers

Future studies should integrate tissue-based molecular analyses, such as transcriptomic or phosphoproteomic profiling, with circulating biomarker measurements. This approach would enhance the biological interpretation of serum-based composite indices by linking systemic signals to intratumoural pathway activity. Establishing concordance

between tissue and blood-based markers would also increase confidence in the use of minimally invasive biomarkers for monitoring disease biology and treatment response.

5.4.4 Functional and Mechanistic Validation

To move beyond associative findings, functional validation in experimental NF-PitNET models should be pursued. In vitro, ex vivo, or patient-derived systems could be used to test the causal relevance of key signalling pathways identified in this study, including the PI3K/AKT, MAPK, mTOR, and Wnt pathways, particularly in the context of oestrogen receptor modulation. Such studies would help clarify whether the identified biomarkers and pathways are drivers of treatment response or secondary correlates.

5.4.5 Clinical Translation, Subtype-Specific Trials, and Biomarker-Guided Strategies

From a translational perspective, the pathway-based framework developed in this study provides a rational basis for future biomarker-guided approaches to patient stratification and treatment monitoring. Importantly, future clinical trials should be designed according to specific NF-PitNET subtypes, recognising the biological and clinical heterogeneity within this tumour group. Subtype-stratified or subtype-enriched trial designs would allow more precise evaluation of treatment effects and may help identify subgroups that derive the greatest benefit from tamoxifen or related endocrine strategies. In addition, the convergence on growth and survival pathways supports the systematic evaluation of combination strategies integrating endocrine modulation with targeted therapies, subject to appropriate safety and feasibility assessment.

5.4.6 Methodological Considerations for Future Trials

Future NF-[illegible]
practical constraints, such as those experienced during the COVID-19 pandemic. This may include decentralised follow-up, extended assessment windows, and remote data capture where appropriate. More adaptive trial designs could also enhance efficiency in rare tumour research while maintaining methodological rigour and interpretability.

5.5 CONCLUSION

This study first characterised oestrogen receptor expression in residual NF-PitNETs, and established a biological rationale for targeting oestrogen signalling in this tumour subtype. Building on this foundation, the study shows that tamoxifen is associated with favourable modulation of tumour growth trajectories in a subset of patients with residual NF-PitNETs, based on longitudinal MRI volumetric assessment. The observed tumour shrinkage and stabilisation in treated patients suggest a disease-modifying effect in a context with limited medical treatment options. At the molecular level, single-analyte serum biomarkers showed modest and heterogeneous changes, highlighting the limitations of isolated markers in a biologically complex disease. In contrast, multivariate modelling identified coherent biological axes and a robust growth–angiogenic composite construct that better capture coordinated, pathway-level modulation under therapy. Integration with bioinformatic enrichment further supports a systems-level model centred on PI3K/AKT and MAPK signalling hubs. Collectively, these findings indicate that tamoxifen acts by rebalancing interconnected signalling networks rather than targeting a single pathway, providing a mechanistic basis for the observed volumetric responses. Despite the pilot nature of the study, this work establishes the feasibility and scientific value of a pathway-based, multivariate approach to biomarker analysis in NF-PitNETs and provides a strong foundation for future confirmatory, mechanistically integrated and precision-oriented therapeutic strategies.

REFERENCES

Acunzo, J., et al. 2011. Inactivation of PITX2 transcription factor induced apoptosis of gonadotroph tumoral cells. *Endocrinology* 152(10): 3884–3892.

Aflorei, E.D. & Korbonits, M. 2014. Epidemiology and etiopathogenesis of pituitary adenomas. *Journal of Neuro-oncology* 117(3): 379–394.

Agustsson, T.T., et al. 2015. The epidemiology of pituitary adenomas in Iceland, 1955-2012. *European Journal of Endocrinology* 173(5): 655–664.

Ajlan, A., et al. 2017. Cavernous Sinus Involvement by Pituitary Adenomas: Clinical Implications and Outcomes. *Journal of Neurological Surgery Part B* 78(3): 273–282.

Almeida, J.P., et al. 2019. Clinical, pathologic, and imaging characteristics of pituitary null cell adenomas (2017 WHO criteria). *Pituitary* 22(5): 514–519.

Alrezk, R., Hannah-Shmouni, F. & Stratakis, C.A. 2017. MEN4 and CDKN1B mutations: the latest of the MEN syndromes. *Endocrine-related Cancer* 24(10): T195–T208.

Amalina, H.A.T., et al. 2024. Tumor shrinkage in a tamoxifen-treated non-functioning pituitary neuroendocri□ *J. Clin. Transl. Endocrinol. Case Reports* 33: 100174.

Andersson, S., et al. 2017. Insufficient antibody validation challenges oestrogen receptor beta research. *Nature Communications* 8: 15840.

Araujo-Castro, M., et al. 2020. Pituitary tumors: epidemiology and clinical presentation spectrum. *Hormones* 19(2): 145–155.

Araujo-Castro, M., et al. 2025. Validation and Limitations of the PANOMEN-3 Predictive Model for Tumor Recurrence. *Journal of Clinical Endocrinology & Metabolism* 110(12): 3391–3399.

Asa, S.L., et al. 2017. From pituitary adenoma to pituitary neuroendocrine tumor (PitNET): an International proposal. *Endocrine-Related Cancer* 24(4): C5–C8.

Asa, S.L., et al. 2022. Overview of the 2022 WHO Classification of Pituitary Tumors. *Endocrine Pathology* 33(1): 6–26.

Asa, S.L., Ezzat, S. & Mete, O. 2025. Clinical integration and application of the 2022 WHO pituitary tumor classification. *Neuro-Oncology Advances* 7(S1): i10–i16.

Asioli, S., et al. 2019. Validation of a clinicopathological score for the prediction of post-surgical evolution. *European Journal of Endocrinology* 180(2): 127–134.

Ayuk, J. & Stewart, P.M. 2009. Mortality following pituitary radiotherapy. *Pituitary* 12(1): 35–39.

Baharudin, R., et al. 2020. Epigenetics of SFRP1: The Dual Roles in Human Cancers. *Cancers* 12(2).

Bai, J., et al. 2012. Effects of fulvestrant on biological activity and Wnt expression in rat GH3 cells. *Neural Regeneration Research* 7(4): 283–289.

Balili, I. & Barkan, A. 2014. Tamoxifen as a therapeutic agent in acromegaly. *Pituitary* 17(6): 500–504.

Balogun, J.A., et al. 2015. Null cell adenomas of the pituitary gland: an institutional review. *Endocrine Pathology* 26(1): 63–70.

Bao, J., Zheng, J.J. & Wu, D. 2012. The structural basis of DKK-mediated inhibition of Wnt/LRP signaling. *Science Signaling* 5(224): pe22.

Bao, X.J., et al. 2021. Transcriptomic analysis identifies a tumor subtype mRNA classifier for invasive NF-PitNET. *Theranostics* 11(1): 132–146.

[illegible] agonists/antagonists. *Molecular Pharmacology* 54(1): 105–112.

[illegible] 5 [illegible] *Journal of the Royal Statistical Society* 16(2): 296–298.

Batista, R.L., et al. 2018. NFPA Recurrence and Its Relationship with Sex, Size, and Hormonal Profile. *World Neurosurgery* 120: e241–e246.

Batista, R.L., et al. 2019. Cabergoline in the Management of Residual Nonfunctioning Pituitary Adenoma. *American Journal of Clinical Oncology* 42(2): 221–227.

Beckers, A. & Daly, A.F. 2007. The clinical, pathological, and genetic features of familial isolated pituitary adenomas. *European Journal of Endocrinology* 157(4): 371–382.

Ben-Shlomo, A. & Cooper, O. 2018. Silent corticotroph adenomas. *Pituitary* 21(2): 183–193.

Berardinelli, J., et al. 2024. KLHL14 and E-Cadherin Nuclear Co-Expression as Predicting Factor of Nonfunctioning PitNET Invasiveness. *Journal of Clinical Medicine* 13(15).

Birgersson, M., et al. 2022. Antibody Validation for Estrogen Receptor Beta. *Methods in Molecular Biology* 2418: 1–23.

Bogush, T., et al. 2012. Tamoxifen non-estrogen receptor mediated molecular targets. *Oncology Reviews* 6(2): e15.

Botelho, M.S., Franzini, Í.A., Nunes, V. dos S. & Boguszewski, C.L. 2022. Treatment of non-functioning pituitary adenoma with cabergoline: a systematic review and meta-analysis. *Pituitary* 25(6): 810–818.

Brochier, S., et al. 2010. Factors predicting relapse of NF-macroadenomas after neurosurgery. *European Journal of Endocrinology* 163(2): 193–200.

Brufsky, A.M. & Dickler, M.N. 2018. Estrogen Receptor-Positive Breast Cancer: Exploiting Signaling Pathways Implicated in Endocrine Resistance. *The Oncologist* 23(5): 528–539.

Camilletti, M.A., et al. 2019. Role of GPER in the anterior pituitary gland focusing on lactotroph function. *The Journal of Endocrinology* 240(2): 99–110.

Castellanos, L.E., et al. 2022. Epidemiology of common and uncommon adult pituitary tumors in the U.S. *Pituitary* 25(1): 201–209.

Č □ □ □ ý □ □□ □ □ □□ □ □ □□ □ □ □2 □ 2 5 □□ □ □ □ □ □ □ □□ □ □□ □ □ □ □ □ □ □ □ □ adenoma. *Journal of Neurosurgery* 143(2): 413–422.

Chaidarun, S.S., Klibanski, A. & Alexander, J.M. 1997. Tumor-specific expression of alternatively spliced ER mRNA variants. *JCE&M* 82(4): 1058–1065.

Chaidarun, S.S., Swearingen, B. & Alexander, J.M. 1998. Differential expression of □ □ β □□ □ □□ □ □ □ □ □ □□ □ *JCE&M* 83(9): 3308–3315. □ □ □ □

Chanson, P. & Brochier, S. 2005. Non-functioning pituitary adenomas. *Journal of Endocrinological Investigation* 28(11 Suppl): 93–99.

Chanson, P., et al. 2018. Physiopathology, Diagnosis, and Treatment of Nonfunctioning Pituitary Adenomas. *Endocrinology (Switzerland)*: 93–128.

Chanson, P., Dormoy, A. & Dekkers, O.M. 2019. Use of radiotherapy after pituitary surgery for NFPA. *European Journal of Endocrinology* 181(1): D1–D13.

Chen, X.-Y., et al. 2020. Relationship Between Pituitary Adenoma Consistency and Extent of Resection (TCTI Ratio). *Medical Science Monitor* 26: e919565.

Chen, Y., et al. 2012. Natural history of postoperative nonfunctioning pituitary adenomas. *Neuroendocrinology* 96(4): 333–342.

Chen, Y., et al. 2017. A Novel Invasive-Related Biomarker in Three Subtypes of NFPA. *World Neurosurgery* 100: 514–521.

Cheng, J., et al. 2019. FGF-2 signaling activation in the hippocampus contributes to the responses to puerarin. *Biochemical Pharmacology* 168: 91–99.

Cheng, S., et al. 2019. Predicting the regrowth of clinically NFPA with a statistical model. *Journal of Translational Medicine* 17(1): 164.

Chiloiro, S., et al. 2025. The clinicopathological PANOMEN-3 classification predicts pituitary adenoma prognosis. *Pituitary* 28(5): 97.

Chin, B.M., Orlandi, R.R. & Wiggins, R.H. 2012. Evaluation of the sellar and parasellar regions. *MRI Clinics of North America* 20(3): 515–543.

Chin, C.-H., et al. 2014. cytoHubba: identifying hub objects and sub-networks from complex interactome. *BMC Systems Biology* 8(S4): S11.

Cironi, K.A., et al. 2020. Arterial Supply to the Pituitary Gland: A Comprehensive Review. *World Neurosurgery* 142: 206–211.

Clarke, I.J. 2002. Multifarious effects of estrogen on the pituitary gonadotrope. *Archives of Physiology and Biochemistry* 110(1–2): 62–73.

Colao, A., et al. 2008. Medical therapy for clinically non-functioning pituitary adenomas. *Endocrine-related Cancer* 15(4): 905–915.

Colao, A., Faggiano, A. & Pivonello, R. 2010. Somatostatin analogues: treatment of pituitary and neuroendocrine tumors. *Progress in Brain Research* 182: 281–294.

Cooper, O. & Greenman, Y. 2018. Dopamine Agonists for Pituitary Adenomas. *Frontiers in Endocrinology* 9: 469.

Corsello, S. M., et al. 2017. The Drug Repurposing Hub: a next-generation drug library and information resource. *Nature Medicine* 23(4): 405–408.

Cox, F.F., et al. 2013. The neural cell adhesion molecule-derived peptide, FGL, attenuates LPS-induced changes. *Neuroscience* 235: 141–148.

Cristina, C., et al. 2010. VEGF and CD31 association in pituitary adenomas. *Endocrine Pathology* 21(3): 154–160.

D, G., et al. 2020. SwissTargetPrediction: A Web Server for Target Prediction. [https://pubmed.ncbi.nlm.nih.gov/24792161/].

Dai, C., et al. 2013. Inhibition of PI3K/AKT/mTOR pathway enhances temozolomide-induced cytotoxicity. *Endocrinology* 154(3): 1247–1259.

Dai, C., et al. 2021. Anti-VEGF Therapy in Refractory Pituitary Adenomas and Pituitary Carcinomas: A Review. *Frontiers in Oncology* 11: 773905.

Daly, A.F., et al. 2006. High prevalence of pituitary adenomas: a cross-sectional study in Liege, Belgium. *JCE&M* 91(12): 4769–4775.

Davies, C., et al. 2013. Long-term effects of continuing adjuvant tamoxifen (ATLAS trial). *Lancet* 381(9869): 805–816.

de Divitiis, E., et al. 2015. The current status of endoscopy in transsphenoidal surgery: an international survey. *World Neurosurgery* 83(4): 447–454.

de Laat, J.M., et al. 2015. Long-Term Natural Course of Pituitary Tumors in Patients With MEN1. *JCE&M* 100(9): 3288–3296.

Derwich, A., et al. 2023. The Role of PI3K/AKT/mTOR and RAF/MEK/ERK in Aggressive Pituitary Adenomas. *Int. J. Mol. Sci.* 24(13).

Di Ieva, A., et al. 2014. Aggressive pituitary adenomas—diagnosis and emerging treatments. *Nature Reviews Endocrinology* 10(7): 423–435.

Drange, M.R., et al. 2000. Pituitary Tumor Registry: A Novel Clinical Resource. *JCE&M* 85(1): 168–174.

Drummond, J., et al. 2019. Clinical and Pathological Aspects of Silent Pituitary Adenomas. *JCE&M* 104(7): 2473–2489.

Dubois, P.M. & ElAmraoui, A. 1995. Embryology of the pituitary gland. *Trends in Endocrinology & Metabolism* 6(1): 1–7.

Elston, M.S. & Clifton-Bligh, R.J. 2010. Identification of Wnt family inhibitors: a whole genome approach. *Molecular and Cellular Endocrinology* 326(1–2): 48–54.

Erickson, D., et al. 2009. Silent subtype 3 pituitary adenoma: clinicopathologic analysis (Mayo Clinic). *Clinical Endocrinology* 71(1): 92–99.

Esmaeili Motlagh, P., et al. 2024. Expression assays of selected lncRNAs in NFPA. *Discover Oncology* 15(1).

Esslimani-[illegible] 2 [illegible] β [illegible] breast cancer. *Clinical Cancer Research* 10(17): 5769–5776.

Ezzat, S., et al. 2004. The prevalence of pituitary adenomas: a systematic review. *Cancer* 101(3): 613–619.

Famini, P., et al. 2011. Pituitary MRI for sellar and parasellar masses: ten-year experience. *JCE&M* 96(6): 1633–1641.

Feng, J., et al. 2016. IL-6R/JAK2/STAT3/MMP9 signaling pathway correlated with invasion of null cell adenomas. *Mol. Cell. Endocrinol.* 436: 195–203.

Feng, T., et al. 2023a. Identification of cholesterol metabolism-related subtypes in NF-PitNETs. *Lipids in Health and Disease* 22(1): 127.

Feng, Y., et al. 2023b. A Network Pharmacology Prediction and Molecular Docking-Based Strategy for Glioma. *Int. J. Mol. Sci.* 24(22).

Fernandez, A., Brada, M., et al. 2009. Radiation-induced hypopituitarism. *Endocrine-related Cancer* 16(3): 733–772.

Fernandez, A., Karavitaki, N. & Wass, J.A.H. 2010. Prevalence of pituitary adenomas in Banbury (UK). *Clinical Endocrinology* 72(3): 377–382.

Fernández-Balsells, M.M., et al. 2011. Natural history of NFPA and incidentalomas: A systematic review. *JCE&M* 96(4): 905–912.

Fleseriu, M., Gurnell et al. 2025. Pituitary incidentaloma: a Pituitary Society international consensus guideline statement. *Nature reviews. Endocrinology*

21(10): 638–655.

Florio, T., et al. 2008. Efficacy of BIM-23A760 in the control of cell growth in NFPA. *Endocrine-related Cancer* 15(2): 583–596.

Fong, K.Y., et al. 2023. Postsurgical outcomes of NFPA: a patient-level meta-analysis. *Pituitary* 26(4): 461–473.

Formosa, R., et al. 2012. Expression and clinical significance of Wnt players and survivin in pituitary tumours. *Endocrine Pathology* 23(2): 123–131.

Freda, P.U., et al. 2011. Pituitary incidentaloma: an endocrine society clinical practice guideline. *JCE&M* 96(4): 894–904.

Freda, P.U., et al. 2020. Presenting features in 269 patients with clinically NFPA. *Journal of the Endocrine Society* 4(4): 1–13.

Fusco, A., et al. 2012. Treatment with octreotide LAR in clinically NFPA: results from a case–control study. *Pituitary* 15(4): 571–578.

Gaia, F., et al. 2022. Analyzing giant pituitary adenomas: An 8-year review (2012–2020) at a reference center in Brazil. *Clinical Neurology and Neurosurgery* 213: 107138.

Gao, H., et al. 2017. ESR1 and its antagonist fulvestrant in pituitary adenomas. *Molecular and Cellular Endocrinology* 443: 32–41.

García-Campos, M.A., et al. 2015. Pathway Analysis: State of the Art. *Frontiers in Physiology* 6: 383.

Gfeller, D., et al. 2014. SwissTargetPrediction: a web server for target prediction. *Nucleic Acids Research* 42(W1): W32-8.

Ghadir, M., et al. 2020. Cell proliferation, apoptosis, and angiogenesis in NFPA. *Endocrine* 69(3): 596–603.

Ghafouri-Fard, S., et al. 2022. Expression pattern of non-coding RNAs in NFPA. *Frontiers in Oncology* 12.

□ □ □ □ □ □ □ □□ □ □ □ □ □□ □ □□ □ □ □2 □ □ □ □ □ □□ □ □ □ □ □ □ □ □□ □ □ □ □ □ □ □ females. *Endocrinology* 149(1): 20–27.

Gil, J., et al. 2023. Molecular characterization of EMT and medical treatment related-genes in NF-PitNETs. *Frontiers in Endocrinology* 14.

Goshtasbi, K., et al. 2021. Endoscopic versus nonendoscopic surgery for resection of pituitary adenomas. *Journal of Neurosurgery* 134(3): 816–824.

Gough, P. & Myles, I.A. 2020. Tumor Necrosis Factor Receptors: Pleiotropic Signaling Complexes. *Frontiers in Immunology* 11: 585880.

Goyal-Honavar, A., et al. 2025. Early adjuvant radiation reduces the rate of recurrence in silent corticotroph PitNETs. *Clin. Neurol. Neurosurg.* 256: 109023.

Greenman, Y., et al. 2016. Treatment of clinically NFPA with dopamine agonists. *European Journal of Endocrinology* 175(1): 63–72.

Greenman, Y. & Stern, N. 2009. Non-functioning pituitary adenomas. *Best Practice & Res. Clin. Endocrinol. Metab.* 23(5): 625–638.

Gu, Y.-H. & Feng, Y.-G. 2018. Down-regulation of TGF-β [illegible] and invasion in NFPA. *Journal of Clinical Neuroscience* 47: 264–268.

Guerreiro, V.A., et al. 2023. Incidental versus symptomatic NFPA: Are they different? *Endocrinology, Diabetes and Metabolism* 6(6).

Guo, J., et al. 2021. Screening and Identification of Key Microenvironment-Related Genes in NFPA. *Frontiers in Genetics* 12: 627117.

Hadjimarkou, M.M. & Vasudevan, N. 2018. GPER1/GPR30 in the brain: Crosstalk with classical ER. *J. Steroid Biochem. Mol. Biol.* 176: 57–64.

Hair, J.F., et al. 2022. *A primer on partial least squares structural equation modeling (PLS-SEM)* (3rd ed.). Sage.

[illegible] β [illegible] *Endocrinology* 140(12): 5566–5578.

Hallén, T., et al. 2021. MCM7 as a marker of postsurgical progression in NFPA. *European Journal of Endocrinology* 184(4): 521–531.

Hallén, T., et al. 2022. Genome-wide DNA Methylation Differences in NFPA With and Without Postsurgical Progression. *JCE&M* 107(8): 2318–2328.

Hallén, T., et al. 2024. Proteomic Profiles Associated With Postsurgical Progression in NFPA. *JCE&M* 109(6): 1485–1493.

Han, S., et al. 2020. Overrepresentation of highly functional T regulatory cells in patients with NFPA. *Human Immunology* 81(6): 314–319.

[illegible] 2 [illegible] α [illegible] β [illegible] aging. *The Journal of Neuroscience* 33(6): 2671–2683.

Hannen, R., et al. 2019. Effects of anti-estrogens on cell invasion and survival in pituitary adenoma cells. *J. Steroid Biochem. Mol. Biol.* 187: 88–96.

Hattori, Y., et al. 2020. Accurate assessment of ER profiles in NFPA using RT-digital PCR. *Life Sciences* 260: 118416.

Haydar Ali Tajuddin, A., et al. 2020. Estrogen Receptors in NF-PitNETs: Review on Expression and Gonadotroph Functions. *Journal of the Endocrine Society* 4(12): bvaa157.

Haydar Ali Tajuddin, A., et al. 2025a. Tamoxifen for residual NF-PitNETs: A Proof-of-Concept study. *Endocrine*.

Haydar Ali Tajuddin, A., et al. 2025b. Biomarkers Driving Precision Medicine in NF-PitNETs: A Systematic Review. *JCE&M*: dgaf650.

Hazell, G.G., et al. 2009. Localisation of GPR30 suggests multiple functions in rodent brain. *Journal of Endocrinology* 202: 223–236.

He, W., et al. 2017. Relationship between RSUME and HIF-[illegible] α [illegible]-A with invasion of pituitary adenoma. *Gene* 603: 54–60.

Heaney, A.P., Fernando, M. & Melmed, S. 2002. Functional role of estrogen in pituitary tumor pathogenesis. *The Journal of Clinical Investigation* 109(2): 277–283.

Hefner, N.A. & Cooper, O.B. 2025. Management of Recurrent and Aggressive Non-Functioning Pituitary Adenomas. *Journal of Clinical Medicine* 14(15).

[illegible] 2 [illegible]-cadherin [illegible] protein levels. *Cancer Research* 68(21): 8695–8704.

Hemaidia, R.-M., et al. 2024. Radiation therapy in functioning and NF-PitNET: systematic review. *Frontiers in Endocrinology* 15: 1468724.

Herkenham, M. 2005. FS Cells of the Anterior Pituitary Mediate Interactions between Endocrine and Immune Systems. *Endocrinology* 146(1): 33–34.

Hickman, R.A., et al. 2021. Gonadotroph tumours with a low SF-1 labelling index enrichment of the PI3K-AKT pathway. *Neuropathology and Applied Neurobiology* 47(3): 415–427.

Ho, K., et al. 2021. Pituitary Neoplasm Nomenclature Workshop: Does Adenoma Stand the Test of Time? *Journal of the Endocrine Society* 5(3).

Ho, K.K.Y., et al. 2024. A proposed clinical classification for pituitary neoplasms to guide therapy and prognosis. *The Lancet Diabetes & Endocrinology* 12(3): 209–214.

Honegger, J. & Grimm, F. 2018. The experience with transsphenoidal surgery and its importance to outcomes. *Pituitary* 21(5): 545–555.

Hong, G.K., Payne, S.C. & Jane, J.A.J. 2016. Anatomy, Physiology, and Laboratory Evaluation of the Pituitary Gland. *Otolaryngologic Clinics of North America* 49(1): 21–32.

Hopewell, S., et al. 2025. CONSORT 2025 statement: updated guideline for reporting randomised trials. *The Lancet* 405(10489): 1633–1640.

Hossain, M.G., et al. 2009. Expression of p18(INK4C) is down-regulated in human pituitary adenomas. *Endocrine Pathology* 20(2): 114–121.

Hosseinkhan, N., et al. 2022. A systematic review of molecular alterations in invasive NFPA. *Endocrine* 77(3): 500–509.

Hou, X.-Z., et al. 2010. Expression of hepatocyte growth factor and c-Met in human pituitary adenomas. *Neuro-oncology* 12(8): 799–803.

Huang, D.W., Sherman, B.T. & Lempicki, R.A. 2009. Bioinformatics Enrichment Tools for Large Gene Lists. *Nucleic Acids Research* 37(1): 1–13.

Huang, X., et al. 2021. Alterations in CD8+ Tregs and NK Cells Associated With Invasiveness of NFPA. *Pathology and Oncology Research* 27.

Hussein, I.H., Mansour, A.A. & Jameel, N.A. 2023. Comparing MRI volume measurement techniques for pituitary macroadenoma. *Journal of Medicine and Life* 16(7): 998–1006.

Hussaini, I.M., et al. 2007. Matrix metalloproteinase-9 increases invasion in human pituitary adenoma cell line. *American Journal of Pathology* 170(1): 356–365.

Hwang, J., et al. 2016. Therapeutic Strategy for Cavernous Sinus-Invading NFPA Based on Knosp Grading. *Brain Tumor Research and Treatment* 4(2): 63–69.

Ibáñez-Costa, A., et al. 2016. Octreotide and pasireotide (dis)similarly inhibit pituitary tumor cells in vitro. *Journal of Endocrinology* 231(2): 135–145.

Ilie, M.D., Lasolle, H. & Raverot, G. 2019. Emerging and Novel Treatments for Pituitary Tumors.

Inoshita, N. & Nishioka, H. 2018. The 2017 WHO classification of pituitary adenoma: overview and comments. *Brain Tumor Pathology* 35(2): 51–56.

Johansson, A., Dar, H., et al. 2025. Differential long-term tamoxifen therapy benefit by menopausal status in breast cancer patients: secondary analysis of a controlled randomized clinical trial. *Journal of the National Cancer Institute* 117(5): 868–878.

Jordan, V.C. 2003. Tamoxifen: a most unlikely pioneering medicine. *Nature reviews. Drug discovery* 2(3): 205–213.

Juthani, R.G., et al. 2021. Radiographic and clinical outcomes using iMRI for resection of pituitary adenomas. *Journal of Neurosurgery* 134(6): 1824–1835.

Kagey, M.H. & He, X. 2017. Rationale for targeting the Wnt signalling modulator Dickkopf-1 for oncology. *British Journal of Pharmacology* 174(24): 4637–4650.

Kaiser, H.F. 1974. An index of factorial simplicity. *Psychometrika* 39(1): 31–36.

Kanehisa, M., et al. 2017. KEGG: New Perspectives on Genomes, Pathways, Diseases and Drugs. *Nucleic Acids Research* 45(D1): D353–D361.

Karavitaki, N., et al. 2006. Do the limits of serum prolactin in disconnection hyperprolactinaemia need re-definition? *Clinical endocrinology* 65(4): 524–529.

Kelly, M.J. & Levin, E.R. 2001. Rapid actions of plasma membrane estrogen receptors. *Trends in Endocrinology & Metabolism* 12(4): 152–156.

Kerekes, K., et al. 2021. Wnt Inhibitory Factor 1 Binds to and Inhibits the Activity of Sonic Hedgehog. *Cells* 10(12).

Khamseh, M.E., et al. 2022. Evaluation of necroptosis pathway mediators in functional and NFPA. *BMC Endocrine Disorders* 22(1).

Khayer, N., et al. 2021. Nkx3-1 and Fech genes might be switch genes involved in NFPA invasiveness. *Scientific Reports* 11(1).

Kim, B.-R., et al. 2012. Dickkopf-1 interrupts FAK/PI3K/mTOR pathway by interaction of CA9. *Cellular Signalling* 24(7): 1406–1413.

Kim, S.H., Lee, K.C. & Kim, S.H. 2007. Cranial nerve palsies accompanying pituitary tumour. *Journal of Clinical Neuroscience* 14(12): 1158–1162.

Kim, Y.J., et al. 2025. Natural history and predictors of growth in conservatively managed NF-macroadenomas. *Clin. Neurol. Neurosurg.* 254: 108920.

Kimura, N., et al. 2008. Identification of transcriptional regulatory elements in the human sst2 promoter. *Journal of molecular endocrinology* 40(2): 75–91.

Kinoshita, Y., Kurisu, K. & Arita, K. 2018. Nonfunctioning pituitary adenomas in elderly patients. *Journal of Clinical Neuroscience* 53: 127–131.

Kober, P., et al. 2018. DNA methylation profiling in nonfunctioning pituitary adenomas. *Molecular and Cellular Endocrinology* 473: 194–204.

Komm, B.S. & Mirkin, S. 2014. An overview of current and emerging SERMs. *The Journal of steroid biochemistry and molecular biology* 143: 207–222.

Kopp, C., et al. 2012. Tumor shrinkage assessed by volumetric MRI after radiotherapy of NFPA. *Int. J. Rad. Oncol. Biol. Phys.* 82(3): 1262–1267.

Kostanek, J., et al. 2024. Bootstrap Method as a Tool for Analyzing Data with Atypical Distributions.

Krzentowska, A., et al. 2025a. The Roles of PD-L1, Ki-67, P53, and Cyclin D1 in PitNETs. *Int. J. Mol. Sci.* 26(16).

Krzentowska, A., et al. 2025b. Radiological and Immunohistochemical Characteristics of PitNETs in 79 Patients.

Kuhl, H. 2005. Pharmacology of estrogens and progestogens: influence of routes of administration. *Climacteric* 8(S1): 3–63.

[illegible] *Endocrinology* 138(3): 863–870.

Kulkarni, V.S., et al. 2023. Drug Repurposing: An Effective Tool in Modern Drug Discovery. *Russian Journal of Bioorganic Chemistry* 49(2): 157–166.

Kunselman, A.R. 2024. A brief overview of pilot studies and their sample size justification. *Fertility and Sterility* 121(6): 899–901.

La Rosa, S., et al. 2008. Characterization of C-Kit (CD117) Expression in Human Normal Pituitary Cells and Adenomas. *Endocrine Pathology* 19(2): 104–111.

Langlois, F., et al. 2018. Silent somatotroph pituitary adenomas: an update. *Pituitary* 21(2): 194–202.

[illegible] 2 [illegible] α [illegible] *Neuroscience* 163(1): 233–243.

Lelotte, J., et al. 2018. Both invasiveness and proliferation criteria predict recurrence of NF-macroadenomas. *European Journal of Endocrinology* 178(3): 237–246.

Lenders, N.F., et al. 2016. Longitudinal evaluation of the natural history of conservatively managed NFPA. *Clinical Endocrinology* 84(2): 222–228.

Lenders, N.F., et al. 2023. The evolution in pituitary tumour classification: a clinical perspective. *Endocrine Oncology* 3(1): e220079.

Levin, E.R. & Hammes, S.R. 2016. Nuclear receptors outside the nucleus: extranuclear signalling. *Nature Reviews Molecular Cell Biology* 17(12): 783–797.

Li, L. & Kar, S. 2025. Leveraging network pharmacology for drug discovery. *Medicine in Drug Discovery* 27: 100220.

Li, W., et al. 2014. Wnt4 is overexpressed in human pituitary adenomas and associated with invasion. *Journal of Clinical Neuroscience* 21(1): 137–141.

Lien, E.A., Solheim, E. & Ueland, P.M. 1991. Distribution of tamoxifen and its metabolites in rat and human tissues. *Cancer Research* 51(18): 4837–4844.

Lin, K., et al. 2022. Metabolic Characteristics and M2 Macrophage Infiltrates in Invasive NFPA. *Frontiers in Endocrinology* 13.

Lin, S., et al. 2024. Targeting HTR2B suppresses NFPA growth via inhibiting [illegible] α [illegible] γ *Neuro-Oncology* 26(11): 2010–2026.

Lin, Y., et al. 2009. Frequent mutations and amplifications of the PIK3CA gene in pituitary tumors. *Endocrine-related Cancer* 16(1): 301–310.

Little, A.S., et al. 2020. Pituitary gland recovery following endoscopic surgery for NFPA. *Journal of Neurosurgery* 133(6): 1732–1738.

Liu, C., et al. 2016. Smad3 and phospho-Smad3 are potential markers of invasive NFPA. *OncoTargets and Therapy* 9: 2265–2271.

[illegible] β-catenin and c-myc expression predict aggressive growth of NFPA. *Molecular Medicine Reports* 15(4): 1793–1799.

Liu, D., et al. 2020. Integration of quantitative phosphoproteomics and transcriptomics. *EPMA Journal* 11(3): 419–467.

Liu, H., et al. 2022. Expression and clinical significance of Cathepsin K and MMPs in invasive NFPA. *Frontiers in Oncology* 12.

Loeffler, J.S. & Shih, H.A. 2011. Radiation therapy in the management of pituitary adenomas. *JCE&M* 96(7): 1992–2003.

Lohrer, P., et al. 2001. VEGF Production and Regulation in Rodent and Human Pituitary Tumor Cells in vitro. *Neuroendocrinology* 74(2): 95–105.

Long, N., et al. 2017. Tamoxifen and ICI 182,780 activate hypothalamic GPER1 to facilitate lordosis. *Hormones and Behavior* 89: 98–103.

Lopes, M.B. 2025. The 5th Edition of the WHO Classification of Pituitary Tumors: Strengths and limitations. *Brain Pathology* 35(1): e13323.

Lopes, M.B.S. 2017. The 2017 WHO classification of tumors of the pituitary gland: a summary. *Acta Neuropathologica* 134(4): 521–535.

Losa, M., et al. 2016. Temozolomide therapy in patients with aggressive pituitary adenomas or carcinomas. *Journal of Neuro-Oncology 126(3): 519–525.

Lu, L., et al. 2022. Classifying Pituitary Adenoma Invasiveness Based on Radiological and Histological Features. *Journal of Clinical Medicine* 11(9).

Lüdecke, D.K., et al. 2007. Pathohistological classification of pituitary tumors: 10 years of German Registry. *European Journal of Endocrinology*.

[illegible] 2 [illegible] 5 [illegible] -related behaviors. *Endocrinology* 146(2): 797–807.

Lv, T., et al. 2022. Tamoxifen Exerts Anticancer Effects on Pituitary Adenoma via Inducing Apoptosis. *Int. J. Mol. Sci.* 23(5).

Lyu, L., et al. 2021. Exosomal miRNA Profiling is a Potential Screening Route for NFPA. *Frontiers in Cell and Dev. Bio.* 9: 771354.

Maclean, J., et al. 2014. Peptide receptor radionuclide therapy for aggressive atypical pituitary adenoma. *Pituitary* 17(6): 530–538.

responsiveness. *BMC Cancer* 13: 425.

Maggiolini, M. & Picard, D. 2010. The unfolding stories of GPR30, a new membrane-bound ER. *Journal of Endocrinology* 204: 105–114.

Mann, J., et al. 2002. CD40 Induces IL-6 Gene Transcription in Dendritic Cells. *Journal of Biological Chemistry* 277(19): 17125–17138.

adenomas. *Anticancer Research* 30(7): 2897–2904.

Manojlovic-Gacic, E., et al. 2018. Histopathological classification of NF-PitNETs. *Pituitary* 21(2): 119–129.

Martensson, U.E., et al. 2009. Deletion of the GPER30 impairs glucose tolerance. *Endocrinology* 150: 687–698.

Martinkovich, S., et al. 2014. Selective estrogen receptor modulators: tissue specificity and clinical utility. *Clinical Interventions in Aging* 9: 1437–1452.

Mayson, S.E. & Snyder, P.J. 2015. Silent pituitary adenomas. *Endocrinol Metab Clin North Am* 44(1): 79–87.

McCabe, C.J., et al. 2002. VEGF, KDR/Flk-1, and PTTG in pituitary tumors. *JCE&M* 87(9): 4238–4244.

McClure, J.J., et al. 2024. Conditioned recurrence-free survival following resection of NFPA. *Journal of Neurosurgery* 140(6): 1614–1619.

McCormack, A., et al. 2018. Treatment of aggressive pituitary tumours and carcinomas: ESE survey 2016. *European Journal of Endocrinology* 178(3): 265–276.

McDowell, B.D., et al. 2011. Demographic differences in incidence for pituitary adenoma. *Pituitary* 14(1): 23–30.

Melmed, S., et al. 2022. Clinical Biology of the Pituitary Adenoma. *Endocrine Reviews* 43(6): 1003–1037.

Meng, J.H., et al. 2023. Network Pharmacology to Explore the Mechanism of Prunella vulgaris L. Against Prolactinoma. *Pharmacognosy Magazine* 20(1): 127–136.

Mete, O., Cintosun, A., Pressman, I. & Asa, S.L. 2018. Epidemiology and biomarker profile of pituitary adenohypophysial tumors. *Modern Pathology* 31(6): 900–909.

Mete, O., Ezzat, S. & Asa, S.L. 2012. Biomarkers of aggressive pituitary adenomas. *Journal of Molecular Endocrinology* 49(2): R69-78.

Mete, O., et al. 2013. The role of mediators of cell invasiveness in silent corticotroph adenomas. *Endocrine Pathology* 24(4): 191–198.

Mete, O., et al. 2016. Silent subtype 3 pituitary adenomas represent monomorphous plurihormonal Pit-1 lineage. *Modern Pathology* 29(2): 131–142.

Mete, O. & Lopes, M.B. 2017. Overview of the 2017 WHO Classification of Pituitary Tumors. *Endocrine Pathology* 28(3): 228–243.

Metin-Armagan, D., et al. 2020. A Novel Expression Profile of Cell Cycle and DNA Repair Proteins in NFPA. *Endocrine Pathology* 31(1): 2–13.

Mikelman, S., et al. 2017a. Tamoxifen and amphetamine abuse: Are there therapeutic possibilities? *Journal of chemical neuroanatomy* 83–84: 50–58.

Mikelman, S.R., et al. 2017b. Tamoxifen and its active metabolites inhibit dopamine transporter function. *Journal of neurochemistry* 141(1): 31–36.

Mikelman, S.R., et al. 2018. Tamoxifen Directly Interacts with the Dopamine Transporter. *Journal of Pharmacology and Experimental Therapeutics* 367(1): 119–128.

Mindermann, T. & Wilson, C.B. 1994. Age-related and gender-related occurrence of pituitary adenomas. *Clinical Endocrinology* 41(3): 359–364.

Minniti, G., et al. 2016. Stereotactic radiotherapy and radiosurgery for NF and secreting pituitary adenomas. *Rep. Pract. Oncol. Radiother.* 21(4): 370–378.

Möller, M.W., et al. 2020. Endoscopic vs. microscopic transsphenoidal pituitary surgery. *Scientific Reports* 10(1): 21942.

Möller-Goede, D.L., et al. 2011. Pituitary apoplexy: re-evaluation of risk factors and impact on outcome. *European Journal of Endocrinology* 164(1): 37–43.

Monné Rodríguez, J.M., et al. 2023. ESTP: Review of In Situ Hybridization Techniques for Drug Research. *Toxicologic Pathology* 51(3): 92–111.

Moreno, C.S., et al. 2005. Novel molecular signaling and classification of human NFPA. *Cancer Research* 65(22): 10214–10222.

□ β □ □ □ □ □ □ □ □ □ □ □ □ □ □ □ □ □ □ ER. *FEBS letters* 392(1): 49–53.

Muskens, I.S., et al. 2017. Visual outcomes after endoscopic endonasal pituitary adenoma resection: meta-analysis. *Pituitary* 20(5): 539–552.

Namvar, M., et al. 2023. Complications in Endoscopic Endonasal Pituitary Adenoma Surgery: 310 Patients. *J. Neurol. Surg. Part B* 84(3): 255–265.

Nasi-Kordhishti, I., et al. 2025. Transcription factor-based classification of pituitary adenomas / PitNETs. *Acta Neuropathologica Communications* 13(1): 135.

Nathan, M.R. & Schmid, P. 2017. A Review of Fulvestrant in Breast Cancer. *Oncology and therapy* 5(1): 17–29.

Neou, M., et al. 2020. Pangenomic Classification of Pituitary Neuroendocrine Tumors. *Cancer Cell* 37(1): 123-134.e5.

Newton, C.J. 1995. ER blockade by ZM 182780 induces death of pituitary tumour cells. *J. Steroid Biochem. Mol. Biol.* 55(3): 327–336.

Nishioka, H. & Inoshita, N. 2018. New WHO classification of pituitary adenomas (4th ed.): prognostic histological factors. *Brain Tumor Pathology* 35(2): 57–61.

Nishioka, H., et al. 2011. Co-[illegible] α [illegible] patients. *Molecular and Cellular Endocrinology* 331(1): 73–78.

Nishioka, H., et al. 2015. The Complementary Role of Transcription Factors in Accurate Diagnosis of NFPA. *Endocrine Pathology* 26(4): 349–355.

Noh, T., et al. 2009. Predicting recurrence of nonfunctioning pituitary adenomas. *JCE&M* 94(11): 4406–4413.

Novick, A.M., et al. 2020. Neuropsychiatric effects of tamoxifen: Challenges and opportunities. *Frontiers in Neuroendocrinology* 59: 100869.

Ntali, G., et al. 2016. Mortality in patients with NFPA is increased: systematic analysis of 546 cases. *European Journal of Endocrinology* 174(2): 137–145.

Ntali, G. & Wass, J.A. 2018. Epidemiology, clinical presentation and diagnosis of NFPA. *Pituitary* 21(2): 111–118.

Oh, J.S., et al. 2021. Incidence, mortality, and cardiovascular diseases in pituitary adenoma in Korea. *Pituitary* 24(1): 38–47.

Ooi, G.T., Tawadros, N. & Escalona, R.M. 2004. Pituitary cell lines and their endocrine applications. *Molecular and Cellular Endocrinology* 228(1–2): 1–21.

Ostrom, Q.T., Price, M. & Ryan, K. 2022. CBTRUS statistical report: Primary brain tumors diagnosed in the US 2015–2019. *Neuro-Oncology* 24(S5): v1–v95.

Øystese, K[illegible] 2 [illegible]-Dependent Predictor of Aggressiveness in NFPA. *JCE&M* 102(9): 3581–3590.

[illegible] 2 [illegible]-[illegible] selective ligands. *Steroids* 90: 13–29.

Patisaul, H.B., et al. 2003. Immediate and residual effects of tamoxifen in the female rat hypothalamus. *Brain Research* 978(1–2): 185–193.

Pedersen, M.B., et al. 2022. Endocrine Function after Transsphenoidal Surgery in Patients with NFPA: meta-analysis. *Neuroendocrinology* 112(9): 823–834.

Pepe, S., Korbonits, M. & Iacovazzo, D. 2019. Germline and mosaic mutations causing pituitary tumours. *The Journal of Endocrinology* 240(2): R21–R45.

Pereira-[illegible] 2 [illegible] α [illegible] cellular replication. *Neuroendocrinology* 79(3): 119–124.

Perez-Castro, C., et al. 2012. Cellular and molecular specificity of pituitary gland physiology. *Physiological Reviews* 92(1): 1–38.

[illegible] 2 [illegible] 5 [illegible] n. [illegible] *Molecular and Cellular Endocrinology* 415: 100–113.

Portovedo, S., et al. 2019. Differential Expression of HMGA1 and HMGA2 in pituitary neuroendocrine tumors. *Molecular and Cellular Endocrinology* 490: 80–87.

Prossnitz, E.R. & Hathaway, H.J. 2015. What have we learned about GPER function from knockout mice? *J. Steroid Biochem. Mol. Biol.* 153: 114–126.

Pushpakom, S., Iorio, F. & Eyers, P.A. 2019. Drug repurposing: progress, challenges and recommendations. *Nature Reviews Drug Discovery* 18(1): 41–58.

Qin, J., et al. 2021. A comparative study of functioning and non-functioning pituitary adenomas. *Medicine* 100(14).

Quirke, V.M. 2017. Tamoxifen from Failed Contraceptive Pill to Best-Selling Breast Cancer Medicine. *Frontiers in pharmacology* 8: 620.

Raappana, A., et al. 2010. Incidence of pituitary adenomas in Northern Finland in 1992-2007. *JCE&M.*

Radandish, M., et al. 2025. In-depth insight into tumor-infiltrating stromal cells linked to TLS. *Exp. Hematol. Oncol.* 14(1): 105.

Rai, A., et al. 2021. Phosphorylated EGFR as a Novel Predictor of Recurrence in NFPA. *Frontiers in Endocrinology* 12.

[illegible] 2 [illegible] 2 2-catenin at Serine552 correlates with invasion [illegible] β of NF-PitNETs. *Acta Neuropathologica Communications* 10(1).

Rai, P.D., et al. 2020. Comparison of Various Scoring Systems for Evaluating Hormone Receptors in Carcinoma of Breast. *J. Datta Meghe Inst. Med. Sci. Univ.* 15(2).

Ramírez-Rentería, C., et al. 2012. Expression of Ki-67, PTTG1, FGFR4, and SSTR 2, 3, and 5 in NFPA. *JCE&M* 97(5): 1745–1751.

Ratnasingam, J., et al. 2017. Predictors for secondary therapy after surgical resection of NFPA. *Clinical Endocrinology* 87(6): 717–724.

Raverot, G., et al. 2017. Risk of Recurrence in PitNETs: A Prospective Study Using a Five-Tiered Classification. *JCE&M* 102(9): 3368–3374.

Raverot, G., et al. 2018. ESE Clinical Practice Guidelines for the management of aggressive pituitary tumours. *European Journal of Endocrinology* 178(1): G1–G24.

Raverot, G., et al. 2025. Revised ESE Clinical Practice Guideline for the management of aggressive pituitary tumours. *European Journal of Endocrinology* 192(6): G1–G34.

Rees, D.A., et al. 2003. Adenosine-induced IL-6 expression in pituitary FS cells via A2b receptors. *British Journal of Pharmacology* 140(4): 764–772.

Ren, Y., et al. 2022. Diagnosis of invasive NFPA using exosomal biomarkers. *Clinica Chimica Acta* 529: 25–33.

Richardson, T.E., et al. 2017. Aggressive Behavior in Silent Subtype III Pituitary Adenomas: suppression of Local Immune Response. *J. Neuropathol. Exp. Neurol.* 76(10): 874–882.

Righi, A., et al. 2017. The changing faces of corticotroph cell adenomas: role of PC 1/3. *Endocrine* 56(2): 286–297.

Rizzoli, P., et al. 2016. Headache in Patients With Pituitary Lesions: A Longitudinal Cohort Study. *Neurosurgery* 78(3): 316–323.

Rouhimoghadam, M., et al. 2018. Tamoxifen-Induced Apoptosis of MCF-7 Cells via GPR30/PI3K/MAPKs Interactions. *Frontiers in Physiology* 9: 907.

Rubinfeld, H., et al. 2024. Erythropoietin-producing hepatocellular receptor B6 in NF-PitNETs. *Molecular Biology Reports* 51(1): 297.

Rudolf, F.O. & Kadokawa, H. 2013. Expression of ER, GPR30, in bovine anterior pituitary. *Animal Reproduction Science* 139: 9–17.

Sá, S.I., et al. 2016. Induction of PR A and B by tamoxifen in hypothalamic ventromedial neurons. *Molecular and Cellular Endocrinology* 420: 1–10.

Sahakian, N., et al. 2022. Real-life clinical impact of a five-tiered classification of pituitary tumors. *European Journal of Endocrinology* 187(6): 893–904.

Sam, A.H., et al. 2015. Clinical outcomes in patients with NFPA managed conservatively. *Clinical Endocrinology* 83(6): 861–865.

Sánchez-□ □ □ □ □ □ □ □□ □ □ □ □ □□ □ □□ □ □ □2 □ □ □ □ □□ □ □ □ □ □ □ □ □ □□ □ expression. *Neuroendocrinology* 79(5): 247–258.

Sato, M., et al. 2019. Analysis of Tumor Angiogenesis and Immune Microenvironment in NF-PitNETs. *Journal of Clinical Medicine* 8(5).

Sattler, M.G.A., et al. 2015. Brain abnormalities on MRI in NFPA patients treated with or without radiotherapy. *Radiotherapy and Oncology* 114(2): 239–244.

Sav, A., et al. 2012. Biomarkers of pituitary neoplasms. *Anticancer Research* 32(11): 4639–4654.

Schmitz, V., et al. 2022. Suppression of GPER1 Enhances Anti-invasive Efficacy of β. *Anticancer Research* 42(11): 5187–5194.

Scarpetti, L., et al. 2023. Therapeutic Role of Tamoxifen for TNBC: Interaction β. *The Oncologist* 28(4): 358–363.

Scully, K.M. & Rosenfeld, M.G. 2002. Pituitary development: regulatory codes in mammalian organogenesis. *Science* 295(5563): 2231–2235.

Seilicovich, A. 2010. Cell life and death in the anterior pituitary gland: role of oestrogens. *Journal of Neuroendocrinology* 22(7): 758–764.

Serioli, S., et al. 2023. Aggressive PitNETs and Potential Target Therapies: Systematic Review.

Shannon, P., et al. 2003. Cytoscape: A Software Environment for Integrated Models of Biomolecular Interaction Networks. *Genome Research* 13: 2498–2504.

Shariq, O.A. & Lines, K.E. 2019. Epigenetic Dysregulation in Pituitary Tumors. *Int. J. Endocrine Oncology* 6(3): IJE19.

Sheehan, J.P., et al. 2012. External Beam Radiation Therapy and Stereotactic Radiosurgery for Pituitary Adenomas. *Neurosurgery Clinics of North America* 23(4): 571–586.

Sheehan, J.P., et al. 2013. Gamma Knife radiosurgery for the management of NFPA: A multicenter study. *Journal of Neurosurgery* 119(2): 446–456.

Shen, D.-W., et al. 2019. MicroRNA-543 promotes cell invasion in pituitary adenoma -catenin pathway. *Biosci. Biotechnol. Biochem.* 83(6): 1035–1044.

Shen, M., et al. 2020. Surgical Outcomes and Predictors of Visual Function Alterations After Transcranial Surgery. *World Neurosurgery* 141: e60–e69.

Shi, C., et al. 2020. BRD4 as a therapeutic target for nonfunctioning and GH pituitary adenoma. *Neuro-Oncology* 22(8): 1114–1125.

pituitary tumors. *JCE&M* 83(11): 3965–3972.

Solari, D., et al. 2019. Pituitary Adenomas: What Are the Key Features? Where Is the Future Taking Us? *World Neurosurgery* 127: 695–709.

Solarski, M., et al. 2017. Alpha subunit in clinically NFPA: An immunohistochemical study. *Pathology - Research and Practice* 213(9): 1130–1133.

Song, S., et al. 2022. Endoscopic vs. microscopic transsphenoidal surgery outcomes in 514 NFPA cases. *Neurosurgical Review* 45(3): 2375–2383.

Song, W., et al. 2018. Aberrant expression of sFRP and WIF1 genes in invasive NFPA. *Molecular and Cellular Endocrinology* 474: 168–175.

□ □ □ □ □ □□ □ □ □ □ □ □□ □ □□ □ □ □2 □ □ □ □ □□ □ □ □□ □ α □□ □ □ □ □ □ □ □□ □
pituitary tumours. *The Journal of Endocrinology* 240(2): 229–241.

Stone, J.C., et al. 2014. Estrogen and SERMs for the treatment of acromegaly: a meta-analysis. *Pituitary* 17(3): 284–295.

Szklarczyk, D., et al. 2019. STRING V11: Protein–Protein Association Networks with Increased Coverage. *Nucleic Acids Research* 47: D607–D613.

Taghavi, S.F., et al. 2023. Evaluating the expression pattern of the opioid receptor in PitNET. *Biomedicine & Pharmacotherapy* 157: 114022.

Tampourlou, M., et al. 2018. Mortality in patients with non-functioning pituitary adenoma. *Pituitary* 21(2): 203–207.

□ □ □ □ □ □□ □ □ □□ □ □ □□ □ □ □2 □ □ □ □ □□ □ □ 2 □□ □ □ □ □ □ -catenin to
promote proliferation. *Oncology Letters* 18(1): 81–86.

Taniguchi-Ponciano, K., et al. 2020. Molecular alterations in non-functioning pituitary adenomas. *Cancer Biomarkers* 28(2): 193–199.

Thodou, E., Argyrakos, T. & Kontogeorgos, G. 2007. Galectin-3 as a marker distinguishing functioning from silent corticotroph adenomas. *Hormones* 6(3): 227–232.

Treeck, O., et al. 2008. Effects of exon-□ □ □ □ □ □ □ □□ □ β □□ □ □ □ □ □ □ □ □ □□ □ □ □
apoptosis. *Breast Cancer Research and Treatment* 110(3): 507–520.

Trott, G., et al. 2019. PTTG overexpression in NFPA: Correlation with invasiveness, female gender and younger age. *Annals of diagnostic pathology* 41: 83–89.

Trouillas, J., et al. 2013. A new prognostic clinicopathological classification of pituitary adenomas. *Acta Neuropathologica* 126(1): 123–135.

Turgeon, J.L. & Waring, D.W. 2000. Progesterone regulation of the PR in rat gonadotropes. *Endocrinology* 141(9): 3422–3429.

Turlej, E., et al. 2025. Cross-Talk Between Cancer and Its Cellular Environment. *Cells* 14(6).

Vamvoukaki, R., et al. 2023. Pituitary Tumorigenesis-Implications for Management. *Medicina* 59(4).

Van Iersel, L., et al. 2019. Pathophysiology and Treatment of Hypothalamic Obesity Following Craniopharyngioma. *Endocrine Reviews* 40(1): 193–235.

Vargas, G., et al. 2015. Clinical characteristics and treatment outcome of 485 patients with NF-macroadenomas. *Int. J. Endocrinol.* 2015: 756069.

Varlamov, E.V., McCartney, S. & Fleseriu, M. 2019. Functioning Pituitary Adenomas - Treatment Options and Medical Therapies. *European Endocrinology* 15(1): 30–40.

Vasilev, V., et al. 2011. Familial pituitary tumor syndromes. *Endocrine Practice* 17(S3): 41–46.

Velázquez-Zamora, D.A., et al. 2012. Effects of SERMs on allocentric working memory performance. *Hormones and behavior* 61(4): 512–517.

Villa, C., et al. 2023. The WHO classifications of PitNETs: a clinico-pathological appraisal. *Endocrine-Related Cancer* 30(8): e230021.

Voellger, B., et al. 2021. Targeting Aggressive Pituitary Adenomas at the Molecular Level-A Review. *Journal of Clinical Medicine* 11(1).

Voltan, G., et al. 2023. Role of Estrogen and ER in GH-Secreting Adenomas. *Int. J. Mol. Sci.* 24(12).

Wang, J.-S., Wang, H.-J. & Qian, H.-L. 2018a. Biological effects of radiation on cancer cells. *Military Medical Research* 5(1): 20.

Wang, P.-F., et al. 2018b. Expression profile of PD-L1 and CD8(+) lymphocyte in pituitary adenomas. *Journal of Neuro-oncology* 139(1): 89–95.

Wang, R.-S., Maron, B.A. & Loscalzo, J. 2015. Systems medicine: evolution of systems biology from bench to bedside. *Wiley Interdiscip. Rev. Syst. Biol. Med.* 7(4): 141–161.

Wang, W., et al. 2023. Research progress on the role of the Wnt signaling pathway in pituitary adenoma. *Frontiers in Endocrinology* 14: 1216817.

Wang, X., et al. 2020. SDF-□ α □ □ □ □-134 Axis Regulates NF-PitNET Growth via Targeting VEGFA. *Frontiers in Endocrinology* 11: 566761.

Wang, Y., et al. 2014. Expression profile of D2 receptor, MGMT and VEGF in subtypes of pituitary adenomas. *J. Exp. Clin. Cancer Res.* 33(1): 56.

Wen, S., et al. 2021. Quantitative Acetylomics Revealed Acetylation-Mediated Molecular Network Changes in NF-PitNETs. *Frontiers in Endocrinology* 12.

Wen, S., Li, C. & Zhan, X. 2022. Multi-omics integration analysis revealed molecular network alterations in NF-PitNETs. *EPMA Journal* 13(1): 9–37.

Whitehead, A.L., et al. 2016. Estimating the sample size for a pilot randomised trial. *Statistical Methods in Medical Research* 25(3): 1057–1073.

Whyte, E., et al. 2023. Update on Evidence for Diagnosis and Management of NF-PitNETs. *Endocrinology and Metabolism* 38(6): 631–654.

Woo, C.S.-L., et al. 2024. A clinicopathological study of NF-PitNETs using the WHO 2022 classification. *Frontiers in Endocrinology* 15: 1368944.

Wu, H., et al. 2024. Genetic and Functional Changes in Mitochondria in the Pituitary Adenoma. *Antioxidants* 13(12).

Wu, J., et al. 2023. Identification of biomarkers associated with invasion of NF-PitNETs. *Frontiers in Endocrinology* 14.

Wu, X., et al. 2024. TNF-α [illegible] MAPK/MMP9 in pituitary adenoma. *CNS Neuroscience & Therapeutics* 30(5): e14749.

Wu, Y., et al. 2015. Low expression of sFRP 4 in aggressive pituitary adenoma. *Pituitary* 18(3): 335–342.

[illegible] 2 [illegible] -catenin [illegible] 2 [illegible] in aggressive NFPA. *Oncology Letters* 12(1): 199–206.

Wu, Z., et al. 2025. GALR1 and PENK serve as potential biomarkers in invasive NF-PitNETs. *Gene* 950.

Xiao, Z., et al. 2011. TNF-α-Induced VEGF and MMP-9 Expression Promotes Hemorrhagic Transformation.

Yamakawa, K. & Arita, J. 2004. Cross-talk between ER-, PKA-, and MAPK-signaling pathways. *J. Steroid Biochem. Mol. Biol.* 88(2): 123–130.

Yao, X., et al. 2017. Analysis of Ki67, HMGA1, MDM2, and RB expression in NFPA. *Journal of Neuro-Oncology* 132(2): 199–206.

Yavropoulou, M.P., et al. 2020. The natural history and treatment of NF-PitNETs. *Endocrine-Related Cancer* 27(10): R375–R390.

Yeung, C.-M., et al. 2006. Cells of the anterior pituitary. *The International Journal of Biochemistry & Cell Biology* 38(9): 1441–1449.

Yi, L.S., et al. 2019. Endocrinological Outcome of Endoscopic Transsphenoidal Surgery for Pituitary Adenoma. *Malaysian Journal of Medical Sciences* 26(3): 64–71.

Yin, P. & Arita, J. 2002. Proestrous surge of GnRH inhibits apoptosis of anterior pituitary cells. *Neuroendocrinology* 76(5): 272–282.

Yu, S., et al. 2018. Outcomes of endoscopic and microscopic transsphenoidal surgery: meta-analysis. *J. Cell. Mol. Med.* 22(3): 2023–2027.

[illegible] 2 [illegible] 2 5 [illegible] -MMP pathway associated [illegible] α [illegible] with invasion in null cell adenomas. *Endocrine-Related Cancer* 32(2).

Zatelli, M.C., et al. 2010. Effect of everolimus on cell viability in NFPA. *JCE&M* 95(2): 968–976.

Zavadil, J. & Böttinger, E.P. 2005. TGF-beta and EMT. *Oncogene* 24(37): 5764–5774.

Zemková, H. & Stojilkovic, S.S. 2018. Neurotransmitter receptors as signaling platforms in anterior pituitary cells. *Molecular and cellular endocrinology* 463: 49–64.

Zhan, X., Wang, X. & Cheng, T. 2016. Human Pituitary Adenoma Proteomics: New Progresses and Perspectives. *Frontiers in Endocrinology* 7: 54.

Zhang, Q., et al. 2021. Potential biomarkers of miRNA in NFPA. *World Journal of Surgical Oncology* 19(1).

Zhang, W., et al. 2022. CircVPS13C promotes pituitary adenoma growth by decreasing stability of IFITM1 mRNA. *Oncogene* 41(11): 1550–1562.

Zhang, X., et al. 2002. Loss of expression of GADD45 gamma in human pituitary adenomas. *JCE&M* 87(3): 1262–1267.

Zhang, X., et al. 2003. A Pituitary-Derived MEG3 Isoform Functions as a Growth Suppressor. *JCE&M*.

Zhao, C., □ □ □ □ □ □ -2Catenin5knocβdown inhibits pituitary adenoma cell proliferation and invasion. *International Journal of Oncology* 46(4): 1643–1650.

Zhao, H., et al. 2021. Inflammation and tumor progression: signaling pathways and targeted intervention. *Signal Transduction and Targeted Therapy* 6(1): 263.

Zheng, B., et al. 2024. The current state of MRI-based radiomics in pituitary adenoma. *Frontiers in Endocrinology* 15: 1426781.

Zheng, G., et al. 2020. Clinical Profiles of Silent Corticotroph Adenomas That Have Transformed to Functional Type. *Frontiers in Endocrinology* 11: 558593.

Zhou, K., et al. 2013. Expression and significance of E-□ □ □ □ □ □ -catenins in □β pituitary adenoma. *International journal of surgical pathology* 21(4): 363–367.

Zhou, W., et al. 2011. In NFPA, ER and slug contribute to development of invasiveness. *JCE&M* 96(8): E1237-45.

Zhu, H., et al. 2018. Association of TGF-β □ Primary/Recurrent NFPA. *World Neurosurgery* 119: e23–e31.

APPENDIX A

LIST OF STATISTICAL DATA

Table A1 Normality Z-Skewness and Z-Kurtosis

Variables	N	Skewness Statistic	Skewness Std. Error	Kurtosis Statistic	Kurtosis Std. Error	Z-Skewness	Z-Kurtosis	Normality (±2.00)
AGE	20	-0.06	0.51	-0.77	0.99	-0.12	6.34	No
AGEATDX	20	0.2	0.51	-0.65	0.99	0.39	-1.68	Yes
T0VOL2	20	0.78	0.51	0.17	0.99	1.53	0.11	Yes
T1VOL2	20	0.25	0.62	-1.23	1.19	0.4	-3.05	No
T2VOL2	20	0.16	0.51	-1.08	0.99	0.3	-3.55	No
totalchange	20	-0.66	0.51	4.43	0.99	-1.28	-3.46	No
percentchange	20	1.04	0.51	5.37	0.99	2.02	2.66	No
HSCOREA	20	4.01	0.51	16.77	0.99	7.84	2.14	No
HSCOREB	20	0.77	0.51	-1.26	0.99	1.5	-0.84	Yes
postopduration	20	1.7	0.51	2.77	0.99	3.33	0.83	No
CD40pre	20	1.88	0.51	2.21	0.99	3.68	0.6	No
HGFpre	20	2.07	0.51	5.97	0.99	4.04	1.48	No
SCFpre	20	1.91	0.51	3.43	0.99	3.73	0.92	No
TGFalphapre	20	2.76	0.51	8.71	0.99	5.39	1.61	No
FGFpre	20	0.19	0.51	-1.25	0.99	0.38	-3.28	No
TNFalphapre	20	-1.8	0.51	1.82	0.99	-3.52	-0.52	No
IL6pre	20	0.59	0.51	0.17	0.99	1.15	0.14	Yes
VEGFpre	20	1.56	0.51	2.21	0.99	3.04	0.73	No
DKK1pre	20	0.44	0.51	-0.49	0.99	0.87	-0.56	Yes
SFRP1pre	20	2.76	0.51	8.04	0.99	5.38	1.49	No
CD40post	10	0.77	0.69	-0.99	1.33	1.12	-0.89	No
HGFpost	10	-0.2	0.69	-0.16	1.33	-0.28	0.57	Yes
SCFpost	10	1.34	0.69	1.43	1.33	1.95	0.73	Yes
TGFalphapost	10	-0.86	0.69	0.45	1.33	-1.25	-0.36	Yes
FGFpost	10	2.16	0.69	5.52	1.33	3.15	1.75	No

TNFalphapost	10	0.98	0.79	2.82	1.59	1.23	2.28	No
IL6post	10	0.56	0.69	-0.8	1.33	0.81	-0.99	Yes
VEGFpost	10	1.95	0.69	4.59	1.33	2.84	1.62	No
DKK1post	10	0.28	0.69	-1.94	1.33	0.41	-4.78	No
SFRP1post	10	1.85	0.69	2.84	1.33	2.69	1.06	No
Δ □ □ □ □	10	1.77	0.69	2.66	1.33	2.58	1.03	No
Δ □ □ □	10	0.28	0.69	-1.53	1.33	0.41	-3.69	No
Δ □ □ □	10	1.49	0.69	2.28	1.33	2.16	1.05	No
Δ □ □ □ □ □ □	10	-0.73	0.69	1.44	1.33	-1.06	-1.36	Yes
Δ □ □ □	10	2.29	0.69	6.14	1.33	3.33	1.84	No
Δ □ □ □ □ □ □	10	0.87	0.79	-1.11	1.59	1.09	-1.01	Yes
Δ □ □ □	10	0.46	0.69	-0.96	1.33	0.68	-1.42	Yes
Δ □ □ □ □	10	1.96	0.69	4.86	1.33	2.86	1.70	No
Δ □ □ □ □	10	0.96	0.69	0.68	1.33	1.40	0.49	Yes
Δ □ □ □ □	10	1.88	0.69	4.83	1.33	2.74	1.76	No

Table A2 Descriptive statistics of categorical demographic, clinical, volumetric, immunohistochemical, and serum biomarker variables among NF-PitNET patients (N = 20)

Variables	Group	Frequency	Percent
STUDYARM	control	10	50.0
	tamoxifen	10	50.0
GENDER	Male	10	50.0
	Female	10	50.0
RACE	malay	17	85.0
	Chinese	3	15.0
headache	Yes	8	40.0
	No	12	60.0
visionprob	Yes	19	95.0
	No	1	5.0
hypocortisol	Yes	9	45.0
	No	11	55.0
hypogonad	Yes	6	30.0

	No	14	70.0
hypothyroid	Yes	5	25.0
	No	15	75.0
panhypopit	Yes	2	10.0
	No	18	90.0
pitapoplexy	No	20	100.0
incidental	No	20	100.0
cranialnerve	Yes	1	5.0
	No	19	95.0
preopmeds	Yes	17	85.0
	No	3	15.0
hydrocort	Yes	16	80.0
	No	4	20.0
thyroxine	Yes	10	50.0
	No	10	50.0
testoHRT	Yes	5	25.0
	No	15	75.0
minirin	No	20	100.0
postopmeds	Yes	16	80.0
	No	4	20.0
cortisol_A	Yes	11	55.0
	No	9	45.0
thyroxine_A	Yes	12	60.0
	No	8	40.0
testoHRT_A	Yes	7	35.0
	No	13	65.0
minirin_A	No	20	100.0
SUPRASELLAR	Yes	20	100.0
PARASELLAR	Yes	13	65.0
	No	7	35.0
INFRASELLAR	Yes	2	10.0
	No	18	90.0

outcome	shrinkage (volume reduction >25%)	4	20.0
	stabilization (volume change ≤ 25 %)	14	70.0
	regrowth (volume increment > 25%)	2	10.0
ERalpha	present	3	15.0
	absent	17	85.0
ERbeta	present	10	50.0
	absent	10	50.0
SUBTYPES	null cell adenoma	8	40.0
	silent gonadotroph tumor	9	45.0
	silent corticotroph tumor	2	10.0
	plurihormonal tumor	1	5.0
repeatop	Yes	9	45.0
	No	11	55.0
	Total	20	100.0

TABLE A3 Descriptive statistics of continuous demographic, clinical, volumetric, immunohistochemical and serum biomarker variables among Nf-PitNET patients (N = 20)

Variables	N	Mean	Median	Std. Deviation	Minimum	Maximum	Percentiles 25	Percentiles 75	IQR
AGE	20	53.60	54.50	10.99	32.00	72.00	45.25	61.50	16.25
AGEATDX	20	48.85	48.00	10.29	32.00	66.00	40.50	57.00	16.50
T0VOL2	20	2.07	2.01	1.40	0.38	5.51	0.77	2.95	2.18
T1VOL2	20	2.47	2.65	1.61	0.53	4.89	0.65	3.94	3.30
T2VOL2	20	2.13	2.45	1.46	0.17	4.89	0.56	3.16	2.60
totalchange	20	0.06	0.03	0.80	-2.28	1.98	-0.17	0.41	0.58
percentchange	20	2.12	4.67	40.08	-86.29	127.74	-18.04	14.75	32.79
HSCOREA	20	2.75	0.00	9.10	0.00	40.00	0.00	0.00	0.00
HSCOREB	20	91.25	5.00	118.36	0.00	300.00	0.00	227.50	227.50
postopduration	20	27.95	24.00	16.13	13.00	75.00	15.25	34.75	19.50
CD40pre	20	2107.51	437.05	3372.95	75.30	10518.26	183.23	2373.42	2190.19

HGFpre	20	2739.63	2316.51	1803.29	858.23	8777.76	1455.62	3456.01	2000.39
SCFpre	20	71.94	62.59	47.12	29.44	195.20	36.01	77.18	41.17
TGFalphapre	20	6.10	3.65	6.62	1.17	29.79	2.03	6.51	4.48
FGFpre	20	10.34	10.73	7.34	2.05	23.83	2.05	16.35	14.30
TNFalphapre	20	44.65	49.73	11.16	15.48	53.16	49.73	49.73	0.00
IL6pre	20	61.11	53.98	18.89	24.40	100.36	49.12	68.24	19.12
VEGFpre	20	334.30	271.73	281.41	56.39	1117.59	130.39	447.48	317.09
DKK1pre	20	4447.85	4271.50	2464.28	455.00	9428.00	2166.00	6161.50	3995.50
SFRP1pre	20	97.96	54.78	105.19	34.75	466.90	46.15	80.33	34.18
Δ □□□□□	10	357.20	-73.60	1244.47	-932.70	3220.64	-254.24	555.37	809.62
Δ □□□	10	-237.28	-266.68	892.32	-1238.08	1109.36	-1085.54	484.69	1570.23
Δ □□□	10	5.96	-9.16	38.90	-32.70	95.32	-20.21	26.35	46.57
Δ □□□□□□□	10	-0.55	-1.20	3.89	-8.82	5.12	-2.15	3.02	5.17
Δ □□□	10	4.10	0.00	19.32	-12.49	54.67	-7.82	8.05	15.88
Δ □□□□□□□	10	-25.68	-27.81	10.30	-34.25	-10.10	-34.25	-12.72	21.53
Δ □□□	10	5.60	0.00	18.31	-18.19	34.37	-9.49	23.56	33.04
Δ □□□□□	10	121.36	25.73	404.22	-316.01	1139.25	-109.98	263.14	373.11
Δ □□□□□	10	-431.00	-805.00	2250.40	-2936.00	4281.00	-2469.50	1210.25	3679.75
Δ □□□□□	10	13.30	9.40	38.57	-27.28	110.10	-12.32	23.16	35.48

Table A4 Crosstabulation of baseline categorical demographic and clinical characteristics between control and tamoxifen-□□□□□□□□□□□□□□□□□□□□□□□□□□□□□’ □□□

		STUDYARM		Total	Fisher's Exact Test
Variables	Groups	Control (N=10)	Tamoxifen (N=10)		*p*
GENDER	Male	5	5	10	1.000
	Female	5	5	10	
RACE	Malay	9	8	17	1.000
	Chinese	1	2	3	
headache	Yes	4	4	8	1.000
	No	6	6	12	

visionprob	Yes	10	9	19	1.000
	No	0	1	1	
hypocortisol	Yes	5	4	9	1.000
	No	5	6	11	
hypogonad	Yes	3	3	6	1.000
	No	7	7	14	
hypothyroid	Yes	4	1	5	0.303
	No	6	9	15	
panhypopit	Yes	2	0	2	0.474
	No	8	10	18	
pitapoplexy	No	10	10	20	
incidental	No	10	10	20	
cranialnerve	Yes	1	0	1	1.000
	No	9	10	19	
PREOPMEDS	Yes	8	9	17	1.000
	No	2	1	3	
hydrocort	Yes	8	8	16	1.000
	No	2	2	4	
thyroxine	Yes	5	5	10	1.000
	No	5	5	10	
testoHRT	Yes	2	3	5	1.000
	No	8	7	15	
minirin	No	10	10	20	
postopmeds	Yes	7	9	16	0.582
	No	3	1	4	
cortisol_A	Yes	4	7	11	0.370
	No	6	3	9	
thyroxine_A	Yes	5	7	12	0.650
	No	5	3	8	
testoHRT_A	Yes	4	3	7	1.000
	No	6	7	13	

minirin_A	No	10	10	20	
SUPRASELLAR	Yes	10	10	20	
PARASELLAR	Yes	6	7	13	1.000
	No	4	3	7	
INFRASELLAR	Yes	0	2	2	0.474
	No	10	8	18	
outcome	shrinkage (volume reduction >25%)	0	4	4	0.014*
	stabilization (volume change ≤ 2 5 %)	8	6	14	
	regrowth (volume increment > 25%)	2	0	2	
ERalpha	present	2	1	3	1.000
	absent	8	9	17	
ERbeta	present	6	4	10	0.656
	absent	4	6	10	
SUBTYPES	null cell adenoma	3	5	8	0.189
	silent gonadotroph tumor	4	5	9	
	silent corticotroph tumor	2	0	2	
	plurihormonal tumor	1	0	1	
repeatop	Yes	5	4	9	1.000
	No	5	6	11	

Table A5 Comparison of continuous baseline and pre-treatment parameters between control and tamoxifen groups using independent-sample t-test (N = 20).

	STUDYARM						
	Control (N=10)		tamoxifen (N=10)				Mean Difference
Variables	Mean	Std. Deviation	Mean	Std. Deviation	t	*p*	
AGE	54.80	11.03	52.40	11.39	0.48	0.638	2.40
AGEATDX	49.40	11.21	48.30	9.87	0.23	0.818	1.10
T0VOL2	2.24	1.31	1.90	1.54	0.53	0.602	0.34

T1VOL2	2.72	1.72	2.18	1.59	0.59	0.566	0.55
T2VOL2	2.60	1.54	1.66	1.27	1.49	0.153	0.94
totalchange	0.36	0.68	-0.25	0.84	1.77	0.094	0.60
percentchange	16.66	41.31	-12.42	34.85	1.70	0.106	29.08
HSCOREA	1.50	3.37	4.00	12.65	-0.60	0.553	-2.50
HSCOREB	94.50	127.55	88.00	115.26	0.12	0.906	6.50
postopduration	24.00	11.31	31.90	19.66	-1.10	0.285	-7.90
CD40pre	3419.29	4371.37	795.74	1041.55	1.85	0.081	2623.55
HGFpre	3084.24	2305.49	2395.02	1133.96	0.85	0.407	689.22
SCFpre	83.07	60.61	60.82	27.19	1.06	0.304	22.24
TGFalphapre	6.44	8.78	5.76	3.89	0.22	0.825	0.68
FGFpre	9.04	8.02	11.65	6.75	-0.79	0.441	-2.61
TNFalphapre	46.65	11.00	42.64	11.54	0.79	0.437	4.01
IL6pre	53.71	17.17	68.51	18.36	-1.86	0.079	-14.80
VEGFpre	384.72	373.04	283.88	149.57	0.79	0.438	100.84
DKK1pre	5155.10	2861.38	3740.60	1876.45	1.31	0.208	1414.50
SFRP1pre	75.14	70.96	120.77	131.03	-0.97	0.346	-45.63

TABLE A6 NON-PARAMETRIC COMPARISON OF CONTINUOUS CLINICAL, VOLUMETRIC, AND BIOCHEMICAL PARAMETERS BETWEEN CONTROL AND TAMOXIFEN GROUPS USING MANN–WHITNEY U TEST (N = 20).

			Percentiles							
Variables	STUDYARM	N	50th (Median)	25th	75th	IQR	Mean Rank	Sum of Ranks	Mann-Whitney U	*p*
AGE	control	10	57.00	44.00	63.25	19.25	10.95	109.50	45.50	0.733
	tamoxifen / intervention group	10	52.00	45.50	61.50	16.00	10.05	100.50		
AGEATDX	control	10	48.00	39.75	59.75	20.00	10.65	106.50	48.50	0.910
	tamoxifen / intervention group	10	47.50	41.25	55.25	14.00	10.35	103.50		
T0VOL2	control	10	2.18	0.90	3.54	2.65	11.50	115.00	40.00	0.450

	tamoxifen / intervention group	10	1.58	0.72	2.63	1.91	9.50	95.00		
T1VOL2	control	10	2.89	0.63	4.58	3.95	7.71	54.00	16.00	0.475
	tamoxifen / intervention group	10	2.18	0.63	3.23	2.60	6.17	37.00		
T2VOL2	control	10	2.74	0.93	3.77	2.84	12.70	127.00	28.00	0.096
	tamoxifen / intervention group	10	1.64	0.40	2.91	2.51	8.30	83.00		
totalchange	control	10	0.03	-0.08	0.58	0.67	11.85	118.50	36.50	0.307
	tamoxifen / intervention group	10	0.06	-0.44	0.27	0.71	9.15	91.50		
percentchange	control	10	3.20	-0.71	21.58	22.29	11.50	115.00	40.00	0.450
	tamoxifen / intervention group	10	5.32	-38.17	12.24	50.41	9.50	95.00		
HSCOREA	control	10	0.00	0.00	1.25	1.25	10.90	109.00	46.00	0.627
	tamoxifen / intervention group	10	0.00	0.00	0.00	0.00	10.10	101.00		
HSCOREB	control	10	25.00	0.00	240.00	240.00	11.20	112.00	43.00	0.571
	tamoxifen / intervention group	10	0.00	0.00	232.50	232.50	9.80	98.00		
postopduration	control	10	24.00	15.75	24.25	8.50	9.90	99.00	44.00	0.648
	tamoxifen / intervention group	10	27.00	15.00	42.25	27.25	11.10	111.00		
CD40pre	control	10	1192.41	220.55	9069.32	8848.77	11.65	116.50	38.50	0.384
	tamoxifen / intervention group	10	353.28	175.45	1056.84	881.39	9.35	93.50		
HGFpre	control	10	2879.47	1117.51	3773.89	2656.38	11.10	111.00	44.00	0.650
	tamoxifen / intervention group	10	1899.74	1497.68	3447.97	1950.29	9.90	99.00		
SCFpre	control	10	62.74	49.66	103.20	53.54	10.80	108.00	47.00	0.821
	tamoxifen / intervention group	10	62.59	34.29	82.46	48.18	10.20	102.00		
TGFalphapre	control	10	2.57	1.80	7.39	5.59	8.90	89.00	34.00	0.225

	tamoxifen / intervention group	10	3.95	3.48	7.18	3.70	12.10	121.00		
FGFpre	control	10	7.20	2.05	15.17	13.11	9.40	94.00	39.00	0.394
	tamoxifen / intervention group	10	11.82	6.74	17.56	10.82	11.60	116.00		
TNFalphapre	control	10	49.73	49.73	49.73	0.00	11.70	117.00	38.00	0.233
	tamoxifen / intervention group	10	49.73	28.20	49.73	21.53	9.30	93.00		
IL6pre	control	10	49.12	49.12	60.96	11.84	8.05	80.50	25.50	0.052
	tamoxifen / intervention group	10	67.32	49.12	84.92	35.80	12.95	129.50		
VEGFpre	control	10	196.94	127.98	731.14	603.16	10.30	103.00	48.00	0.880
	tamoxifen / intervention group	10	290.23	152.10	385.50	233.40	10.70	107.00		
DKK1pre	control	10	5063.00	2101.00	8033.25	5932.25	11.70	117.00	38.00	0.364
	tamoxifen / intervention group	10	4199.00	2134.75	4912.00	2777.25	9.30	93.00		
SFRP1pre	control	10	52.16	43.23	73.24	30.02	8.60	86.00	31.00	0.151
	tamoxifen / intervention group	10	64.65	52.01	162.90	110.90	12.40	124.00		

Table A7 a) Mean Tumour Volumes at Baseline, 6 Months, and 12 Months by Study Arm

Variables	STUDYARM	N	Mean	Std. Deviation
T0VOL2	control	10	2.24	1.31
	tamoxifen / intervention group	10	1.90	1.54
T1VOL2	control	10	2.76	1.40
	tamoxifen / intervention group	10	2.19	1.18
T2VOL2	control	10	2.60	1.54
	tamoxifen / intervention group	10	1.66	1.27

b) Multivariate Tests of Time and Time × Study Arm Effects on Tumour Volume (RM- GLM)

Effect		Value	F	Hypothesis df	*p*	Partial Eta Squared	Noncent. Parameter	Observed Power[c]
Time	Pillai's Trace	0.23	2.495[b]	2.00	0.112	0.23	4.99	0.43
	Wilks' Lambda	0.77	2.495[b]	2.00	0.112	0.23	4.99	0.43
	Hotelling's Trace	0.29	2.495[b]	2.00	0.112	0.23	4.99	0.43
	Roy's Largest Root	0.29	2.495[b]	2.00	0.112	0.23	4.99	0.43
Time * STUDYARM	Pillai's Trace	0.15	1.505[b]	2.00	0.250	0.15	3.01	0.28
	Wilks' Lambda	0.85	1.505[b]	2.00	0.250	0.15	3.01	0.28
	Hotelling's Trace	0.18	1.505[b]	2.00	0.250	0.15	3.01	0.28
	Roy's Largest Root	0.18	1.505[b]	2.00	0.250	0.15	3.01	0.28

c) Mauchly's Test of Sphericity

Within Subjects Effect	Mauchly's W	Approx. Chi-Square	*p*	Greenhouse-Geisser	Huynh-Feldt	Lower-bound
Time	0.991	0.16	0.920	0.99	1.000	0.50

d) Tests of Within-Subjects Effects

Source		Type III Sum of Squares	Mean Square	F	*p*	Partial Eta Squared	Noncent. Parameter	Observed Power[a]
Time	Sphericity Assumed	1.86	0.93	2.89	0.069	0.14	5.78	0.53
	Greenhouse-Geisser	1.86	0.94	2.89	0.069	0.14	5.72	0.53
	Huynh-Feldt	1.86	0.93	2.89	0.069	0.14	5.78	0.53
	Lower-bound	1.86	1.86	2.89	0.106	0.14	2.89	0.36
Time * STUDYARM	Sphericity Assumed	0.93	0.47	1.44	0.249	0.07	2.89	0.29
	Greenhouse-Geisser	0.93	0.47	1.44	0.249	0.07	2.86	0.29
	Huynh-Feldt	0.93	0.47	1.44	0.249	0.07	2.89	0.29
	Lower-bound	0.93	0.93	1.44	0.245	0.07	1.44	0.21

e) Tests of Within-Subjects Contrasts

Source		Type III Sum of Squares	Mean Square	F	*p*	Partial Eta Squared	Noncent. Parameter	Observed Power[a]
Time	Level 1 vs. Level 2	3.17	3.17	4.69	0.044	0.21	4.69	0.54
	Level 2 vs. Level 3	2.35	2.35	3.49	0.078	0.16	3.49	0.42
Time * STUDYARM	Level 1 vs. Level 2	0.26	0.26	0.38	0.543	0.02	0.38	0.09
	Level 2 vs. Level 3	0.71	0.71	1.05	0.320	0.05	1.05	0.16

Table A8 ANOVA by Treatment Outcome

Variables	Outcome	N	Mean	Std. Deviation	95% Confidence Interval for Mean Lower Bound	95% Confidence Interval for Mean Upper Bound	F	*p*
AGE	shrinkage (volume reduction >25%)	4	49.75	15.63	24.88	74.62	0.323	0.729
	stabilization (volume □ □ □ □ □ □ □ ≤ 2 5 %	14	54.86	10.24	48.94	60.77		
	regrowth (volume increment > 25%)	2	52.50	10.61	-42.80	147.80		
AGEATDX	shrinkage (volume reduction >25%)	4	46.25	14.29	23.51	68.99	0.185	0.832
	stabilization (volume □ □ □ □ □ □ □ ≤ 2 5 %	14	49.21	9.89	43.50	54.93		
	regrowth (volume increment > 25%)	2	51.50	9.19	-31.09	134.09		
T0VOL2	shrinkage (volume reduction >25%)	4	2.03	2.34	-1.69	5.75	0.194	0.825
	stabilization (volume □ □ □ □ □ □ □ ≤ 2 5 %	14	2.00	1.17	1.32	2.67		
	regrowth (volume increment > 25%)	2	2.69	1.61	-11.74	17.11		
T1VOL2	shrinkage (volume reduction >25%)	4	2.04	1.98	-1.12	5.20	1.522	0.247
	stabilization (volume □ □ □ □ □ □ □ ≤ 2 5 %	14	2.39	1.01	1.81	2.98		
	regrowth (volume increment > 25%)	2	3.89	1.41	-8.82	16.60		
T2VOL2	shrinkage (volume reduction >25%)	4	1.08	1.44	-1.21	3.37	4.062	0.036*

	stabilization (volume □□□□□□≤25%	14	2.13	1.25	1.41	2.85		
	regrowth (volume increment > 25%)	2	4.21	0.96	-4.43	12.85		
totalchange	shrinkage (volume reduction >25%)	4	-0.95	0.97	-2.50	0.60	18.625	0.001*
	stabilization (volume □□□□□□≤25%	14	0.13	0.22	0.01	0.26		
	regrowth (volume increment > 25%)	2	1.53	0.64	-4.26	7.31		
percentchange	shrinkage (volume reduction >25%)	4	-48.53	25.67	-89.37	-7.68	21.675	0.001*
	stabilization (volume □□□□□□≤25%	14	5.77	11.26	-0.73	12.27		
	regrowth (volume increment > 25%)	2	77.88	70.52	-555.72	711.47		
HSCOREA	shrinkage (volume reduction >25%)	4	10.00	20.00	-21.82	41.82	1.720	0.209
	stabilization (volume □□□□□□≤25%	14	1.07	2.89	-0.60	2.74		
	regrowth (volume increment > 25%)	2	0.00	0.00	0.00	0.00		
HSCOREB	shrinkage (volume reduction >25%)	4	102.50	121.76	-91.24	296.24	0.563	0.580
	stabilization (volume □□□□□□≤25%	14	100.36	125.61	27.83	172.88		
	regrowth (volume increment > 25%)	2	5.00	7.07	-58.53	68.53		
postopduration	shrinkage (volume reduction >25%)	4	26.25	10.81	9.04	43.46	0.277	0.761
	stabilization (volume □□□□□□≤25%	14	29.50	18.39	18.88	40.12		
	regrowth (volume increment > 25%)	2	20.50	6.36	-36.68	77.68		
CD40pre	shrinkage (volume reduction >25%)	4	355.88	153.43	111.74	600.02	1.205	0.324
	stabilization (volume □□□□□□≤25%	14	2225.13	3337.99	297.83	4152.42		
	regrowth (volume increment > 25%)	2	4787.48	6664.03	-55086.43	64661.38		
HGFpre	shrinkage (volume reduction >25%)	4	1964.33	214.45	1623.10	2305.56	0.515	0.606
	stabilization (volume □□□□□□≤25%	14	3001.90	2019.56	1835.84	4167.95		

	regrowth (volume increment > 25%)	2	2454.40	2257.31	-17826.76	22735.55		
SCFpre	shrinkage (volume reduction >25%)	4	61.59	29.15	15.21	107.97	1.076	0.363
	stabilization (volume □ □ □ □ □ □ ≤ 2 5 %	14	80.66	51.80	50.75	110.57		
	regrowth (volume increment > 25%)	2	31.64	3.11	3.66	59.62		
TGFalphapre	shrinkage (volume reduction >25%)	4	4.09	1.28	2.06	6.12	0.213	0.810
	stabilization (volume □ □ □ □ □ □ ≤ 2 5 %	14	6.65	7.62	2.25	11.05		
	regrowth (volume increment > 25%)	2	6.28	7.23	-58.67	71.22		
FGFpre	shrinkage (volume reduction >25%)	4	14.99	4.39	8.00	21.98	1.022	0.381
	stabilization (volume □ □ □ □ □ □ ≤ 2 5 %	14	9.31	7.73	4.84	13.77		
	regrowth (volume increment > 25%)	2	8.30	8.83	-71.03	87.63		
TNFalphapre	shrinkage (volume reduction >25%)	4	42.78	13.90	20.65	64.90	0.244	0.786
	stabilization (volume □ □ □ □ □ □ ≤ 2 5 %	14	44.45	11.51	37.81	51.10		
	regrowth (volume increment > 25%)	2	49.73	0.00	49.73	49.73		
IL6pre	shrinkage (volume reduction >25%)	4	75.38	15.30	51.03	99.73	1.790	0.197
	stabilization (volume □ □ □ □ □ □ ≤ 2 5 %	14	58.75	19.42	47.54	69.96		
	regrowth (volume increment > 25%)	2	49.12	0.00	49.12	49.12		
VEGFpre	shrinkage (volume reduction >25%)	4	320.85	127.16	118.51	523.20	0.218	0.807
	stabilization (volume □ □ □ □ □ □ ≤ 2 5 %	14	319.58	289.01	152.71	486.44		
	regrowth (volume increment > 25%)	2	464.26	576.83	-4718.33	5646.86		
DKK1pre	shrinkage (volume reduction >25%)	4	3093.25	1407.02	854.37	5332.13	0.814	0.460
	stabilization (volume □ □ □ □ □ □ ≤ 2 5 %	14	4876.43	2645.24	3349.11	6403.74		
	regrowth (volume increment > 25%)	2	4157.00	2897.72	-21878.01	30192.01		

SFRP1pre	shrinkage (volume reduction >25%)	4	113.71	67.05	7.03	220.39	0.399	0.677
	stabilization (volume □ □ □ □ □ □ ≤ 2 5 %	14	85.47	110.58	21.62	149.31		
	regrowth (volume increment > 25%)	2	153.88	168.47	-1359.75	1667.50		

*Signifikan p <0.05

Table A9 ANOVA by Tumour Subtypes

					95% Confidence Interval for Mean			
Variables	SUBTYPES	N	Mean	Std. Deviation	Lower Bound	Upper Bound	F	p
AGE	null cell adenoma	8	49.00	9.38	41.16	56.84	2.69	0.081
	silent gonadotroph tumor	9	55.11	10.58	46.98	63.24		
	silent corticotroph tumor	2	69.50	3.54	37.73	101.27		
	plurihormonal tumor	1	45.00					
AGEATDX	null cell adenoma	8	43.38	8.33	36.41	50.34	3.76	0.032*
	silent gonadotroph tumor	9	50.44	9.32	43.28	57.60		
	silent corticotroph tumor	2	65.50	0.71	59.15	71.85		
	plurihormonal tumor	1	45.00					
T0VOL2	null cell adenoma	8	2.30	1.85	0.75	3.84	0.70	0.567
	silent gonadotroph tumor	9	2.22	1.07	1.40	3.04		
	silent corticotroph tumor	2	0.76	0.31	-2.04	3.56		
	plurihormonal tumor	1	1.55					

T1VOL2	null cell adenoma	8	2.58	1.55	1.29	3.87	0.28	0.836
	silent gonadotroph tumor	9	2.51	1.20	1.59	3.43		
	silent corticotroph tumor	2	1.66	1.48	-11.62	14.93		
	plurihormonal tumor	1	2.89					
T2VOL2	null cell adenoma	8	1.97	1.62	0.61	3.32	1.11	0.374
	silent gonadotroph tumor	9	2.43	1.36	1.38	3.48		
	silent corticotroph tumor	2	0.72	0.42	-3.09	4.53		
	plurihormonal tumor	1	3.53					
totalchange	null cell adenoma	8	-0.33	0.90	-1.09	0.42	3.82	0.031*
	silent gonadotroph tumor	9	0.21	0.43	-0.12	0.53		
	silent corticotroph tumor	2	-0.04	0.11	-1.06	0.98		
	plurihormonal tumor	1	1.98					
percentchange	null cell adenoma	8	-11.14	34.84	-40.26	17.99	7.11	0.003*
	silent gonadotroph tumor	9	2.43	23.03	-15.27	20.13		
	silent corticotroph tumor	2	-9.07	18.60	-176.16	158.02		
	plurihormonal tumor	1	127.74					
HSCOREA	null cell adenoma	8	0.00	0.00	0.00	0.00	0.71	0.560
	silent gonadotroph tumor	9	6.11	13.18	-4.02	16.24		

	silent corticotroph tumor	2	0.00	0.00	0.00	0.00		
	plurihormonal tumor	1	0.00					
HSCOREB	null cell adenoma	8	135.00	146.09	12.86	257.14	0.73	0.550
	silent gonadotroph tumor	9	74.44	101.26	-3.39	152.28		
	silent corticotroph tumor	2	37.50	53.03	-438.98	513.98		
	plurihormonal tumor	1	0.00					
postopduration	null cell adenoma	8	29.88	19.66	13.44	46.31	0.39	0.763
	silent gonadotroph tumor	9	29.44	15.26	17.72	41.17		
	silent corticotroph tumor	2	19.50	6.36	-37.68	76.68		
	plurihormonal tumor	1	16.00	-				
CD40pre	null cell adenoma	8	3278.50	4138.77	-181.60	6738.59	3.95	0.028*
	silent gonadotroph tumor	9	458.56	580.88	12.05	905.06		
	silent corticotroph tumor	2	1147.81	1275.42	-10311.38	12607.00		
	plurihormonal tumor	1	9499.65					
HGFpre	null cell adenoma	8	2528.06	1079.94	1625.21	3430.91	0.42	0.741
	silent gonadotroph tumor	9	2995.24	2460.65	1103.81	4886.66		
	silent corticotroph tumor	2	1780.23	823.06	-5614.64	9175.09		
	plurihormonal tumor	1	4050.56					
SCFpre	null cell adenoma	8	65.98	25.54	44.63	87.33	0.49	0.696

	silent gonadotroph tumor	9	84.51	65.28	34.33	134.68		
	silent corticotroph tumor	2	58.31	1.73	42.73	73.88		
	plurihormonal tumor	1	33.84					
TGFalphapre	null cell adenoma	8	5.41	1.84	3.87	6.95	0.55	0.658
	silent gonadotroph tumor	9	7.08	9.56	-0.28	14.43		
	silent corticotroph tumor	2	1.80	0.00	1.80	1.80		
	plurihormonal tumor	1	11.39					
FGFpre	null cell adenoma	8	9.41	6.80	3.72	15.10	0.91	0.457
	silent gonadotroph tumor	9	12.80	7.88	6.74	18.85		
	silent corticotroph tumor	2	7.20	7.28	-58.20	72.61		
	plurihormonal tumor	1	2.05					
TNFalphapre	null cell adenoma	8	40.87	12.38	30.52	51.22	2.23	0.124
	silent gonadotroph tumor	9	50.11	1.14	49.23	50.99		
	silent corticotroph tumor	2	32.60	24.22	-184.99	250.20		
	plurihormonal tumor	1	49.73					
IL6pre	null cell adenoma	8	55.03	19.64	38.61	71.45	1.54	0.242
	silent gonadotroph tumor	9	70.52	17.88	56.77	84.26		
	silent corticotroph tumor	2	49.12	0.00	49.12	49.12		
	plurihormonal tumor	1	49.12					

VEGFpre	null cell adenoma	8	323.94	223.88	136.77	511.11	1.76	0.195
	silent gonadotroph tumor	9	329.05	312.30	89.00	569.10		
	silent corticotroph tumor	2	130.41	0.03	130.16	130.67		
	plurihormonal tumor	1	872.14					
DKK1pre	null cell adenoma	8	3828.25	2510.26	1729.62	5926.88	0.72	0.554
	silent gonadotroph tumor	9	5105.22	2633.69	3080.79	7129.66		
	silent corticotroph tumor	2	3089.00	1426.94	-9731.56	15909.56		
	plurihormonal tumor	1	6206.00					
SFRP1pre	null cell adenoma	8	128.14	143.90	7.84	248.44	0.49	0.696
	silent gonadotroph tumor	9	90.09	77.13	30.80	149.38		
	silent corticotroph tumor	2	44.20	9.20	-38.46	126.85		
	plurihormonal tumor	1	34.75					

*Significant, p <0.05

Table A10 ANOVA Post Hoc Test by Outcome

Dependent Variable	I	J	Mean Difference (I-J)	*P*	95% Confidence Interval	
					Lower Bound	Upper Bound
T2VOL2	shrinkage (volume reduction >25%)	regrowth (volume increment > 25%)	-3.13	0.011	-5.45	-0.81
	stabilization (volume change ≤ 2 5 %)	regrowth (volume increment > 25%)	-2.08	0.044	-4.1	-0.06

totalchange	shrinkage (volume reduction >25%)	stabilization (volume change ≤ 2 5 %)	-1.08	0.001	-1.65	-0.51
		regrowth (volume increment > 25%)	-2.48	0	-3.35	-1.6
	stabilization (volume change ≤ 2 5 %)	regrowth (volume increment > 25%)	-1.39	0.001	-2.15	-0.63
percentchange	shrinkage (volume reduction >25%)	stabilization (volume change ≤ 2 5 %)	-54.29	0.001	-81.19	-27.39
		regrowth (volume increment > 25%)	-126.40	0	-167.49	-85.31
	stabilization (volume change ≤ 2 5 %)	regrowth (volume increment > 25%)	-72.11	0.001	-107.97	-36.24

Table A11 Comparison between shrinkage and stabilisation in the tamoxifen group using independent-sample t-test (N = 20)

	shrinkage (volume reduction >25%) N=4		stabilization (volume □ □ □ □ □ □ □ ≤ 2 N=6				95% Confidence Interval of the Difference		
Variables	Mean	Std. Deviation	Mean	Std. Deviation	t	*p*	Mean Difference	Lower	Upper
AGE	49.75	15.63	54.17	8.82	-0.58	0.579	-4.42	-22.04	13.21
AGEATDX	46.25	14.29	49.67	6.86	-0.51	0.621	-3.42	-18.74	11.91
T0VOL2	2.03	2.34	1.82	0.99	0.20	0.846	0.21	-2.22	2.64
T1VOL2	2.04	1.98	2.29	0.36	-0.30	0.769	-0.25	-2.10	1.61
T2VOL2	1.08	1.44	2.04	1.10	-1.20	0.265	-0.96	-2.81	0.89
totalchange	-0.95	0.97	0.22	0.18	-2.97	0.018*	-1.17	-2.08	-0.26
percentchange	-48.53	25.67	11.65	7.30	-5.57	0.001*	-60.17	-85.09	-35.25
HSCOREA	10.00	20.00	0.00	0.00	1.26	0.242	10.00	-8.23	28.23
HSCOREB	102.50	121.76	78.33	121.39	0.31	0.766	24.17	-156.73	205.07

postopduration	26.25	10.81	35.67	24.15	-0.72	0.491	-9.42	-39.49	20.66
CD40pre	355.88	153.43	1088.98	1296.38	-1.10	0.302	-733.09	-2265.03	798.85
HGFpre	1964.33	214.45	2682.15	1428.16	-0.98	0.357	-717.82	-2409.78	974.14
SCFpre	61.59	29.15	60.31	28.64	0.07	0.947	1.29	-41.63	44.20
TGFalphapre	4.09	1.28	6.87	4.75	-1.12	0.295	-2.77	-8.49	2.94
FGFpre	14.99	4.39	9.42	7.46	1.33	0.220	5.57	-4.07	15.22
TNFalphapre	42.78	13.90	42.55	11.12	0.03	0.978	0.23	-17.99	18.44
IL6pre	75.38	15.30	63.93	20.09	0.96	0.364	11.45	-16.00	38.90
VEGFpre	320.85	127.16	259.23	169.54	0.62	0.555	61.62	-169.11	292.36
DKK1pre	3093.25	1407.02	4172.17	2142.74	-0.88	0.405	-1078.92	-3907.88	1750.05
SFRP1pre	113.71	67.05	125.48	167.75	-0.13	0.899	-11.77	-218.42	194.88
CD40post	1009.96	1596.30	1248.26	1071.60	-0.29	0.783	-238.29	-2163.77	1687.18
HGFpost	2090.31	1091.41	2202.69	989.16	-0.17	0.870	-112.38	-1643.61	1418.85
SCFpost	63.35	40.86	69.08	46.50	-0.20	0.847	-5.73	-71.92	60.46
TGFalphapost	5.53	2.15	4.99	2.07	0.39	0.704	0.53	-2.59	3.66
FGFpost	14.21	7.30	16.77	20.53	-0.24	0.819	-2.56	-27.62	22.49
TNFalphapost	23.53	13.94	13.67	8.47	1.17	0.293	9.86	-11.72	31.44
IL6post	80.77	11.14	69.67	32.50	0.65	0.536	11.10	-28.48	50.67
VEGFpost	457.27	571.88	370.55	193.62	0.35	0.734	86.72	-482.19	655.63
DKK1post	2363.40	2385.41	3940.40	2488.82	-1.00	0.348	-1577.00	-5224.70	2070.70
SFRP1post	146.60	117.18	125.72	171.58	0.21	0.838	20.88	-207.54	249.31
Δ □ □ □ □	654.08	1713.29	159.28	953.37	0.59	0.569	494.80	-1428.12	2417.72
Δ □ □ □	125.98	983.30	-479.46	822.90	1.06	0.321	605.44	-714.07	1924.94
Δ □ □ □	1.75	32.00	8.77	45.67	-0.26	0.798	-7.02	-68.16	54.13
Δ □ □ □ □ □ □ □ □ [	1.43	3.17	-1.87	4.00	1.38	0.205	3.31	-2.22	8.83
Δ □ □ □	-0.78	9.32	7.35	24.25	-0.63	0.546	-8.13	-37.91	21.65
Δ □ □ □ □ □ □ □ □ [	-26.20	13.94	-25.29	9.05	-0.11	0.920	-0.91	-23.03	21.21
Δ □ □ □	5.39	21.91	5.74	17.77	-0.03	0.978	-0.35	-29.26	28.56
Δ □ □ □ □	136.42	675.40	111.32	141.82	0.09	0.930	25.10	-612.76	662.96
Δ □ □ □ □	-729.85	3371.86	-231.77	1474.79	-0.33	0.753	-498.08	-4027.76	3031.60
Δ □ □ □ □	32.89	53.67	0.24	20.92	1.37	0.206	32.65	-22.11	87.42

*Siognificant, p <0.05

Table A12 Spearman Correlation Analysis of Clinical and Biomarker Variables with Baseline (T0VOL2) and Final Tumour Volume (T2VOL2) in the Control Group

	Independent variable			
	T0VOL2		T2VOL2	
	r	*P*	r	*P*
T0VOL2	1.000		.855**	0.002
T2VOL2	.855**	0.002	1.000	
AGE	-0.365	0.300	-0.413	0.235
AGEATDX	-0.200	0.580	-0.164	0.651
T1VOL2	.855**	0.002	.927**	0.000
totalchange	0.248	0.489	0.576	0.082
percentchange	0.297	0.405	.648*	0.043
HSCOREA	0.277	0.439	0.026	0.943
HSCOREB	-0.013	0.973	-0.226	0.530
postopduration	0.389	0.267	0.307	0.388
CD40pre	-0.382	0.276	-0.212	0.556
HGFpre	-0.382	0.276	-0.248	0.489
SCFpre	-0.091	0.803	-0.406	0.244
TGFalphapre	-0.244	0.497	-0.075	0.837
FGFpre	0.376	0.284	0.318	0.371
TNFalphapre	0.156	0.668	0.156	0.668
IL6pre	0.348	0.324	0.178	0.624
VEGFpre	-0.498	0.143	-0.359	0.309
DKK1pre	0.370	0.293	0.321	0.365
SFRP1pre	0.382	0.276	0.127	0.726

**. Correlation is significant at the 0.01 level (2-tailed).

*. Correlation is significant at the 0.05 level (2-tailed).

Table A13 Spearman Correlation Analysis of Clinical and Biomarker Variables with Baseline (T0VOL2) and Final Tumour Volume (T2VOL2) in the Tamoxifen Group

	Independent variable			
	T0VOL2		T2VOL2	
	r	*p*	r	*p*
T0VOL2	1.000		.855**	0.002
T2VOL2	.855**	0.002	1.000	
AGE	0.152	0.676	0.212	0.556
AGEATDX	0.103	0.777	0.164	0.651
T1VOL2	0.590	0.073	.748*	0.013
totalchange	0.188	0.603	0.358	0.310
percentchange	0.139	0.701	0.394	0.260
HSCOREA	-0.406	0.244	-0.406	0.244
HSCOREB	-0.178	0.622	-0.487	0.154
postopduration	0.122	0.738	0.073	0.841
CD40pre	-0.576	0.082	-0.345	0.328
HGFpre	-0.321	0.365	-0.067	0.855
SCFpre	-0.273	0.446	-0.115	0.751
TGFalphapre	-0.182	0.614	-0.079	0.828
FGFpre	0.055	0.880	-0.128	0.724
TNFalphapre	-0.337	0.341	-0.472	0.168
IL6pre	0.191	0.598	-0.148	0.684
VEGFpre	0.152	0.676	-0.030	0.934
DKK1pre	-0.467	0.174	-0.285	0.425
SFRP1pre	-0.406	0.244	-0.527	0.117
CD40post	-.661*	0.038	-0.418	0.229
HGFpost	0.042	0.907	0.273	0.446
SCFpost	-0.188	0.603	-0.139	0.701
TGFalphapost	0.091	0.802	0.097	0.789

FGFpost	0.043	0.906	-0.025	0.946
TNFalphapost	-0.473	0.284	-0.374	0.408
IL6post	0.419	0.228	0.225	0.532
VEGFpost	-0.564	0.090	-0.358	0.310
DKK1post	-.782**	0.008	-0.539	0.108
SFRP1post	-0.212	0.556	-0.430	0.214

**. Correlation is significant at the 0.01 level (2-tailed).

*. Correlation is significant at the 0.05 level (2-tailed).

Table A14 Spearman Correlation Analysis Between □ Tumour Volumetric Outcomes

Factors	totalchange		percentchange		T0VOL2		T1VOL2		T2VOL2	
	r	*p*	r	*p*	r	*p*	r	*p*	r	*p*
Δ □ □ □ □ □	0.370	0.293	0.406	0.244	0.188	0.603	-0.359	0.309	0.176	0.627
Δ □ □ □	-0.091	0.803	-0.103	0.777	0.224	0.533	0.073	0.841	0.285	0.425
Δ □ □ □	0.406	0.244	0.285	0.425	-0.079	0.829	-0.729	0.017*	-0.200	0.580
Δ □ □ □ □ □ □	-0.539	0.108	-0.624	0.054	0.127	0.726	0.243	0.498	0.018	0.960
Δ □ □ □	0.316	0.374	0.188	0.602	-0.030	0.934	-0.073	0.841	0.043	0.907
Δ □ □ □ □ □ □	-0.043	0.906	0.178	0.622	0.092	0.800	0.185	0.608	0.295	0.407
Δ □ □ □	-0.031	0.933	0.067	0.853	0.350	0.322	0.375	0.285	0.485	0.156
Δ □ □ □ □	0.382	0.276	0.382	0.276	-0.430	0.214	-0.219	0.544	-0.152	0.676
Δ □ □ □ □	0.055	0.881	0.127	0.726	-0.394	0.260	0.109	0.763	-0.139	0.701
Δ □ □ □ □	-0.018	0.960	-0.079	0.829	-0.091	0.803	-.0796	0.006**	-0.418	0.229

**. Correlation is significant at the 0.01 level (2-tailed).

*. Correlation is significant at the 0.05 level (2-tailed).

Table A15 Paired t-Test Comparison of Pre- and Post-Treatment Serum Biomarker Levels (N = 10)

Paired Samples	N	Mean	Std. Deviation	Paired Differences Mean	t	*p*
TGFalphapre	10	5.76	3.89	0.55	0.45	0.665
TGFalphapost	10	5.21	2.00			
TNFalphapre	10	42.64	11.54	15.11	2.34	0.044
TNFalphapost	10	27.53	18.06			
IL6pre	10	68.51	18.36	-5.60	-0.97	0.359
IL6post	10	74.11	25.71			
DKK1pre	10	3740.60	1876.45	431.00	0.61	0.560
DKK1post	10	3309.60	2449.73			

Table A16 Wilcoxon Signed-Rank Test Comparing Pre- and Post-Treatment Serum Biomarker Levels (N=10)

Paired		N	Mean Rank	Sum of Ranks	Z	*p*
CD40post - CD40pre	Negative Ranks	6[a]	5.17	31.00	-.357[b]	0.721
	Positive Ranks	4[b]	6.00	24.00		
	Ties	0[c]				
	Total	10				
HGFpost - HGFpre	Negative Ranks	6[d]	6.17	37.00	-.968[b]	0.333
	Positive Ranks	4[e]	4.50	18.00		
	Ties	0[f]				
	Total	10				
SCFpost - SCFpre	Negative Ranks	6[g]	4.67	28.00	-.051[b]	0.959
	Positive Ranks	4[h]	6.75	27.00		
	Ties	0[i]				
	Total	10				
FGFpost - FGFpre	Negative Ranks	4[m]	4.25	17.00	-.140[c]	0.889
	Positive Ranks	4[n]	4.75	19.00		
	Ties	2[o]				

	Total	10				
VEGFpost - VEGFpre	Negative Ranks	5[v]	4.20	21.00	-.663[c]	0.508
	Positive Ranks	5[w]	6.80	34.00		
	Ties	0[x]				
	Total	10				
SFRP1post - SFRP1pre	Negative Ranks	3[ab]	5.67	17.00	-1.070[c]	0.285
	Positive Ranks	7[ac]	5.43	38.00		
	Ties	0[ad]				
	Total	10				

a. CD40post < CD40pre

b. CD40post > CD40pre

c. CD40post = CD40pre

d. HGFpost < HGFpre

e. HGFpost > HGFpre

f. HGFpost = HGFpre

g. SCFpost < SCFpre

h. SCFpost > SCFpre

i. SCFpost = SCFpre

j. TGFalphapost < TGFalphapre

k. TGFalphapost > TGFalphapre

l. TGFalphapost = TGFalphapre

m. FGFpost < FGFpre

n. FGFpost > FGFpre

o. FGFpost = FGFpre

p. TNFalphapost < TNFalphapre

q. TNFalphapost > TNFalphapre

r. TNFalphapost = TNFalphapre

s. IL6post < IL6pre

t. IL6post > IL6pre

u. IL6post = IL6pre

v. VEGFpost < VEGFpre

w. VEGFpost > VEGFpre

x. VEGFpost = VEGFpre

y. DKK1post < DKK1pre

z. DKK1post > DKK1pre

aa. DKK1post = DKK1pre

ab. SFRP1post < SFRP1pre

ac. SFRP1post > SFRP1pre

ad. SFRP1post = SFRP1pre

Table A17 The Benjamini-Hochberg (BH) False Discovery Rate (N=10)

No (m)	Paired variables	*p*	*q*	Mean Rank (i)	(i/10) ×0.05 (m)	BH critical value	Decision
1	TNFalpha	0.044	0.05	1	10	0.005	NS
2	SFRP1	0.304	0.05	2	10	0.01	NS
3	IL6	0.359	0.05	3	10	0.015	NS
4	VEGF	0.367	0.05	4	10	0.02	NS
5	CD40L	0.388	0.05	5	10	0.025	NS
6	HGF	0.422	0.05	6	10	0.03	NS
7	FGF	0.519	0.05	7	10	0.035	NS
8	DKK1	0.560	0.05	8	10	0.04	NS
9	SCF	0.639	0.05	9	10	0.045	NS
10	TGFalpha	0.665	0.05	10	10	0.05	NS

NS – not significant

Table A18 Simple Linear Regression Analyses of Clinical, Volumetric, ER Expression, and Biomarker Predictors of Final Tumour Volume ($T2VOL_2$)

					95.0% Confidence Interval for B		Collinearity Statistics			
Factors	B	Beta	t	*p*	Lower Bound	Upper Bound	Tolerance	VIF	R Square	Adjusted R Square
totalchange	**0.62**	**0.34**	**1.55**	**0.140**	**-0.22**	**1.46**	**1.00**	**1.00**	**0.12**	**0.07**
percentchange	**0.02**	**0.50**	**2.45**	**0.025***	**0.00**	**0.03**	**1.00**	**1.00**	**0.25**	**0.21**
HSCOREA	-0.04	-0.23	-0.99	0.333	-0.11	0.04	1.00	1.00	0.05	0.00
HSCOREB	0.00	-0.28	-1.23	0.235	-0.01	0.00	1.00	1.00	0.08	0.03
postopduration	0.01	0.07	0.31	0.762	-0.04	0.05	1.00	1.00	0.01	-0.05
CD40pre	0.00	-0.02	-0.07	0.942	0.00	0.00	1.00	1.00	0.00	-0.06
HGFpre	0.00	-0.04	-0.15	0.881	0.00	0.00	1.00	1.00	0.00	-0.05
SCFpre	0.00	0.03	0.14	0.892	-0.01	0.02	1.00	1.00	0.00	-0.05
TGFalphapre	0.01	0.05	0.19	0.848	-0.10	0.12	1.00	1.00	0.00	-0.05
FGFpre	0.02	0.09	0.37	0.713	-0.08	0.12	1.00	1.00	0.01	-0.05
TNFalphapre	0.01	0.09	0.40	0.696	-0.05	0.08	1.00	1.00	0.01	-0.05
IL6pre	0.00	-0.02	-0.06	0.949	-0.04	0.04	1.00	1.00	0.00	-0.06
VEGFpre	0.00	-0.05	-0.20	0.847	0.00	0.00	1.00	1.00	0.00	-0.05
DKK1pre	0.00	0.15	0.65	0.522	0.00	0.00	1.00	1.00	0.02	-0.03
SFRP1pre	0.00	-0.13	-0.58	0.571	-0.01	0.00	1.00	1.00	0.02	-0.04
CD40post	**0.00**	**-0.45**	**-1.43**	**0.191**	**0.00**	**0.00**	**1.00**	**1.00**	**0.20**	**0.10**
HGFpost	0.00	0.17	0.50	0.629	0.00	0.00	1.00	1.00	0.03	-0.09
SCFpost	0.00	0.05	0.15	0.884	-0.02	0.03	1.00	1.00	0.00	-0.12
TGFalphapost	0.02	0.04	0.11	0.915	-0.49	0.54	1.00	1.00	0.00	-0.12
FGFpost	0.02	0.20	0.56	0.589	-0.05	0.08	1.00	1.00	0.04	-0.08
TNFalphapost	0.00	0.06	0.18	0.859	-0.05	0.06	1.00	1.00	0.00	-0.12
IL6post	0.02	0.35	1.05	0.322	-0.02	0.05	1.00	1.00	0.12	0.01
VEGFpost	0.00	-0.33	-0.98	0.355	0.00	0.00	1.00	1.00	0.11	0.00
DKK1post	**0.00**	**-0.47**	**-1.49**	**0.175**	**0.00**	**0.00**	**1.00**	**1.00**	**0.22**	**0.12**
SFRP1post	**0.00**	**-0.50**	**-1.61**	**0.145**	**-0.01**	**0.00**	**1.00**	**1.00**	**0.25**	**0.15**
CBI pre	0.00	-0.04	-0.16	0.874	0.00	0.00	1.00	1.00	0.00	-0.05

CBI post	0.00	0.04	0.12	0.910	0.00	0.00	1.00	1.00	0.00	-0.12
shrinkage	0.01	0.00	0.01	0.993	-1.53	1.54	1.00	1.00	0.00	-0.06
stabilization	0.01	0.00	0.01	0.993	-1.53	1.54	1.00	1.00	0.00	-0.06
regrowth	**2.31**	**0.49**	**2.37**	**0.029***	**0.27**	**4.36**	**1.00**	**1.00**	**0.24**	**0.20**
STUDYARM	**-0.94**	**-0.33**	**-1.49**	**0.153**	**-2.27**	**0.38**	**1.00**	**1.00**	**0.11**	**0.06**

Dependent Variable: $T2VOL_2$

Table A19 Multiple Linear Regression Model for Predictors of Final Tumour Volume ($T2VOL_2$)

					95.0% Confidence Interval for B		Collinearity Statistics			
	B	Beta	t	Sig.	Lower Bound	Upper Bound	Tolerance	VIF	R Square	Adjusted R Square
(Constant)	3.34		6.78	0.000	2.18	4.51			0.72	0.63
percentchange	0.03	0.77	3.50	0.010*	0.01	0.05	0.83	1.20		
DKK1post	0.00	-0.78	-3.53	0.010*	0.00	0.00	0.83	1.20		

Dependent Variable: $T2VOL_2$

Table A20 Binary Logistic Regression Analysis of Clinical, Radiological, and Biomarker Predictors of Tumour Shrinkage

					95% C.I.for EXP(B)			
Factors	B	Wald	*p*	Exp(B)	Lower	Upper	Cox & Snell R Square	Nagelkerke R Square
T0VOL2	-0.13	0.14	0.709	0.88	0.44	1.75	0.01	0.01
T1VOL2	-0.17	0.18	0.669	0.85	0.40	1.81	0.01	0.01
T2VOL2	0.00	0.00	0.992	1.00	0.51	1.97	0.00	0.00
totalchange	0.42	0.43	0.511	1.52	0.44	5.29	0.02	0.03
percentchange	0.01	0.39	0.530	1.01	0.98	1.04	0.02	0.03
HSCOREA	-0.07	1.05	0.306	0.93	0.81	1.07	0.07	0.11
HSCOREB	0.00	0.29	0.592	1.00	0.99	1.01	0.01	0.02
postopduration	0.02	0.43	0.511	1.02	0.95	1.10	0.02	0.04
CD40pre	0.00	0.06	0.808	1.00	1.00	1.00	0.00	0.00
HGFpre	0.00	0.95	0.330	1.00	1.00	1.00	0.06	0.09
SCFpre	0.03	1.33	0.249	1.03	0.98	1.07	0.11	0.16

TGFalphapre	0.06	0.31	0.577	1.06	0.87	1.29	0.02	0.03
FGFpre	-0.07	0.94	0.332	0.93	0.81	1.07	0.05	0.07
TNFalphapre	-0.01	0.01	0.904	0.99	0.91	1.09	0.00	0.00
IL6pre	-0.02	0.74	0.389	0.98	0.93	1.03	0.04	0.05
VEGFpre	0.00	0.13	0.715	1.00	1.00	1.00	0.01	0.01
DKK1pre	0.00	1.38	0.240	1.00	1.00	1.00	0.08	0.11
SFRP1pre	0.00	0.63	0.428	1.00	0.99	1.01	0.03	0.04
CD40post	0.00	0.10	0.752	1.00	1.00	1.00	0.01	0.01
HGFpost	0.00	0.04	0.850	1.00	1.00	1.00	0.00	0.00
SCFpost	0.00	0.05	0.824	1.00	0.97	1.04	0.01	0.01
TGFalphapost	-0.15	0.19	0.666	0.86	0.43	1.73	0.02	0.03
FGFpost	0.01	0.07	0.794	1.01	0.93	1.11	0.01	0.01
TNFalphapost	-0.01	0.15	0.694	0.99	0.91	1.06	0.02	0.02
IL6post	-0.02	0.48	0.489	0.98	0.93	1.04	0.05	0.07
VEGFpost	0.00	0.15	0.700	1.00	1.00	1.00	0.01	0.02
DKK1post	0.00	1.03	0.310	1.00	1.00	1.00	0.11	0.15
CBI pre	0.00	0.67	0.413	1.00	1.00	1.00	0.04	0.06
CBI post	0.00	0.00	0.973	1.00	1.00	1.00	0.00	0.00

Dependent variable: shrinkage (yes)

Table A21 Z-Score–Standardised Clinical, Radiological, and Biomarker Variables

Variables	N	Minimum	Maximum	Mean	Std. Deviation
Zscore(CD40pre)	20020	-0.60	2.49	0.00	0.97
Zscore(HGFpre)	20020	-1.04	3.35	0.00	0.97
Zscore(SCFpre)	20020	-0.90	2.62	0.00	0.97
Zscore(TGFalphapre)	20020	-0.75	3.58	0.00	0.97
Zscore(FGFpre)	20020	-1.13	1.84	0.00	0.97
Zscore(TNFalphapre)	20020	-2.61	0.76	0.00	0.97
Zscore(IL6pre)	20020	-1.94	2.08	0.00	0.97
Zscore(VEGFpre)	20020	-0.99	2.78	0.00	0.97
Zscore(DKK1pre)	20020	-1.62	2.02	0.00	0.97
Zscore(SFRP1pre)	20020	-0.60	3.51	0.00	0.97
Zscore: T0VOL2	20020	-1.21	2.45	0.00	0.97
Zscore(T1VOL2)	20020	-1.20	1.50	-0.01	0.78
Zscore: T2VOL2	20020	-1.34	1.89	0.00	0.97
Zscore(totalchange)	20020	-2.90	2.39	0.00	0.97
Zscore(percentchange)	20020	-2.21	3.13	0.00	0.97
Zscore(HSCOREA)	20020	-0.30	4.09	0.00	0.97
Zscore(HSCOREB)	20020	-0.77	1.76	0.00	0.97
Zscore(postopduration)	20020	-0.93	2.92	0.00	0.97
Zscore(CD40post)	10010	-0.89	1.84	0.00	0.95
Zscore(HGFpost)	10010	-1.66	1.68	0.00	0.95
Zscore(SCFpost)	10010	-1.10	2.16	0.00	0.95
Zscore(TGFalphapost)	10010	-2.02	1.32	0.00	0.95
Zscore(FGFpost)	10010	-0.86	2.57	0.00	0.95
Zscore(TNFalphapost)	7007	-1.42	1.92	0.00	0.93
Zscore(IL6post)	10010	-0.97	1.83	0.00	0.95
Zscore(VEGFpost)	10010	-0.99	2.50	0.00	0.95
Zscore(DKK1post)	10010	-1.14	1.40	0.00	0.95
Zscore(SFRP1post)	10010	-0.62	2.35	0.00	0.95
□ □ □ □ □ □ □ □Δ □ □ □ □	10010	-1.04	2.30	0.00	0.95
□ □ □ □ □ □ □ □Δ □ □ □	10010	-1.12	1.51	0.00	0.95

□ □ □ □ □ □ □ □Δ □ □ □	10010	-0.99	2.30	0.00	0.95
□ □ □ □ □ □ □ □Δ □ □ □ □ □ □ □ □	10010	-2.12	1.46	0.00	0.95
□ □ □ □ □ □ □ □Δ □ □ □ □	10010	-0.86	2.62	0.00	0.95
□ □ □ □ □ □ □ □Δ □ □ □ □ □ □ □ □	7007	-0.83	1.51	0.00	0.93
□ □ □ □ □ □ □ □Δ □ □ □ □	10010	-1.30	1.57	0.00	0.95
□ □ □ □ □ □ □ □Δ □ □ □ □ □	10010	-1.08	2.52	0.00	0.95
□ □ □ □ □ □ □ □Δ □ □ □ □ □	10010	-1.11	2.09	0.00	0.95
□ □ □ □ □ □ □ □Δ □ □ □ □ □	10010	-1.05	2.51	0.00	0.95

Table A22 Bootstrapping Exploratory Factor Analysis of Baseline, Post-Treatment, and Change □ Δ) □□ □ □ □ □ □ □□ □ □ □ □ □ □ □ □ □ □

			Initial Eigenvalues			Kaiser-Meyer-Olkin Measure of Sampling Adequacy.	Bartlett's Test of Sphericity	
Component	Variable	Loading	Total	% of Variance	Cumulative %		Approx. Chi-Square	*p*
1	HGFpre	0.94	3.60	36.02	36.02	0.56	147304.99	0.000
	SCFpre	0.66						
	TGFalphapre	0.91						
	VEGFpre	0.83						
2	CD40pre	-0.81	2.18	21.83	57.85			
	FGFpre	0.81						
	IL6pre	0.79						
3	SFRP1pre	0.75	1.37	13.68	71.53			
4	TNFalphapre	0.69	1.04	10.43	81.96			
1	Zscore(HGFpre)	0.95	3.60	36.02	36.02	0.56	147304.99	0.000
	Zscore(TGFalphapre)	0.95						
	Zscore(VEGFpre)	0.86						
2	Zscore(FGFpre)	0.79	2.18	21.83	57.85			
	Zscore(CD40pre)	-0.80						
	Zscore(IL6pre)	0.82						
3	Zscore(DKK1pre)	0.69	1.37	13.68	71.53			

	Zscore(SFRP1pre)	-0.74			
4	Zscore(TNFalphapre)	0.91	1.04	10.43	81.96
1	CD40post	0.90	5.35	53.48	53.48
	HGFpost	0.74			
	SCFpost	0.77			
	TGFalphapost	0.84			
	TNFalphapost	0.92			
	VEGFpost	0.98			
	DKK1post	0.75			
2	FGFpost	0.62	1.89	18.85	72.34
	IL6post	0.92			
3	SFRP1post	0.96	1.37	13.73	86.06
1	Δ □ □ □	0.97	5.21	47.35	47.35
	Δ □ □ □ □ □ □ □ □	0.68			
	Δ □ □ □	0.77			
2	Δ □ □ □ □	0.68	2.14	19.47	66.82
	Δ □ □ □ □ □ □ □ □	0.94			
	Δ □ □ □ □	0.90			
	Δ □ □ □ □	0.83			
3	Δ □ □ □	0.87	1.78	16.19	83.01
	Δ □ □ □	0.74			
4	Δ □ □ □ □	0.95	1.43	12.98	95.98
1	Zscore(CD40post)	0.90	5.35	53.48	53.48
	Zscore(HGFpost)	0.74			
	Zscore(SCFpost)	0.77			
	Zscore(TGFalphapost)	0.84			
	Zscore(TNFalphapost)	0.92			
	Zscore(VEGFpost)	0.98			
	Zscore(DKK1post)	0.75			
2	Zscore(FGFpost)	0.62	1.89	18.85	72.34
	Zscore(IL6post)	0.92			
3	Zscore(SFRP1post)	0.96	1.37	13.73	86.06

1	□ □ □ □ □ □ □ □ □ Δ □ [	0.74	4.64	46.43	46.43
	□ □ □ □ □ □ □ □ □ Δ □ [	0.93			
	□ □ □ □ □ □ □ □ □ Δ □ [	0.93			
	□ □ □ □ □ □ □ □ □ Δ □ [	0.84			
2	□ □ □ □ □ □ □ □ □ Δ □ [	0.98	2.13	21.34	67.78
	□ □ □ □ □ □ □ □ □ Δ □ [	0.66			
	□ □ □ □ □ □ □ □ □ Δ □ [	0.86			
3	□ □ □ □ □ □ □ □ □ Δ □ [	0.71	1.51	15.15	82.92
	□ □ □ □ □ □ □ □ □ Δ □ [	0.88			
4	□ □ □ □ □ □ □ □ □ Δ □ [	0.93	1.38	13.79	96.71

Figure A2 PLS-SEM Measurement Model of the Composite Biomarker Index (CBI) in the Intervention Cohort

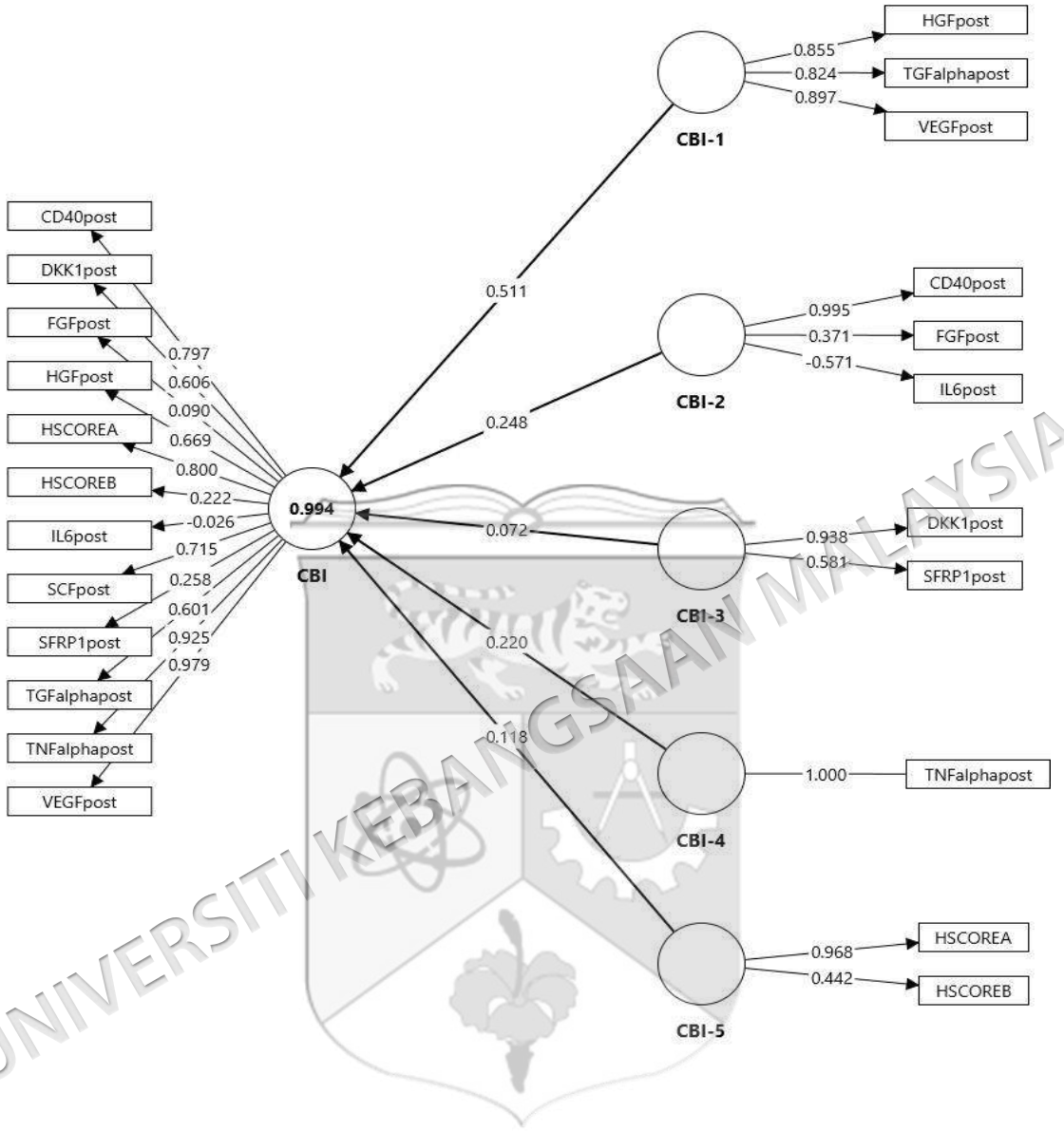

Table A23 Top 10 Pathways Significantly Associated with Targeted Genes

KEGG pathways	**Count**	**Genes**	**Fold Enrichment**	**FDR**
hsa04080:Neuroactive ligand-receptor interaction	42	*CHRM2, OPRD1, CHRM3, CHRM1, CHRM4, CHRNA7, NPY2R, CHRM5, HTR2B, HTR2C, ADRA1D, ADRB1, HTR2A, ADRA1A, CRHR1, HTR6, HRH3, HRH2, ADORA3, GNRHR, DRD1, DRD2, DRD3, DRD4, HTR1F, HTR1D, AVPR2, TACR2, NPY1R, OPRK1, TACR1, AVPR1A, OPRM1, ADRA2C, HTR5A, F2, ADRA2B, ADRA2A, MC1R, ADORA2A, ADRB3, MC5R*	10.32415	1.58E-29
hsa04020:Calcium signaling pathway	22	*CHRM2, CHRM3, CHRM1, CHRNA7, CHRM5, TACR2, HTR2B, HTR2C, ADRA1D, ADRB1, AVPR1A, TACR1, HTR2A, HTR5A, ADRA1A, EGFR, HTR6, ADORA2A, ADRB3, HRH2, ERBB2, DRD1*	7.835047	1.70E-11
hsa04024:cAMP signaling pathway	15	*CHRM2, CHRM1, HTR1F, HTR1D, NPY1R, ADRB1, PLD1, CRHR1, PLD2, HTR6, ADORA2A, AKT2, AKT1, DRD1, DRD2*	6.003928	6.37E-06
hsa04218:Cellular senescence	12	*CCNB3, CCNB2, CCNB1, CCND1, CCNE2, CCNE1, CDK4, AKT2, CDK2, CDK1, AKT1, MAPK14*	6.914078	3.45E-05
hsa05200:Pathways in cancer	20	*FLT3, XIAP, F2, PLD1, ESR1, EGFR, ESR2, PLD2, AR, CCNE2, CCND1, CCNE1, CDK4, AKT2, ERBB2, CDK2, PIM1, AKT1, PIM2, BIRC2*	3.394341	1.02E-04
hsa04725:Cholinergic synapse	10	*CHRM2, ACHE, CHRM3, CHRM1, AKT2, CHRNA7, CHRM4, CHRM5, AKT1, FYN*	7.798205	1.02E-04
hsa05222:Small cell lung cancer	9	*CCND1, CCNE2, CCNE1, CDK4, AKT2, CDK2, XIAP, AKT1, BIRC2*	8.754115	1.42E-04
hsa05215:Prostate cancer	9	*AR, CCND1, CCNE2, CCNE1, AKT2, ERBB2, CDK2, AKT1, EGFR*	8.307476	1.70E-04

Figure A3 Tamoxifen associated genes are involved in the regulation of hsa04080: Neuroactive Ligand-Receptor Interaction

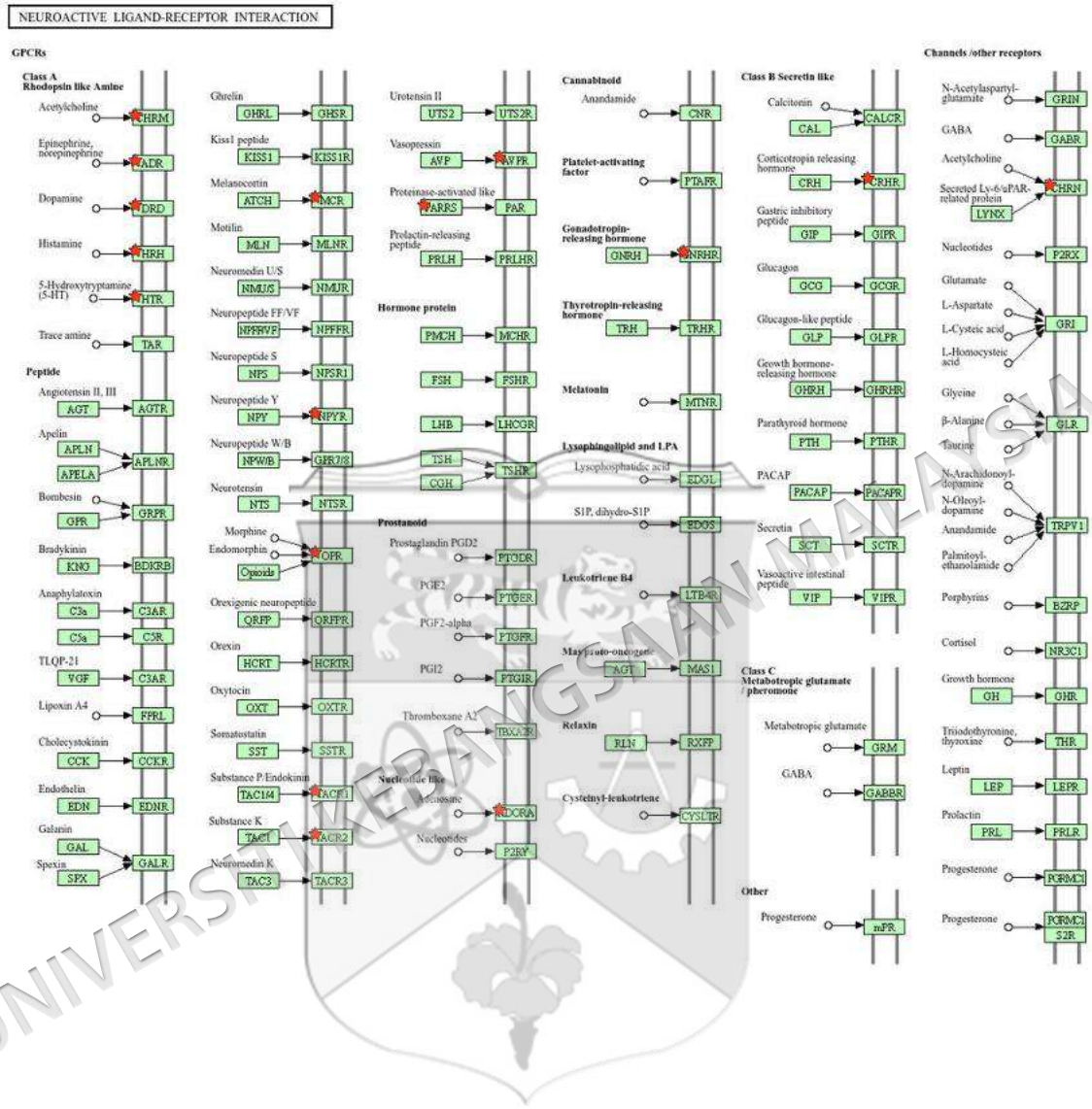

Figure A4 Tamoxifen associated genes are involved in the regulation of hsa04725: Cholinergic Synapse pathway

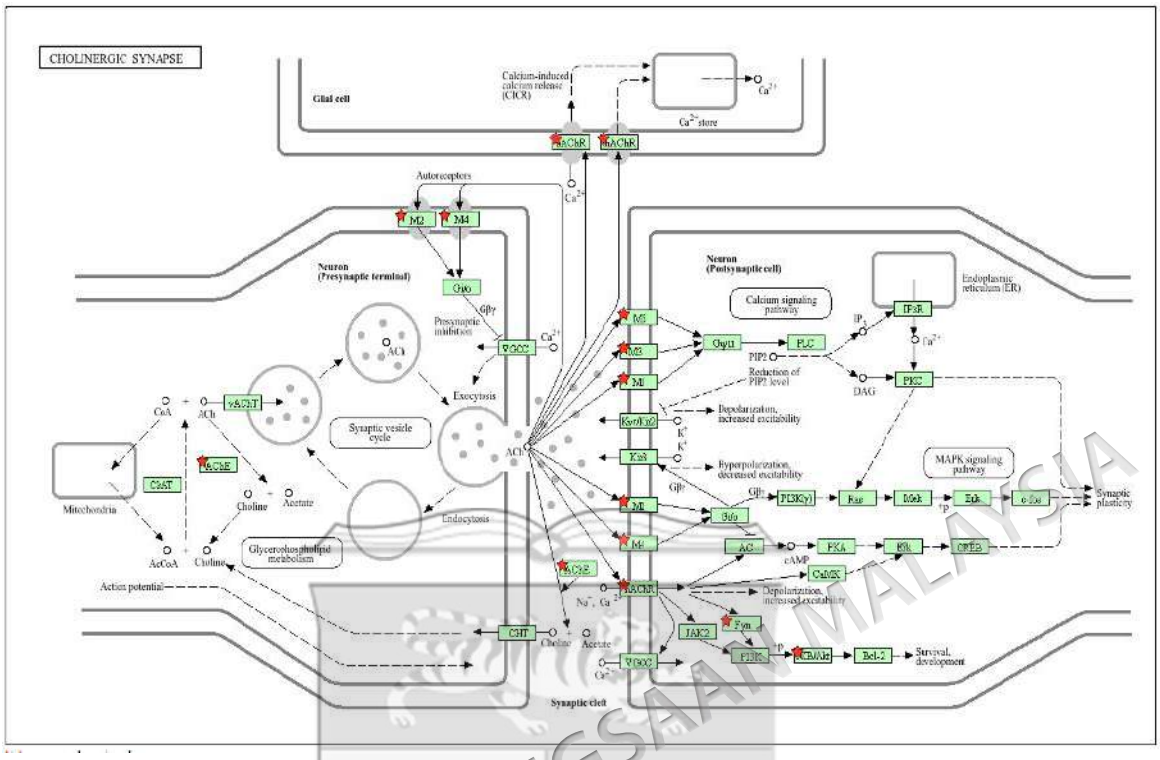

APPENDIX B

Consort Diagram

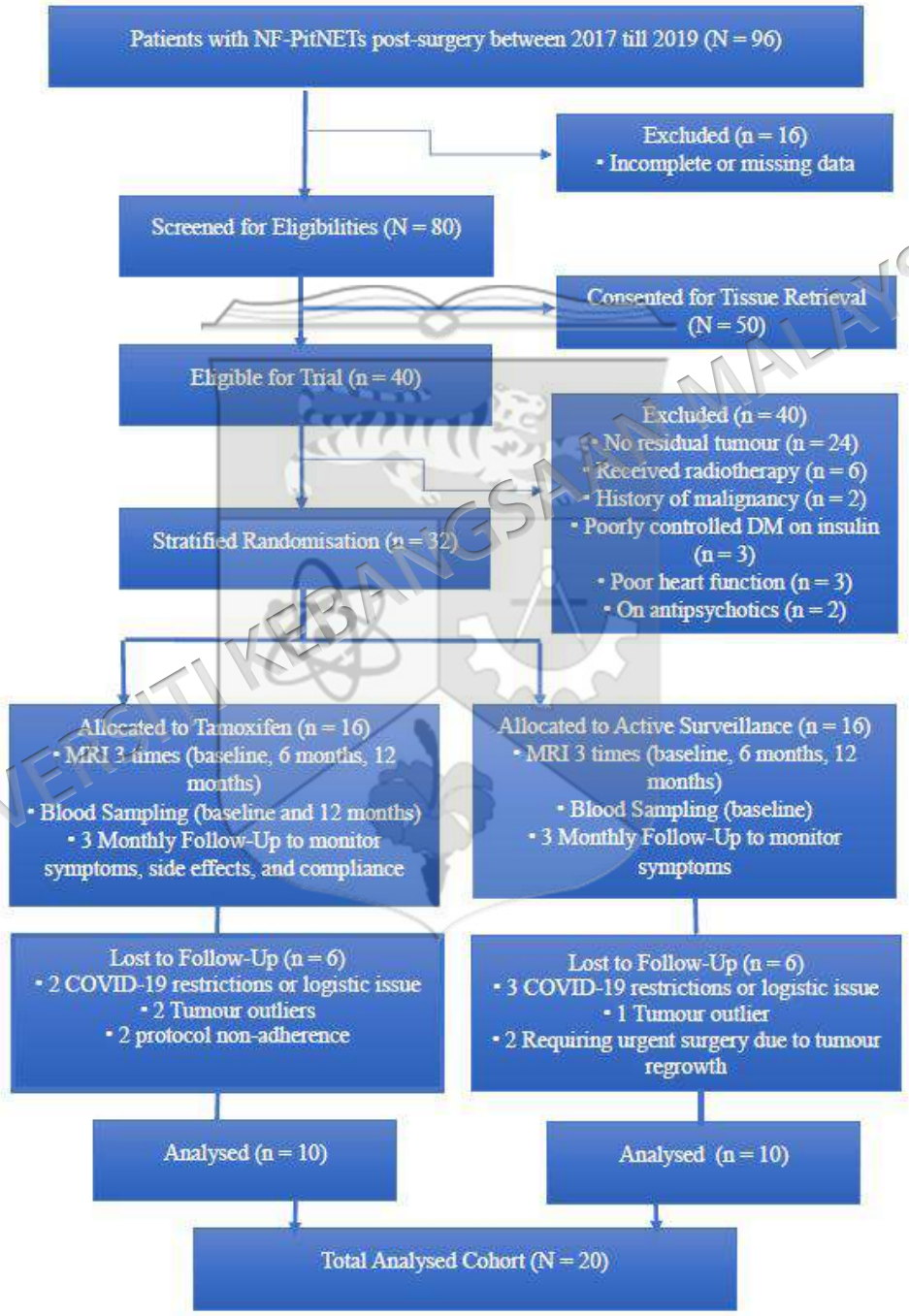

APPENDIX C

CALIBRATION AND VALIDATION FOR MULTIPLEX IMMUNOASSAY

Luminex

Calibration and Verification Report

22-Jul-25 1:57:40PM

Date/Time: 22-Jul-25 through 22-Jul-25

CAL1

Date	Time	Serial	User	Version		Lot	Pressure	Status
				Firmware	LXR			
7/22/2025	11:30 AM	LX10015041401		2.6.1	2.1.495.0	C08158	7.86	Pass

Channel	Temp	Volt	DAC	R-Val	Result	Target	Status
DD	21.79	95.09	1,527	745	10,055.00	10,100.00	Pass
CL1	21.57	114.64	1,841	1,322	3,658.18	3,656.00	Pass
CL2	22.22	117.01	1,879	1,417	3,664.04	3,658.00	Pass
Final Result Code	The operation completed successfully. (0x00000000)						

Luminex

Calibration and Verification Report

22-Jul-25 1:57:40PM

Date/Time: 22-Jul-25 through 22-Jul-25

CAL1

Date	Time	Serial	User	Version		Lot	Pressure	Status
				Firmware	LXR			
7/22/2025	11:30 AM	LX10015041401		2.6.1	2.1.495.0	C08158	7.86	Pass

Channel	Temp	Volt	DAC	R-Val	Result	Target	Status
DD	21.79	95.09	1,527	745	10,055.00	10,100.00	Pass
CL1	21.57	114.64	1,841	1,322	3,658.18	3,656.00	Pass
CL2	22.22	117.01	1,879	1,417	3,664.04	3,658.00	Pass
Final Result Code	The operation completed successfully. (0x00000000)						

Luminex

Calibration and Verification Report

22-Jul-25 1:57:40PM

Date/Time: 22-Jul-25 through 22-Jul-25

CAL1

Date	Time	Serial	User	Version		Lot	Pressure	Status
				Firmware	LXR			
7/22/2025	11:30 AM	LX100150414 01		2.6.1	2.1.495.0	C08158	7.86	Pass

Channel	Temp	Volt	DAC	R-Val	Result	Target	Status
DD	21.79	95.09	1,527	745	10,055.00	10,100.00	Pass
CL1	21.57	114.64	1,841	1,322	3,658.18	3,656.00	Pass
CL2	22.22	117.01	1,879	1,417	3,664.04	3,658.00	Pass
Final Result Code		The operation completed successfully. (0x00000000)					

Luminex

Calibration and Verification Report

22-Jul-25 1:57:40PM

Date/Time: 22-Jul-25 through 22-Jul-25

CAL1

Date	Time	Serial	User	Version		Lot	Pressure	Status
				Firmware	LXR			
7/22/2025	11:30 AM	LX100150414 01		2.6.1	2.1.495.0	C08158	7.86	Pass

Channel	Temp	Volt	DAC	R-Val	Result	Target	Status
DD	21.79	95.09	1,527	745	10,055.00	10,100.00	Pass
CL1	21.57	114.64	1,841	1,322	3,658.18	3,656.00	Pass
CL2	22.22	117.01	1,879	1,417	3,664.04	3,658.00	Pass
Final Result Code		The operation completed successfully. (0x00000000)					

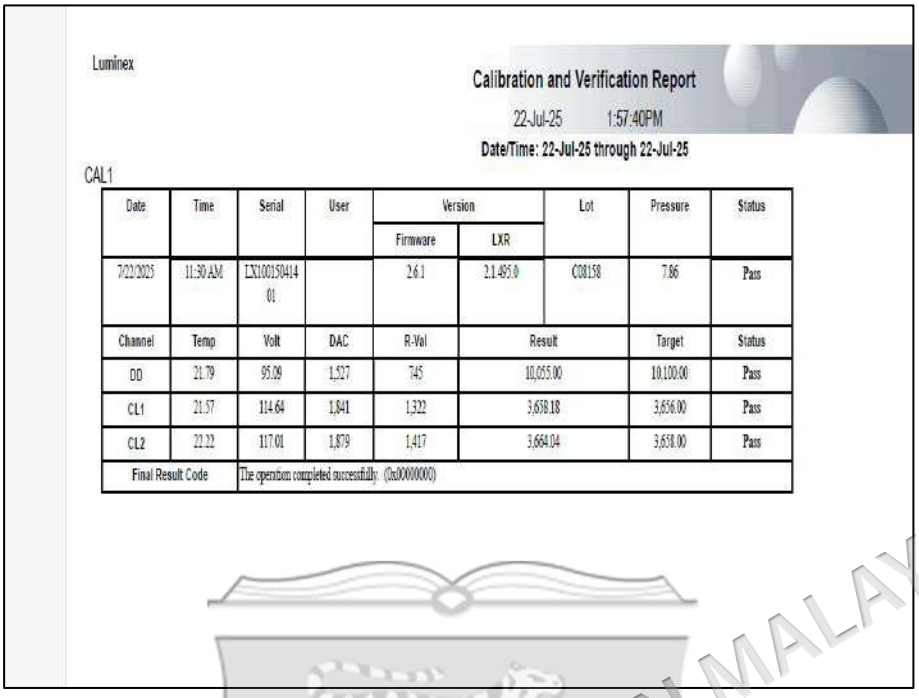

Luminex

Calibration and Verification Report

22-Jul-25 1:57:40PM

Date/Time: 22-Jul-25 through 22-Jul-25

CAL1

Date	Time	Serial	User	Version		Lot	Pressure	Status
				Firmware	LXR			
7/22/2025	11:30 AM	LX10015041401		2.6.1	2.1.495.0	C08158	7.86	Pass

Channel	Temp	Volt	DAC	R-Val	Result	Target	Status
DD	21.79	95.09	1,527	745	10,055.00	10,100.00	Pass
CL1	21.57	114.64	1,841	1,322	3,638.18	3,656.00	Pass
CL2	22.22	117.01	1,879	1,417	3,664.04	3,658.00	Pass
Final Result Code		The operation completed successfully. (0x00000000)					

Luminex

Calibration and Verification Report

22-Jul-25 1:57:40PM

Date/Time: 22-Jul-25 through 22-Jul-25

CAL1

Date	Time	Serial	User	Version		Lot	Pressure	Status
				Firmware	LXR			
7/22/2025	11:30 AM	LX10015041401		2.6.1	2.1.495.0	C08158	7.86	Pass

Channel	Temp	Volt	DAC	R-Val	Result	Target	Status
DD	21.79	95.09	1,527	745	10,055.00	10,100.00	Pass
CL1	21.57	114.64	1,841	1,322	3,638.18	3,656.00	Pass
CL2	22.22	117.01	1,879	1,417	3,664.04	3,658.00	Pass
Final Result Code		The operation completed successfully. (0x00000000)					

APPENDIX D

CERTIFICATE OF ANALYSIS FOR MULTIPLEX IMMUNOASSAY

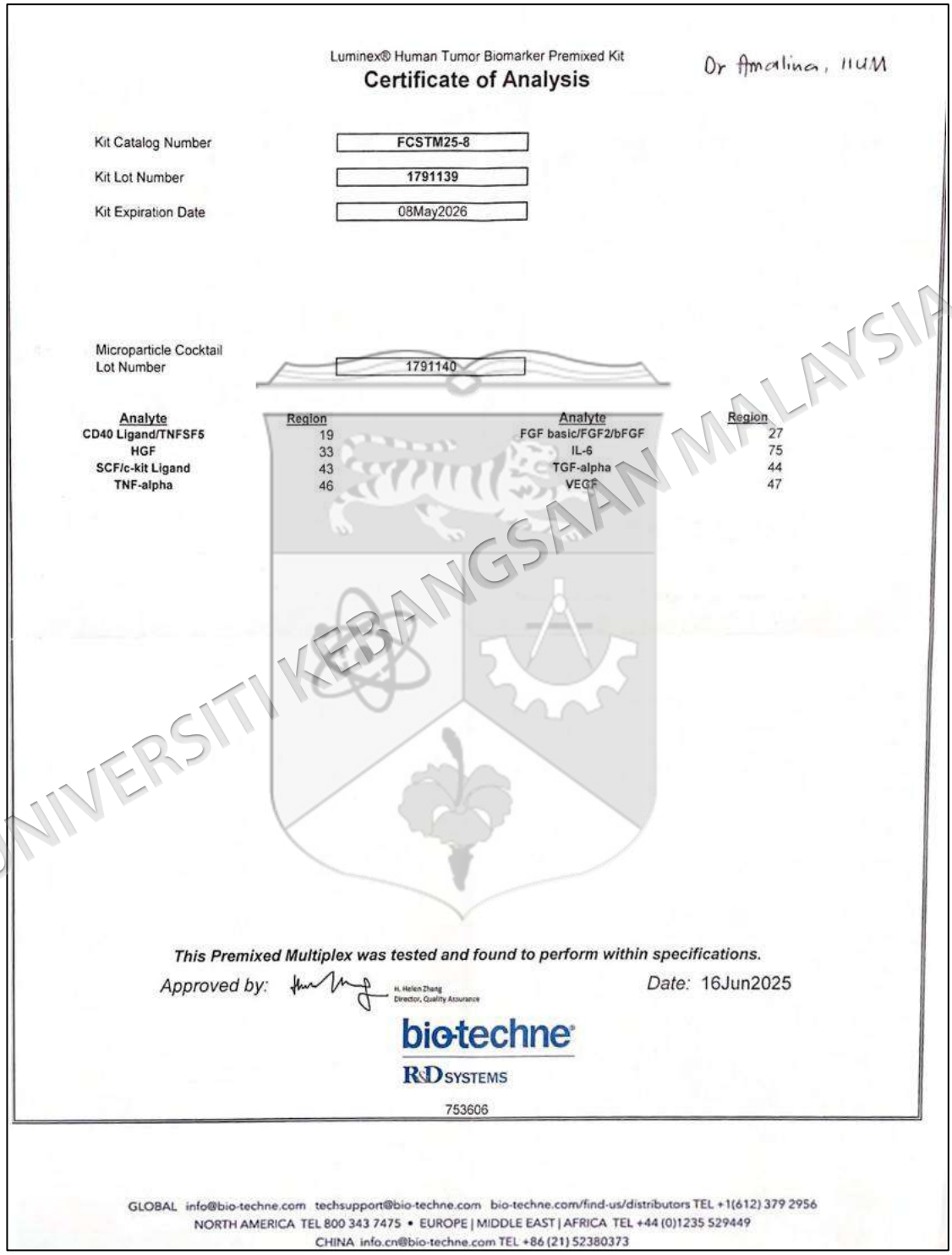

Luminex® Human Tumor Biomarker Premixed Kit

Certificate of Analysis

Dr Amalina, IIUM

Kit Catalog Number	FCSTM25-8
Kit Lot Number	1791139
Kit Expiration Date	08May2026

Microparticle Cocktail Lot Number	1791140

Analyte	Region	Analyte	Region
CD40 Ligand/TNFSF5	19	FGF basic/FGF2/bFGF	27
HGF	33	IL-6	75
SCF/c-kit Ligand	43	TGF-alpha	44
TNF-alpha	46	VEGF	47

This Premixed Multiplex was tested and found to perform within specifications.

Approved by: H. Helen Zhang, Director, Quality Assurance *Date:* 16Jun2025

bio-techne® R&D SYSTEMS

753606

GLOBAL info@bio-techne.com techsupport@bio-techne.com bio-techne.com/find-us/distributors TEL +1(612) 379 2956
NORTH AMERICA TEL 800 343 7475 • EUROPE | MIDDLE EAST | AFRICA TEL +44 (0)1235 529449
CHINA info.cn@bio-techne.com TEL +86 (21) 52380373

Human Tumor Biomarker Luminex® Performance Assay Control Values

Low Control	Part #: 899543	Lot #: P436937	Recon. Volume: 1.0 mL	Expiration Date: 11 JAN 2028
High Control	Part #: 899542	Lot #: P436935	Recon. Volume: 1.0 mL	Expiration Date: 11 JAN 2028

Analyte	Low (pg/mL)	High (pg/mL)	Analyte	Low (pg/mL)	High (pg/mL)
α-Fetoprotein/AFP	443	3953	HE4/WFDC2	381	3446
CA125-MUC16	104	913	HGF	2988	25,123
CA15-3/MUC-1	715	6776	IL-6	314	2856
CA19-9	9.46 U/mL	83.0 U/mL	IL-8	4.81	40.7
CD40 Ligand/TNFSF5	1244	11,293	Leptin	36.0	328
CEACAM-5	307	2672	MIF	1826	17,122
Chromogranin A	395	3303	Osteopontin/OPN	958	8587
CYFRA21-1	180	1769	Prolactin	1240	11,664
ENO-2	817	7272	Stem Cell Factor	45.1	407
Fas Ligand/TNFSF6	443	3968	TGF-α	43.9	388
Fas/TNFRSF6/CD95	417	3775	Thyroglobulin	1568	13,841
FGF Basic/FGF2/bFGF	205	1823	TNF-α	1135	9172
Glypican-1	4098	37,433	Total PSA	187	1636
HCG-B	47.9	424	VEGF	123	1057

700176.3

Discard reconstituted controls after use.

bio-techne® | R&D SYSTEMS

Human Tumor Biomarker Luminex® Performance Assay Standard Values

Standard Cocktail 1 Part #: 899540 Lot #: P436906
Recon. Volume: 0.50 mL Expiration Date: 13DEC2027

Standard Cocktail 2 Part #: 899541 Lot #: P436911
Recon. Volume: 0.50 mL Expiration Date: 10DEC2027

Analyte	Concentration (pg/mL)	Analyte	Concentration (pg/mL)
α-Fetoprotein/AFP	19,000	HE4/WFDC2	16,500
CA125-MUC16	5100	HGF	115,000
CA15-3/MUC-1	33,000	IL-6*	14,000
CA19-9	350 U/mL	IL-8	230
CD40 Ligand/TNFSF5	60,000	Leptin	1500
CEACAM-5	14,000	MIF*	91,000
Chromogranin A	24,260	Osteopontin/OPN	46,500
CYFRA21-1	8800	Prolactin	62,500
ENO-2	54,000	Stem Cell Factor	1600
Fas Ligand/TNFSF6	19,180	TGF-α	1970
Fas/TNFRSF6/CD95	20,000	Thyroglobulin	62,290
FGF Basic/FGF2/bFGF	9000	TNF-α	36,250
Glypican-1	167,000	Total PSA	7800
HCG-B	2000	VEGF*	5300

*Generate a 7-point curve for all analytes except analytes marked with an asterisk (*) as these analytes require a 6-point standard curve (remove the lowest standard point for IL-6, MIF, and VEGF).

700177.4 Discard reconstituted standards after use. biotechne | R&D SYSTEMS

APPENDIX E

LIST OF RAW BIOMARKER DATA FOR MULTIPLEX IMMUNOASSAY

PRIMANEXUS®
LEADING THE CONNECTION

28-1B, Jalan Puteri 1/2, Bandar Puteri Puchong, 47100 Selangor, Malaysia.
Tel: +603 5891 0194 | Fax: +603 58910195 | Website: www.primanexus.com.my
Company registered number: 1055479-X

VEGF
Logistic5p: y = a+((b-a)/(1+((x/c)^d))^f)

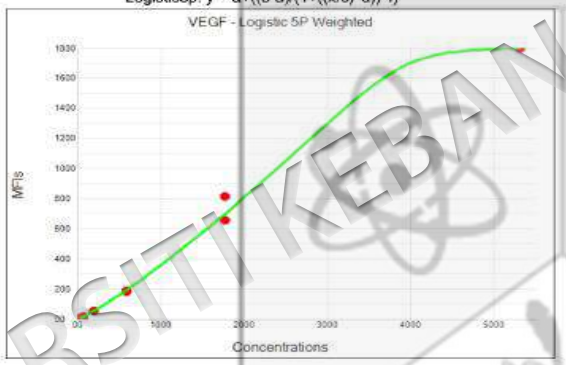

R-Squared	0.9893117184
Sum of Residuals	57.20839607
Average Residuals	5.200763279
Relative Sum of Squares Absolute	15407.92727
Relative Sum of Squares Relative	12.5735489
Standard Error of the Estimate	1.447615793
Adjusted Coefficient of Multiple Determination	0.9821861973
Coefficient a	1.882287784
Coefficient b	1801.565268
Coefficient c	3948.989706
Coefficient d	-12.77808877
Coefficient f	0.09212155302

Standard	Well	Net MFI	Expected Concentration (pg/mL)	Tested Concentration (pg/mL)	Recovery (%)	CV of Replicates (%)	Remarks
Standard 1	1(1,A1)	-	5300	-	-	-	
	2(1,B1)	1797.75		5299.664931	99.99		
Mean	-	1797.75		5299.664931	-		
Standard 2	3(1,C1)	815.25	1767	2011.339947	113.85	13.12099343	
	4(1,D1)	655.25		1669.905367	94.52		
Mean	-	735.25		1840.572657	-		
Standard 3	5(1,E1)	186.25		570.0040817	96.79		

Standard 3	6(1,F1)	184.75	589	566.0620184	96.12	0.49072164	
Mean	-	185.5		568.033049	-		
Standard 4	7(1,G1)	55.25	196	198.834555	101.29	0	
	8(1,H1)	55.25		198.834555	101.29		
Mean	-	55.25		198.834555	-		
Standard 5	9(1, A2)	15.25	65	61.33990055	93.75	12.13238488	
	10(1, B2)	18.25		72.85520856	111.34		
Mean	-	16.75		67.09599308	-		
Standard 6	11(1,C2)	6.75	22	26.00350838	119.22	21.95036234	
	12(1,D2)	5.25		19.01592894	87.19		
Mean	-	6		22.50971866	-		
Blank	15(1,G2)	0.25	0	-	-	-	
	16(1,H2)	-0.25		-	-		
Mean	-	0		-	-		

Quality Control	Well	Net MFI	Expected Concentration (pg/mL)	Tested Concentration (pg/mL)	CV of Replicates (%)	Remarks
Low Control	17(1,A3)	29.75	123	114.4925024	8.979943115	
	18(1,B3)	34.25		130.0184037		
Mean	-	32		122.2554531		
High Control	19(1,C3)	341.25	1057	957.1680316	2.257903727	
	20(1,D3)	354.25		988.2278139		
Mean	-	347.75		972.6979228		

Sample				Net MFI	Test Result (pg/mL)	CV of Replicates (%)
No.	Well	Sample ID	Grouping			
1	21(1,E3)	EN2183843	Pre	72.25	502.9729767	7.243316921
	22(1,F3)			64.25	453.9607589	
Mean	-			68.25	478.4668678	
2	23(1,G3)	EN2183837	Pre	39.25	283.786353	3.131477655
	24(1,H3)			41.25	307.0915262	
Mean	-			40.25	300.4389396	
3	25(1,A4)	EN2183830	Pre	45.25	333.4033679	6.549988895
	26(1,B4)			50.25	365.7866439	
Mean	-			47.75	349.5950059	
4	27(1,C4)	EN2183834	Pre	20.25	160.6959388	11.80769371
	28(1,D4)			24.25	189.9744638	

Mean	-			22.25	175.3352013	
5	29(1,E4)	EN2183835	Pre	48.75	356.1270063	0.644285054
	30(1,F4)			48.25	352.8968473	
Mean	-			48.5	354.5119268	
6	31(1,G4)	EN2183817	Pre	32.25	246.3220118	17.01611596
	32(1,H4)			42.25	313.7057315	
Mean	-			37.25	280.0138716	
7	33(1,A5)	EN2183859	Pre	67.75	475.5133859	12.29323937
	34(1,B5)			82.75	566.0529216	
Mean	-			75.25	520.7831538	
8	35(1,C5)	EN2183855	Pre	9.25	73.95743949	14.37668413
	36(1,D5)			11.25	90.69584699	
Mean	-			10.25	82.32664324	
9	37(1,E5)	EN2183863	Pre	27.75	214.9467159	5.638988567
	38(1,F5)			30.25	232.4705113	
Mean	-			29	223.7086136	
10	39(1,G5)	EN2183871	Pre	10.25	82.40208913	-
	40(1,H5)			0.25	< 21.8106995	
Mean	-			5.25	82.40208913	
11	41(1,A6)	EN2183852	Post	22.25	175.4435453	11.30202857
	42(1,B6)			18.75	149.4767562	
Mean	-			20.5	162.4601508	
12	43(1,C6)	EN2183845	Post	54.25	391.3299397	1.745656799
	44(1,D6)			52.75	381.7868507	
Mean	-			53.5	386.5583952	
13	45(1,E6)	EN2183847	Post	18.25	145.7041712	6.919567062
	46(1,F6)			20.25	160.6959388	
Mean	-			19.25	153.200055	
14	47(1,G6)	EN2183856	Post	276.75	1600.469805	30.7545623
	48(1,H6)			165.25	1028.708681	
Mean	-			221	1314.58924	
15	49(1,A7)	EN2183846	Post	63.25	447.7697958	35.55692093
	50(1,B7)			114.25	748.5566499	
Mean	-			88.75	598.1632229	
16	51(1,C7)	EN2183848	Post	23.25	182.7345979	11.45510554
	52(1,D7)			27.75	214.9467159	
Mean	-			25.5	198.8406569	
17	53(1,E7)			75.75	524.1475214	

17	54(1,F7)	EN20203773	Post	72.25	502.9729767	2.915463991
Mean	-			74	513.5602491	
18	55(1,G7)	EN20203775	Post	6.25	47.43231912	0
	56(1,H7)			6.25	47.43231912	
Mean	-			6.25	47.43231912	
19	57(1,A8)	EN20203776	Post	10.75	86.56657071	98.09665326
	58(1,B8)			68.25	478.5780693	
Mean	-			39.5	282.57232	
20	59(1,C8)	EN20203774	Post	56.25	403.9904297	-
	60(1,D8)			-3.75	< 21.8106995	
Mean	-			26.25	403.9904297	
22	61(1,E8)	EN2183865	Control	17.25	138.1062141	8.365572245
	62(1,F8)			15.25	122.6798011	
Mean	-			16.25	130.8930076	
23	63(1,G8)	EN2183861	Control	34.25	260.0368075	1.827669647
	64(1,H8)			35.25	266.8460177	
Mean	-			34.75	263.4414126	
25	65(1,A9)	EN2187421	Post	37.25	280.3735304	3.495999344
	66(1,B9)			35.25	266.8460177	
Mean	-			36.25	273.609774	
27	67(1,C9)	EN20212578	Control	81.75	560.1009542	3.292029943
	68(1,D9)			86.25	586.7986753	
Mean	-			84	573.4498148	
28	69(1,E9)	EN2183839	Control	8.75	69.67132681	14.74918569
	70(1,F9)			7.25	56.51141427	
Mean	-			8	63.09137054	
29	71(1,G9)	EN2183844	Control	8.25	65.3379533	22.45484574
	72(1,H9)			6.25	47.43231912	
Mean	-			7.25	56.38513621	
30	73(1,A10)	EN2183836	Control	134.25	860.3196948	27.42016665
	74(1,B10)			85.25	580.8847667	
Mean	-			109.75	720.6022307	
31	75(1,C10)	EN2183838	Control	14.75	118.7705175	2.289730618
	76(1,D10)			15.25	122.6798011	
Mean	-			15	120.7251593	
32	77(1,E10)	EN2183841	Control	54.25	391.3299397	40.08836097
	78(1,F10)			28.25	218.4711405	
Mean	-			41.25	304.9005401	

34	79(1,G10)	EN2183829	Control	177.25	1092.555432	3.168495244
	80(1,H10)			186.75	1142.634059	
Mean	-			182	1117.594745	
35	81(1,A11)	EN2183840	Control	35.25	266.8460177	6.795788013
	82(1,B11)			39.25	293.786353	
Mean	-			37.25	280.3161853	
36	83(1,C11)	EN2183831	Control	17.25	138.1062141	8.365572245
	84(1,D11)			15.25	122.6798011	
Mean	-			16.25	130.3930076	
37	85(1,E11)	EN2183832	Control	46.75	343.1746296	0.673165456
	86(1,F11)			46.25	339.9230854	
Mean	-			46.5	341.5488575	
38	87(1,G11)	EN2183872	Control	16.25	130.4334348	0
	88(1,H11)			16.25	130.4334348	
Mean	-			16.25	130.4334348	
39	89(1,A12)	EN20212576	Control	122.75	796.3938055	12.28315271
	90(1,B12)			150.25	947.8938265	
Mean	-			136.5	872.143866	
40	91(1,C12)	EN2183873	Control	19.25	153.2325479	9.556853805
	92(1,D12)			22.25	175.4435453	
Mean	-			20.75	164.3380466	
41	93(1,E12)	EN2183860	Control	95.25	639.565911	9.21296367
	94(1,F12)			110.75	728.7024232	
Mean	-			103	684.1341671	
43	95(1,G12)	EN2183874	Pre	28.75	221.9855217	4.645046459
	96(1,H12)			26.75	207.8668326	
Mean				27.75	214.9261772	

PRIMANEXUS®
LEADING THE CONNECTION
28-1B, Jalan Puteri 1/2, Bandar Puteri Puchong, 47100 Selangor, Malaysia.
Tel: +603 5891 0194 | Fax: +603 58910195 | Website: www.primanexus.com.my
Company registered number: 1055479-X

IL-6
Logistic5p: y = a+((b-a)/(1+((x/c)^d))^f)

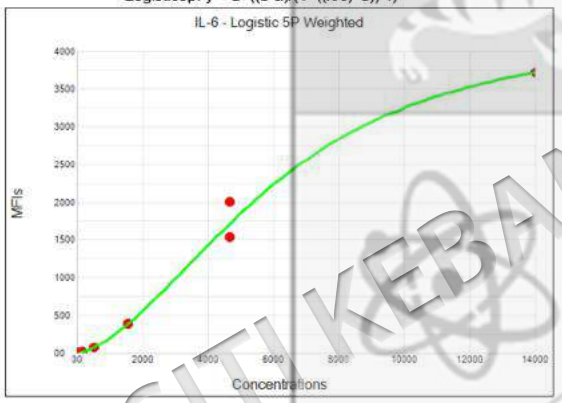

R-Squared	0.9957518364
Sum of Residuals	120.8291248
Average Residuals	10.98446589
Relative Sum of Squares Absolute	115195.7559
Relative Sum of Squares Relative	0.7571553735
Standard Error of the Estimate	0.3552359248
Adjusted Coefficient of Multiple Determination	0.9929197274
Coefficient a	-0.7681398614
Coefficient b	4275.798644
Coefficient c	7599.96746
Coefficient d	-2.330326596
Coefficient f	0.6453723614

Standard	Well	Net MFI	Expected Concentration (pg/mL)	Tested Concentration (pg/mL)	Recovery (%)	CV of Replicates (%)	Remarks
Standard 1	1(1,A1)	-	14000	-	-	-	
	2(1,B1)	3721		14014.97038	100.11		
Mean	-	3721		14014.97038	-		
Standard 2	3(1,C1)	2006.5	4667	5388.600708	115.47	16.5849342	
	4(1,D1)	1541		4257.385135	91.23		
Mean	-	1773.75		4822.992921	-		
Standard 3	5(1,E1)	386		1553.89499	99.89		

Standard 3	6(1,F1)	391	1556	1567.558041	100.77	0.619021718	
Mean	-	388.5		1560.726515	-		
Standard 4	7(1,G1)	73		511.3798089	98.62		
	8(1,H1)	75	519	520.5748519	100.4	1.260109083	
Mean	-	74		515.9773304	-		
Standard 5	9(1, A2)	14		175.36687	101.46		
	10(1, B2)	13.5	173	171.3956603	99.16	1.619592107	
Mean	-	13.75		173.3812652	-		
Standard 6	11(1,C2)	2		57.60084178	99.98		
	12(1,D2)	2	58	57.60084178	99.98	0	
Mean	-	2		57.60084178	-		
Blank	15(1,G2)	-1		-	-		
	16(1,H2)	1	0	-	-	-	
Mean	-	0		-			

Quality Control	Well	Net MFI	Expected Concentration (pg/mL)	Tested Concentration (pg/mL)	CV of Replicates (%)	Remarks
Low Control	17(1,A3)	36		321.6946401		
	18(1,B3)	38.5	314	336.0875794	3.094442102	
Mean	-	37.25		328.8911097		
High Control	19(1,C3)	871		2742.3379		
	20(1,D3)	1011	2856	3059.71749	7.735922706	
Mean	-	941		2901.027695		

Sample				Net MFI	Test Result (pg/mL)	CV of Replicates (%)
No.	Well	Sample ID	Grouping			
1	21(1,E3)	EN2183843	Pre	1.5	100.909051	11.68221618
	22(1,F3)			1	85.50978463	
Mean	-			1.25	93.20941783	
2	23(1,G3)	EN2183837	Pre	1	85.50978463	20.92092023
	24(1,H3)			2	115.2016836	
Mean	-			1.5	100.3557341	
3	25(1,A4)	EN2183830	Pre	0.5	68.5541543	23.35558552
	26(1,B4)			0	49.12033794	
Mean	-			0.25	58.83724612	
4	27(1,C4)	EN2183834	Pre	2	115.2016836	56.87194835
	28(1,D4)			0	49.12033794	

Mean	-			1	82.16101075	
5	29(1,E4)	EN2183835	Pre	0.5	68.5541543	-
	30(1,F4)			-1	< 57.613168	
Mean	-			-0.25	68.5541543	
6	31(1,G4)	EN2183817	Pre	0	49.12033794	38.2250629
	32(1,H4)			1	85.50978463	
Mean	-			0.5	67.31506129	
7	33(1,A5)	EN2183859	Pre	0	49.12033794	0
	34(1,B5)			0	49.12033794	
Mean	-			0	49.12033794	
8	35(1,C5)	EN2183855	Pre	0	49.12033794	38.2250629
	36(1,D5)			1	85.50978463	
Mean	-			0.5	67.31506129	
9	37(1,E5)	EN2183863	Pre	0	49.12033794	0
	38(1,F5)			0	49.12033794	
Mean	-			0	49.12033794	
10	39(1,G5)	EN2183871	Pre	0	49.12033794	0
	40(1,H5)			0	49.12033794	
Mean	-			0	49.12033794	
11	41(1,A6)	EN2183852	Post	1	85.50978463	0
	42(1,B6)			1	85.50978463	
Mean	-			1	85.50978463	
12	43(1,C6)	EN2183845	Post	1.5	100.909051	23.64325557
	44(1,D6)			3	141.4228387	
Mean	-			2.25	121.1659449	
13	45(1,E6)	EN2183847	Post	1.5	100.909051	11.68221618
	46(1,F6)			1	85.50978463	
Mean	-			1.25	93.20941783	
14	47(1,G6)	EN2183856	Post	1	85.50978463	38.2250629
	48(1,H6)			0	49.12033794	
Mean	-			0.5	67.31506129	
15	49(1,A7)	EN2183846	Post	1	85.50978463	20.92092023
	50(1,B7)			2	115.2016836	
Mean	-			1.5	100.3557341	
16	51(1,C7)	EN2183848	Post	1	85.50978463	15.56424075
	52(1,D7)			0.5	68.5541543	
Mean	-			0.75	77.03196947	
17	53(1,E7)			0	49.12033794	

17	54(1,F7)	EN20203773	Post	0	49.12033794	0
Mean	-			0	49.12033794	
18	55(1,G7)	EN20203775	Post	0	49.12033794	0
	56(1,H7)			0	49.12033794	
Mean	-			0	49.12033794	
19	57(1,A8)	EN20203776	Post	0	49.12033794	0
	58(1,B8)			0	49.12033794	
Mean	-			0	49.12033794	
20	59(1,C8)	EN20203774	Post	0	49.12033794	0
	60(1,D8)			0	49.12033794	
Mean	-			0	49.12033794	
22	61(1,E8)	EN2183865	Control	0	49.12033794	0
	62(1,F8)			0	49.12033794	
Mean	-			0	49.12033794	
23	63(1,G8)	EN2183861	Control	0	49.12033794	-
	64(1,H8)			-1	< 57.613168	
Mean	-			-0.5	49.12033794	
25	65(1,A9)	EN2187421	Post	0	49.12033794	0
	66(1,B9)			0	49.12033794	
Mean	-			0	49.12033794	
27	67(1,C9)	EN20212578	Control	1	85.50978463	0
	68(1,D9)			1	85.50978463	
Mean	-			1	85.50978463	
28	69(1,E9)	EN2183839	Control	2	115.2016836	20.92092023
	70(1,F9)			1	85.50978463	
Mean	-			1.5	100.3557341	
29	71(1,G9)	EN2183844	Control	-1	< 57.613168	-
	72(1,H9)			0	49.12033794	
Mean	-			-0.5	49.12033794	
30	73(1,A10)	EN2183836	Control	3	141.4228387	34.84426269
	74(1,B10)			1	85.50978463	
Mean	-			2	113.4663117	
31	75(1,C10)	EN2183838	Control	0.5	68.5541543	35.90066541
	76(1,D10)			2	115.2016836	
Mean	-			1.25	91.87791893	
32	77(1,E10)	EN2183841	Control	1	85.50978463	38.2250629
	78(1,F10)			0	49.12033794	
Mean	-			0.5	67.31506129	

34	79(1,G10)	EN2183829	Control	1	85.50978463	38.2250629
	80(1,H10)			0	49.12033794	
Mean	-			0.5	67.31506129	
35	81(1,A11)	EN2183840	Control	0	49.12033794	68.50701806
	82(1,B11)			3	141.4228387	
Mean	-			1.5	95.27158833	
36	83(1,C11)	EN2183831	Control	-1	< 57.613168	-
	84(1,D11)			0	49.12033794	
Mean	-			-0.5	49.12033794	
37	85(1,E11)	EN2183832	Control	0.5	68.5541543	23.35558552
	86(1,F11)			0	49.12033794	
Mean	-			0.25	58.83724612	
38	87(1,G11)	EN2183872	Control	-2	< 57.613168	-
	88(1,H11)			0	49.12033794	
Mean	-			-1	49.12033794	
39	89(1,A12)	EN20212576	Control	0	49.12033794	0
	90(1,B12)			0	49.12033794	
Mean	-			0	49.12033794	
40	91(1,C12)	EN2183873	Control	1	85.50978463	0
	92(1,D12)			1	85.50978463	
Mean	-			1	85.50978463	
41	93(1,E12)	EN2183860	Control	-1	< 57.613168	-
	94(1,F12)			-0.5	24.39707603	
Mean	-			-0.75	24.39707603	
43	95(1,G12)	EN2183874	Pre	0	49.12033794	0
	96(1,H12)			0	49.12033794	
Mean	-			0	49.12033794	

PRIMANEXUS®
LEADING THE CONNECTION
28-1B, Jalan Puteri 1/2, Bandar Puteri Puchong, 47100 Selangor, Malaysia.
Tel: +603 5891 0194 | Fax: +603 58910195 | Website: www.primanexus.com.my
Company registered number: 1055479-X

TNF-alpha
Logistic5p: y = a+((b-a)/(1+((x/c)^d))^f)

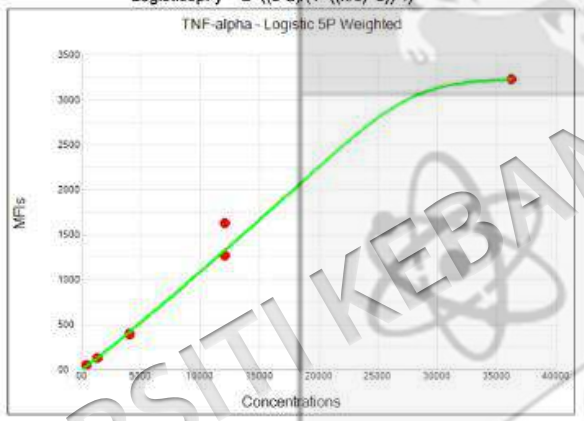

R-Squared	0.9918461212
Sum of Residuals	191.044744
Average Residuals	14.69574954
Relative Sum of Squares Absolute	94191.13737
Relative Sum of Squares Relative	8.404635006
Standard Error of the Estimate	1.024977744
Adjusted Coefficient of Multiple Determination	0.9877691818
Coefficient a	0.4423526107
Coefficient b	3236.146885
Coefficient c	28179.67471
Coefficient d	-11.9752142
Coefficient f	0.08825176224

Standard	Well	Net MFI	Expected Concentration (pg/mL)	Tested Concentration (pg/mL)	Recovery (%)	CV of Replicates (%)	Remarks
Standard 1	1(1,A1)	-	36250	-	-	-	
	2(1,B1)	3222.5		36246.84049	99.99		
Mean	-	3222.5		36246.84049	-		
Standard 2	3(1,C1)	1622	12083	14657.13661	121.3	16.51135482	
	4(1,D1)	1266		11592.42403	95.94		
Mean	-	1444		13124.78032	-		
Standard 3	5(1,E1)	393		3829.430247	95.08		

Standard 3	6(1,F1)	384	4028	3746.304344	93.01	1.551767408	
Mean	-	389.5		3787.867295	-		
Standard 4	7(1,G1)	130	1343	1341.480548	99.92	0.518435592	
	8(1,H1)	129		1331.681023	99.19		
Mean	-	129.5		1336.580785	-		
Standard 5	9(1, A2)	41	448	447.0116819	99.88	1.629620623	
	10(1, B2)	42		457.4337495	102.21		
Mean	-	41.5		452.2227157	-		
Standard 6	11(1,C2)	14	149	158.4975258	106.25	5.124312564	
	12(1,D2)	13		147.4130514	98.82		
Mean	-	13.5		152.9552886	-		
Standard 7	13(1, E2)	5	50	56.49882741	113.62	16.49813579	
	14(1, F2)	4		44.69375744	89.88		
Mean	-	4.5		50.59629242	-		
Blank	15(1,G2)	0	0	-	-	-	
	16(1,H2)	0		-	-		
Mean	-	0		-	-		

Quality Control	Well	Net MFI	Expected Concentration (pg/mL)	Tested Concentration (pg/mL)	CV of Replicates (%)	Remarks
Low Control	17(1,A3)	100	1135	1045.556394	7.905406175	
	18(1,B3)	112.5		1169.370035		
Mean	-	106.25		1107.463215		
High Control	19(1,C3)	997.5	9172	9250.83762	0.434769409	
	20(1,D3)	1004		9307.892426		
Mean	-	1000.75		9279.365023		

Sample				Net MFI	Test Result (pg/mL)	CV of Replicates (%)
No.	Well	Sample ID	Grouping			
1	21(1,E3)	EN2183843	Pre	-0.5	< 49.72565	0
	22(1,F3)			-1	< 49.72565	
Mean	-			-0.75	< 49.72565	
2	23(1,G3)	EN2183837	Pre	0	< 49.72565	0
	24(1,H3)			-1	< 49.72565	
Mean	-			-0.5	< 49.72565	
3	25(1,A4)	EN2183830	Pre	1.5	28.36520805	41.56338307
	26(1,B4)			1	15.47939022	

Mean	-			1.25	21.92229913	
4	27(1,C4)	EN2183834	Pre	-1	< 49.72565	0
	28(1,D4)			-0.5	< 49.72565	
Mean	-			-0.75	< 49.72565	
5	29(1,E4)	EN2183835	Pre	-1	< 49.72565	0
	30(1,F4)			-2	< 49.72565	
Mean	-			-1.5	< 49.72565	
6	31(1,G4)	EN2183817	Pre	-3	< 49.72565	0
	32(1,H4)			0	< 49.72565	
Mean	-			-1.5	< 49.72565	
7	33(1,A5)	EN2183859	Pre	-2	< 49.72565	0
	34(1,B5)			-1	< 49.72565	
Mean	-			-1.5	< 49.72565	
8	35(1,C5)	EN2183855	Pre	1	15.47939022	63.78411964
	36(1,D5)			2	40.91407391	
Mean	-			1.5	28.19673207	
9	37(1,E5)	EN2183863	Pre	1	15.47939022	0
	38(1,F5)			1	15.47939022	
Mean	-			1	15.47939022	
10	39(1,G5)	EN2183871	Pre	2	40.91407391	63.78411964
	40(1,H5)			1	15.47939022	
Mean	-			1.5	28.19673207	
11	41(1,A6)	EN2183852	Post	0	< 49.72565	-
	42(1,B6)			1	15.47939022	
Mean	-			0.5	15.47939022	
12	43(1,C6)	EN2183845	Post	1	15.47939022	-
	44(1,D6)			0	< 49.72565	
Mean	-			0.5	15.47939022	
13	45(1,E6)	EN2183847	Post	-1	< 49.72565	0
	46(1,F6)			0	< 49.72565	
Mean	-			-0.5	< 49.72565	
14	47(1,G6)	EN2183856	Post	3.5	77.45306296	134.9698465
	48(1,H6)			0.5	1.807905543	
Mean	-			2	39.63048425	
15	49(1,A7)	EN2183846	Post	1.5	28.36520805	41.56338307
	50(1,B7)			1	15.47939022	
Mean	-			1.25	21.92229913	
16	51(1,C7)			1	15.47939022	

16	52(1,D7)	EN2183848	Post	1	15.47939022	0
Mean	-			1	15.47939022	
17	53(1,E7)	EN20203773	Post	-1	< 49.72565	0
	54(1,F7)			-1	< 49.72565	
Mean	-			-1	< 49.72565	
18	55(1,G7)	EN20203775	Post	0.5	1.807905543	-
	56(1,H7)			0	< 49.72565	
Mean	-			0.25	1.807905543	
19	57(1,A8)	EN20203776	Post	1	15.47939022	0
	58(1,B8)			1	15.47939022	
Mean	-			1	15.47939022	
20	59(1,C8)	EN20203774	Post	1	15.47939022	0
	60(1,D8)			1	15.47939022	
Mean	-			1	15.47939022	
22	61(1,E8)	EN2183865	Control	-1.5	< 49.72565	0
	62(1,F8)			-2	< 49.72565	
Mean	-			-1.75	< 49.72565	
23	63(1,G8)	EN2183861	Control	-1	< 49.72565	0
	64(1,H8)			-1	< 49.72565	
Mean	-			-1	< 49.72565	
25	65(1,A9)	EN2187421	Post	0	< 49.72565	0
	66(1,B9)			-1	< 49.72565	
Mean	-			-0.5	< 49.72565	
27	67(1,C9)	EN20212578	Control	2	40.91407391	0
	68(1,D9)			2	40.91407391	
Mean	-			2	40.91407391	
28	69(1,E9)	EN2183839	Control	1	15.47939022	-
	70(1,F9)			0	< 49.72565	
Mean	-			0.5	15.47939022	
29	71(1,G9)	EN2183844	Control	-2	< 49.72565	-
	72(1,H9)			-1	< 49.72565	
Mean	-			-1.5	< 49.72565	
30	73(1,A10)	EN2183836	Control	0	< 49.72565	-
	74(1,B10)			1	15.47939022	
Mean	-			0.5	15.47939022	
31	75(1,C10)	EN2183838	Control	-1	< 49.72565	0
	76(1,D10)			-1	< 49.72565	
Mean	-			-1	< 49.72565	

32	77(1,E10)	EN2183841	Control	2	40.91407391	-
	78(1,F10)			0	< 49.72565	
Mean	-			1	40.91407391	
34	79(1,G10)	EN2183829	Control	3	65.41270772	32.58473515
	80(1,H10)			2	40.91407391	
Mean	-			2.5	53.16339082	
35	81(1,A11)	EN2183840	Control	-2	< 49.72565	0
	82(1,B11)			0	< 49.72565	
Mean	-			-1	< 49.72565	
36	83(1,C11)	EN2183831	Control	0	< 49.72565	-
	84(1,D11)			1	15.47939022	
Mean	-			0.5	15.47939022	
37	85(1,E11)	EN2183832	Control	0	< 49.72565	0
	86(1,F11)			0	< 49.72565	
Mean	-			0	< 49.72565	
38	87(1,G11)	EN2183872	Control	-3	< 49.72565	0
	88(1,H11)			-2.5	< 49.72565	
Mean	-			-2.75	< 49.72565	
39	89(1,A12)	EN20212576	Control	-2	< 49.72565	0
	90(1,B12)			0	< 49.72565	
Mean	-			-1	< 49.72565	
40	91(1,C12)	EN2183873	Control	0	< 49.72565	0
	92(1,D12)			-1	< 49.72565	
Mean	-			-0.5	< 49.72565	
41	93(1,E12)	EN2183860	Control	0	< 49.72565	0
	94(1,F12)			0	< 49.72565	
Mean	-			0	< 49.72565	
43	95(1,G12)	EN2183874	Pre	-1	< 49.72565	0
	96(1,H12)			-1	< 49.72565	
Mean	-			-1	< 49.72565	

PRIMANEXUS®
LEADING THE CONNECTION
28-1B, Jalan Puteri 1/2, Bandar Puteri Puchong, 47100 Selangor, Malaysia.
Tel: +603 5891 0194 | Fax: +603 58910195 | Website: www.primanexus.com.my
Company registered number: 1055479-X

TGF-alpha
Logistic5p: y = a+((b-a)/(1+((x/c)^d))^f)

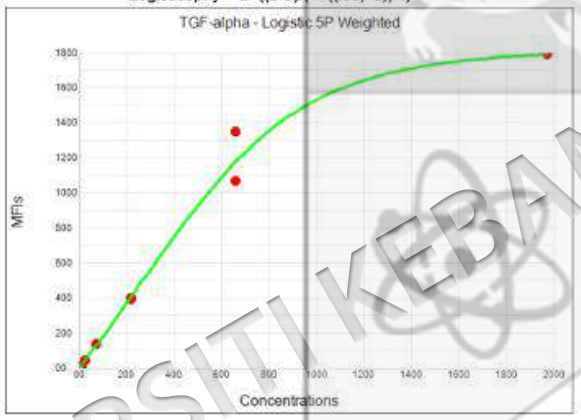

R-Squared	0.9947698435
Sum of Residuals	54.96805257
Average Residuals	4.228311736
Relative Sum of Squares Absolute	42054.84099
Relative Sum of Squares Relative	4.495274686
Standard Error of the Estimate	0.7496061204
Adjusted Coefficient of Multiple Determination	0.9921547652
Coefficient a	-0.3935405307
Coefficient b	1835.203428
Coefficient c	933.9275911
Coefficient d	-3.362276728
Coefficient f	0.3076413323

Standard	Well	Net MFI	Expected Concentration (pg/mL)	Tested Concentration (pg/mL)	Recovery (%)	CV of Replicates (%)	Remarks
Standard 1	1(1,A1)	-	1970	-	-	-	
	2(1,B1)	1790		1948.047273	98.89		
Mean	-	1790		1948.047273	-		
Standard 2	3(1,C1)	1349.5	657	795.4072522	121.13	21.39040072	
	4(1,D1)	1069.5		586.4041657	89.3		
Mean	-	1209.5		690.9057089	-		
Standard 3	5(1,E1)	397		213.1759443	97.39		

Standard 3	6(1,F1)	394	219	211.6092613	96.67	0.521586972	
Mean	-	395.5		212.3926028	-		
Standard 4	7(1,G1)	134	73	74.58872879	102.23	0.506880357	
	8(1,H1)	135		75.12533174	102.96		
Mean	-	134.5		74.85703027	-		
Standard 5	9(1, A2)	42.5	24	24.72544314	101.66	5.359611167	
	10(1, B2)	46		26.67336408	109.67		
Mean	-	44.25		25.69940361	-		
Standard 6	11(1,C2)	13	8	8.025019043	98.99	5.302112661	
	12(1,D2)	12		7.445022463	91.83		
Mean	-	12.5		7.735020753	-		
Standard 7	13(1, E2)	4	3	2.731823939	101.09	0	
	14(1, F2)	4		2.731823939	101.09		
Mean	-	4		2.731823939	-		
Blank	15(1,G2)	0	0	-	-	-	
	16(1,H2)	0		-	-		
Mean	-	0		-	-		

Quality Control	Well	Net MFI	Expected Concentration (pg/mL)	Tested Concentration (pg/mL)	CV of Replicates (%)	Remarks
Low Control	17(1,A3)	81.5	43.9	46.20327258	5.987039329	
	18(1,B3)	89		50.28821673		
Mean	-	85.25		48.24574466		
High Control	19(1,C3)	704	388	375.0146439	6.827234888	
	20(1,D3)	774		413.0595902		
Mean	-	739		394.0371171		

Sample				Net MFI	Test Result (pg/mL)	CV of Replicates (%)
No.	Well	Sample ID	Grouping			
1	21(1,E3)	EN2183843	Pre	4	5.463647878	7.361309416
	22(1,F3)			4.5	6.063671576	
Mean	-			4.25	5.763659727	
2	23(1,G3)	EN2183837	Pre	2	3.037209999	23.64077255
	24(1,H3)			3	4.25646004	
Mean	-			2.5	3.646835019	
3	25(1,A4)	EN2183830	Pre	4	5.463647878	71.31956861
	26(1,B4)			1	1.80036579	

Mean	-			2.5	3.632006834	
4	27(1,C4)	EN2183834	Pre	2	3.037209999	15.95049828
	28(1,D4)			1.5	2.421534305	
Mean	-			1.75	2.729372152	
5	29(1,E4)	EN2183835	Pre	12	14.89004493	5.302112661
	30(1,F4)			13	16.05003809	
Mean	-			12.5	15.47004151	
6	31(1,G4)	EN2183817	Pre	2	3.037209999	40.38653914
	32(1,H4)			4	5.463647878	
Mean	-			3	4.250428938	
7	33(1,A5)	EN2183859	Pre	7	9.036674348	4.784923001
	34(1,B5)			6.5	8.445184144	
Mean	-			6.75	8.740929246	
8	35(1,C5)	EN2183855	Pre	2	3.037209999	23.64077255
	36(1,D5)			3	4.25646004	
Mean	-			2.5	3.646835019	
9	37(1,E5)	EN2183863	Pre	2	3.037209999	23.64077255
	38(1,F5)			3	4.25646004	
Mean	-			2.5	3.646835019	
10	39(1,G5)	EN2183871	Pre	5	6.661657691	0
	40(1,H5)			5	6.661657691	
Mean	-			5	6.661657691	
11	41(1,A6)	EN2183852	Post	3.5	4.861345557	9.382052444
	42(1,B6)			3	4.25646004	
Mean	-			3.25	4.558902799	
12	43(1,C6)	EN2183845	Post	5	6.661657691	0
	44(1,D6)			5	6.661657691	
Mean	-			5	6.661657691	
13	45(1,E6)	EN2183847	Post	5	6.661657691	0
	46(1,F6)			5	6.661657691	
Mean	-			5	6.661657691	
14	47(1,G6)	EN2183856	Post	7	9.03667435	21.39578115
	48(1,H6)			5	6.66165769	
Mean	-			6	7.849166019	
15	49(1,A7)	EN2183846	Post	3	4.25646004	50.85515356
	50(1,B7)			7	9.036674348	
Mean	-			5	6.646567194	
16	51(1,C7)			2	3.037209999	

16	52(1,D7)	EN2183848	Post	2	3.037209999	0
Mean	-			2	3.037209999	
17	53(1,E7)	EN20203773	Post	4.5	6.063671576	7.361309416
	54(1,F7)			4	5.463647878	
Mean	-			4.25	5.763659727	
18	55(1,G7)	EN20203775	Post	3	4.25646004	0
	56(1,H7)			3	4.25646004	
Mean	-			3	4.25646004	
19	57(1,A8)	EN20203776	Post	7	9.036674348	0
	58(1,B8)			7	9.036674348	
Mean	-			7	9.036674348	
20	59(1,C8)	EN20203774	Post	4	5.463647878	0
	60(1,D8)			4	5.463647878	
Mean	-			4	5.463647878	
22	61(1,E8)	EN2183865	Control	2.5	3.646594398	12.93229738
	62(1,F8)			2	3.037209999	
Mean	-			2.25	3.342902197	
23	63(1,G8)	EN2183861	Control	4	5.463647878	0
	64(1,H8)			4	5.463647878	
Mean	-			4	5.463647878	
25	65(1,A9)	EN2187421	Post	0	0.5302489315	77.07050292
	66(1,B9)			1	1.80036579	
Mean	-			0.5	1.165307361	
27	67(1,C9)	EN20212578	Control	3	4.25646004	17.5638113
	68(1,D9)			4	5.463647878	
Mean				3.5	4.860053959	
28	69(1,E9)	EN2183839	Control	4	5.463647878	71.31956861
	70(1,F9)			1	1.80036579	
Mean	-			2.5	3.632006834	
29	71(1,G9)	EN2183844	Control	1	1.80036579	77.07050292
	72(1,H9)			0	0.5302489315	
Mean	-			0.5	1.165307361	
30	73(1,A10)	EN2183836	Control	5	6.661657691	52.8488814
	74(1,B10)			2	3.037209999	
Mean	-			3.5	4.849433845	
31	75(1,C10)	EN2183838	Control	1	1.80036579	0
	76(1,D10)			1	1.80036579	
Mean	-			1	1.80036579	

32	77(1,E10)	EN2183841	Control	4	5.463647878	71.31956861
	78(1,F10)			1	1.80036579	
Mean	-			2.5	3.632006834	
34	79(1,G10)	EN2183829	Control	26	30.92345093	5.384292865
	80(1,H10)			24	28.65513336	
Mean	-			25	29.78929215	
35	81(1,A11)	EN2183840	Control	1	1.80036579	71.31956861
	82(1,B11)			4	5.463647878	
Mean	-			2.5	3.632006834	
36	83(1,C11)	EN2183831	Control	1	1.80036579	0
	84(1,D11)			1	1.80036579	
Mean	-			1	1.80036579	
37	85(1,E11)	EN2183832	Control	2	3.037209999	38.15781812
	86(1,F11)			1	1.80036579	
Mean	-			1	1.80036579	
38	87(1,G11)	EN2183872	Control	1	1.80036579	0
	88(1,H11)			1	1.80036579	
Mean	-			1	1.80036579	
39	89(1,A12)	EN20212576	Control	8	10.21575516	14.55844724
	90(1,B12)			10	12.56042049	
Mean	-			9	11.38808783	
40	91(1,C12)	EN2183873	Control	1	1.80036579	38.15781812
	92(1,D12)			2	3.037209999	
Mean	-			1.5	2.418787894	
41	93(1,E12)	EN2183860	Control	4	5.463647878	13.9727755
	94(1,F12)			5	6.661657691	
Mean	-			4.5	6.062652784	
43	95(1,G12)	EN2183874	Pre	2	3.037209999	0
	96(1,H12)			2	3.037209999	
Mean	-			2	3.037209999	

PRIMANEXUS®
LEADING THE CONNECTION
28-1B, Jalan Puteri 1/2, Bandar Puteri Puchong, 47100 Selangor, Malaysia.
Tel: +603 5891 0194 | Fax: +603 58910195 | Website: www.primanexus.com.my
Company registered number: 1055479-X

FGF Basic/FGF2/bFGF
Logistic5p: y = a+((b-a)/(1+((x/c)^d))^f)

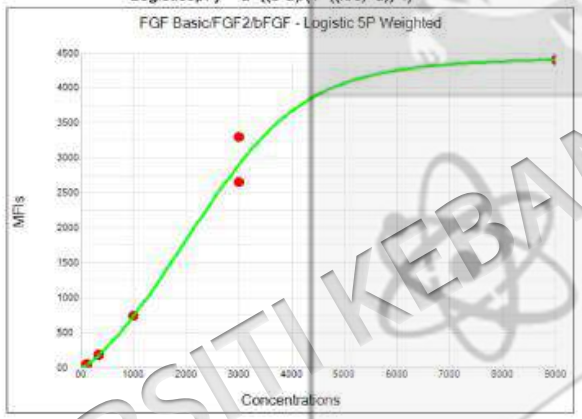

R-Squared	0.9597696665
Sum of Residuals	135.4034393
Average Residuals	10.41564918
Relative Sum of Squares Absolute	210211.4772
Relative Sum of Squares Relative	1.285833515
Standard Error of the Estimate	0.4009104505
Adjusted Coefficient of Multiple Determination	0.9396544998
Coefficient a	-1.580580543
Coefficient b	4440.184436
Coefficient c	3852.232417
Coefficient d	-4.291339469
Coefficient f	0.3091383487

Standard	Well	Net MFI	Expected Concentration (pg/mL)	Tested Concentration (pg/mL)	Recovery (%)	CV of Replicates (%)	Remarks
Standard 1	1(1,A1)	-	9000	-	-	-	
	2(1,B1)	4404.5		8982.215021	99.8		
Mean	-	4404.5		8982.215021	-		
Standard 2	3(1,C1)	3293.5	3000	3438.991058	114.63	15.73248443	
	4(1,D1)	2659.5		2750.444433	91.68		
Mean	-	2976.5		3094.717746	-		
Standard 3	5(1,E1)	734		993.9289008	99.39		

Standard 3	6(1,F1)	738	1000	998.0126432	99.8	0.289932386	
Mean	-	736		995.970772	-		
Standard 4	7(1,G1)	170.5	333	332.2669392	99.68	3.44753833	
	8(1,H1)	182		348.8715824	104.66		
Mean	-	176.25		340.5692608	-		
Standard 5	9(1, A2)	39.5	111	112.8628524	101.58	5.457605869	
	10(1, B2)	35.5		104.4755251	94.03		
Mean	-	37.5		108.6691887	-		
Standard 6	11(1,C2)	7.5	37	36.17594937	97.68	5.565674643	
	12(1,D2)	8.5		39.14002951	105.68		
Mean	-	8		37.65798944	-		
Standard 7	13(1, E2)	0.5	12	11.91361306	96.5	20.76803633	
	14(1, F2)	1.5		16.01498962	129.72		
Mean	-	1		13.96430134	-		
Blank	15(1,G2)	0	0	-	-	-	
	16(1,H2)	0		-	-		
Mean	-	0		-	-		

Quality Control	Well	Net MFI	Expected Concentration (pg/mL)	Tested Concentration (pg/mL)	CV of Replicates (%)	Remarks
Low Control	17(1,A3)	89.5	205	205.6866598	2.290712742	
	18(1,B3)	93.5		212.4597047		
Mean	-	91.5		209.0731823		
High Control	19(1,C3)	1624	1823	1822.386321	2.163105613	
	20(1,D3)	1688.5		1879.000763		
Mean	-	1656.25		1850.693542		

Sample				Net MFI	Test Result (pg/mL)	CV of Replicates (%)
No.	Well	Sample ID	Grouping			
1	21(1,E3)	EN2183843	Pre	0	19.3684271	-
	22(1,F3)			-2	< 12.3456790	
Mean	-			0	19.3684271	
2	23(1,G3)	EN2183837	Pre	-0.5	14.54111376	106.4031777
	24(1,H3)			-1.5	2.054692932	
Mean	-			-1	8.297903346	
3	25(1,A4)	EN2183830	Pre	-0.5	14.54111376	0
	26(1,B4)			-0.5	14.54111376	

Mean	-			-0.5	14.54111376	
4	27(1,C4)			-0.5	14.54111376	
	28(1,D4)	EN2183834	Pre	0	19.3684271	20.13254035
Mean	-			-0.25	16.95477043	
5	29(1,E4)			1	28.02710685	
	30(1,F4)	EN2183835	Pre	-0.5	14.54111376	44.80355077
Mean	-			0.25	21.28411031	
6	31(1,G4)			-2.5	< 12.3456790	
	32(1,H4)	EN2183817	Pre	-1	9.103897017	
Mean	-			-1	9.103897017	
7	33(1,A5)			-0.5	14.54111376	
	34(1,B5)	EN2183859	Pre	-0.5	14.54111376	0
Mean	-			-0.5	14.54111376	
8	35(1,C5)			-1.5	2.054692932	
	36(1,D5)	EN2183855	Pre	-0.5	14.54111376	106.4031777
Mean	-			-1	8.297903346	
9	37(1,E5)			-1.5	2.054692932	
	38(1,F5)	EN2183863	Pre	-1.5	2.054692932	0
Mean	-			-1.5	2.054692932	
10	39(1,G5)			-1.5	2.054692932	
	40(1,H5)	EN2183871	Pre	-1.5	2.054692932	0
Mean	-			-1.5	2.054692932	
11	41(1,A6)			-1.5	2.054692932	
	42(1,B6)	EN2183852	Post	-0.5	14.54111376	106.4031777
Mean	-			-1	8.297903346	
12	43(1,C6)			0	19.3684271	
	44(1,D6)	EN2183845	Post	-0.5	14.54111376	20.13254035
Mean	-			-0.25	16.95477043	
13	45(1,E6)			-0.5	14.54111376	
	46(1,F6)	EN2183847	Post	-1.5	2.054692932	106.4031777
Mean	-			-1	8.297903346	
14	47(1,G6)			1.5	32.02997924	
	48(1,H6)	EN2183856	Post	-0.5	14.54111376	53.10803152
Mean	-			0.5	23.2855465	
15	49(1,A7)			-0.5	14.54111376	
	50(1,B7)	EN2183846	Post	-0.5	14.54111376	0
Mean	-			-0.5	14.54111376	
16	51(1,C7)			0	19.3684271	

16	52(1,D7)	EN2183848	Post	-0.5	14.54111376	20.13254035
Mean	-			-0.25	16.95477043	
17	53(1,E7)	EN20203773	Post	-2.5	< 12.3456790	-
	54(1,F7)			-1.5	2.054692932	
Mean	-			-1.5	2.054692932	
18	55(1,G7)	EN20203775	Post	-1.5	2.054692932	106.4031777
	56(1,H7)			-0.5	14.54111376	
Mean	-			-1	8.297903348	
19	57(1,A8)	EN20203776	Post	-1.5	2.054692932	0
	58(1,B8)			-1.5	2.054692932	
Mean	-			-1.5	2.054692932	
20	59(1,C8)	EN20203774	Post	-1.5	2.054692932	0
	60(1,D8)			-1.5	2.054692932	
Mean	-			-1.5	2.054692932	
22	61(1,E8)	EN2183865	Control	-2.5	< 12.3456790	0
	62(1,F8)			-2	< 12.3456790	
Mean	-			-2.25	< 12.3456791	
23	63(1,G8)	EN2183861	Control	-1.5	2.054692932	0
	64(1,H8)			-1.5	2.054692932	
Mean	-			-1.5	2.054692932	
25	65(1,A9)	EN2187421	Post	5.5	59.9799578	8.106558768
	66(1,B9)			4.5	53.47640891	
Mean	-			5	56.72818335	
27	67(1,C9)	EN20212578	Control	1.5	32.02997924	53.10803152
	68(1,D9)			-0.5	14.54111376	
Mean	-			0.5	23.2855465	
28	69(1,E9)	EN2183839	Control	0.5	23.82722612	34.22755868
	70(1,F9)			-0.5	14.54111376	
Mean	-			0	19.18416994	
29	71(1,G9)	EN2183844	Control	-0.5	14.54111376	0
	72(1,H9)			-0.5	14.54111376	
Mean	-			-0.5	14.54111376	
30	73(1,A10)	EN2183836	Control	4.5	53.47640891	66.21741925
	74(1,B10)			0	19.3684271	
Mean	-			2.25	36.422418	
31	75(1,C10)	EN2183838	Control	1.5	32.02997924	124.3710258
	76(1,D10)			-1.5	2.054692932	
Mean	-			0	17.04233608	

32	77(1,E10)	EN2183841	Control	-0.5	14.54111376	106.4031777
	78(1,F10)			-1.5	2.054692932	
Mean	-			-1	8.297903346	
34	79(1,G10)	EN2183829	Control	0.5	23.82722612	0
	80(1,H10)			0.5	23.82722612	
Mean	-			0.5	23.82722612	
35	81(1,A11)	EN2183840	Control	-1.5	2.054692932	118.9672669
	82(1,B11)			0.5	23.82722612	
Mean	-			-0.5	12.94095953	
36	83(1,C11)	EN2183831	Control	-1.5	2.054692932	0
	84(1,D11)			-1.5	2.054692932	
Mean	-			-1.5	2.054692932	
37	85(1,E11)	EN2183832	Control	-2.5	< 12.3456790	-
	86(1,F11)			-1.5	2.054692932	
Mean	-			-1.5	2.054692932	
38	87(1,G11)	EN2183872	Control	-1	9.103897017	-
	88(1,H11)			-2.5	< 12.3456790	
Mean	-			-1	9.103897017	
39	89(1,A12)	EN20212576	Control	-2.5	< 12.3456790	0
	90(1,B12)			-2	< 12.3456790	
Mean	-			-2.25	< 12.3456790	
40	91(1,C12)	EN2183873	Control	-1.5	2.054692932	-
	92(1,D12)			-2.5	< 12.3456790	
Mean	-			-1.5	2.054692932	
41	93(1,E12)	EN2183860	Control	-2.5	< 12.3456790	-
	94(1,F12)			-1.5	2.054692932	
Mean	-			-1.5	2.054692932	
43	95(1,G12)	EN2183874	Pre	-1.5	2.054692932	0
	96(1,H12)			-1.5	2.054692932	
Mean	-			-1.5	2.054692932	

PRIMANEXUS®
LEADING THE CONNECTION
28-1B, Jalan Puteri 1/2, Bandar Puteri Puchong, 47100 Selangor, Malaysia.
Tel: +603 5891 0194 | Fax: +603 58910195 | Website: www.primanexus.com.my
Company registered number: 1055479-X

HGF

Logistic5p: y = a+((b-a)/(1+((x/c)^d))^f)

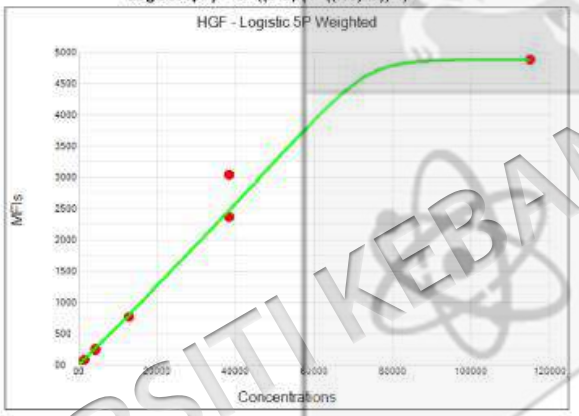

R-Squared	0.9935490343
Sum of Residuals	379.7947294
Average Residuals	29.21497918
Relative Sum of Squares Absolute	337461.1452
Relative Sum of Squares Relative	16.77596078
Standard Error of the Estimate	1.448100513
Adjusted Coefficient of Multiple Determination	0.9903235514
Coefficient a	-1.936619924
Coefficient b	4881.062968
Coefficient c	74258.29285
Coefficient d	-14.76364304
Coefficient f	0.06962498082

Standard	Well	Net MFI	Expected Concentration (pg/mL)	Tested Concentration (pg/mL)	Recovery (%)	CV of Replicates (%)	Remarks
Standard 1	1(1,A1)	-	115000	-	-	-	
	2(1,B1)	4880.5		114573.6809	99.63		
Mean	-	4880.5		114573.6809	-		
Standard 2	3(1,C1)	3041.5	38333	46884.81585	122.31	17.14115006	
	4(1,D1)	2367.5		36747.99747	95.86		
Mean	-	2704.5		41816.40666	-		
Standard 3	5(1,E1)	759.5		12179.00109	95.31		

Standard 3	6(1,F1)	769.5	12778	12334.57693	96.53	0.897533073	
Mean	-	764.5		12256.78901	-		
Standard 4	7(1,G1)	234.5	4259	3903.801996	91.65	6.249170279	
	8(1,H1)	257		4264.756778	100.13		
Mean	-	245.75		4084.279387	-		
Standard 5	9(1, A2)	82.5	1420	1433.670794	100.98	0.80990051	
	10(1, B2)	83.5		1450.186243	102.14		
Mean	-	83		1441.928518	-		
Standard 6	11(1,C2)	25	473	471.778564	99.69	6.101528561	
	12(1,D2)	27.5		514.3232588	108.68		
Mean	-	26.25		493.0509114	-		
Standard 7	13(1, E2)	7	158	161.2808087	102.24	3.369606133	
	14(1, F2)	6.5		152.4954977	96.67		
Mean	-	6.75		156.8881532	-		
Blank	15(1,G2)	-0.5	0	-	-	-	
	16(1,H2)	0.5		-	-		
Mean	-	0		-	-		

Quality Control	Well	Net MFI	Expected Concentration (pg/mL)	Tested Concentration (pg/mL)	CV of Replicates (%)	Remarks
Low Control	17(1,A3)	187.5	2939	3146.669882	3.018904802	
	18(1,B3)	196		3283.943218		
Mean	-	191.75		3215.306455		
High Control	19(1,C3)	1602.5	25 123	25148.32471	3.162678088	
	20(1,D3)	1678		26298.8645		
Mean	-	1640.25		25723.5946		

Sample No.	Well	Sample ID	Grouping	Net MFI	Test Result (pg/mL)	CV of Replicates (%)
1	21(1,E3)	EN2183843	Pre	53	1887.471813	7.947487351
	22(1,F3)			47	1686.6179	
Mean	-			50	1787.044857	
2	23(1,G3)	EN2183837	Pre	40.5	1468.265337	4.697102444
	24(1,H3)			43.5	1569.148575	
Mean	-			42	1518.706956	
3	25(1,A4)	EN2183830	Pre	62.5	2204.295878	4.141768979
	26(1,B4)			66.5	2337.304499	

Mean	-			64.5	2270.800188	
4	27(1,C4)	EN2183834	Pre	53	1887.471813	4.247381335
	28(1,D4)			56.5	2004.357141	
Mean	-			54.75	1945.914477	
5	29(1,E4)	EN2183835	Pre	140.5	4768.726819	1.196880096
	30(1,F4)			143	4850.133352	
Mean	-			141.75	4809.430085	
6	31(1,G4)	EN2183817	Pre	44.5	1602.735525	19.13746961
	32(1,H4)			59.5	2104.392829	
Mean	-			52	1853.564177	
7	33(1,A5)	EN2183859	Pre	91.5	3164.251842	12.08936858
	34(1,B5)			109.5	3755.811711	
Mean	-			100.5	3460.031777	
8	35(1,C5)	EN2183855	Pre	39	1417.751846	0.835103907
	36(1,D5)			39.5	1434.595173	
Mean	-			39.25	1426.17351	
9	37(1,E5)	EN2183863	Pre	81.5	2834.300061	3.378868642
	38(1,F5)			77.5	2702.025024	
Mean	-			79.5	2768.162542	
10	39(1,G5)	EN2183871	Pre	100.5	3460.385143	0.674833036
	40(1,H5)			99.5	3427.517517	
Mean	-			100	3443.95133	
11	41(1,A6)	EN2183852	Post	13.5	548.9646467	0
	42(1,B6)			13.5	548.9646467	
Mean	-			13.5	548.9646467	
12	43(1,C6)	EN2183845	Post	71.5	2503.269848	2.382385326
	44(1,D6)			69	2420.326897	
Mean	-			70.25	2461.798373	
13	45(1,E6)	EN2183847	Post	75.5	2635.820183	1.799932534
	46(1,F6)			73.5	2569.56888	
Mean	-			74.5	2602.694532	
14	47(1,G6)	EN2183856	Post	107.5	3690.219277	29.39015557
	48(1,H6)			69	2420.326897	
Mean	-			88.25	3055.273087	
15	49(1,A7)	EN2183846	Post	83.5	2900.372486	33.07236695
	50(1,B7)			137.5	4670.987677	
Mean	-			110.5	3785.680082	
16	51(1,C7)			58.5	2071.062668	

16	52(1,D7)	EN2183848	Post	63.5	2237.568533	5.465189314
Mean	-			61	2154.315601	
17	53(1,E7)	EN20203773	Post	70	2453.513451	1.939489461
	54(1,F7)			68	2387.127634	
Mean	-			69	2420.320543	
18	55(1,G7)	EN20203775	Post	24.5	926.5141045	0
	56(1,H7)			24.5	926.5141045	
Mean	-			24.5	926.5141045	
19	57(1,A8)	EN20203776	Post	139.5	4736.153376	1.918349947
	58(1,B8)			143.5	4866.410061	
Mean	-			141.5	4801.281719	
20	59(1,C8)	EN20203774	Post	63.5	2237.568533	1.059344359
	60(1,D8)			62.5	2204.295878	
Mean	-			63	2220.932205	
22	61(1,E8)	EN2183865	Control	23.5	892.4016115	2.75862019
	62(1,F8)			22.5	858.2526657	
Mean	-			23	875.3271386	
23	63(1,G8)	EN2183861	Control	95.5	3295.958085	0.70964102
	64(1,H8)			94.5	3263.045531	
Mean	-			95	3279.501808	
25	65(1,A9)	EN2187421	Post	38.5	1400.902931	0
	66(1,B9)			38.5	1400.902931	
Mean	-			38.5	1400.902931	
27	67(1,C9)	EN20212578	Control	71.5	2503.269848	3.202270861
	68(1,D9)			75	2619.261762	
Mean	-			73.25	2561.265805	
28	69(1,E9)	EN2183839	Control	38.5	1400.902931	3.488684347
	70(1,F9)			36.5	1333.449936	
Mean	-			37.5	1367.176433	
29	71(1,G9)	EN2183844	Control	21.5	824.0657331	5.630257188
	72(1,H9)			23.5	892.4016115	
Mean	-			22.5	858.2336723	
30	73(1,A10)	EN2183836	Control	134.5	4573.1914	32.42289155
	74(1,B10)			82.5	2867.341587	
Mean	-			108.5	3720.266494	
31	75(1,C10)	EN2183838	Control	73.5	2569.56888	4.839118163
	76(1,D10)			79	2751.648887	
Mean	-			76.25	2660.608884	

32	77(1,E10)	EN2183841	Control	100.5	3460.385143	32.38013258
	78(1,F10)			61.5	2171.009195	
Mean	-			81	2815.697169	
34	79(1,G10)	EN2183829	Control	263	8721.728789	0.902804113
	80(1,H10)			266.5	8833.79958	
Mean	-			264.75	8777.764185	
35	81(1,A11)	EN2183840	Control	78.5	2735.110398	0.849926969
	82(1,B11)			79.5	2768.184602	
Mean	-			79	2751.6475	
36	83(1,C11)	EN2183831	Control	66.5	2337.304499	1.491407883
	84(1,D11)			68	2387.127634	
Mean	-			67.25	2362.216066	
37	85(1,E11)	EN2183832	Control	91.5	3164.251842	3.00933071
	86(1,F11)			87.5	3032.392326	
Mean	-			89.5	3098.322084	
38	87(1,G11)	EN2183872	Control	33.5	1232.089935	3.99523563
	88(1,H11)			31.5	1164.387943	
Mean	-			32.5	1198.238889	
39	89(1,A12)	EN20212576	Control	115.5	3952.399504	3.427077164
	90(1,B12)			121.5	4148.714571	
Mean	-			118.5	4050.557037	
40	91(1,C12)	EN2183873	Control	58.5	2071.062668	4.407120709
	92(1,D12)			62.5	2204.295878	
Mean	-			60.5	2137.679273	
41	93(1,E12)	EN2183860	Control	98	3378.199546	11.65693677
	94(1,F12)			116.5	3985.137236	
Mean	-			107.25	3681.668391	
43	95(1,G12)	EN2183874	Pre	39.5	1434.595173	0
	96(1,H12)			39.5	1434.595173	
Mean	-			39.5	1434.595173	

PRIMANEXUS®
LEADING THE CONNECTION
28-1B, Jalan Puteri 1/2, Bandar Puteri Puchong, 47100 Selangor, Malaysia.
Tel: +603 5891 0194 | Fax: +603 58910195 | Website: www.primanexus.com.my
Company registered number: 1055479-X

CD40 Ligand/TNFSF5

Logistic5p: y = a+((b-a)/(1+((x/c)^d))^f)

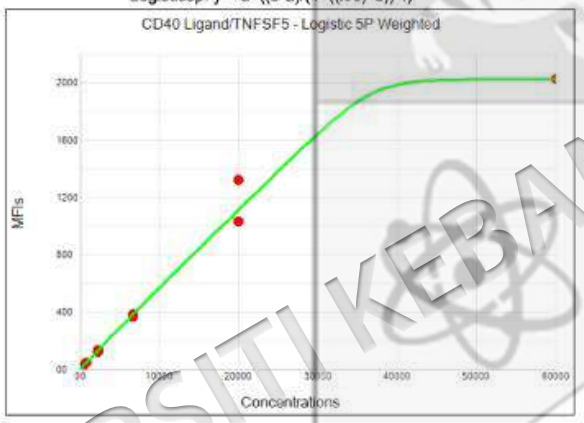

R-Squared	0.9919933531
Sum of Residuals	109.0089081
Average Residuals	8.385300626
Relative Sum of Squares Absolute	51449.15662
Relative Sum of Squares Relative	8.541396919
Standard Error of the Estimate	1.033283415
Adjusted Coefficient of Multiple Determination	0.9879900296
Coefficient a	-1.06022982
Coefficient b	2027.160271
Coefficient c	37074.24455
Coefficient d	-14.23631399
Coefficient f	0.0680192016

Standard	Well	Net MFI	Expected Concentration (pg/mL)	Tested Concentration (pg/mL)	Recovery (%)	CV of Replicates (%)	Remarks
Standard 1	1(1,A1)	-	60000	-	-	-	
	2(1,B1)	2027		59594.84029	99.32		
Mean	-	2027		59594.84029	-		
Standard 2	3(1,C1)	1325	20000	23908.15571	119.54	18.14159421	
	4(1,D1)	1032		18471.65485	92.36		
Mean	-	1178.5		21189.90528	-		
Standard 3	5(1,E1)	367.5		6371.673643	95.58		

Standard 3	6(1,F1)	384	6667	6666.463897	100	3.197514788	
Mean	-	375.75		6519.06877	-		
Standard 4	7(1,G1)	123	2222	2069.751777	93.14	7.270503793	
	8(1,H1)	136		2294.098293	103.23		
Mean	-	129.5		2181.925035	-		
Standard 5	9(1, A2)	45.5	741	752.2919446	101.56	0.779982521	
	10(1, B2)	46		760.6362113	102.69		
Mean	-	45.75		756.4640779	-		
Standard 6	11(1,C2)	14	247	234.5188199	94.98	9.092783073	
	12(1,D2)	16		266.7481217	108.03		
Mean	-	15		250.6334708	-		
Standard 7	13(1, E2)	4	82	76.03810652	92.39	13.13062091	
	14(1, F2)	5		91.60318297	111.8		
Mean	-	4.5		83.82064474	-		
Blank	15(1,G2)	-1	0	-	-	-	
	16(1,H2)	1		-	-		
Mean	-	0		-	-		

Quality Control	Well	Net MFI	Expected Concentration (pg/mL)	Tested Concentration (pg/mL)	CV of Replicates (%)	Remarks
Low Control	17(1,A3)	76	1244	1265.771036	7.20633811	
	18(1,B3)	84		1401.695826		
Mean	-	80		1333.733431		
High Control	19(1,C3)	646	11 293	11394.12368	2.876351742	
	20(1,D3)	672		11867.2836		
Mean	-	659		11630.67864		

Sample No.	Well	Sample ID	Grouping	Net MFI	Test Result (pg/mL)	CV of Replicates (%)
1	21(1,E3)	EN2183843	Pre	15	501.2341177	26.90480227
	22(1,F3)			10	341.0022803	
Mean	-			12.5	421.118199	
2	23(1,G3)	EN2183837	Pre	3.5	136.5842518	7.589865745
	24(1,H3)			4	152.076213	
Mean	-			3.75	144.3302324	
3	25(1,A4)	EN2183830	Pre	8	277.5238956	3.92155743
	26(1,B4)			8.5	293.3541136	

Mean	-			8.25	285.4390046	
4	27(1,C4)	EN2183834	Pre	4	152.076213	24.08427319
	28(1,D4)			6	214.5056678	
Mean	-			5	183.2909404	
5	29(1,E4)	EN2183835	Pre	18	598.2029245	3.934282872
	30(1,F4)			17	565.8202865	
Mean	-			17.5	582.0116055	
6	31(1,G4)	EN2183817	Pre	13.5	452.9653153	21.39112644
	32(1,H4)			18.5	614.4152736	
Mean	-			16	533.6902945	
7	33(1,A5)	EN2183859	Pre	65	2159.275907	18.35539478
	34(1,B5)			84	2803.391652	
Mean	-			74.5	2481.333779	
8	35(1,C5)	EN2183855	Pre	3	121.1478315	28.83614611
	36(1,D5)			5	183.2063859	
Mean	-			4	152.1770987	
9	37(1,E5)	EN2183863	Pre	114	3829.760711	2.255550439
	38(1,F5)			110.5	3709.51566	
Mean	-			112.25	3769.638186	
10	39(1,G5)	EN2183871	Pre	91	3041.95027	2.419006378
	40(1,H5)			88	2939.635496	
Mean	-			89.5	2990.792883	
11	41(1,A6)	EN2183852	Post	4.5	167.6183797	6.283690573
	42(1,B6)			5	183.2063659	
Mean	-			4.75	175.4123728	
12	43(1,C6)	EN2183845	Post	5	183.2063659	28.83614611
	44(1,D6)			3	121.1478315	
Mean	-			4	152.1770987	
13	45(1,E6)	EN2183847	Post	5.5	198.8365012	5.361066364
	46(1,F6)			6	214.5056678	
Mean	-			5.75	206.6710845	
14	47(1,G6)	EN2183856	Post	125	4208.43707	33.42448355
	48(1,H6)			78	2599.421542	
Mean	-			101.5	3403.929306	
15	49(1,A7)	EN2183846	Post	14	469.0376399	42.75005394
	50(1,B7)			26.5	875.4655259	
Mean	-			20.25	672.2515829	
16	51(1,C7)			7.5	261.7222264	

16	52(1,D7)	EN2183848	Post	7	245.9507192	4.393494705
Mean	-			7.25	253.8364728	
17	53(1,E7)	EN20203773	Post	71	2362.098562	2.978037012
	54(1,F7)			74	2463.720179	
Mean	-			72.5	2412.909371	
18	55(1,G7)	EN20203775	Post	1	60.12407696	0
	56(1,H7)			1	60.12407696	
Mean	-			1	60.12407696	
19	57(1,A8)	EN20203776	Post	194	6605.559614	4.004944897
	58(1,B8)			205	6990.59226	
Mean	-			199.5	6798.075937	
20	59(1,C8)	EN20203774	Post	63	2091.799514	2.3159434
	60(1,D8)			61	2024.391969	
Mean	-			62	2058.095741	
22	61(1,E8)	EN2183865	Control	13	436.6110277	5.015062355
	62(1,F8)			14	469.0376399	
Mean	-			13.5	452.9743338	
23	63(1,G8)	EN2183861	Control	303	10447.28084	0.954352015
	64(1,H8)			307	10589.24135	
Mean	-			305	10518.26109	
25	65(1,A9)	EN2187421	Post	63	2091.799514	2.795189051
	66(1,B9)			65.5	2176.155523	
Mean	-			64.25	2133.977519	
27	67(1,C9)	EN20212578	Control	162	5489.651851	3.922116927
	68(1,D9)			171	5802.832587	
Mean	-			166.5	5646.242219	
28	69(1,E9)	EN2183839	Control	6	214.5056678	24.08427319
	70(1,F9)			4	152.076213	
Mean	-			5	183.2909404	
29	71(1,G9)	EN2183844	Control	1	60.12407696	28.49754357
	72(1,H9)			2	90.46999713	
Mean	-			1.5	75.29703704	
30	73(1,A10)	EN2183836	Control	14	469.0376399	44.12555041
	74(1,B10)			7	245.9507192	
Mean	-			10.5	357.4941795	
31	75(1,C10)	EN2183838	Control	9	309.2114335	16.13640263
	76(1,D10)			11.5	388.862821	
Mean	-			10.25	349.0371272	

32	77(1,E10)	EN2183841	Control	15	501.2341177	48.31806356
	78(1,F10)			7	245.9507192	
Mean	-			11	373.5924185	
34	79(1,G10)	EN2183829	Control	59.5	1973.882776	3.077953415
	80(1,H10)			57	1889.792143	
Mean	-			58.25	1931.83746	
35	81(1,A11)	EN2183840	Control	4	152.076213	41.29650121
	82(1,B11)			8	277.5238956	
Mean	-			6	214.8000543	
36	83(1,C11)	EN2183831	Control	7	245.9507192	0
	84(1,D11)			7	245.9507192	
Mean	-			7	245.9507192	
37	85(1,E11)	EN2183832	Control	3.5	136.5842618	7.589865745
	86(1,F11)			4	152.076213	
Mean	-			3.75	144.3302324	
38	87(1,G11)	EN2183872	Control	61	2024.391989	1.74387527
	88(1,H11)			62.5	2074.941092	
Mean	-			61.75	2049.66653	
39	89(1,A12)	EN20212576	Control	288.5	9225.492067	4.081447428
	90(1,B12)			284	9773.815728	
Mean	-			276.25	9499.653897	
40	91(1,C12)	EN2183873	Control	48	1588.083951	1.47340325
	92(1,D12)			49	1621.523354	
Mean	-			48.5	1604.803652	
41	93(1,E12)	EN2183860	Control	243	8325.681251	9.509403798
	94(1,F12)			277	9526.061709	
Mean	-			260	8925.87148	
43	95(1,G12)	EN2183874	Pre	5	183.2063659	0
	96(1,H12)			5	183.2063659	
Mean	-			5	183.2063659	

PRIMANEXUS®
LEADING THE CONNECTION

28-1B, Jalan Puteri 1/2, Bandar Puteri Puchong, 47100 Selangor, Malaysia.
Tel: +603 5891 0194 | Fax: +603 58910195 | Website: www.primanexus.com.my
Company registered number: 1055479-X

SCF/c-kit Ligand
Logistic5p: y = a+((b-a)/(1+((x/c)^d))^f)

R-Squared	0.9901418221
Sum of Residuals	156.349811
Average Residuals	12.02690854
Relative Sum of Squares Absolute	62457.98605
Relative Sum of Squares Relative	4.049949732
Standard Error of the Estimate	0.7115080579
Adjusted Coefficient of Multiple Determination	0.9852127332
Coefficient a	-0.3479289258
Coefficient b	2456.427224
Coefficient c	1331.213681
Coefficient d	-10.06229601
Coefficient f	0.1036854255

Standard	Well	Net MFI	Expected Concentration (pg/mL)	Tested Concentration (pg/mL)	Recovery (%)	CV of Replicates (%)	Remarks
Standard 1	1(1,A1)	-	1600	-	-	-	
	2(1,B1)	2419.5		1599.871993	99.99		
Mean	-	2419.5		1599.871993	-		
Standard 2	3(1,C1)	1188.5	533	663.949815	124.49	19.40245804	
	4(1,D1)	891		503.746446	94.45		
Mean	-	1039.75		583.8481308	-		
Standard 3	5(1,E1)	281		166.8003696	93.83		

Standard 3	6(1,F1)	291	178	172.4787154	97.02	2.366899085	
Mean	-	286		169.6395425	-		
Standard 4	7(1,G1)	90	59	56.15029366	94.75	2.935678899	
	8(1,H1)	94		58.53088977	98.77		
Mean	-	92		57.34059172	-		
Standard 5	9(1, A2)	29	20	19.11106497	96.75	10.64220534	
	10(1, B2)	34		22.22140597	112.5		
Mean	-	31.5		20.66623547	-		
Standard 6	11(1,C2)	9	7	6.383372621	96.95	6.882649474	
	12(1,D2)	10		7.036486022	106.87		
Mean	-	9.5		6.709929322	-		
Standard 7	13(1, E2)	3	2	2.385746589	108.7	10.94071023	
	14(1, F2)	2.5		2.043118496	93.09		
Mean	-	2.75		2.214432542	-		
Blank	15(1,G2)	-1	0	-	-	-	
	16(1,H2)	1		-	-		
Mean	-	0		-	-		

Quality Control	Well	Net MFI	Expected Concentration (pg/mL)	Tested Concentration (pg/mL)	CV of Replicates (%)	Remarks
Low Control	17(1,A3)	77.5	46.1	48.68189975	1.763883996	
	18(1,B3)	75.5		47.48229022		
Mean	-	76.5		48.08199498		
High Control	19(1,C3)	688	407	393.2150624	2.370137014	
	20(1,D3)	712.5		406.6198147		
Mean	-	700.25		399.9174385		

Sample				Net MFI	Test Result (pg/mL)	CV of Replicates (%)
No.	Well	Sample ID	Grouping			
1	21(1,E3)	EN2183843	Pre	31	40.7153	6.812507517
	22(1,F3)			28	36.97292589	
Mean	-			29.5	38.84411294	
2	23(1,G3)	EN2183837	Pre	48	61.67579726	2.746857295
	24(1,H3)			50	64.11913926	
Mean	-			49	62.89746826	
3	25(1,A4)	EN2183830	Pre	71	89.55751649	6.338904382
	26(1,B4)			78	97.962702	

Mean	-			74.5	93.76010925	
4	27(1,C4)	EN2183834	Pre	63	79.90929733	2.174108384
	28(1,D4)			61	77.48956251	
Mean	-			62	78.69942992	
5	29(1,E4)	EN2183835	Pre	49.5	63.50868785	2.774974346
	30(1,F4)			47.5	61.06431248	
Mean	-			48.5	62.28650016	
6	31(1,G4)	EN2183817	Pre	21	28.17289563	27.8003768
	32(1,H4)			32	41.95938326	
Mean	-			26.5	35.06613945	
7	33(1,A5)	EN2183859	Pre	45	58.00284911	19.24737908
	34(1,B5)			60	76.27847295	
Mean	-			52.5	67.14066103	
8	35(1,C5)	EN2183855	Pre	23	30.69795628	5.567471866
	36(1,D5)			25	33.21404198	
Mean	-			24	31.95599913	
9	37(1,E5)	EN2183863	Pre	45	58.00284911	1.478263577
	38(1,F5)			46	59.22825435	
Mean	-			45.5	58.61555173	
10	39(1,G5)	EN2183871	Pre	90	112.3005873	5.462958429
	40(1,H5)			83	103.9471639	
Mean	-			86.5	108.1238756	
11	41(1,A6)	EN2183852	Post	43	55.54864493	6.556981852
	42(1,B6)			39	50.6258777	
Mean	-			41	53.08726132	
12	43(1,C6)	EN2183845	Post	36	46.92024112	1.839328427
	44(1,D6)			37	48.15681484	
Mean	-			36.5	47.53852798	
13	45(1,E6)	EN2183847	Post	46	59.22825435	4.249520016
	46(1,F6)			49	62.89798218	
Mean	-			47.5	61.06311826	
14	47(1,G6)	EN2183856	Post	119	146.6424318	33.28913011
	48(1,H6)			72	90.76027962	
Mean	-			95.5	118.7013557	
15	49(1,A7)	EN2183846	Post	96	119.439212	34.25040491
	50(1,B7)			161	195.7815664	
Mean	-			128.5	157.6103892	
16	51(1,C7)			14	19.24992766	

16	52(1,D7)	EN2183848	Post	16	21.81472834	8.832841338
Mean	-			15	20.532328	
17	53(1,E7)	EN20203773	Post	39	50.6258777	3.534811715
	54(1,F7)			37	48.15681484	
Mean	-			38	49.39134627	
18	55(1,G7)	EN20203775	Post	22	29.43659904	6.34994971
	56(1,H7)			20	26.90673139	
Mean	-			21	28.17166521	
19	57(1,A8)	EN20203776	Post	71	89.55751649	1.873597679
	58(1,B8)			73	91.96235275	
Mean	-			72	90.75993462	
20	59(1,C8)	EN20203774	Post	64	81.11796953	1.06151004
	60(1,D8)			63	79.90929733	
Mean	-			63.5	80.51363343	
22	61(1,E8)	EN2183865	Control	43	55.54864499	1.581766018
	62(1,F8)			42	54.31979199	
Mean	-			42.5	54.93421846	
23	63(1,G8)	EN2183861	Control	51	65.39928976	1.307193501
	64(1,H8)			52	66.6584541	
Mean	-			51.5	65.94887193	
25	65(1,A9)	EN2187421	Post	41	53.08973365	5.102727579
	66(1,B9)			38	49.3920146	
Mean	-			39.5	51.24087412	
27	67(1,C9)	EN20212576	Control	60	76.27847295	1.11384611
	68(1,D9)			61	77.48956251	
Mean	-			60.5	76.88401773	
28	69(1,E9)	EN2183839	Control	42	54.31979199	1.619563235
	70(1,F9)			41	53.08973365	
Mean	-			41.5	53.70476282	
29	71(1,G9)	EN2183844	Control	23	30.69795628	6.065777709
	72(1,H9)			21	28.17289563	
Mean	-			22	29.43542595	
30	73(1,A10)	EN2183836	Control	163	198.1070448	29.29687942
	74(1,B10)			105	130.1129236	
Mean	-			134	164.1099842	
31	75(1,C10)	EN2183838	Control	157.5	191.7090894	2.528192103
	76(1,D10)			163.5	198.6882292	
Mean	-			160.5	195.1986593	

32	77(1,E10)	EN2183841	Control	74	93.16374567	35.77091687
	78(1,F10)			43	55.54864493	
Mean	-			58.5	74.3561953	
34	79(1,G10)	EN2183829	Control	160.5	195.2000104	0.211008666
	80(1,H10)			160	194.6183793	
Mean	-			160.25	194.9091948	
35	81(1,A11)	EN2183840	Control	4	6.129827772	0
	82(1,B11)			4	6.129827772	
Mean	-			4	6.129827772	
36	83(1,C11)	EN2183831	Control	46	59.22825435	0.727233565
	84(1,D11)			46.5	59.84054397	
Mean	-			46.25	59.53439916	
37	85(1,E11)	EN2183832	Control	60	76.27847295	7.09146462
	86(1,F11)			54	68.99390197	
Mean	-			57	72.63618746	
38	87(1,G11)	EN2183872	Control	44	56.77632143	0.759846525
	88(1,H11)			44.5	57.3897272	
Mean	-			44.25	57.08302432	
39	89(1,A12)	EN20212576	Control	24	31.95707197	7.866931538
	90(1,B12)			27	35.72189066	
Mean	-			25.5	33.83948131	
40	91(1,C12)	EN2183873	Control	52	66.5584541	2.639865057
	92(1,D12)			50	64.11913926	
Mean	-			51	65.33879668	
41	93(1,E12)	EN2183860	Control	44	56.77632143	21.81711809
	94(1,F12)			61	77.48956251	
Mean	-			52.5	67.13294197	
43	95(1,G12)	EN2183874	Pre	22	29.43659904	0
	96(1,H12)			22	29.43659904	
Mean	-			22	29.43659904	

APPENDIX F

RAW BIOMARKER DATA FOR ELISA

PRIMANEXUS®
LEADING THE CONNECTION

28-1B, Jalan Puteri 1/2, Bandar Puteri Puchong, 47100 Selangor, Malaysia.
Tel: +603 5891 0194 | Fax: +603 58910195 | Website: www.primanexus.com
Company registered number: 1055479-X

Dr Amalina IIUM

Human DKK1 (Dickkof Related Protein 1)
Catalogue No.: E-EL-H0057
Lot: WA12TN8408941
Exp: 7/16/2026

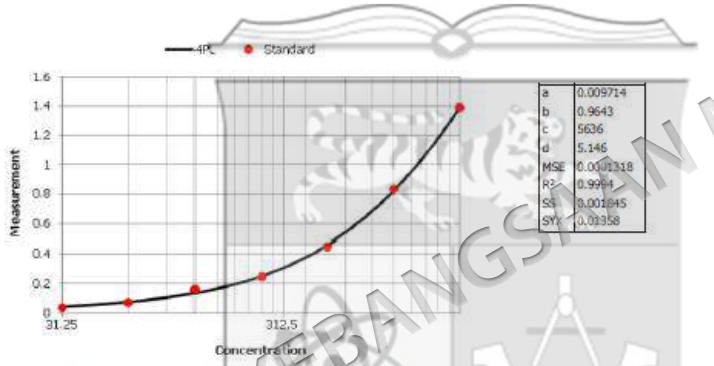

Calibrator	Conc.	Wells	Raw (Corrected)	SEM	Backfit	Recovery %
Standard1	2000	A1	1.39	0.0025	2002	100.1
		A2	1.39		1992	99.58
Standard2	1000	B1	0.834	0	1013	101.3
		B2	0.834		1013	101.3
Standard3	500	C1	0.451	0.0015	485.3	97.06
		C2	0.448		481.5	96.31
Standard4	250	D1	0.248	0.001	245.1	98.05
		D2	0.246		242.9	97.16
Standard5	125	E1	0.161	0.0005	150.3	120.2
		E2	0.16		149.2	119.4
Standard6	62.5	F1	0.072	0.001	58.78	94.05
		F2	0.07		56.8	90.88
Standard7	31.25	G1	0.037	0.0005	24.8	79.35
		G2	0.036		23.85	76.32

Sample	Dilution	Wells	Raw	Background Corrected	Conc.	Conc. (Average) pg/mL	%CV	SD	SEM	
EN2183843	10	A3	0.524	0.378	4007	3953	1.93	76.4	54	pre
		A4	0.515		3899					
EN2183837	10	B3	0.464	0.322	3297	3291	0.25	8.24	5.83	pre
		B4	0.463		3285					
EN2183830	10	C3	0.381	0.238	2351	2340	0.672	15.7	11.1	pre
		C4	0.379		2329					
EN2183834	10	D3	0.305	0.163	1524	1519	0.495	7.51	5.31	pre
		D4	0.304		1513					
EN2183835	10	E3	0.561	0.418	4457	4445	0.39	17.3	12.3	pre
		E4	0.559		4432					
EN2183817	10	F3	0.571	0.427	4580	4561	0.573	26.1	18.5	pre

		F4	0.568		4543					pre
EN2183859	10	G3	0.588	0.444	4791	4772	0.553	26.4	18.7	pre
		G4	0.585		4753					
EN2183855	10	H3	0.201	0.0585	459.9	455	1.52	6.9	4.88	pre
		H4	0.2		450.1					
EN2183863	10	A5	0.677	0.53	5924	5852	1.73	101	71.4	pre
		A6	0.666		5781					
EN2183871	10	B5	0.632	0.489	5344	5332	0.337	18	12.7	pre
		B6	0.63		5319					
EN2183852	10	C5	0.257	0.115	1022	1017	0.714	7.26	5.14	post
		C6	0.256		1012					
EN2183845	10	D5	0.419	0.276	2778	2761	0.873	24.1	17	post
		D6	0.416		2744					
EN2183847	10	E5	0.208	0.0655	528.5	523.6	1.33	6.96	4.92	post
		E6	0.207		518.7					
EN2183856	10	F5	0.668	0.526	5807	5800	0.158	9.17	6.48	post
		F6	0.667		5794					
EN2183846	10	G5	0.342	0.199	1922	1911	0.804	15.4	10.9	post
		G6	0.34		1900					
EN2183848	10	H5	0.361	0.218	2130	2113	1.1	23.3	16.5	post
		H6	0.358		2097					
EN20203773	10	A7	0.681	0.535	5976	5917	1.4	82.9	58.6	post
		A8	0.672		5859					
EN20203775	10	B7	0.222	0.079	667.4	657.4	2.15	14.1	9.97	post
		B8	0.22		647.4					
EN20203776	10	C7	0.7	0.557	6225	6206	0.45	27.9	19.8	post
		C8	0.697		6186					
EN20203774	10	D7	0.741	0.597	6771	6738	0.705	47.5	33.6	post
		D8	0.736		6704					
EN2183857	10	E7	0.687	0.543	6055	6028	0.614	37	26.2	control
		E8	0.683		6002					
EN2183865	10	F7	0.461	0.318	3262	3250	0.606	16.4	11.6	control
		F8	0.459		3238					
EN2183861	10	G7	0.877	0.734	8667	8546	0.354	30.6	21.6	control
		G8	0.874		8624					
EN2183864	10	H7	0.33	0.188	1792	1786	0.427	7.63	5.4	control
		H8	0.329		1781					
EN2187421	10	A9	0.661	0.515	5716	5658	1.45	82	58	post
		A10	0.652		5600					
EN20212577	10	B9	0.849	0.706	8266	8252	0.244	20.1	14.2	control
		B10	0.847		8238					
EN20212578	10	C9	0.339	0.196	1889	1878	0.817	15.3	10.8	control
		C10	0.337		1867					
EN2183839	10	D9	0.357	0.215	2086	2080	0.373	7.76	5.49	control
		D10	0.356		2075					
EN2183844	10	E9	0.36	0.217	2119	2108	0.737	15.5	11	control
		E10	0.358		2097					
EN2183836	10	F9	0.338	0.195	1878	1868	0.821	15.3	10.8	control
		F10	0.336		1857					
EN2183838	10	G9	0.931	0.787	9457	9428	0.445	41.9	29.6	control
		G10	0.927		9398					
EN2183841	10	H9	0.468	0.325	3343	3332	0.496	16.5	11.7	control
		H10	0.466		3320					
EN2183842	10	A11	0.457	0.312	3215	3180	1.55	49.2	34.8	control
		A12	0.451		3146					
EN2183829	10	B11	0.819	0.676	7843	7829	0.253	19.8	14	control
		B12	0.817		7815					
EN2183840	10	C11	0.848	0.704	8252	8231	0.366	30.1	21.3	control
		C12	0.845		8209					
EN2183831	10	D11	0.533	0.39	4116	4098	0.625	25.6	18.1	pre
		D12	0.53		4080					
Blank		H1	0.142	0	< Curve	-	-	-	-	
		H2	0.142		< Curve					

PRIMANEXUS®
LEADING THE CONNECTION

28-1B, Jalan Puteri 1/2, Bandar Puteri Puchong, 47100 Selangor, Malaysia.
Tel: +603 5891 0194 | Fax: +603 58910195 | Website: www.primanexus.com.my
Company registered number: 1055479-X

Human SFRP1
Dr Amalina IIUM

Catalogue no: E2336Hu
Lot: 202507011
Exp : 2026/7/14

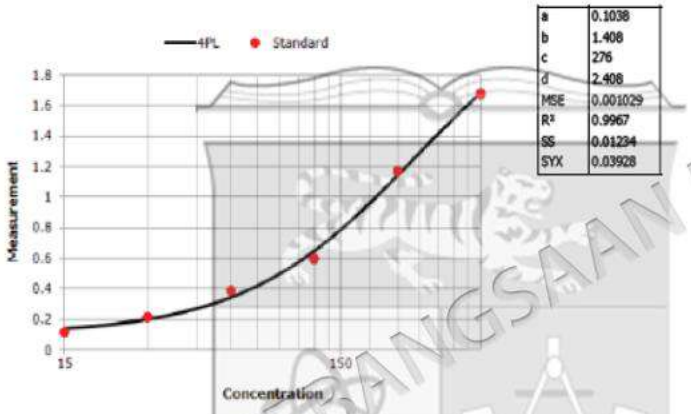

a	0.1038
b	1.408
c	276
d	2.408
MSE	0.001029
R^2	0.9967
SS	0.01234
SYX	0.03928

Calibrator	Wells	Conc.	Raw (Corrected)	SEM	Backfit	Recovery %
Standard1	A1	480	1.68	0.006	479.6	99.92
	A2		1.67		471.5	98.23
Standard2	B1	240	1.17	0.0035	249.3	103.9
	B2		1.17		247.2	103
Standard3	C1	120	0.599	0.0025	109.9	91.56
	C2		0.593		108.9	90.72
Standard4	D1	60	0.388	0.0005	68.44	114.1
	D2		0.387		68.25	113.7
Standard5	E1	30	0.216	0.001	33.31	111
	E2		0.214		32.86	109.5
Standard6	F1	15	0.118	0.0005	7.27	48.47
	F2		0.116		6.887	45.91

Sample	Wells	Raw	Background Corrected	Conc.	Conc. (Average) ng/L	%CV	SD	SEM	
EN2183843	A3	1.06	0.945	185.2	186.3	0.846	1.58	1.12	pre
	A4	1.07		187.4					
EN2183837	B3	0.442	0.318	55.03	54.73	0.776	0.424	0.3	pre
	B4	0.439		54.43					
EN2183830	C3	0.442	0.319	55.03	54.83	0.516	0.283	0.2	pre
	C4	0.44		54.63					
EN2183834	D3	0.936	0.813	155.3	155.1	0.205	0.318	0.225	pre
	D4	0.934		154.9					
EN2183835	E3	0.386	0.265	43.62	43.83	0.672	0.295	0.208	pre
	E4	0.388		44.03					
EN2183817	F3	0.462	0.338	59.01	58.61	0.957	0.561	0.397	pre
	F4	0.458		58.21					

EN2183859	G3	1.79	1.66	469.5	466.9	0.798	3.72	2.63	pre
	G4	1.78		464.2					
EN2183855	H3	0.535	0.413	73.32	73.32	0	0	0	pre
	H4	0.535		73.32					
EN2183863	A5	0.429	0.314	52.42	53.82	3.69	1.99	1.4	pre
	A6	0.443		55.23					
EN2183871	B5	0.522	0.399	70.78	70.69	0.195	0.138	0.0975	pre
	B6	0.521		70.59					
EN21838S2	C5	1.43	1.31	295.7	296.4	0.35	1.04	0.733	post
	C6	1.44		297.1					
EN2183845	D5	0.491	0.37	64.72	64.92	0.427	0.277	0.196	post
	D6	0.493		65.11					
EN2183847	E5	0.401	0.279	46.72	46.72	0	0	0	post
	E6	0.401		46.72					
EN2183856	F5	1.05	0.932	183	183	0	0	0	post
	F6	1.05		183					
EN2183846	G5	0.495	0.372	65.51	65.41	0.212	0.139	0.098	post
	G6	0.494		65.31					
EN2183848	H5	0.468	0.346	60.19	60.29	0.232	0.14	0.0988	post
	H6	0.469		60.39					
EN20203773	A7	1.8	1.68	472.8	475.5	0.805	3.83	2.71	post
	A8	1.8		478.2					
EN20203775	B7	0.41	0.287	48.57	48.36	0.597	0.289	0.204	post
	B8	0.408		48.16					
EN20203776	C7	0.344	0.222	34.64	34.75	0.448	0.156	0.11	post
	C8	0.345		34.86					
EN20203774	D7	0.386	0.263	43.62	43.41	0.68	0.295	0.209	post
	D8	0.384		43.2					
EN21838S7	E7	0.586	0.46	83.25	82.66	1	0.826	0.584	control
	E8	0.58		82.08					
EN2183865	F7	0.414	0.292	49.38	49.38	0	0	0	control
	F8	0.414		49.38					
EN2183861	G7	0.435	0.313	53.62	53.62	0	0	0	control
	G8	0.435		53.62					
EN2183864	H7	0.784	0.662	122.7	122.7	0	0	0	control
	H8	0.784		122.7					
EN2187421	A9	0.451	0.328	56.62	56.2	0.248	0.141	0.0995	post
	A10	0.45		56.62					
EN20212577	B9	0.367	0.244	39.62	39.4	0.766	0.302	0.213	control
	B10	0.365		39.19					
EN20212578	C9	0.524	0.396	71.18	70.1	2.17	1.52	1.07	control
	C10	0.513		69.03					
EN2183839	D9	0.36	0.236	38.12	37.69	1.62	0.61	0.431	control
	D10	0.356		37.26					
EN2183844	E9	1.38	1.25	274.9	273	0.959	2.62	1.85	control
	E10	1.36		271.2					
EN2183836	F9	0.438	0.315	54.23	54.02	0.525	0.284	0.2	control
	F10	0.436		53.82					
EN2183838	G9	0.44	0.317	54.63	54.43	0.52	0.283	0.2	control
	G10	0.438		54.23					
EN2183841	H9	0.378	0.256	41.94	41.94	0	0	0	control
	H10	0.378		41.94					
EN2183842	A11	0.377	0.266	41.73	44.02	7.35	3.24	2.29	control
	A12	0.399		46.31					
EN2183829	B11	0.393	0.271	45.07	45.07	0	0	0	control
	B12	0.393		45.07					
EN2183840	C11	0.383	0.259	42.99	42.68	1.04	0.444	0.314	control
	C12	0.38		42.36					
EN2183831	D11	0.422	0.298	51	50.7	0.847	0.43	0.304	pre
	D12	0.419		50.4					
Blank	G1	0.123	0	< Curve	-	-	-	-	
	G2	0.122		< Curve					

APPENDIX G

CASE REPORT FORM

45144 CONFIDENTIAL TAMONFPA

PATIENT BASELINE INFORMATION D D M M M Y Y Y Y

Participant IC No

Participant ID No E N

Study site

Study Arm

Date of Birth D D M M M Y Y Y Y

Age (yo)

Gender
☐1 Male
☐2 Female

Race
☐1 Malay ☐2 Chinese
☐3 Indian ☐4 Others

Date of Enrolment D D M M M Y Y Y Y

Date of Completion D D M M M Y Y Y Y

Date of Informed Consent D D M M M Y Y Y Y

45144 CONFIDENTIAL TAMONFPA

Symptoms upon first presentation	Headache ☐ Yes ☐ No Visual Disturbance ☐ Yes ☐ No Hypocortisol symptom ☐ Yes ☐ No Hypogonadism symptom ☐ Yes ☐ No Hypothyroid symptom ☐ Yes ☐ No H/o Pituitary apoplexy ☐ Yes ☐ No Asymptomatic ☐ Yes ☐ No
Previous dopamine agonist therapy ☐ Yes ☐ No	If yes; Cabergoline ☐1 Cumulative dose _____/week Bromocriptine ☐2 Cumulative dose _____/week Total Duration Months Years
Baseline Tumor Grade (Knosp Grading)	☐1 Grade 0 ☐2 Grade 1 ☐3 Grade 2 ☐4 Grade 3A ☐5 Grade 3B ☐6 Grade 4

45144 CONFIDENTIAL TAMONFPA

VISIT NO:	D D M M M Y Y Y Y
IC NO	
Ongoing Symptoms	Headache ☐ Yes ☐ No Visual Disturbance ☐ Yes ☐ No Hypocortisol symptom ☐ Yes ☐ No Hypogonadism symptom ☐ Yes ☐ No Hypothyroid symptom ☐ Yes ☐ No H/o Pituitary apoplexy ☐ Yes ☐ No Asymptomatic ☐ Yes ☐ No
Adverse Events	☐1. Yes ☐2. No

If yes;

Nausea / Vomiting	☐ Yes	☐ No	Hot flush	☐ Yes	☐ No
Weight gain	☐ Yes	☐ No	Vaginal discharge	☐ Yes	☐ No
Headache	☐ Yes	☐ No	Fluid retention	☐ Yes	☐ No
Transaminitis	☐ Yes	☐ No	Renal impairment	☐ Yes	☐ No
Others	☐ Yes	☐ No			

State _____

Plan of action;

Monitor and continue treatment ☐1.

Discontinue treatment ☐2

45144 CONFIDENTIAL TAMONFPA

INTERVENTION & IMAGING	
First Surgery D D M M M Y Y Y Y	Transphenoidal surgery ☐1 Transfrontal surgery ☐2 Others ☐3 Complication _____
Repeated surgery D D M M M Y Y Y Y	Transphenoidal surgery ☐1 Transfrontal surgery ☐2 Others ☐3 Complication _____
Baseline MRI Pituitary (pre op) D D M M M Y Y Y Y	Tumor size _____ Tumor volume _____ mm^3 (first observer) Tumor size _____ Tumor volume _____ mm^3 (second observer) Inter-observer variability _____

45144 CONFIDENTIAL TAMONFPA

Baseline MRI Pituitary (post op) D D M M M Y Y Y Y	Tumor size _____ Tumor volume _____mm^3 (first observer) Tumor size_____ Tumor volume _____mm^3 (second observer) Inter-observer variability_____
1st MRI Pituitary D D M M M Y Y Y Y	Tumor size_____ Tumor volume _____mm^3 _____% change from baseline (first observer) Tumor size_____ Tumor volume _____mm^3 _____% change from baseline (second observer) Inter-observer variability _____
2nd MRI Pituitary D D M M M Y Y Y Y	Tumor size_____ Tumor volume _____mm^3 _____% change from baseline (first observer) Tumor size_____ Tumor volume _____mm^3 _____% change from baseline (second observer) Inter-observer variability _____

45144 CONFIDENTIAL TAMONFPA

HISTOPATHOLOGY

HPE Date D D M M M Y Y Y Y **Code No** _____

Subtype;

Null cell adenoma ☐1. Silent Gonadotroph adenoma ☐2

Silent Corticotroph adenoma ☐3 Silent Somatotroph adenoma ☐4

Silent Lactotroph adenoma ☐5 Silent Thyrotroph adenoma ☐6

Others _____

Receptors;

Null ☐ Yes ☐ No α-subunit ☐ Yes ☐ No

ACTH ☐ Yes ☐ No TSH ☐ Yes ☐ No

PRL ☐ Yes ☐ No FSH ☐ Yes ☐ No

LH ☐ Yes ☐ No GH ☐ Yes ☐ No

Estrogen receptor;

ERα ☐ Yes ☐ No

ERβ ☐ Yes ☐ No

Ki67 index _____%

Mitotic count no _____ /10 HPF

p53 positivity ☐1 Yes _____ nuclei /10 HPF

☐2 No

Tumor grade:

Grade 1a ☐1. Grade 1b ☐2

Grade 2a ☐3 Grade 2b ☐4

Grade 3 ☐5

HORMONAL PROFILES

DATE					
Cortisol					
TSH					
T4					
FSH					
LH					
Testosterone					
Estradiol					
Prolactin					

APPENDIX H

PATIENT INFORMATION SHEET AND INFORMED CONSENT

1. **Title of study**: Identification of Putative Protein Profiles Associated with Tamoxifen Therapy Effectiveness in Residual Non-functioning Pituitary Neuroendocrine Tumors

2. **Name of investigator and institution:**

   -Dr Amalina Haydar Ali Tajuddin (HCTM/HKL)

   -Prof Dr Norazmi Kamaruddin (HCTM)

   -Prof Dr Norlela Sukor (HCTM)

   -Dr Elena Aisha Azizan (HCTM)

   -Assoc Prof Dr Tan Geok Chin (HCTM)

   -Assoc. Prof Dr Shahizon Azura Mohamed Mukari (HCTM)

   -Assoc Prof Dr Ahmad Marzuki Omar (UIAM)

   -Dr Azmi Alias (HKL)

   -Dr Kartikasalwah Abd Latif (HKL)

   -Datin Dr Fauziah Kassim (HKL)

3. **Name of sponsor**:

   Fundamental Research Grant Scheme (FGRS) by Ministry of Higher Education

4. **Introduction:**

   You are invited to participate in this research study because you have residual pituitary tumors that were not completely removed during surgical resection and require further monitoring. This study aims to explore the alternative treatment approach in patients with residual pituitary tumors. It is done by comparing the outcomes of treatment with alternative agent versus standard care in order to assess the efficacy of the alternative agent.

The details of the research trial are described in this document. It is important that you understand why the research is being done and what it will involve. Please take your time to read through and consider this information carefully before you decide if you are willing to participate. Ask the study staff if anything is unclear or if you like more information. After you are properly satisfied that you understand this study, and that you wish to participate, you must sign this informed consent form. To participate in this study, you may be required to provide your doctor with information on your health history; you may harm yourself if you are not truthful with the information provided.

Your participation in this study is voluntary. You do not have to be in this study if you do not want to. You may also refuse to answer any questions you do not want to answer. If you volunteer to be in this study, you may withdraw from it at any time. If you withdraw, any data collected from you up to your withdrawal will still be used for the study. Your refusal to participate or withdrawal will not affect any medical or health benefits to which you are otherwise entitled.

This study has been approved by the Medical Research and Ethics Committee, Ministry of Health Malaysia and UKM Ethics Committee.

5. What is the purpose of the study?

The purpose of this study is to compare the effects of tamoxifen versus continuous observation for the treatment of residual pituitary tumors following surgical resection. Your pituitary tumors are non-functioning type, which means type of pituitary tumors that do not produce excess hormones. Current local practices for those patients are observation only, repeat surgery or radiotherapy. A recent study assessed that patients managed by the observation only approach is estimated to lead to a 63.4% risk of regrowth at 5 years. The proven efficacy of radiation therapy in preventing tumor regrowth has to be weighed against potential side effects, particularly pituitary hormone deficiencies, stroke and mortality.

Studies have shown that estrogen regulates pituitary tumors growth. Tamoxifen, a selective antiestrogen, is currently widely used as a medical therapy for estrogen-receptor positive breast cancer patients after surgery. Previous studies have demonstrated that tamoxifen administration prevents occurrence of pituitary tumors in animals. Tamoxifen has also been shown to be effective in slowing the growth of pituitary carcinoma that had failed to respond to first line therapy. Tamoxifen was also found to be effective in patients with acromegaly whose disease activity is not controlled by standard medication therapy.

In this study, patients with residual tumors will be enrolled and prospectively followed up for 12 months. Treatment outcomes will include serial assessment of clinical symptoms, change in tumor volume detected by pituitary magnetic resonance imaging, tumor grading and potential biomarkers detected from blood and tissue samples.

A total of 50 subjects like you from HKL and HCTM will be participating in this study. The whole study will last about 24 months and your participation will be about 16 months.

6. What kind of study products will I receive?

If you agree to participate in the study, the doctor may need to perform some tests and examinations to determine if you are suitable for the study. If you are deemed suitable, you will be randomly assigned to one of the treatment groups below. There will be 2 general groups (intervention and control), and further subdivided into 4 groups according to your tumor size and age. You will have equal chance (1/2) of being assigned to either intervention or control group. You will be informed which group you are assigned to. Study drug (Tamoxifen) does not contain porcine, bovine or animal components.

Intervention Groups (tumor < 10mm or ≥ 10mm / age > 40 years old or ≥ 40 years old)

Participants will receive tamoxifen 20mg daily in the first month followed by 40mg daily in the subsequent months up to a total of 12 months therapy. Clinic visits every 4-monthly.

Observation (Control) groups (tumor < 10mm or ≥ □□ □ □age□ > □40 years old or ≥ □ 40 years old)

Participant will be observed and monitored. Clinic visits every 4-monthly (similar assessments will be done as in intervention group).

7. What will happen if I decide to take part?

a) You will have to sign a consent letter
b) Your baseline clinical data and laboratory results will be recorded in the case report form
c) 10mls of blood (1 table spoon) will be withdrawn at baseline and at the end of study (twice). Additional blood taking will be informed if required.
d) You will be randomly assigned to one of the treatment groups (intervention or control group) based on tumor size and age group. It is an open-label study and you will be informed which group you are assigned to
e) Slide of your pituitary tumor tissue that was removed during previous operation will be retrieved for the purpose of tumor grading and detection of potential biomarker.
f) You will have to attend clinic visits every 4-monthly (at 4, 8, 12 and 16 months of treatment)
g) You will be required to perform MRI Pituitary twice (after 6 and 12 months of treatment). These MRIs are considered as part of your routine monitoring in order to detect tumor regrowth and treatment outcomes.

Subjects will be informed of the study findings. Subjects will be informed if new information relevant to consent becomes available.

8. When will I receive the trial product and how should it be kept?

For those in the intervention group, you will be given the study drug (tamoxifen) at each study visit throughout the treatment period of the study. You must not give it to anyone else. The study staff will instruct you on how the tamoxifen bottles must be handled and stored. Please ensure that you keep your used and partly used study tamoxifen bottles after you have finished with them. For some visits you will need to bring back all tamoxifen bottles (partly used, unused and empty packaging material) to your study site.

9. What are my responsibilities when taking part in this study?

It is important that you answer all of the questions asked by the study staff honestly and completely. If your condition or circumstances change during the study, you must tell the investigator. You must not take any other medications without consulting your study doctor. You must inform your investigator immediately if you make any changes to any of your current treatments, even those which you have been taking for a long time.

It is very important that your investigator be informed very rapidly of any eventual changes to your health during your participation in the study. For your own
□ □ □□ □□ □ □ □ □□ □ □□ □ □□ □ □ □ □ □ □ □ □□ □ □ □ □□ □ □ □□ □ □ □ □ □
throughout the entire duration of the study.

10. What kind of treatment will I receive after my participation in the trial?

Study drug (tamoxifen) will not be given to you at the end of your participation in the study. Whether you complete the study or withdraw early, your doctor will discuss the best alternatives for your future treatment with you.

11. What are the potential risks and side effects of being in this study?

You may develop the side effects related to tamoxifen therapy. Baseline blood investigations will be reviewed prior to initiation of treatment regime. This will minimize any potential side effects. Potential side effects of tamoxifen include;

- Hot flashes
- Nausea
- Fatigue
- Mood swings
- Headache
- Constipation

- Dry skin
- Vaginal discharge
- Increased liver enzymes

For women, you should not become pregnant while in this study. Women subjects should not breastfeed a child while in the study. Notify your study doctor immediately if you think that you have become pregnant during the study. If you are pregnant, you will be removed from the study regardless of treatment arm.

Please ask your investigator if you need more information on risks and side effects.

12. What are the benefits of being in this study?

There may or may not be any benefits to you. Information obtained from this study will help improve the treatment or management of other participants with the same disease or condition.

13. What if I am injured during this study?

If you are injured as a result of being in this study, you should contact your investigator. In the event of a bodily injury or illness directly resulting from tamoxifen therapy or a medical procedure required for this study, the investigator will pay for reasonable and necessary treatment. The investigator is not responsible for medical expenses due to pre-existing medical conditions, any underlying diseases, any ongoing treatment process, your negligence or willful misconduct, the negligence or willful misconduct of your investigator or the study site or any third parties. You do not lose any of your legal rights to seek compensation by signing this form.

14. What are my alternatives if I do not participate in this study?

You do not have to participate in this study to get treatment for your disease or condition. Alternate treatments which are available are observation alone, radiotherapy or repeated surgeries. The study doctor will discuss in more details the benefits and risks of those treatments with you.

15. Who is funding the research?

This study is sponsored by Fundamental Research Grant Scheme (FRGS) under Ministry of Higher Education who will pay for the total cost of the study, including study drug, MRI Pituitary, blood and tissue tests. All other drugs and procedures that are part of your routine medical care will have to be paid by you or your insurance. The sponsor will financially compensate the time spent by the study staff, use of facilities, etc., for including you in the study. You will be reimbursed RM25 for your travel expenses for each study visits.

16. Can the research or my participation be terminated early?

The investigator may due to concerns for your safety, stop the study or your participation at any time. If the study is stopped early for any reason you will be informed and arrangements made for your future care. You may be asked to attend a final follow-up visit.

17. Will my medical information be kept private?

All your information obtained in this study will be kept and handled in a confidential manner, in accordance with applicable laws and/or regulations. When publishing or presenting the study results, your identity will not be revealed without your expressed consent. Individuals involved in this study and in your medical care, qualified monitors and auditors or regulatory authorities may inspect and copy your medical records, where appropriate and necessary.

Your blood specimens will be sent to laboratories in another country for testing. If this is required, your blood specimens will be coded and information that can identify you will be removed. Only your investigator and study staff will be able to link the code with you.

Data from the study will be archived and may be transmitted outside the country for the purpose of analysis or presentation, but your identity will not be revealed at any time.

18. Who should I call if I have questions?

If you have any questions about the study or if you think you have a study related injury and you want information about treatment, please contact the investigator, Dr Amalina Haydar Ali Tajuddin, at telephone number 013-3539557.

If you have any questions about your rights as a participant in this study, please contact the Secretary, Medical Research & Ethics Committee (MREC) at;

Ministry of Health Malaysia,
Block A, Kompleks Institut Kesihatan Negara (NIH)
No 1 Jalan Setia Murni U13/52,
Seksyen U13 Bandar Setia Alam,
40170 Shah Alam
Phone: 03-3362 8888/8205
Email: nihsec@moh.gov.my

APPENDIX I

BORANG MAKLUMAT PESAKIT DAN BORANG KEIZINAN

RISALAH MAKLUMAT PESAKIT DAN BORANG KEIZINAN PESAKIT

1. Tajuk penyelidikan: Mengenalpasti profil protein yang terlibat dalam keberkesanan rawatan ubat tamoxifen untuk merawat sisa ketumbuhan pada kelenjar pituitary jenis tanpa fungsi

2. Nama Institusi dan nama penyelidik:

-Dr Amalina Haydar Ali Tajuddin (HCTM/HKL)

-Prof Dr Norazmi Kamaruddin (HCTM)

-Prof Dr Norlela Sukor (HCTM)

-Dr Elena Aisha Azizan (HCTM)

-Assoc Prof Dr Tan Geok Chin (HCTM)

-Assoc. Prof Dr Shahizon Azura Mohamed Mukari (HCTM)

-Assoc Prof Dr Ahmad Marzuki Omar (UIAM)

-Dr Azmi Alias (HKL)

-Dr Kartikasalwah Abd Latif (HKL)

-Datin Dr Fauziah Kassim (HKL)

3. Nama penaja: Skim Geran Penyelidikan Fundamental (FRGS) di bawah Kementerian Pengajian Tinggi

4. Pengenalan:

Anda telah dijemput untuk menyertai penyelidikan ini kerana anda mempunyai sisa ketumbuhan kelenjar pituitari yang tidak dibuang sepenuhnya semasa pembedahan yang lalu dan memerlukan pemerhatian lanjut. Kajian ini dijalankan untuk meneroka rawatan alternatif untuk pesakit yang mempunyai lebihan ketumbuhan pada kelenjar pituitari. Ini dilaksanakan melalui kaedah perbandingan antara kesan rawatan alternatif dengan rawatan sedia ada agar keberkesanan rawatan alternatif dapat dinilai.

Risalah ini menjelaskan hal-hal berkenaan penyelidikan tersebut dengan lebih mendalam dan terperinci. Amat penting anda memahami mengapa penyelidikan ini dilakukan dan apa yang dilakukan dalam penyelidikan ini.Sila ambil masa yang secukupnya untuk membaca dan mempertimbangkan dengan teliti penerangan yang diberi sebelum anda bersetuju untuk menyertai penyelidikan ini. Jika ada sebarang

kemusykilan ataupun maklumat lanjut yang anda ingin tahu, anda boleh bertanya dengan mana-mana kakitangan yang terlibat dalam penyelidikan ini. Setelah anda berpuas hati bahawa anda memahami penyelidikan ini, dan anda berminat untuk turut serta, anda dikehendaki untuk menandatangani Borang Persetujuan atau Keizinan Pesakit pada muka surat akhir risalah ini. Untuk menyertai penyelidikan ini, anda perlu memberi doktor anda maklumat sejarah kesihatan ataupun penyakit anda yang lalu; jika anda tidak berterus terang anda mungkin boleh menimbulkan masalah pada diri anda di kemudian hari.

Penyertaan anda dalam penyelidikan ini adalah secara sukarela. Anda tidak perlu menyertai penyelidikan ini jika anda tidak mahu. Anda juga mempunyai hak untuk tidak menjawab mana-mana soalan yang anda tidak mahu jawab. Anda juga boleh menarik diri daripada penyelidikan ini pada bila-bila masa. Jika anda menarik diri, segala maklumat yang telah diperolehi sebelum anda menarik diri tetap akan digunakan dalam penyelidikan ini. Jika anda tidak mahu menyertai ataupun menarik diri dari penyelidikan ini, tindakan anda tidak akan menjejaskan segala hak dan keistimewaan perkhidmatan perubatan dan kesihatan yang selayaknya anda terima.

Penyelidikan ini telah mendapat kelulusan Jawatankuasa Etika dan Penyelidikan Perubatan, Kementerian Kesihatan Malaysia and Jawatankuasa Etika UKM.

5. Apakah tujuan penyelidikan ini dilakukan?

Tujuan penyelidikan ini dilakukan adalah untuk membandingkan antara kesan rawatan ubat tamoxifen dengan kaedah pemerhatian berterusan terhadap perubahan saiz ukuran sisa ketumbuhan kelenjar pituitari yang tertinggal selepas pembedahan. Ketumbuhan pada kelenjar pituitari yang dihidapi ialah jenis tanpa fungsi, iaitu ketumbuhan yang tidak menghasilkan sebarang hormon secara berlebihan. Kaedah rawatan yang diamalkan buat masa sekarang untuk pesakit sedemikian adalah samada pemerhatian sahaja, pembedahan berulang atau radioterapi. Kajian terkini menunjukkan bahawa terdapat risiko sebanyak 63.4% untuk sisa ketumbuhan tersebut membesar kembali dalam masa 5 tahun. Manakala kaedah rawatan radioterapi pula harus mengambil kira kesan sampingan yang mungkin berlaku seperti kekurangan hormon pituitari, stroke dan risiko kematian.

Hasil kajian terdahulu menunjukkan bahawa estrogen terlibat dalam tumbesaran ketumbuhan pada kelenjar pituitari. Tamoxifen ialah sejenis ubat anti-estrogen, merupakan rawatan yang digunakan secara meluas untuk pesakit yang menghidap kanser payudara jenis positive estrogen-receptor. Kajian terdahulu telah membuktikan bahawa tamoxifen menghalang tumbesaran ketumbuhan pada kelenjar pituitari yang ditanam pada haiwan kajian. Tamoxifen juga mampu melambatkan tumbesaran kanser pada kelenjar pituitari walaupun kanser tersebut tidak dapat dikawal sepenuhnya oleh rawatan biasa. Tamoxifen juga didapati berkesan di kalangan pesakit ketumbuhan □ ‘ □ □ □ □ □ □ □ □ □ □ ’ □ □ □ □ □ pertumbuhan tersebut.

Dalam kajian ini, pesakit yang mempunyai sisa ketumbuhan pada kelenjar pituitari akan dipilih dan dinilai secara berkala selama 12 bulan. Kesan rawatan yang akan dinilai adalah termasuk simptom pesakit, perubahan pada saiz ukuran sisa ketumbuhan

yang tertinggal pada kelenjar pituitari berdasarkan ujian MRI, tahap ketumbuhan dan penanda tertentu yang dikesan dalam sampel darah dan tisu.

Sejumlah 50 pesakit seperti anda daripada Hospital Kuala Lumpur (HKL) dan Hospital Canselor Tuanku Muhriz (HCTM) akan menyertai penyelidikan ini. Penyelidikan ini akan berlangsung selama 24 bulan dan tempoh pembabitan anda dianggarkan selama 16 bulan.

6. Apakah produk penyelidikan yang akan saya terima?

Sekiranya anda bersetuju untuk menyertai penyelidikan ini, doktor mungkin perlu menjalankan beberapa ujian dan pemeriksaan terhadap diri anda bagi menentukan samada anda sesuai untuk menyertai penyelidikan ini. Sekiranya anda didapati layak, anda akan ditentukan secara rawak kepada salah satu kumpulan rawatan yang dinyatakan di bawah. Sebanyak 2 kumpulan umum (intervensi atau kontrol) yang akan dibahagikan secara sama rata, dan seterusnya dibahagikan kepada 4 sub-kumpulan bergantung kepada saiz tumor dan umur pesakit. Peluang untuk anda dimasukkan ke dalam kumpulan rawatan (intervensi atau kontrol) adalah sama (1/2). Anda akan diberitahu kumpulan rawatan yang mana yang telah ditentukan untuk anda. Ubat kajian (Tamoxifen) tidak mengandungi sebarang unsur-unsur yang berkaitan dengan khinzir, lembu atau pun produk yang berasaskan haiwan.

Kumpulan Intervensi (tumor < 10mm atau ≥ 10mm, umur < 40 tahun atau ≥ 40 tahun)

Peserta akan dikehendaki mengambil ubat tamoxifen sebanyak 20mg setiap hari dalam bulan pertama kajian, diikuti dengan 40mg setiap hari untuk bulan berikutnya sehingga cukup tempoh 12 bulan. Perlu menghadiri lawatan susulan setiap 4 bulan.

Kumpulan Kontrol (tumor < 10mm atau ≥ 10mm, umur < 40 tahun atau ≥ 40 tahun)

Peserta akan diletakkan di bawah kaedah rawatan pemerhatian. Perlu menghadiri lawatan susulan setiap 4 bulan (penilaian yang sama akan dilaksanakan seperti mana kumpulan intervensi)

7. Apakah yang terjadi kepada saya sekiranya saya bersetuju untuk menyertai penyelidikan ini?

a) Anda perlu menandatangani borang keizinan pesakit
b) Maklumat klinikal dan keputusan ujian makmal anda yang sedia ada akan direkodkan ke dalam borang maklumat kes
c) Sebanyak 10ml darah (1 sudu makan) akan diambil dari setiap pesakit sebelum dan selepas selesai kajian (dua kali). Ujian darah tambahan akan diberitahu sekiranya perlu.
d) Anda akan ditentukan secara rawak ke dalam salah satu kumpulan rawatan (Kumpulan Intervensi atau Kontrol) bergantung kepada saiz ketumbuhan yang ada dan kumpulan umur. Kajian ini adalah kajian terbuka, dan setiap pesakit akan diberitahu tentang kumpulan rawatan yang ditetapkan untuk mereka.

e) Slaid tisu kelenjar pituitari anda yang dibuang semasa pembedahan lalu akan diperoleh semula untuk tujuan penilaian tahap ketumbuhan dan mengesan penanda yang berkaitan.
f) Anda perlu menghadiri lawatan susulan setiap 4 bulan (bulan ke 4, 8, 12 dan 16 selepas rawatan bermula)
g) Anda dikehendaki menjalani MRI Pituitari sebanyak 2 kali (selepas 6 bulan dan 12 bulan rawatan). MRI tersebut adalah sebahagian dari rutin pemerhatian yang harus dilakukan oleh pesakit bagi mengesan sebarang tumbesaran pada sisa ketumbuhan dan menilai keberkesanan rawatan.

Peserta kajian akan dimaklumkan berkenaan keputusan kajian yang dijalankan. Peserta kajian akan dimaklumkan berkenaan apa-apa hal berkaitan dengan borang keizinan pesakit sekiranya terdapat maklumat tambahan.

8. Bilakah saya akan menerima produk penyelidikan dan bagaimana cara menyimpannya?

Bagi peserta kumpulan intervensi, anda akan diberikan produk penyelidikan setiap kali anda hadir untuk lawatan susulan di sepanjang tempoh rawatan penyelidikan ini. Anda tidak boleh memberi bekalan ubat kajian (tamoxifen) kepada orang lain. Kakitangan penyelidikan ini akan menerangkan kepada anda cara-cara mengendali dan menyimpan ubat tamoxifen tersebut. Sila pastikan anda menyimpan kesemua botol yang mengandungi tamoxifen selepas selesai menggunakannya, samaada ianya habis digunakan ataupun tidak. Kadangkala semasa lawatan susulan, anda mungkin dikehendaki membawa semula semua botol tersebut ke pusat kajian anda (samada separuh guna, belum digunakan atau botol yang kosong).

9. Apakah tanggungjawab saya sewaktu menyertai penyelidikan ini?

Amat penting anda menjawab kesemua soalan yang ditanyakan oleh kakitangan penyelidikan dengan jujur dan lengkap. Jika keadaan atau kesihatan anda berubah sepanjang penyelidikan ini, anda mesti memberitahu penyelidik anda. Mungkin terdapat ubat-ubat yang tidak boleh anda ambil sepanjang penyertaan anda dalam penyelidikan ini. Penyelidik akan berbincang dengan anda mengenai ubat-ubat itu. Anda tidak boleh mengambil apa-apa ubat tanpa berbincang terlebih dahulu dengan penyelidik anda. Anda mesti memberitahu penyelidik anda dengan segera, sekiranya anda membuat sebarang perubahan dalam rawatan yang sedia ada (yang sedang anda ambil), walaupun jika anda telah lama mengambil ubat tersebut.

Adalah amat penting untuk memberitahu dengan segera kepada penyelidik anda jika berlaku sebarang perubahan pada kesihatan anda sepanjang penyertaan anda dalam penyelidikan ini. Demi keselamatan anda, adalahjuga amat penting anda mengikut semua arahan yang diberikan oleh penyelidik anda sepanjang penyelidikan ini dijalankan.

Sila bertanya kepada penyelidik anda jika anda mahukan lebih banyak maklumat mengenai risiko dan kesan sampingan dalam penyelidikan ini.

10. Apakah jenis rawatan yang akan saya terima selepas menyertai penyelidikan ini?

Ubat tamoxifen tidak akan diberikan lagi kepada anda selepas tamat tempoh penyelidikan. Sama ada anda mengikuti penyelidikan ini dengan sepenuhnya ataupun menarik diri di pertengahan penyelidikan, doktor anda akan berbincang dengan anda mengenai rawatan alternatif yang terbaik untuk rawatan anda di masa hadapan.

11. Apakah risiko dan kesan-kesan sampingan menyertai penyelidikan ini?

Anda mungkin mengalami kesan sampingan. Status kesihatan berdasarkan ujian darah yang terdahulu akan dinilai sebelum rawatan dimulakan. Ini untuk mengurangkan risiko untuk kesan sampingan. Kesan sampingan tersebut adalah seperti berikut;

- Rasa panas yang berlebihan
- Loya
- Keletihan
- Mood berubah-ubah
- Sakit kepala
- Sembelit
- Kulit kering
- Cecair yang berlebihan dari vagina
- Enzim hati meningkat

Bagi peserta wanita, anda tidak boleh mengandung ataupun membuat pasangan anda hamil. Pesakit-pesakit wanita yang menyertai penyelidikan ini juga tidak dibenarkan menyusu badan. Beritahu penyelidik anda secepat mungkin, jika anda syak bahawa anda telah mengandung. Jika perkara ini terjadi, rawatan akan dihentikan dengan serta-merta dan penyertaan anda dalam penyelidikan ini akan ditamatkan.

Sila bertanya kepada penyelidik anda sekiranya anda ingin mengetahui lebih lanjut berkenaan risiko dan kesan sampingan yang boleh terjadi.

12. Apakah manfaatnya saya menyertai kajian ini?

Penyelidikan ini mungkin akan mendatangkan manfaat ataupun langsung tiada memberi apa- apa manfaat kepada anda. Segala maklumat yang diperolehi daripada penyelidikan ini akan dapat membantu dalam memperbaik kaedah rawatan atau pengurusan pesakit lain yang menghidap penyakit atau masalah kesihatan yang sama dengan anda

13. Apakah yang akan terjadi sekiranya saya tercedera semasa menyertai kajian ini?

Jika anda tercedera kerana penyertaan anda dalam penyelidikan ini, anda haruslah menghubungi doktor penyelidikan anda. Sekiranya kecederaan fizikal/badan atau penyakit terhasil secara langsung akibat daripada rawatan ataupun prosedur perubatan yang dijalankan dalam penyelidikan ini, pihak penyelidik akan membayar segala kos rawatan berpatutan yang diperlukan. Tetapi pihak penyelidik tidak akan bertanggungjawab terhadap perbelanjaan perubatan bagi penyakit atau rawatan yang telah wujud sebelum penyertaan anda dalam penyelidikan ini, ataupun mana-mana proses rawatan yang sedang anda ikuti, ataupun sebarang masalah yang timbul samaada daripada kecuaian anda sendiri atau salah laku yang disengajakan, ataupun kecuaian atau salahlaku yang disengajakan samaada oleh pihak penyelidik anda, pihak tapak/lokasi/pusat penyelidikan, mahupun mana- mana pihak ketiga yang terlibat. Walaubagaimanapun, anda tetap tidak kehilangan mana-mana hak anda di sisi undang-undang untuk mendapatkan pampasan sekalipun anda sudah menandatangani borang ini.

14. Apakah rawatan alternatif lain sekiranya saya tidak menyertai penyelidikan ini?

Anda tidak perlu menyertai kajian ini untuk mendapatkan rawatan bagi penyakit atau masalah kesihatan anda. Rawatan alternative yang telah sedia adalah pemerhatian sahaja, radioterapi atau pembedahan berulang. Penyelidik akan berbincang dengan anda secara terperinci mengenai risiko dan manfaat rawatan tersebut.

15. Siapakah yang membiayai penyelidikan ini?

Kajian ini ditaja sepenuhnya oleh Skim Geran Penyelidikan Fundamental (FRGS) di bawah Kementerian Pengajian Tinggi yang akan membayar semua kos kajian termasuklan rawatan tamoxifen, MRI Pituitari, ujian darah dan sampel tisu yang berkaitan. Mana-mana prosedur dan rawatan lain yang tidak diperlukan dalam penyelidikan ini tetapi merupakan sebahagian daripada rawatan anda adalah tanggungan anda sendiri ataupun pihak insurans anda. Pihak penaja akan membayar kakitangan penyelidikan kerana meluangkan masa, penggunaan kemudahan kesihatan dan makmal, dan sebagainya, kerana melibatkan anda dalam penyelidikan ini. Anda juga akan dibayar sejumlah wang RM25 sebagai perbelanjaan perjalanan bagi setiap lawatan susulan untuk penyelidikan ini.

16. Bolehkah penyelidikan ataupun penyertaan saya ditamatkan lebih awal daripada yang dirancang?

Penyelidik boleh menamatkan penyelidikan ini ataupun menamatkan penyertaan anda dalam penyelidikan ini pada bila-bila masa, jika ia perlu demi keselamatan anda. Jika penyelidikan ini dihentikan terlebih awal, di atas sebab-sebab tertentu,

anda akan dimaklumkan dan rawatan yang bakal anda terima selepas itu akan diuruskan. Anda mungkin akan diminta menghadiri satu lawatan susulan terakhir untuk penyelidikan ini.

17. Adakah maklumat perubatan saya akan dirahsiakan?

Segala maklumat anda yang diperolehi dalam penyelidikan ini akan disimpan dan dikendalikan secara sulit. Sekiranya hasil penyelidikan ini diterbitkan atau dibentangkan kepada orang ramai, identiti anda tidak akan didedahkan tanpa kebenaran anda terlebih dahulu. Pihak tertentu seperti individu yang terlibat dalam penyelidikan dan rawatan perubatan anda, juruaudit dan jurupantau yang terlatih, boleh memeriksa dan membuat salinan laporan perubatan anda jika berkenaan dan diperlukan.

Spesimen biologikal anda mungkin akan dihantar ke makmal di luar Negara untuk diuji. Jika perkara ini diperlukan, specimen tersebut akan dikodkan dan maklumat yang boleh mengenal pasti identiti anda akan dipadam. Hanya penyelidik yang terlibat sahaja yang dapat menghubungkan kod tersebut dengan identiti anda.

18. Siapakah yang perlu saya hubungi sekiranya saya mempunyai sebarang pertanyaan?

Anda boleh menghubungi penyelidik ini, Dr Amalina Haydar Ali Tajuddin pada sambungan telefon 013-3539557 sekiranya anda mempunyai sebarang pertanyaan mengenai penyelidikan ini atau jika anda mengesyaki anda mengalami kecederaan yang terhasil daripada penyelidikan ini dan anda mahukan maklumat tentang rawatannya.

Jika anda mempunyai sebarang pertanyaan berkaitan dengan hak-hak anda sebagai pesakit dalam penyelidikan ini, sila hubungi: Setiausaha, Jawatankuasa Etika & Penyelidikan Perubatan, di alamat;

Kementerian Kesihatan Malaysia,

Block A, Kompleks Institut Kesihatan Negara (NIH)
No 1 Jalan Setia Murni U13/52,
Seksyen U13 Bandar Setia Alam,
40170 Shah Alam
Phone: 03-3362 8888/8205
Email: nihsec@moh.gov

BORAG PERSETUJUAN/ KEIZINAN PESAKIT

Tajuk Penyelidikan: Mengenalpasti profil protein yang terlibat dalam keberkesanan rawatan ubat tamoxifen untuk merawat sisa ketumbuhan pada kelenjar pituitary jenis tanpa fungsi

Dengan menandatangani di bawah, saya mengesahkan bahawa:

- Saya telah diberi maklumat tentang penyelidikan di atas secara lisan dan bertulis and saya telah membaca dan memahami segala maklumat yang diberikan dalam risalah ini.

- Saya telah diberikan masa yang secukupnya untuk mempertimbangkan penyertaan saya dalam penyelidikan ini dan telah diberi peluang untuk bertanyakan soalan dan semua persoalan saya telah dijawab dengan sempurna dan memuaskan.

- Saya juga faham bahawa penyertaan saya adalah secara sukarela dan pada bila-bila masa saya bebas menarik diri daripada penyelidikan ini tanpa harus memberi sebarang alasan dan ianya sama sekali tidak akan menjejaskan rawatan perubatan saya pada masa akan datang. Saya tidak mengambil bahagian dalam mana-mana penyelidikan lain pada masa ini. Saya juga memahami tentang risiko dan manfaat penyelidikan ini dan saya secara sukarela memberi persetujuan untuk menyertai penyelidikan inidi bawah syarat-syarat yang telah dinyatakan di atas. Saya faham saya harus mematuhi nasihat dan arahan yang berkaitan dengan penyertaan saya dalam penyelidikan ini daripada doktor penyelidikan (penyelidik).

- Saya faham bahawa kakitangan penyelidikan, pemantau dan juruaudit terlatih , pihak penaja atau gabungannya, dan pihak berkuasa kerajaan atau undang-undang, mempunyai akses langsung dan boleh menyemak laporan perubatan saya bagi memastikan penyelidikan ini dijalankan dengan betul dan data direkodkan dengan betul. Segala maklumat dan data peribadi akan dianggap sebagai SULIT.

- Saya akan menerima satu salinan Maklumat Pesakit dan Borang Persetujuan atau Keizinan Pesakit' yang telah lengkap dengan tarikh dan tandatangan untuk dibawa pulang ke rumah.

- Saya bersetuju/tidak bersetuju* untuk doktor yang biasa merawat saya diberitahu tentang penyertaan saya dalam penyelidikan ini.*(*Potong mana yang tidak berkenaan)*

Subjek:

Tandatangan: Nombor K/P:

Penyelidik yang mengendalikan proses menandatangani boring keizinan:

Tandatangan: Nombor K/P:

Saksi tidak-berpihak/adil: *(Diperlukan; jika subjek adalah buta huruf dan kandungan risalah maklumat pesakit disampaikan secara lisan kepada subjek)*

Tandatangan: Nombor K/P:

APPENDIX J

ETHICAL APPROVAL

JAWATANKUASA ETIKA & PENYELIDIKAN PERUBATAN
(Medical Research & Ethics Committee)
KEMENTERIAN KESIHATAN MALAYSIA
d/a Kompleks Institut Kesihatan Negara
Blok A, No 1, Jalan Setia Murni U13/52,
Seksyen U13, Bandar Setia Alam,
40170 Shah Alam, Selangor.
Tel: 03-3362 8888/8205

Ruj.Kami:(15)KKM/NIHSEC/ P19-653
Tarikh: 23-August-2019

Prof. Dr. Nor Azmi Kamaruddin
PUSAT PERUBATAN UNIVERSITI KEBANGSAAN MALAYSIA (PPUKM)

Dato'/ Tuan/ Puan,

SURAT KELULUSAN ETIKA:

NMRR-18-3778-45144 (IIR)
IDENTIFICATION OF PUTATIVE PROTEIN PROFILES ASSOCIATED WITH TAMOXIFEN THERAPY EFFECTIVENESS IN RESIDUAL NON-FUNCTIONING PITUITARY NEUROENDOCRINE TUMORS

Dengan hormatnya perkara di atas adalah dirujuk.

2. Bersama dengan surat ini dilampirkan surat kelulusan saintifik dan etika bagi projek ini. Segala rekod dan data subjek adalah **SULIT** dan hanya digunakan untuk tujuan kajian dan semua isu serta prosedur mengenai data confidentiality mesti dipatuhi. Kebenaran daripada Pengarah Hospital / Institusi di mana kajian akan dijalankan mesti diperolehi terlebih dahulu sebelum kajian dijalankan. Dato'/ Tuan/ Puan perlu akur dan mematuhi keputusan tersebut dan undang-undang lain yang berkaitan termasuk Akta Akses kepada Sumber Biologi dan Perkongsian Faedah 2017.

3. Penyelidik- penyelidik dan lokasi penyelidikan yang terlibat ialah:

HOSPITAL KUALA LUMPUR
Dr Amalina binti Haydar Ali Tajuddin
Dr Azmi Alias
Dr Fauziah Kassim
Dr KARTIKASALWAH BINTI ABD LATIF

INTERNATIONAL ISLAMIC UNIVERSITY MALAYSIA (IIUM) - KUANTAN CAMPUS
Dr Ahmad Marzuki Omar

PUSAT PERUBATAN UNIVERSITI KEBANGSAAN MALAYSIA (PPUKM)
Prof. Dr. Nor Azmi Kamaruddin (Penyelidik Utama)
Assoc. Prof. Dr. Norlela Sukor
Dr Amalina binti Haydar Ali Tajuddin
Dr Elena Aisha Binti Azizan
Dr Tan Geok Chin

4. Adalah dimaklumkan bahawa kelulusan ini adalah sah sehingga **22-August-2020.** Tuan/Puan perlu menghantar dokumen-dokumen seperti berikut selepas mendapat kelulusan etika. Borang-borang berkaitan boleh dimuat turun daripada laman web Jawatakuasa Etika & Penyelidikan Perubatan (JEPP) (http://www.nih.gov.my/mrec).

Ruj.Kami:(15)KKM/NIHSEC/ P19-653
Tarikh: 23-August-2019

i. ***Continuing Review Form*** selewat-lewatnya **2 bulan (60 hari)** sebelum tamat tempoh kelulusan ini bagi memperbaharui kelulusan etika.
ii. ***Study Final Report*** pada penghujung kajian.
iii. Mendapat kelulusan etika sekiranya terdapat pindaan ke atas sebarang dokumen kajian/ lokasi kajian/ penyelidik. Pihak JEPP mempunyai hak untuk menarik balik kelulusan etika sekiranya terdapat perubahan dokumen kajian yang tidak diisytiharkan.
iv. Kajian berkenaan intervensi klinikal sahaja: Laporan mengenai ***all Serious Adverse Events (SAEs), Suspected Unexpected Serious Adverse Reaction (SUSARs)*** dan ***Protocol Deviation/Violation*** di lokasi kajian yang diluluskan oleh JEPP jika berkenaan. *SAE* perlu dilaporkan dalam tempoh 15 hari kalender dari kesedaran kejadian (*awareness of event)* oleh penyelidik. Laporan awal *SUSAR* perlu dikemukakan seawal mungkin tapi tidak melewati 7 hari calendar dari kesedaran kejadian oleh penyelidik, disusuli dengan laporan lengkap dalam tempoh tambahan 8 hari kalender.

5. Bilangan subjek yang disasarkan untuk menyertai kajian ini di Malaysia adalah **50 orang.**

6. Sila ambil maklum bahawa sebarang urusan surat-menyurat berkaitan dengan penyelidikan ini haruslah dinyatakan nombor rujukan surat ini untuk melicinkan urusan yang berkaitan.

Komen (jika ada) : tiada

Lokasi Kajian:

HOSPITAL KUALA LUMPUR
INTERNATIONAL ISLAMIC UNIVERSITY MALAYSIA (IIUM) - KUANTAN CAMPUS
PUSAT PERUBATAN UNIVERSITI KEBANGSAAN MALAYSIA (PPUKM)

Keputusan Jawatankuasa Etika dan Penyelidikan Perubatan:
(√) Lulus
( ) Tidak Lulus

Tarikh kelulusan **: 23-August-2019**

Sekian terima kasih.

BERKHIDMAT UNTUK NEGARA

Saya yang menjalankan amanah,

.....
DR HJH SALINA ABDUL AZIZ
Pengerusi
Jawatankuasa Etika & Penyelidikan Perubatan
Kementerian Kesihatan Malaysia
No. MPM: 27117

S.K HRRC HOSPITAL KUALA LUMPUR

\KY\MREC_Share\Approval 2019\full-board\23August2019

JAWATANKUASA ETIKA & PENYELIDIKAN PERUBATAN
(Medical Research & Ethics Committee)
KEMENTERIAN KESIHATAN MALAYSIA
d/a Kompleks Institut Kesihatan Negara
Blok A, No 1, Jalan Setia Murni U13/52,
Seksyen U13, Bandar Setia Alam,
40170 Shah Alam, Selangor.
Tel: 03-3362 8888/8205

Ref:(16)KKM/NIHSEC/ P19-653
Date: 23-August-2019

Prof. Dr. Nor Azmi Kamaruddin
PUSAT PERUBATAN UNIVERSITI KEBANGSAAN MALAYSIA (PPUKM)

Dear Sir/ Mdm,

ETHICS INITIAL APPROVAL:

NMRR-18-3778-45144 (IIR)

IDENTIFICATION OF PUTATIVE PROTEIN PROFILES ASSOCIATED WITH TAMOXIFEN THERAPY EFFECTIVENESS IN RESIDUAL NON-FUNCTIONING PITUITARY NEUROENDOCRINE TUMORS

This letter is made in reference to the above matter.

2. The Medical Research and Ethics Committee (MREC), Ministry of Health Malaysia (MOH) has provided ethical approval for this study. Please take note that all records and data are to be kept strictly **CONFIDENTIAL** and can only be used for the purpose of this study. All precautions are to be taken to maintain data confidentiality. Permission from the District Health officer/Hospital Administrator/ Hospital Director and all relevant heads of departments /units where the study will be carried out must be obtained prior to the study. You are required to follow and comply with their decision and all other relevant regulations, including the Access to the Biological Resources and Benefit Sharing Act 2017.

3. The investigators and study sites involved in this study are:

HOSPITAL KUALA LUMPUR
Dr Amalina binti Haydar Ali Tajuddin
Dr Azmi Alias
Dr Fauziah Kassim
Dr KARTIKASALWAH BINTI ABD LATIF

INTERNATIONAL ISLAMIC UNIVERSITY MALAYSIA (IIUM) - KUANTAN CAMPUS
Dr Ahmad Marzuki Omar

PUSAT PERUBATAN UNIVERSITI KEBANGSAAN MALAYSIA (PPUKM)
Prof. Dr. Nor Azmi Kamaruddin (Penyelidik Utama)
Assoc. Prof. Dr. Norlela Sukor
Dr Amalina binti Haydar Ali Tajuddin
Dr Elena Aisha Binti Azizan
Dr Tan Geok Chin

4. The following study documents have been received and reviewed with reference to the above study:

Ref:(16)KKM/NIHSEC/ P19-653
Date: 23-August-2019

Documents received and reviewed with reference to the above study:

1. Study Protocol version 2, dated 21 June 2019
2. English PIS-ICF. Version 2.0. Date: 21 June 2019
3. Malay Pls-ICF. Version 2.0. Date: 21 June 2019
4. Case report form: Version 2.0: Date 21 June19
5. Investigators' Documents : COI Declaration Form, CV and GCP and IA-HOD:

HOSPITAL KUALA LUMPUR
Dr Amalina binti Haydar Ali Tajuddin
Dr Azmi Alias
Dr Fauziah Kassim
Dr KARTIKASALWAH BINTI ABD LATIF

INTERNATIONAL ISLAMIC UNIVERSITY MALAYSIA (IIUM) - KUANTAN CAMPUS
Dr Ahmad Marzuki Omar

PUSAT PERUBATAN UNIVERSITI KEBANGSAAN MALAYSIA (PPUKM)
Prof. Dr. Nor Azmi Kamaruddin (Penyelidik Utama)
Assoc. Prof. Dr. Norlela Sukor
Dr Amalina binti Haydar Ali Tajuddin
Dr Elena Aisha Binti Azizan
Dr Tan Geok Chin

5. Please note that the approval is valid unti **22-August-2020**. The following are to be reported upon receiving ethical approval. Required forms can be obtained from the Medical Research Ethics Committee (MREC) website (**http://www.nih.gov.my/mrec**).

i. **Continuing Review Form** has to be submitted to MREC **2 months (60 days) prior** to the expiry of ethical approval.
ii. **Study Final Report** upon study completion to the MREC.
iii. Ethical approval is required in the case of **amendments/ changes** to the **study documents/ study sites/ study team**. MREC reserves the right to withdraw ethical approval if changes to study documents are not completely declared.
iv. **Applicable for Clinical Interventional Studies only:** Report occurrences of **all Serious Adverse Events (SAEs), Suspected Unexpected Serious Adverse Reaction (SUSARs)** and **Protocol Deviation/Violation** at all MREC approved sites to MREC. SAEs are to be reported within 15 calendar days from awareness of event by investigator. Initial report of SUSARs are to be reported as soon as possible but not later than 7 calendar days from awareness of event by investigator, followed by a complete report within 8 additional calendar days.

6. Total of **50 subjects** are targeted to enroll this study in Malaysia.

7. Please take note that the reference number for this letter must be stated in all correspondence related to this study to facilitate the process.

Comments (if any): None

Ref:(16)KKM/NIHSEC/ P19-653
Date: 23-August-2019

Project Sites:

HOSPITAL KUALA LUMPUR
INTERNATIONAL ISLAMIC UNIVERSITY MALAYSIA (IIUM) - KUANTAN CAMPUS
PUSAT PERUBATAN UNIVERSITI KEBANGSAAN MALAYSIA (PPUKM)

Decision by Medical Research & Ethics Committee:
(√) Approved
( ) Disapproved

Date of Approval : **23-August-2019**

DR HJH SALINA ABDUL AZIZ
Chairperson
Medical Research & Ethics Committee (MREC)
Ministry of Health
MMC No.:27117

CC: HRRC HOSPITAL KUALA LUMPUR

\KY\MREC_Share\Approval 2019\full-board\23August2019

MEMBERS OF THE MEDICAL RESEARCH & ETHICS COMMITTEE WHO
MEMBERS OF THE MEDICAL RESEARCH & ETHICS COMMITTEE WHO ATTEND
THE MEETING ON
28th May 2019

No	NAME	GENDER	EXPERTISE	DESIGNATION/ AFFILIATION	ROLES	TICK (√) IF PRESENT
1	**MREC Chairman** Dr. Salina binti Abdul Aziz	F	Psychiatry & Clinical Epidemiology	Hospital Kuala Lumpur	Medical member	x
2	**MREC Deputy Chairperson** Dr Nurain bt Mod Noor	F	Endocrinology	Putrajaya Hospital	Medical member	√
3	**MREC Secretary** Dr Lee Keng Yee	F	Bioethics	Clinical Research Centre	Secretary	√
4	Dr Lam Mynn Dee	F	Health Research	Secretariat of the National Institutes of Health	Secretariat of MREC	√
5	Datin Dr Noriah Bidin	F	Public Health	Independent	Medical member (Independent Member)	√
6	Dr Tang Swee Ping	F	Paediatric Rheumatology	Selayang Hospital	Medical member	√
7	Dr Ami Fazlin Syed Mohamed	F	Clinical Pharmacology	Institute for Medical Research	Medical member	√
8	Dr Chin Yin Chung Melvyn	M	Occupational Medicine	Institute of Health Management	Medical member	√

No	NAME	GENDER	EXPERTISE	DESIGNATION/ AFFILIATION	ROLES	TICK (√) IF PRESENT
9	Dr Asiah Kassim	F	Paediatrician	Hospital Kuala Lumpur	Medical Member	x
10	Dr Noraziani Khamis	F	Public Health	Institute of Health Management	Medical Member	x
11	Dr Norsazila Asikin Mohd Azmi	F	Complementary Medicine	Bahagian Perubatan Tradisional & Komplementari, KKM	Medical Member	x
12	Chun Geok Ying	F	Pharmacy	CTU, Hospital Ampang	Scientific member	x
13	Dr Ho Tze Ming	F	Senior Researcher (Acarology)	-	Scientific member	x
14	Assoc Prof Dr Wee Lei Hum	F	Health Behaviour	Faculty of Health Sciences, Universiti Kebangsaan Malaysia	Scientific member	√
15	Dr Neoh Chin Fen	F	Pharmacy	UITM	Scientific member	√
16	Dr Afendi Dahlan	M	Pharmacy	DR Group Holdings Sdn Bhd	Scientific member	x
17	Dr Mohammad Zabri Johari	M	Health Behavioural & Research Method	Institute of Health Behavioural Research	Scientific member	√
18	Dr Wan Rosalina Wan Rosli	F	Pharmacogenetics	Cyberjaya University College of Medical Sciences	Scientific Reviewer (Independent Member)	√

No	NAME	GENDER	EXPERTISE	DESIGNATION/ AFFILIATION	ROLES	TICK (√) IF PRESENT
19	Pn Ang Wei Meng	F	-	Max Station Malaysia Sdn Bhd	Non medical non scientific member	x
20	En Abu Hurairah bin Bahari	M	-	-	Non medical non scientific member	√
21	En. Lim Teng Ann	M	-	-	Non medical non scientific member	x
22	En Mohd Hadziq Mohd Zafari	M	Layperson	PPUKM	medical non scientific member	√

The Medical Research & Ethics Committee, Ministry of Health Malaysia operates in accordance to the International Council for Harmonization of Technical Requirement for Pharmaceutical for Human Use (ICH). Any member of the MREC who is involved in the study / project under review will not participate in the approval of the study / project.

UNIVERSITI KEBANGSAAN MALAYSIA
The National University of Malaysia

Pusat Pengurusan Penyelidikan dan Instrumentasi / *Centre for Research and Instrumentation Management*

Rujukan : UKM PPI/111/8/JEP-2019-055
Tarikh : 10 April 2019

Profesor Dr. Nor Azmi Kamaruddin
Jabatan Perubatan
Hospital Canselor Tuanku Muhriz
Pusat Perubatan UKM

Y.Bhg. Profesor/Datuk/Dato'/Datin/Tuan/Puan,

KELULUSAN ETIKA MENJALANKAN PENYELIDIKAN DI UKM

Tajuk Penyelidikan : *Identification Of Putative Protein Profiles Associated With Tamoxifen Therapy Effectiveness In Residual Non-Functioning Pituitary Neuroendocrine Tumors*

Perkara yang tersebut di atas adalah dirujuk.

2. Sukacita dimaklumkan, Jawatankuasa Etika Penyelidikan UKM meluluskan permohonan penyelidikan Y. Bhg. Profesor/Datuk/Dato'/Datin/Tuan/Puan bagi tajuk diatas. Tempoh kelulusan penyelidikan adalah daripada **30 Mac 2019 – 29 Mac 2021.** Sila kemukakan sebarang Laporan **Kesan Sampingan, Laporan Kemajuan Setiap 6 Bulan** dan **Laporan Akhir** sebaik sahaja penyelidikan tamat kepada Jawatankuasa Etika Penyelidikan UKM.

3. Sukacita diingatkan projek penyelidikan ini hanya boleh dijalankan setelah mendapat **surat kelulusan menjalankan penyelidikan** dari Timbalan Dekan Penyelidikan Fakulti atau Pengarah Pusat/Institut.

Sekian, terima kasih.

Yang benar,

PROFESOR DATO' DR. FUAD ISMAIL
Pengerusi
Jawatankuasa Etika Penyelidikan
Universiti Kebangsaan Malaysia

s.k.
- **Pengarah**
  Pusat Pengurusan Penyelidikan dan Instrumentasi (CRIM)
  Universiti Kebangsaan Malaysia
- **Timbalan Dekan (Penyelidikan & Inovasi)**
  Sekretariat Penyelidikan Perubatan & Inovasi
  Hospital Canselor Tuanku Muhriz
  Pusat Perubatan UKM
- **Ketua Jabatan Perubatan**
  Hospital Canselor Tuanku Muhriz
  Pusat Perubatan UKM

- **Profesor Dr. Norlela Sukor**
- **Dr. Elena Aisha Azizan**
  Jabatan Perubatan
  Hospital Canselor Tuanku Muhriz
  Pusat Perubatan UKM

- **Profesor Madya Dr. Shahizon Azura Mohamed Mukari**
  Jabatan Radiologi
  Hospital Canselor Tuanku Muhriz
  Pusat Perubatan UKM

- **Profesor Madya Dr. Tan Geok Chin**
  Jabatan Patologi
  Hospital Canselor Tuanku Muhriz
  Pusat Perubatan UKM

- **Dr. Nadiah Abu**
  Institut Perubatan Molekul UKM (UMBI)
  Cheras

- **Profesor Madya Dr. Ahmad Marzuki Omar**
  Kulliyyah of Medicine, International Islamic University Malaysia
  Jalan Sultan Ahmad Shah, Bandar Indera Mahkota
  25200 Kuantan
  Pahang Darul Makmur

- **Dr. Azmi Alias**
  Jabatan Neurosurgeri
  Hospital Kuala Lumpur
  50586 Jalan Pahang
  Wilayah Persekutuan Kuala Lumpur

- **Dr. Amalina Haydar Ali Tajuddin**
  Kulliyyah Perubatan
  Universiti Islam Antarabangsa Malaysia
  Jalan Sultan Ahmad Shah, Bandar Indera Mahkota
  25200 Kuantan
  Pahang Darul Makmur

- Fail Surat Kelulusan 2019

FI/FMZ

UNIVERSITI KEBANGSAAN MALAYSIA
The National University of Malaysia

Pusat Pengurusan Penyelidikan dan Instrumentasi / ***Centre for Research and Instrumentation Management***

NAME OF ETHICS COMMITTEE/IRB: Research Ethics Committee, The National University of Malaysia	ETHICS COMMITTEE/IRB REF NO : UKM PPI/111/8/JEP-2019-055

PROTOCOL TITLE :
Identification Of Putative Protein Profiles Associated With Tamoxifen Therapy Effectiveness In Residual Non-Functioning Pituitary Neuroendocrine Tumors

PRINCIPAL INVESTIGATOR :
Professor Dr. Nor Azmi Kamaruddin
Department of Medicine
Hospital Canselor Tuanku Muhriz
UKM Medical Centre

The following items [X] have been received and reviewed in connection with the above study to be conducted by the above investigator.

Documents

- [X] Research Application Form
- [X] Research Proposal / Protocol
- [X] Publication Policy
- [X] Non-Disclosure Agreement
- Information Sheet:-
  - [X] Malay [X] English
- Consent Form:-
  - [X] Malay [X] English
- Questionnaire:-
  - [ ] Malay [ ] English
- Curriculum Vitae of Researcher:-
  - [X] Principal [X] Co-researcher [X] Student
- [X] Good Clinical Practice Certificate (GCP)
- [X] Project Agreement

The Research Ethics Committee, The National University of Malaysia operates in accordance to the International Conference of Harmonization Good Clinical Practice Guidelines.

Comments (if any): Professor Associate Dr. Tan Geok Chin is the co-investigator for this study and also member of Research Ethics Committee. He strictly was not involved in the decision of Research Ethics Committee to approve this study.

Date of Approval: 30 March 2019

PROFESSOR DATO' DR. FUAD ISMAIL
Chairman
Research Ethics Committee
The National University of Malaysia

UNIVERSITI KEBANGSAAN MALAYSIA
The National University of Malaysia

Pusat Pengurusan Penyelidikan dan Instrumentasi / ***Centre for Research and Instrumentation Management***

SENARAI KEHADIRAN
MESYUARAT JAWATANKUASA ETIKA PENYELIDIKAN UKM BIL 04/2019

TEMPAT : Sukmaria
3rd Floor, Block Clinical
UKM Medical Centre, Cheras
TARIKH : 28th February 2019 (Thursday)
MASA : 2.15 P.M

Bil	Nama	UKMPerubatan	Tempoh	Tandatangan
1	Profesor Dato' Dr. Fuad Ismail	K006073	23 Sep 2017 – 22 Sep 2019	
2	Profesor Dr. Mohd Rizal Abdul Manaf	K011625	15 Mac 2017 – 14 Mac 2019	
3	Profesor Dr. Joanna Ooi Su Min	K007291	15 Mac 2017 – 14 Mac 2019	
4	Profesor Dr. Mohd Shahrir Mohamed Said	K012928	15 Mac 2017 – 14 Mac 2019	
5	Profesor Dr. Norazlina Mohamed	K010646	15 Mac 2017 – 14 Mac 2019	
6	Profesor Dr. Zarina Abdul Latiff	K006885	15 Mac 2017 – 14 Mac 2019	
7	Profesor Dr. Suzana Shahar	K006408	15 Mac 2017 – 14 Mac 2019	
8	Profesor Dr. Ahmad Nazrun Shuid	K011442	15 Mac 2018 – 14 Mac 2019	
9	Profesor Madya Dr. Nor Ba'yah Abdul Kadir	K012882	15 Mac 2017 – 14 Mac 2019	
10	Profesor Madya Dr. Nurasyikin Yusof	K010963	15 Mac 2017 – 14 Mac 2019	
11	Profesor Madya Dr. Goon Jo Aan	K015359	15 Mac 2017 – 14 Mac 2019	
12	Profesor Madya Dr. Shahrun Niza Abdullah Suhaimi	K017700	15 Mac 2017 – 14 Mac 2019	
13	Profesor Madya Dr. Nik Ruzyanei Nik Jaafar	K014676	15 Mac 2017 – 14 Mac 2019	
14	Dr. Ixora Kamisan Atan	K013149	15 Mac 2017 – 14 Mac 2019	
15	Profesor Dr. Nor Azlin Mohamed Ismail	K006365	15 Mac 2017 – 14 Mac 2019	

16	Profesor Dr. Norfilza Mohd Mokhtar	K009918	15 Mac 2017 – 14 Mac 2019	
17	Profesor Dr. Shamsul Azhar Shah	K013677	15 Mac 2017 – 14 Mac 2019	
18	Profesor Dr. Poh Bee Koon	K006746	15 Mac 2017 – 14 Mac 2019	
19	Profesor Madya Dr. Wong Sau Wei	K012335	15 Mac 2017 – 14 Mac 2019	
20	Profesor Madya Dr. Tan Geok Chin	K014055	15 Mac 2017 – 14 Mac 2019	
21	Profesor Madya Dr. Alfizah Hanafiah	K009680	15 Mac 2017 – 14 Mac 2019	
22	Profesor Madya Dr. Goh Eng Hong	K013734	15 Mac 2017 – 14 Mac 2019	
23	Profesor Madya Dr. Roszalina Ramli	K007802	15 Mac 2017 – 14 Mac 2019	
24	Profesor Madya Dr. Raja Affendi Raja Ali	K020001	15 Julai 2017 – 14 Mac 2019	
25	Profesor Madya Dr. Hizlinda Tohid	K014095	15 Mac 2017 – 14 Mac 2019	
26	Dr. Mohammad Rahim Kamaluddin	K021070	15 Mac 2017 – 14 Mac 2019	
27	Dr. Mohd Nasri Awang Besar	K017076	15 Mac 2017 – 14 Mac 2019	
28	Dr. Aida Zairani Mohd Zahidin	K012991	15 Mac 2017 – 14 Mac 2019	
29	Dr. Jalina Karim	K015101	15 Mac 2017 – 14 Mac 2019	
30	Dr. Ahmad Khaldun Ismail	K011529	15 Mac 2017 – 14 Mac 2019	
31	Rafidah Mamat	K017170		

UNIVERSITI KEBANGSAAN MALAYSIA
The National University of Malaysia

Pusat Pengurusan Penyelidikan dan Instrumentasi — *Centre for Research and Instrumentation Management*

SENARAI KEHADIRAN (AHLI LUAR)
MESYUARAT JAWATANKUASA ETIKA PENYELIDIKAN UKM BIL 04/2019

TEMPAT : Sukmaria
3rd Floor, Block Clinical
UKM Medical Centre, Cheras
TARIKH : 28th February 2019 (Thursday)
MASA : 2.15 P.M

Bil	Nama	Tempoh	Tandatangan
1	Dr. Ibrahim Abu Bakar	15 Mac 2017 - 14 Mac 2019	
2	Encik Tan Meng Leng	15 Mac 2017 - 14 Mac 2019	
3	Puan Hendon Mohamed	15 Mac 2017 - 14 Mac 2019	28/02/19

APPENDIX K

LIST OF PUBLICATIONS AND PRESENTATION

Haydar Ali Tajuddin, A., Kamaruddin, N., Sukor, N., Azizan, E.A. & Omar, A.M. 2020. Estrogen Receptors in Nonfunctioning Pituitary Neuroendocrine Tumors: Review on Expression and Gonadotroph Functions. Journal of the Endocrine Society 4(12): bvaa157.

Amalina, H.A.T., Norlela, S., Elena Aisha, A., Nor Azmi, K., Ahmad Marzuki, O., Tan, G.C., Muaatamarulain, M., Shahizon Azura, M.M., Azmi, A., Kartikasalwah, A.L., Tay, P. Sen, Nurdillah, I., Fauziah, K. & Wan Ruza Iswati, W.I. 2024. Tumor shrinkage in a tamoxifen-treated non-functioning pituitary neuroendocrine tumor with positive estrogen receptor-[illegible] β) [illegible] and review of the literature. Journal of Clinical and Translational Endocrinology: Case Reports 33: 100174.

Haydar Ali Tajuddin, A., Sukor, N., Azizan, E.A., Kamaruddin, N.A., Omar, A.M., Tan, G.C., Mustangin, M., Alias, A., Wan Ismail, W.R.I., Abd Latif, K., Idris, N., Uddin, M.N., Rullah, K., Isa, N. [illegible] 2 [illegible] 2 5 [illegible] for residual NF-PitNETs: A Proof-of-Concept study integrating receptor [illegible]

Journal of the Endocrine Society, 2020, Vol. 4, No. 12, 1–7
doi:10.1210/jendso/bvaa157
Mini-Review

Mini-Review

Estrogen Receptors in Nonfunctioning Pituitary Neuroendocrine Tumors: Review on Expression and Gonadotroph Functions

Amalina Haydar Ali Tajuddin,[1,2] Norazmi Kamaruddin,[2] Norlela Sukor,[2] Elena Aisha Azizan,[2] and Ahmad Marzuki Omar[1]

[1]Department of Internal Medicine, Kulliyyah of Medicine, International Islamic University Malaysia, Jalan Sultan Ahmad Shah, Bandar Indera Mahkota, 25200, Kuantan, Pahang, Malaysia; and [2]Endocrine Unit, Faculty of Medicine, UKM Medical Centre, Jalan Yaa'cob Latif, Bandar Tun Razak, 56000, Cheras, Kuala Lumpur, Malaysia

ORCiD number: 0000-0002-7243-8824 (A. Haydar Ali Tajuddin)

Abbreviations: E2, 17β-estradiol; ER, estrogen receptor; FSH, follicle-stimulating hormone; GH, growth hormone; GnRH, gonadotropin-releasing hormone; GPER, G protein–coupled estrogen receptor; LH, luteinizing hormone; mRNA, messenger ribonucleic acid; NF-Pitnet, nonfunctioning pituitary neuroendocrine tumor; PR, progesterone receptor; PRL, prolactin; PTTG, pituitary tumor transforming gene; SERM, selective estrogen receptor modulator; TX, tamoxifen.

Received: 22 September 2020; Editorial Decision: 12 October 2020; First Published Online: 19 October 2020; Corrected and Typeset: 17 November 2020.

Abstract

Estrogen (17β-estradiol or E2) is a crucial regulator of the synthesis and secretion of pituitary reproductive hormones luteinizing hormone, follicle-stimulating hormone, and prolactin. In this review, we summarize the role of estrogen receptors in nonfunctioning pituitary neuroendocrine tumors (NF-Pitnets), focusing on immunoexpression and gonadotroph cell proliferation and apoptosis. Gonadotroph tumors are the most common subtype of NF-Pitnets. Two major estrogen receptor (ER) isoforms expressed in the pituitary are estrogen receptor alpha (ERα) and estrogen receptor beta (ERβ). Overall, estrogen actions are mostly exerted through the ERα isoform on the pituitary. The G protein–coupled estrogen receptor (GPER) located at the plasma membrane may contribute to nongenomic effects of estrogen. Nuclear immunoreactivity for ERα and ERβ was highest among gonadotroph and null cell tumors. Silent corticotroph tumors are the least immunoreactive for both receptors. A significantly elevated ERα expression was observed in macroadenomas compared with microadenomas. ERα and ERβ may act in opposite directions to regulate the Slug-E-cadherin pathway and to affect invasiveness of NF-Pitnets. In the cellular pathway, ERs regulate estrogen-induced proliferation and differentiation and impact several signaling pathways including the MAPK and PI3K/Akt pathway. Estrogen was the first-discovered inducer of pituitary tumor transforming gene 1 that was abundantly expressed in NF-Pitnets. ERα can be a potential biomarker for predicting tumor size and invasiveness as well as

ISSN 2472-1972

Journal of Clinical and Translational Endocrinology: Case Reports 33 (2024) 100174

Contents lists available at ScienceDirect

Journal of Clinical and Translational Endocrinology: Case Reports

journal homepage: www.elsevier.com/locate/jctecasereports

Tumor shrinkage in a tamoxifen-treated non-functioning pituitary neuroendocrine tumor with positive estrogen receptor-beta (ERβ): A case report and review of the literature

Haydar Ali Tajuddin Amalina [a,b], Sukor Norlela [b,*], Azizan Elena Aisha [b], Kamaruddin Nor Azmi [b], Omar Ahmad Marzuki [a], Geok Chin Tan [c], Mustangin Muaatamarulain [c], Mohamed Mukari Shahizon Azura [d], Aliae Azmi [e], Abd Latif Kartikasalwah [f], Poh Sen Tay [f], Idris Nurdillah [f], Kasim Fauziah [g], Wan Ismail Wan Ruza Iswati [g]

[a] Department of Internal Medicine, International Islamic University Malaysia, Kuantan Campus, Jalan Sultan Ahmad Shah, Bandar Indera Mahkota, 25200, Kuantan, Pahang, Malaysia
[b] Medical Department, Faculty of Medicine, National University of Malaysia, Jalan Yaacob Latif, Bandar Tun Razak, 56000, Cheras, Kuala Lumpur, Malaysia
[c] Department of Pathology, Faculty of Medicine, National University of Malaysia, Jalan Yaacob Latif, Bandar Tun Razak, 56000, Cheras, Kuala Lumpur, Malaysia
[d] Department of Radiology, Faculty of Medicine, National University of Malaysia, Jalan Yaacob Latif, Bandar Tun Razak, 56000, Cheras, Kuala Lumpur, Malaysia
[e] Department of Neurosurgery, Hospital Kuala Lumpur, Jalan Pahang, 50586, Kuala Lumpur, Malaysia
[f] Department of Radiology, Hospital Kuala Lumpur, Jalan Pahang, 50586, Kuala Lumpur, Malaysia
[g] Department of Pathology, Hospital Kuala Lumpur, Jalan Pahang, 50586, Kuala Lumpur, Malaysia

ARTICLE INFO

Keywords:
Non-functioning pituitary neuroendocrine tumor
Estrogen receptor
Tamoxifen
SERM

ABSTRACT

Administration of selective estrogen receptor modulators (SERMs) and anti-estrogens has been shown to reduce the size of pituitary tumors. However, previous studies were performed on animal pituitary tumors or tissue cultures. We administered oral tamoxifen to a postoperative patient with a nonfunctioning pituitary neuroendocrine tumor (NF-PitNET) to investigate its potential effect on tumor volume. This case report presents the case of a 47-year-old female patient with a null cell adenoma who had undergone surgical resection as primary treatment and was left with a residual tumor that grew significantly. She was treated with tamoxifen 20–40 mg daily for one year. She was followed up to assess tamoxifen adherence, tolerability, and adverse events. The resected pituitary tumor was stained with estrogen receptor alpha (ERα) and beta (ERβ), proliferation markers (ki-67 and p53), and H&E staining for mitotic count. MRI of the pituitary gland was performed before starting treatment, after 6 months, and after 1 year of tamoxifen therapy. Her resected tumor showed high-intensity ERβ staining in the absence of ERα expression. She was able to tolerate oral tamoxifen therapy without side effects. Tamoxifen therapy resulted in a remarkable reduction in residual tumor volume of up to 87 % in this patient. Tamoxifen has a potential therapeutic effect in treating patients with residual NF-PitNET tumors that have regrown after primary resection. This finding may provide an alternative treatment modality for recurrent NF-PitNET. ERβ expression may predict response to tamoxifen in this subset of patients.

1. Introduction

Nonfunctioning pituitary neuroendocrine tumors (NF-PitNET) are pituitary tumors characterized by the absence of hormone hypersecretion. Patients may become symptomatic due to hypopituitarism or compression symptoms in large tumors. Although considered benign tumors, patients with NF-PitNET have increased morbidity and slightly increased mortality, mainly due to circulatory, respiratory, and infectious diseases [1,2]. Surgical removal of the tumor is the first-line treatment in most cases. However, complete removal of very large tumors can be difficult, and these adenomas have a high residual tumor rate [3]. For these residual tumors, radiotherapy is an effective treatment option with tumor control of up to 90 % over 10 years [4,5]. However, this high efficacy is offset by a high incidence of complications

* Corresponding author.
E-mail address: drlela2020@yahoo.com (S. Norlela).

https://doi.org/10.1016/j.jeer.2024.100174
Received 7 December 2023; Received in revised form 31 May 2024; Accepted 26 June 2024
Available online 27 June 2024

Endocrine
https://doi.org/10.1007/s12020-025-04404-7

ORIGINAL ARTICLE

"Tamoxifen for residual NF-PitNETs: A Proof-of-Concept study integrating receptor profiling, pilot trial, and target pathway analysis"

Amalina Haydar Ali Tajuddin[1,4] · Norlela Sukor[4] · Elena Aisha Azizan[4] · Nor Azmi Kamaruddin[4] · Ahmad Marzuki Omar[1] · Geok Chin Tan[5] · Muaatamarulain Mustangin[5] · Azmi Alias[6] · Wan Ruza Iswati Wan Ismail[2] · Kartikasalwah Abd Latif[7] · Nurdillah Idris[7] · Md. Nazim Uddin[8] · Kamal Rullah[3] · Nur Firdaus Isa[9] · Mohd Hamzah Mohd Nasir[9]

Received: 8 June 2025 / Accepted: 23 August 2025

Abstract

Background Non-functioning neuroendocrine pituitary neuroendocrine tumors (NF-PitNETs) pose a therapeutic challenge due to their hormonal inactivity, mass effects and limited medical treatment options for residual or recurrent disease. There is increasing evidence that the oestrogen receptor (ER) is involved in the pathogenesis of these tumours. In this study, the potential therapeutic role of tamoxifen, a selective ER modulator, was investigated.

Methods Fifty NF-PitNET samples were analysed for ERα and ERβ expression by immunohistochemistry. A randomised, open-label clinical trial was conducted in 20 patients with postoperative residual tumours comparing tamoxifen treatment ($n=10$) with observation ($n=10$), with MRI volume analysis performed at baseline and after six months. In parallel, tamoxifen targets were predicted with SwissTargetPrediction and analysed with enrichment tools (DAVID, STRING, Cytoscape).

Results ERβ expression was present in 68% of tumours, while ERα was detected in 18%. In the tamoxifen group, the tumour shrank in 40% of patients and the disease remained stable in 60%. In contrast, tumour progression occurred in 20% of patients in the observation group ($p=0.043$). The computational analysis revealed 109 predicted tamoxifen targets that were significantly enriched in neuroactive ligand–receptor interactions, calcium signalling and cAMP pathways. Gene ontology terms indicated involvement in G protein-coupled receptor activities and synaptic signalling pathways, with key nodes being AKT1, MAPK14, ESR1, DRD2, EGFR and CDKN1B.

Conclusion These preliminary results suggest that tamoxifen may provide clinical benefit in residual NF-PitNETs, particularly those expressing ERβ. Further validation studies are required to confirm efficacy and identify predictive molecular markers.

Keywords Nonfunctioning pituitary neuroendocrine tumors · Nonfunctioning pituitary adenoma · Estrogen receptor · Tamoxifen · Immunohistochemistry · Pilot trial · Target prediction analysis

✉ Amalina Haydar Ali Tajuddin
amalinahaydar@iium.edu.my

[1] Department of Internal Medicine, Kulliyyah of Medicine, International Islamic University Malaysia, Kuantan Campus, Jalan Sultan Ahmad Shah, Bandar Indera Mahkota, Kuantan 25200, Pahang, Malaysia

[2] Department of Pathology, Hospital Kuala Lumpur, Jalan Pahang, Kuala Lumpur 50586, Malaysia

[3] Department of Pharmaceutical Chemistry, Kulliyyah of Pharmacy, International Islamic University Malaysia, Kuantan Campus, Jalan Sultan Ahmad Shah, Bandar Indera Mahkota, Kuantan 25200, Pahang, Malaysia

[4] Medical Department, Faculty of Medicine, National University of Malaysia, Jalan Yaacob Latif, Bandar Tun Razak, Cheras, Kuala Lumpur 56000, Malaysia

[5] Department of Pathology, Faculty of Medicine, National University of Malaysia, Jalan Yaacob Latif, Bandar Tun Razak, Cheras, Kuala Lumpur 56000, Malaysia

[6] Department of Neurosurgery, Hospital Kuala Lumpur, Jalan Pahang, Kuala Lumpur 50586, Malaysia

[7] Department of Radiology, Hospital Kuala Lumpur, Jalan Pahang, Kuala Lumpur 50586, Malaysia

[8] Institute of Food Science and Technology, Bangladesh Council of Scientific and Industrial Research, Dhaka 1205, Bangladesh

[9] Department of Biotechnology, Kulliyyah of Science, International Islamic University Malaysia, Kuantan Campus, Jalan Sultan Ahmad Shah, Bandar Indera Mahkota, Kuantan 25200, Pahang, Malaysia

Published online: 01 September 2025

The 97th
Annual Congress of the Japan Endocrine Society

June 6, 2024

Certificate of Presentation

We hereby confirm the presentation of

Dr. Haydar Ali Tajuddin Amalina

English Session 5 : Thyroid・Pituitary・Phe/PPGL

Title：Tamoxifen and residual tumor volume in postoperative nonfunctioning pituitary neuroendocrine tumors: A pilot study

Abstract Number: O1-5-28

at the 97th Annual Meeting of the Japan Endocrine Society,
on June 6-8, 2024 in Yokohama, Japan.

Tomonobu Hasegawa, M.D., Ph.D.
President of the 97th Annual Congress of the JES
Professor and Chairman
Division of Endocrinology and Metabolism
Department of Pediatrics
Keio University School of Medicine

Congress Secretariat
Convention Linkage, Inc. 株式会社コンベンションリンケージ
2 Sanbancho, Chiyoda-ku, Tokyo, 102-0075, Japan
TEL: +81-3-3263-8688 E-mail: jes2024@c-linkage.co.jp
https://www.c-linkage.co.jp/97jes2024/en/